$^{40}AR/^{39}AR$ MUSCOVITE THERMOCHRONOLOGY AND GEOCHRONOLOGY OF NEW MEXICO PEGMATITES

by

Lisa Anne Gaston

Submitted in partial fulfillment
of the requirements for the

Masters of Science in Geology

New Mexico Institute of Mining and Technology
Department of Earth and Environmental Science

Socorro, New Mexico

May, 2014

ABSTRACT

New $^{40}Ar/^{39}Ar$ muscovite thermochronology data from Precambrian basement rocks of the Manzano, Sandia and Tusas Mountains, along with statewide compilation of geo and thermochronology data, define the onset of Mesoproterozoic magmatism and high-grade metamorphism at 1.46 Ga followed by variable cooling histories. Older Paleoproterozoic muscovite dates near 1.67 Ga are found in a restricted area within the Manzanita Mountains and constrain metamorphic fabric development to be of Mazatzal age.

Fragments of large muscovite grains and whole, unbroken, smaller crystals were dated using high-resolution $^{40}Ar/^{39}Ar$ age spectrum and laser ablation in situ dating. The majority of analyses are on pegmatite samples with lesser focus on metamorphic host rocks. Sixteen Petaca District pegmatites from the Tusas Mountains give muscovite ages between ~1400 and 1350 Ma with most at 1375±10 Ma. Finer grained muscovites yield overall younger ages (1370 to 1350 Ma) demonstrating that physical grain size partially controls bulk argon closure temperature. In situ age data (75x75μm square ablation pits) are fully compatible with the age spectrum data and reveal that maximum ages from age spectra equal the oldest ages given by the in situ method. Additionally, younger apparent ages are found near original grain boundaries, again supporting a physical grain scale control on argon diffusion. The multiple diffusion domain (MDD) approach was evaluated and used to extract quantitative time-temperature paths from muscovite step-heating data from the Tusas Mountain samples. To a first order, the MDD method yields thermal histories compatible with other geological and geochronological data and suggests cooling at 10°C/Ma though 375°C at 1375 Ma. Cooling to ~300°C occurred by about 1325 Ma.

The Sandia and Manzano Mountain pegmatite muscovites are older than those from the Tusas Mountains and range from ~1.44-1.41 Ga. Several muscovite ages are equal to fairly imprecise U/Pb zircon ages suggesting that they record emplacement ages. Three Manzanita Mountain muscovites ages (CB-48, KBP-99-3 and KBP-99-8) are Paleoproterozoic and two (1660 and 1670 Ma) equal the zircon age of the Ojito pluton. These muscovites help to support a Mazatzal-aged deformation fabric in the Manzanita Mountains.

These and published data show that a major tectonothermal event began at about 1.46 Ga that widely impacted the Precambrian rocks of New Mexico. Metamorphism and structural depth are subequal in the Burro Mountains and the Tusas Mountains; however rapid cooling through 300°C occurred in the Burros whereas protracted cooling to this temperature occurred in the Tusas. Thus, along the 1.46 Ga orogenic belt both extensional exhumation and compressional burial were ongoing simultaneously. It is not entirely clear if central NM basement experienced a younger pulse of magmatism at about 1.44 Ga or if the Sandia and Priest plutons are nearer to 1.46 Ga.

The currently debated accretion history of the southern Laurentian margin cannot be fully addressed here, however these data record ages consistent with both the Picuris orogeny at 1.46 Ga and the Mazatzal orogeny at about 1.66 Ga. Based on the observed tectonic and magmatic lull between 1.6 and 1.48 Ga in the Southwest USA it is unlikely that a Mazatzal microcontinent was accreted to Laurentia during a long-lived subduction zone setting. More likely, the Picuris orogeny records intracratonic tectonothermal orogenesis related to collision of the 1.4 Ga Granite-Rhyolite province.

ACKNOWLEDGEMENTS

The funding for this study was provided by the New Mexico Bureau of Geology and Mineral Resources and the New Mexico Geological Society. I would also like to specifically thank the New Mexico Geochronology Research Lab and the New Mexico Tech department of Earth and Environmental Science for their help and support.

I would like to specifically thank Dr. Matt Heizler and Dr. William McIntosh for their insight and help on this project. Without their guidance this project wouldn't have been as successful as it was. I would also like to thank in addition to them, Lisa Peters, Jake Ross and Matt Zimmerer for their patience and perseverance in teaching me how to work in the Argon Lab. I would also like to thank Dr. Kent Condie for serving on my thesis committee and Karl Karlstrom, Mike Williams, Mike Spilde, Steve Dubyk, William Moats and Brian Salem for their help in the field and with analysis of my data.

This project would not have been possible without the support of my family and my friends. Special thanks goes to Annie Riggins and Emily Sotello for being a great support to me during the entire process. And lastly, but most importantly, I would like to thank the Lord for helping get through graduate school and providing for me. Without Him I wouldn't be where I am today.

TABLE OF CONTENTS

LIST OF FIGURES

LIST OF TABLES

This thesis is accepted on behalf of the
faculty of the institute by the following committee:

5/8/2014

Advisor

William C McCutcheon 5/5/2014

5/5/2014

Date

I release this document to the New Mexico Institute of Mining and Technology.

5/7/2014

Student's Signature Date

1.0 Introduction

Geochronology and thermochronology provide important spatial and temporal records of magmatism and thermal histories that contribute to the understanding of the Precambrian history of North America. A long held view for the evolution of North America is that juvenile arc terrains accreted onto the southern margin of Laurentia during the Yavapai orogeny at 1.8-1.7 Ga and the Mazatzal orogeny 1.7-1.66 Ga (Condie, 1982). Following these orogenic events, there appears to have been a tectonic gap until the onset of major magmatism beginning at ~1.46 Ga. Once thought to be anorogenic,(Anderson et al., 1986) it is more recently recognized that in association with the magmatism, the "1.4 Ga" event was associated with significant deformation and metamorphism (e.g. Kirby et al., 1995; Nyman et al., 1994; Amato et al., 2011). In central New Mexico, Kirby et al. (1995) showed that 1.4 Ga deformation occurred in 1.4 Ga pluton aureoles, and Marcoline et al. (1999) argued for 1.4 Ga amphibolite grade metamorphism. Thermochronology studies by Shaw et al. (2005) and Karlstrom et al. (1997) also promoted regional metamorphism and deformation at 1.4 Ga and recently Amato et al. (2011) invoked 1.46 Ga gneiss dome development emphasizing extensional tectonism at this time. In general, all of these studies suggested the "1.4 Ga" event was an intracratonic orogeny driven by accretion with plate margin well outboard of the current study area.

A new view of the 1.4 Ga event, known as the Picuris Orogeny, has recently been suggested by Jones et al. (2011) and Daniel et al. (2013). Their model challenges the very existence of the ~1.65 Ga Mazatzal orogeny by suggesting that accretion of a Mazatzal

terrain occurred at 1.46 Ga during the Picuris orogeny, rather than in the Paleoproterozoic. This hypothesis is mainly supported by the occurrence of 1.49-1.45 Ga detrital zircons in Picuris and Tusas Mountains metasedimentary rocks that were previously thought to have Paleoproterozoic protoliths (Daniel et al., 2013). Doe et al. (2013) have also used detrital zircon dating to demonstrate that several basins in Arizona are Mesoproterozoic rather than Paleoproterozoic. However, the presence of Mesoproterozoic zircons in New Mexico and Arizona does not conflict with a Paleoproterozoic Mazatzal Orogeny.

$^{40}Ar/^{39}Ar$ muscovite data collected from several Precambrian rock locations within New Mexico provide thermal histories between 1.65 and 1.35 Ga for the temperature range 400-300°C. Although no single study will confirm or refute the relative importance of the Mazatzal or Picuris orogenies, this new data, coupled with a large existing New Mexico $^{40}Ar/^{39}Ar$ dataset (Karlstrom et al., 1997; Shaw et al., 2005) emphasize the regional significance of 1.4 Ga heating, magmatism, metamorphism and deformation (Figure 1). However, some $^{40}Ar/^{39}Ar$ dates in central NM that exceed 1.65 Ga also record Mazatzal aged deformation thereby demonstrating some that tectonism predated the vast 1.4 Ga overprint.

Samples of mainly pegmatites and spatially associated metamorphic country rocks from the Tusas, Sandia, Manzanita and Manzano Mountain ranges are used to elucidate regional cooling history patterns, timing of pegmatite emplacement and to determine a minimum age of deformation. All pegmatites appear to be undeformed and were collected from within metamorphic country rocks. In the Tusas Mountains, 1.4 Ga metamorphic temperatures that likely exceeded 500°C (Shaw et al., 2005) prevent

$^{40}Ar/^{39}Ar$ dates of pegmatite muscovites from providing emplacement ages. Important information, however, about thermal history and relationship between grain size and argon closure temperature is obtained. Further south in New Mexico, ~1.44 Ga pegmatite muscovite from some areas in the Sandia and Manzano Mountains equals or approaches emplacement ages, based on correspondence between U/Pb zircon ages and argon ages (Karlstrom et al., 1997). In the Manzanita Mountains, muscovite age spectra get as old as 1.65 Ga and demonstrate deformation fabrics to be at least this old.

Quantitative details of the thermal history between about 375°C and 325°C appear to be obtained by multiple diffusion domain modeling of muscovite $^{40}Ar/^{39}Ar$ data, and potentially provide a new approach for thermal history analysis in this important temperature window. High precision UV laser ablation in situ $^{40}Ar/^{39}Ar$ analysis also contribute to an enhanced understanding of argon systematics and extraction of thermal histories from coarse muscovites. More details of the geologic history of New Mexico and muscovite systematics can be found in Appendix 4.

2.0 Methods

Samples of Precambrian muscovite were collected from four different locations in New Mexico: the Tusas, Sandia, Manzano and Manzanita Mountains. Muscovite bearing samples of pegmatite and in some instances the host country rock was collected. No pegmatites samples were collected from within plutons. Locations for the samples are shown in Figures 2 and 3. UTM coordinates are provided in Table 1. Muscovites were initially separated from crushed and sieved rock by handpicking or cut from large books with little to no effort to obtain original unbroken crystals. Muscovites were also handpicked from the crushed and sieved country rocks. In order to preserve grain size, whole, unbroken, muscovites were resampled by carefully plucking crystals from hand samples. Some of the larger (2cm or bigger) muscovites were subsampled using hole punches to produce 4mm diameter discs for analysis. Attempting to obtain original grains from the fine to very fine-grained muscovite schists required gentle crushing with a mortar and pestle followed by handpicking.

Samples were irradiated in two packages (NM-254 and NM-261) for 40 hours at the UGGS TRIGA reactor in Denver, CO, along with the standard Fish Canyon tuff sanidine as a neutron flux monitor. The flux monitor was assigned an age of 28.201 Ma (Kuiper et al., 2008) and ages where calculated using the total ^{40}K decay constant (5.463e-10 /a) of Min et al. (2000).

NMGRL's fully automated extraction line and the MAP 215-50 extended geometry mass spectrometer operated in static mode were used to extract and measure argon isotopes, respectively (McIntosh et al., 2003). Argon was extracted by the incremental step-heating method with samples enclosed in Cu packets that were dropped

into a double vacuum Mo resistance furnace.

In addition to the step-heating analyses, eight samples were analyzed by the in situ UV laser ablation method with isotopes measured on the ARGUS VI mass spectrometer. Ablation pits were approximately 75□m square and depth varied from about 10 to 30 □m. Initially, argon isotopes were collected in standard multicollection mode with mass 40 through 37 measured on Faraday detectors and mass 36 on an ion counter. However, precision on small ^{39}Ar beams was only about 5%, therefore a magnet peak hop was used to collect ^{39}Ar on the ion counter that improved precision to less than ±0.5% analytical uncertainty.

Details regarding the overall operation and data handling methods employed by the NMGRL can be downloaded from the website: https://geoinfo.nmt.edu/labs/argon/methods/home.html.

Thirty-three individual samples were collected from the Tusas area. Sample locations are given in Figure 2 and Table 1. Ten samples were collected from the Sandia Mountains (Figure 3, Table 1). Muscovite-rich pegmatite, quartzite, gneiss and granite samples were collected. Three pegmatite samples with muscovite were collected from the Manzano Mountains (Figure 3,Table 1). Three muscovite samples were collected from the Manzanita Mountains (Figure 3, Table 1).

Experimental protocols varied throughout the study. All runs on the MAP 215-50 mass spectrometer were age spectrum analyses with variable heating schedules and sample preparation procedures. For the initial experiment, 16 Tusas Mountain samples from irradiation NM-254 were dated. These mineral separates did not preserve original grain size. A second experiment, that attempted to use original unbroken crystals,

consisted of 42 muscovites from the Tusas, Sandia, Manzano and Manzanita Mountains. Lastly, 6 muscovites from NM-261 were step-heated at very high resolution following the methods outlined by Kula and Spell (2012). All step-heating schedules heated the sample to at least 1600°C, however steps above 1100°C commonly did not yield gas concentrations above blank level and thus some high temperature heating step analyses are not reported. All age spectra steps are plotted at 2-sigma uncertainty whereas individual analyses reported in the isotopic data tables are given at 1 sigma. All weighted mean plateau ages, terminal ages and integrated ages are reported at 1 sigma with J-uncertainty included. Additional age calculation information is provided in Appendix 2.

The in situ dating experiment consisted of six muscovites from irradiation NM-264 and two muscovites from irradiation NM-251. For the two NM-251 samples, a fixed $^{37}Ar/^{39}Ar$ value of 0.007 was applied because nearly all ^{37}Ar had decayed. 75 µm square ablation pits were cut by the 193 nm UV excimer laser during a 5-10 second interval of laser firing at a repetition rate of 50-100 Hertz. Ages were collected along traverses across individual mica grains and from points along the edges of the muscovite. Following extraction, gas was cleaned for 60 seconds in a D50 getter operated at 1.6 A and a NP-10 getter heated at 0.54 A.

3.0 Results

3.1 Overview

Sixty-three $^{40}Ar/^{39}Ar$ muscovite analyses from the Tusas, Sandia, Manzanita and Manzano Mountains were obtained to determine crystallization age of pegmatites and the ~400 to 300°C thermal history of Precambrian rocks. Additionally, high-resolution incremental heating analyses were used to evaluate the potential of using fractional loss of ^{39}Ar to calculate accurate argon closure temperatures. Age spectrum analyses were preformed on random crystal fragments, unbroken whole crystals and spatially controlled subsamples of large grains. In situ laser ablation dating was also performed on 4 individual whole crystals and 4 subsamples of a single large grain.

Some generalities are used to interpret the age spectrum results towards assignment of a preferred age and these include the following. Precambrian muscovites are highly enriched in radiogenic argon, and thus excess argon is not considered a likely cause for age spectrum complexity. Minor complexities that commonly manifest in anomalously old and variable apparent ages for high temperature heating steps are generally ignored. This behavior is likely related to degassing of mineral inclusions such as plagioclase or apatite or in some cases contamination by previously analyzed, but not fully degassed, samples. With such an extensive data set it is not feasible to describe each age spectrum individually, instead, samples are grouped below based on reoccurring spectra shape.

3.2 Age spectrum analyses

3.2.a Age spectrum categories

There are three different types of age spectra that reoccur throughout the dataset (Figure 4). Type I spectra are downward-stepping spectra where initially old apparent ages decrease to younger ages during the first ~10% of ^{39}Ar released. Twenty-three spectra show this pattern (Table 1). These spectra generally decline to a flat segment from which a plateau age is calculated (Figure 4a). The plateau age is the preferred age for Type I spectra. Type II spectra are referred to as crankshaft spectra and 15 of the 63 group into this category (Figure 4b). These spectra start with young ages, rise to older ages and then this pattern repeats. The preferred ages for these spectra are the short plateau age segments that correspond to the second (high temperature) segment of the crankshaft. Type III spectra are climbing age spectra and 25 analyses show this pattern (Figure 4c). These climbing spectra begin with young ages and then overall monotonically increase to either a plateau segment or continuously climb to what is referred to as a terminal age. All of the analytical data are given in Appendix 1 and each age spectrum is provided in Appendix 2. Table 1 summarizes sample preferred age, spectrum type, location, grain size as well as additional supporting information.

3.2.b Tusas Mountains

Sixteen pegmatite samples were collected from the Tusas Mountains Petaca District (Figure 3, Table 1). In some cases two samples from a single pegmatite were collected for replicate analyses. In addition, at six of the pegmatite locations a sample of

the Vadito schist country rock was collected. The goal of this was to compare the argon data from fine-grained schist muscovite to the argon data from coarse-grained pegmatite muscovites as a means to evaluate the argon system for possible correlations between apparent age and grain size. From the 22 Tusas Mountains samples 42 age spectra were determined (Appendix 2, Table 1). Nearly all age spectra from pegmatite muscovites are either Type I or Type III and yield plateau ages (Table 1). A few exceptions (e.g. P-01-04; Appendix 2-F) show more complexity and for these a terminal age is chosen as the preferred age. Muscovites from the schists have Type III spectra that rise to either a plateau segment or a terminal age (Table 1).

Preferred ages from the Tusas Mountains range from 1407 Ma to 1351 Ma and age spectra of the pegmatites that have country rock pairs are shown in Figure 5. In Figure 5, there are replicate spectra for samples step-heated using variable analytical protocols or where there are muscovites dated from more than one sample at the same location. In some cases, replicate runs yield analytically identical spectra and preferred ages (e.g. Figures 5B, D), but in other cases replicate spectra show minor differences in shape and preferred age (e.g. Figures 5A, C). Muscovites from the schist samples are typically 10-30 Ma younger than their pegmatite pairs. The schist muscovites have generally climbing spectra (Type III) and yield preferred ages between 1373 and 1348 Ma. A summary of this discordant age relationship between the pegmatite and country rock muscovite pairs is shown in Figure 6. Both the preferred and integrated ages are plotted, and with the exception of one sample, all the preferred ages of pegmatite muscovites are older than their country rock muscovite pairs (Figure 6). In general the age separation between integrated ages is greater than that of preferred ages because the

country rock muscovite spectra have somewhat climbing spectra that yield terminal ages approaching the pegmatite muscovite plateau ages.

3.2.c Sandia Mountains

Samples from the Sandia Mountains include eight pegmatite muscovites and one country rock muscovite (Figure 7; Table 1). Age spectra from these pegmatites range from nearly flat (Figure 7D) to spectra that have quite variable ages (Figure 7E). Preferred ages are substantially older than muscovites from the Tusas Mountains and vary between 1439 and 1408 Ma with most being greater than 1430 Ma (Figure 7, Table 1). The single country rock muscovite age spectrum is shown in Figure 7C with its corresponding pegmatite muscovite. Although the country rock muscovite has a younger integrated age than its pegmatite pair, both muscovites have preferred ages at ~1433 Ma.

3.2.d Manzano and Manzanita Mountains

The muscovite ages and spectra from the Manzano Mountains and the Los Pinos Pluton are overall similar to the Sandia Mountain results with preferred ages between 1444 and 1362 Ma (Figures 8A, B, C). In contrast, sample locations falling between the Sandia and Manzano Mountains yield much older muscovites where the country rock muscovite that defines foliation from the Manzanita Pluton has a preferred age of 1511 Ma, and two from the Ojito Pluton are very old with preferred ages of 1660 Ma and 1670 Ma (Figures 8D, E, F).

3.3 Spatial Sampling Analysis

3.3.a Coarse scale (4 mm) Spatial Sampling of Large Crystals

To further explore muscovite argon systematics with respect to spatially controlled age variation, two large grains were subsampled (Figure 9, Appendix 2). From the Joseph Mine pegmatite near Ojo Caliente, NM, sample 2-4C was subsampled by punching out four 4 mm discs from a single 3.5 cm crystal (Figure 9). The four discs yield preferred ages that range from 1404 Ma to 1394 Ma where 2-4C1, C2 and C4 are nearly identical Type I spectra and 2-4C3 is a Type III spectrum (Figures 9b-e). There is no significant age variation between the 4 discs. This coarse spatial sampling was also done on sample 5 from the Globe mine pegmatite and the age spectra from the 3 discs are given in Appendix 2. Samples 5-1, 5-2 and 5-3 have equal Type 1 age spectra with preferred ages of ~1380 Ma (Appendix 2, Table 1). Like above, these discs show no significant age variation.

3.3.b Fine Scale (75 □m) Spatial Sampling with UV Laser Ablation

Several muscovite crystals were explored for age variation using the in situ UV laser ablation method. Prior to UV laser analysis, single whole grains or the 4 mm punched discs described above were cleaved perpendicular to the c-axis to split the crystal approximately in half so that an age spectrum could be conducted on one half and in situ work could be conducted on the other. Based on an assumed density, sample weight and known crystal area, the cleaved fragments ranged in thickness from about 40 to 10 microns. For the in situ dating, between 2 and 8 traverses using 75 μm^2 ablation pits were cut from the 8 individual crystals (Figures 9, 10). The ablation pit transects are

shown on the crystal photographs along with an age versus distance plot of each transect. The transects and some more randomly clustered spots for each muscovite were designed to sample crystal cores and edges.

Two traverses with an "X" pattern were cut for each of the 4 mm punched discs. Age precision is variable (between ~2 to 50 Ma per spot analysis) and this variation is related to isotope measurement method and crystal thickness. High precision measurements were obtained by a combination of multicollection for argon mass 40, 38, 37, and 36 with an additional magnet-controlled peak hop to obtain a high precision measurement of ^{39}Ar on the ion counting multiplier. Lower precision data are given by multicollection analysis where ^{39}Ar is determined on a less precise Faraday collector. Thinner grains were completely penetrated by the laser beam and thus the overall volume of muscovite sampled was less for thin crystals as compared to thick crystals. Low gas yields from thin grains lead to lower precision age measurements. Combined, the in situ data from all 4 discs show no measureable age variation within a disc or between the discs and spot analyses overlap within error of the preferred ages given by the age spectrum analyses (Figure 9). The two traverses from each disc yield normally distributed ages with weighted mean values of 1404±1, 1409±3, 1414±8 and 1397±3 Ma, for discs 2-4C1, C2, C3 and C4, respectively. Recall that samples 2-4C1, 2-4C2 and 2-4C4 are Type I spectra, with the initial release of ^{39}Ar gas having ages of 1438 ± 5 Ma, 1470 ± 12 Ma, and 1557 ± 32 Ma before stepping down to the preferred plateau age (Fig. 9). These anomalously old ages were not observed within the in situ spot analyses (Figures 9B, C, E).

In addition to the spatial work on the 2-4C samples, four other samples were analyzed using the in situ dating method (Figure 10, Table 1). Samples 2-1 and Queen have Type III spectra where the initial steps are young and monotonically climb. Samples Cribbenville and Meadow have Type II crankshaft spectra. As above, all age spectra preferred ages are in close agreement to the majority of the spot ages obtained for each sample (Figure 10). However, unlike the discs, these preserved whole grains do record overall young ages near crystal edges and for each grain an age map is constructed by contouring the spatial age data (Figure 10). The main outcome of the in situ analyses is the observation that spots located away from original crystal boundaries are approximately equal to corresponding preferred ages and that original crystal boundaries preserve much younger apparent ages.

3.4 Muscovite multiple diffusion domain (MDD) results

Six Tusas Mountain pegmatite muscovite samples (Table 1) were step-heated with high temperature resolution and 20 minute heating duration following the suggestion of Kula and Spell (2012) who concluded that spatially meaningful age gradients and argon kinetic parameters could be extracted under these heating conditions. The intent here is to use unbroken crystals to evaluate Kula and Spell's assertion under a model that assumes diffusion of ^{39}Ar in the laboratory approximates that of $^{40}Ar^*$ diffusion in nature. This approach is exactly analogous to the MDD approach that is successfully used to extract diffusion coefficients and thermal histories from $^{40}Ar/^{39}Ar$ age spectrum analysis of K-feldspar (cf. Lovera et al., 1989).

Age spectra, Arrhenius, and $\log(r/r_o)$ diagrams for these six samples are given in Appendix 5. Two of the six samples have somewhat chaotic age spectra that do not

conform to an MDD model, thus only four of the samples are summarized in Figure 11. The Arrhenius plots for all samples are remarkably similar and can be directly compared because identical heating schedules were used to extract the argon (Figure 11b). Following an approximately horizontal pattern of the first few diffusion coefficients, a linear array with an approximate slope of 64 kcal/mol is defined. At about 30% ^{39}Ar released, a distinct kink is observed for all samples that again is followed by a linear segment with the slope subequal to the initial slope. This pattern conforms to a multiple diffusion length scale model, but the overall significance will be discussed below. Treatment of the Arrhenius diagram in an MDD context allows construction of the $\log(r/r_o)$ plot and in this case a common reference line with kinetic parameters of activation energy 64 kcal/mol and $\log(D/r_o^2)$ of 8.4 /sec yields the $\log(r/r_o)$ plots given in Figure 11c. The $\log(r/r_o)$ patterns are sigmoidal and where values decrease following an increase, the applied reference slope is lower than that of measured data. Again, details of this sigmoidal pattern are discussed below, and to a first order the $\log(r/r_o)$ plots can be approximated by two diffusion domains that differ in radius by about a factor of 5.

From the modeled kinetic data a thermal history can be extracted by forward modeling the age spectrum and these thermal histories are given in Figure 11d. Because age spectra are relatively flat and because the modeled kinetic parameters indicate relatively small differences between diffusion domain lengths, the returned thermal histories require overall rapid cooling (~10°C/Ma) from about 375°C to 300°C at an age that is approximately equal to the preferred age obtained from the measured age spectrum. The thermal histories significance is discussed with geological context below.

4. Discussion

4.1 Muscovite $^{40}Ar/^{39}Ar$ data systematics

4.1.a Age spectra and assignment of preferred age

Prior to discussion of the thermal histories it is necessary to briefly provide an interpretative framework for the muscovite age spectra, in situ analyses and the MDD thermal history modeling. If formed within a magmatic or high-temperature metamorphic event, all accurate muscovite $^{40}Ar/^{39}Ar$ ages will record the time of cooling below the closure temperature for argon diffusion. Typically, the plateau age of a muscovite age spectrum is used to determine the time of closure temperature through a nominal temperature of about 300-350°C (e.g. McDougall and Harrison, 1999). More recently, Harrison et al. (2009) determined a higher closure for muscovite of about 375°C. To a first-order, the plateau age of the Type I spectra likely corresponds to this closure temperature. Type I spectra also show initially old apparent ages that could record degassing of small amounts of excess argon. Alternatively, if these Type I muscovites truly have uniform $^{40}Ar^*$ concentration profiles it is possible that near surface ejection of ^{39}Ar via recoil during irradiation could be causing the initially old apparent ages. This is especially true for crystals that are relatively thin, less than about 50 microns. In either case, (excess argon or ^{39}Ar recoil ejection) the plateau age is considered geologically accurate and records the time of argon closure.

The crankshaft spectra (Type II) is not well understood and could result from a variety of mechanisms. Samples with fine scale potassium concentration variability (e.g. exsolution lamellae; basaltic groundmass, chloritized biotite) can yield complex age spectra that are attributed to ^{39}Ar recoil redistribution. However, muscovite is commonly

chemically homogeneous and devoid of internal complexity, thus it is unlikely that ^{39}Ar recoil is significantly contributing to the crankshaft shape. A more likely explanation for the shape of the spectra is that there is spatial complexity in the distribution of the radiogenic argon and that the age spectrum method is providing an imperfect view of this distribution. Hodges et al. (1994) noted that muscovite spectra can be overall flat, despite having highly variable internal age variations. Kula and Spell (2012) also noted the crankshaft shape in low-resolution step-heating analysis of slowly cooled muscovites and upon high resolution step-heating using long duration heating steps recovered spectra with overall climbing patterns. This observation supports that the crankshaft spectra are a combination of a variable radiogenic argon distribution and the instability of muscovite during the step-heating that makes recovery of the true spatial age distribution difficult. The preferred age for crankshaft style spectra comes from the high-temperature heating steps that define the oldest part of the crankshaft. In the absence of excess ^{40}Ar and ^{39}Ar recoil, the oldest apparent age would best approximate the time of cooling below about 375°C and also would record the age closest to the emplacement age of the pegmatites.

Type III spectra climb with initial steps starting at young ages that increase monotonically or somewhat chaotically across the spectrum. Overall this pattern is indicative of partial argon loss related to slow-cooling and/or an episodic heating event. For samples that rise to a plateau, the plateau is the preferred age for the time of argon closure, however some spectra continuously climb to a maximum that is defined by as few as one step (e.g. Figure 4c). This maximum age is referred to as a terminal age and is the preferred age for the sample because if the pegmatite muscovite underwent argon loss then the oldest apparent age is the most accurate age relative to the emplacement age.

4.1.b Grain-size control on muscovite argon closure temperature

Muscovite argon diffusion kinetics, geometry and radius have been debated since the initial diffusion studies presented in the unpublished master's thesis of Robbins (1972). McDougall and Harrison (1999) suggested that muscovite diffusion length is defined by an effective diffusion radius of about 150 microns, however there is now growing consensus that physical grain size does, at least in part, control the diffusion radius (Hodges et al., 1994; Hames and Bowring, 1994; Heizler et al., 1997; Harrison et al., 2009, 2012; Kula and Spell, 2012). Several observations of this dataset also support that physical grain size has a role in defining closure temperature. Figures 5 and 6 show an overall trend of the pegmatite muscovites being older than their country rock muscovites pairs. The younger muscovites from the country rocks are finer grained than the pegmatite muscovites (Table 1) and because the pegmatites intrude into the country rocks but yield older apparent muscovite ages it is highly suggestive that the coarse pegmatite muscovites have a higher argon closure temperature. Also, there is some variability between replicate muscovite analyses from individual pegmatites (Figures 5A-D). In most cases, the analyzed sample is a fragment of a larger muscovite crystal from an unknown position and thus it is possible that younger apparent ages come from nearer the rim of the large muscovite and that older replicate analyses are fragments obtained from nearer the core of the large crystals.

Spatial distribution sampling was conducted on the Joseph Mine pegmatite muscovite near Ojo Caliente (2-4C) by punching 4 mm fragments from a large grain. These grains were cleaved in ~half for both an age spectrum on a bulk sample and for in situ laser ablation on the other half (Figure 9). As presented above, the in situ age

traverses have results that closely match the plateau ages obtained from the age spectra and the entire 152 hole data set has a normally distributed age distribution (MSWD = 1.97) with a weighted mean of 1404±1 Ma. The uniform distribution of ages cannot be used to determine if grain size is controlling the argon transport distance because without a variation in age one cannot determine a boundary that would control argon transport. However, the very uniform distribution requires the sample to cool quickly and it is possible that the 1404 Ma apparent age is actually recording an emplacement age. An interesting note is that 3 of the 4 age spectra from the punched samples have old ages for initial gas released and these old ages are not observed in the in situ data. Perhaps the age spectrum method can thermally separate tiny fractions of excess ^{40}Ar that is not resolved in the spot dating or the age spectrum can record the effects of surface ejection of ^{39}Ar whereas this effect was lost in the uncertainty of the in situ analyses.

In situ analyses were also conducted on 4 other whole grains to determine the spatial argon distribution and like above a cleavage slice was also dated by the age spectrum method (Figure 10). Most spot analysis ages overlap with the plateau ages, however spots near the edges of the grains are ubiquitously younger and suggest that the crystal edge is acting as a diffusion boundary (Figure 10). Age spectrum analyses record young apparent ages during the initial gas release that are sub-equal to the youngest in situ points and perhaps demonstrates that the age spectrum is recovering the spatial distribution for $^{40}Ar^*$ where crystal rim gas is being evolved during low temperature heating and crystal core gas is being released at higher temperatures. Combined, these data indicate that the physical crystal size is defining the argon diffusion dimension for coarse pegmatite muscovites.

4.1.c Evaluation of the MDD method and muscovite age spectra

Coupled with the recently published high activation energy for muscovite diffusion of 64 kcal/mol (as compared to Robbins' (1972) estimate of ~40 kcal/mol) it is apparent that argon closure temperature can exceed ~400°C for coarse muscovites (cf. Harrison et al., 2009). This overall high closure temperature provides the potential that coarse-grained muscovites from mid-crustal levels could yield $^{40}Ar/^{39}Ar$ ages that closely approximate emplacement ages of igneous rocks and perhaps record a time corresponding to near peak metamorphic conditions. This potential formed the foundation for undertaking this muscovite thermochronology study and below the MDD approach is evaluated towards the goal of recovering a segment of thermal history from the age spectra with coupled diffusion data derived from the release of ^{39}Ar (Figure 11).

Many of the Tusas Mt. muscovite pegmatite age spectra are overall flat and thus do not immediately indicate a protracted thermal history. It is possible there was protracted cooling from peak metamorphic conditions to about 400°C that was then followed by a pulse of cooling though the muscovite closure interval or alternatively the age spectrum analysis is homogenizing natural age gradients due to muscovite instability related to high temperature vacuum extraction of the argon. This follows the ideas of for instance Hodges et al. (1994) and Sletten and Onstott (1998) who invoke catastrophic degassing related to delamination and/or dehydroxilation to explain overall flat age spectra when compared to in situ analyses that record large age variations within the crystals. A seeming resolution of the relationship between highly variable in situ data and flat or complex age spectrum measurements was provided by Kula and Spell (2012). They suggested that if step heating was conducted in a double furnace (as opposed to

direct heating with a laser) using long (~20 minute) heating steps that were closely incremented in temperature, climbing spectra consistent with slow cooling could be recovered.

The MDD analysis of the muscovites is presented in Appendix 5, and a summary of 4 samples are given in Figure 11. Because identical heating schedules were used, the Arrhenius data (Figure 11b) can be directly compared between samples and overall they are very similar. Very low gas yield initial steps define a low slope, but quickly transition to a slope that is approximately the 64 kcal/mol value reported by Harrison et al. (2009). At about 30% gas release there is a well-defined and reproducible kink in the Arrhenius data followed by a return to climbing diffusion coefficients with similar slope to the first linear array prior to the kink (Figure 11b). The $\log(r/r_o)$ patterns shown in Figure 11c are sigmoidal and values decrease following an increase, the slope of the measured data is higher than the measured value. To a first order the $\log(r/r_o)$ plots can be approximated by two diffusion domains that differ in radius by about a factor of 5. Within the MDD framework, this kink would indicate the presence of multiple diffusion domains, however an alternative explanation for the kink in the Arrhenius plot is that during the temperature window where the diffusion coefficients depart from linearity the muscovite is transitioning to a dehydroxilated state that has more retentive diffusion characteristics (cf. Sletten and Onstott, 1998). It is beyond the scope of this work to fully evaluate the relative importance of muscovite stability versus a MDD model, but based on the work of Harrison et al. (2009) and Kula and Spell (2012) it seems worthy to derive thermal histories in order to see if they approximate reasonable temperature paths for northern NM basement rocks.

The thermal histories are similar for each sample because the age spectra vary between about 1375 and 1360 Ma and because the apparent diffusion kinetics are overall similar (Figure 11d). Each sample is required to stay above ~400°C until about 1375 Ma followed by relatively rapid cooling (~10°C/Ma) down to about 250°C by 1360-1350 Ma. Relatively minor variation between thermal histories could be caused by a variety of factors that principally would include geological variations of cooling histories and/or inaccuracy of kinetic parameters (i.e. assuming equal activation for each muscovite). Although not perfect in explanation of all kinetic parameters, the MDD approach provides cooling histories that would be predicted by simply using the kinetics of Harrison et al. (2009) and calculating closure temperatures using the formulation of Dodson (1973). This is encouraging as the experiments of Harrison et al. (2009) were based on diffusion of $^{40}Ar^*$ under isothermal-hydrothermal conditions and these MDD derived thermal histories are based on transport of ^{39}Ar within an ultrahigh vacuum (dry) device at variable temperatures. As will be discussed below, the Tusas Mountains experienced metamorphic temperatures above 500°C between 1.46 and 1.40 Ga, therefore the MDD derived thermal histories that require temperatures above 400°C until about 1375 Ma are consistent with this. Also, Sanders et al. (2006) argue that basement temperatures were between about 275 and 175°C from about 1.2 Ga to 0.8 Ga which again is compatible with the muscovite MDD-derived thermal histories. Therefore, to a first order it is believed that the MDD approach yields accurate thermal histories for these muscovites and thus potentially provides a powerful method to extract detailed and quantitative thermal history information in the temperature range between 400 and 300°C.

In summary, muscovite age spectra from several Precambrian locations in northern and central New Mexico yield a variety of shapes that yield preferred ages corresponding to cooling below ~375°C. Age spectra and spatial sampling of age distributions using in situ methods show that physical grain size is a controlling factor for muscovite argon closure temperature. Detailed step-heating following the methods of Kula and Spell (2012) apparently provides age spectra and ^{39}Ar-derived Arrhenius parameters that can be inverted to yield sensible thermal histories in the temperature range between about 400 and 300°C.

4.2 Thermal history of New Mexico Precambrian rocks

It has been nearly two decades since Karlstrom et al. (1997) presented a comprehensive evaluation of the ^{40}Ar/^{39}Ar derived thermal histories of New Mexico Precambrian exposures. This effort was followed by Shaw et al. (2005) who compiled a large thermochronological dataset of ^{40}Ar/^{39}Ar and K/Ar ages that span from northern New Mexico to southern Wyoming and based on this compilation suggested that the southwest USA underwent a regional thermal episode from 1.45-1.35 Ga. Specifically to New Mexico, this database expanded the work of Karlstrom et al. (1997) and combined, these studies show variable maximum Mesoproterozoic temperatures of currently exposed 1.4 Ga rocks and variable post 1.4 Ga cooling histories with rocks cooling overall earlier in the south-central part of the state as compared to the northern regions (Figure 1). Amato et al. (2011) reported several ^{40}Ar/^{39}Ar mineral ages from the Burro Mountains in southwest New Mexico that were grouped at 1.46 and 1.22 Ga. These cooling ages closely match granitoid emplacement ages based on correspondence with U/Pb zircon data and indicated relatively rapid cooling during 1.46 Ga pluton

emplacement and shallow level pluton emplacement at 1.22 Ga. Below, new $^{40}Ar/^{39}Ar$ muscovite data are discussed for northern and central New Mexico mountain ranges followed by a synthesis of some published $^{40}Ar/^{39}Ar$ data from across New Mexico.

4.2.a Tusas Mountains

Metamorphic temperatures at 1.4 Ga in the Tusas Mountain exceed 500°C despite a notable lack of 1.4 Ga intrusions. Shaw et al. (2005) attributed the high metamorphic temperatures to a midcrustal magma layer that has subsequently been eroded, thereby allowing sampling of high grade metamorphic rocks without encountering associated 1.4 Ga granitoids. Shaw et al. (2005) speculated that the Petaca District pegmatites formed late in 1.4 Ga pluton emplacement and represent the vestiges of a large plutonic episode, however very minimal district wide geochronology has been conducted to confirm this. In this study, coarse-grained pegmatite muscovites were dated with the $^{40}Ar/^{39}Ar$ method in an attempt to determine emplacement age and to confirm that indeed the Petaca District pegmatites are part of a 1.4 Ga magmatic event that is at least partly responsible for driving 1.4 Ga metamorphism.

Petaca pegmatite muscovite ages range from 1407-1351 Ma (Figure 5; Table 1), however proximally located finer grained muscovites from country rocks typically yield younger ages. This broad range of pegmatite apparent ages, coupled with discordance of host rock muscovites ages, strongly implies that all muscovites are recording cooling ages rather than pegmatite emplacement ages. To test this, two monazite samples from the Globe and Meadow pegmatites were dated using the electron microprobe (U+Th)/Pb chemical method by Mike Williams at the University of Massachusetts. This data will

not be fully evaluated here, however the in situ spot data are summarized in Table 2 and show ages ranging between 1460 and 1420 Ma. These ages are significantly older than the muscovite ages and conclusively demonstrate that the pegmatite was not rapidly cooled to below ~375°C following emplacement.

Lanzirotti and Hanson (1997) and more recently, Andronicos et al. (2012) and Aronoff et al. (in review) have dated metamorphic minerals in the Tusas Mountains. Staurolite and garnet U/Pb ages from the Hondo Group are 1454±7 and 1461±13 Ma, respectively (Lanzirotti and Hanson, 1997) and Lu/Hf garnet isochron ages fall between 1450±6 and 1399±9 Ma (Aronoff et al., in review). The variation in Lu/Hf garnet dates is suspected to reflect partial dissolution following initial garnet growth at 1460 Ma, but combined all data demonstrate high-grade metamorphism in the Mesoproterozoic. The Petaca monazite ages (1430±7 Ma) are marginally younger than the interpreted 1460 Ma garnet ages and may signify that pegmatite emplacement post dates metamorphic mineral growth, but considering that a full accounting of systematic errors between dating methods has not been undertaken it is equally likely that pegmatite emplacement is approximately coincident with peak metamorphism

Cooling of the southern Tusas Mountains following peak metamorphism is constrained by the $^{40}Ar/^{39}Ar$ data. Shaw et al. (2005) reported $^{40}Ar/^{39}Ar$ hornblende dates as old as 1395±7 Ma indicating cooling below ~500°C at this time. Muscovite preferred ages and MDD modeling of muscovite age spectrum data suggest cooling below 375°C at 1375±10 Ma. Overall rapid cooling of 10°C/Ma could reflect exhumation driven cooling and/or recovery from transiently high geothermal gradients related to pluton enhanced heat advection to more normal conduction controlled geotherms. Protracted cooling and

perhaps long term crustal residence near 300°C following initial rapid cooling is suggested by the wide distribution of finer-grained muscovite ages reported here as well as highly variable biotite $^{40}Ar/^{39}Ar$ dates summarized by Shaw et al. (2005).

4.2.b Sandia Mountains

Coarse-grained muscovites from the Sandia Mountains yield preferred ages between 1.44 ± 1.5 and 1.41± 1.7 Ga and are significantly older than those from the Tusas Mountains (Figure 7). Age spectra are generally climbing and suggest partial argon loss that is variable from sample to sample that likely relates to minor variation in muscovite closure temperature. The pegmatites occur throughout the Sandia pluton and according to Kirby et al. (1995) are likely temporally related to the Sandia pluton. The Sandia pluton is not well dated, however the U/Pb zircon emplacement age reported by Karlstrom et al., 2004 is 1437 ± 47 Ma and is concordant with at least some of the muscovite preferred ages. The age agreement between the U/Pb zircon and $^{40}Ar/^{39}Ar$ muscovite indicates that in some cases the $^{40}Ar/^{39}Ar$ method can directly date pegmatite intrusion and supports that the Sandia granite and the pegmatites are coeval.

A possible different interpretation could be invoked based on unpublished in situ U/Pb laser ablation dating of zircons from the Sandia pluton (Karlstrom, unpublished data). These recently obtained ages clustering at 1454±8 Ma (Karlstrom Pers. Com.) might demonstrate that the zircons (and thus the Sandia granite) are marginally older than the oldest preferred muscovite ages, however as above, systematic errors between dating methods require full consideration before discordance can be verified.

No matter the exact details, the discordance between emplacement age and muscovite cooling age in the Sandia Mountains is much less then observed in the Tusas Mountains. Like the interpretation of Karlstrom et al. (1997), these new data indicate that the centrally located Sandia Mountains cooled through 375°C about 30 to 50 Ma earlier than the northern New Mexico Tusas Mountains.

4.2.c Manzano Mountains

The new muscovite thermochronology data from the Manzano Mountains is similar to that reported by Heizler et al. (1997) and Marcoline et al. (1999), although the interpretation presented here is somewhat different. Muscovite samples provide Type II and III age spectra and yield preferred ages of 1394 and 1444 Ma (Figures 8A, B) showing that individual grains likely have variable argon closure temperatures. Notably the 1444 Ma preferred age is concordant with the 1427±10 Ma U/Pb zircon age (Karlstrom et al., 2004) of the Priest pluton and appears to show that muscovites can record igneous intrusion ages. A sample of the deformed 1.65 Ga Los Pinos granite (LP-156) has a terminal age of about 1380 Ma and a well-developed age gradient suggestive of significant argon loss and thus records a cooling age (Figure 8C).

Heizler et al. (1997) found flat age spectra for muscovites from undeformed pegmatites with plateau ages at about 1400 Ma that they interpreted as cooling through ~350°C nearly 30 Ma after emplacement of the Priest pluton. However, recalculation of the Heizler et al. (1997) results to the age of Fish Canyon tuff sanidine used here (28.201 Ma) and the decay constants of Min et al. (2000) changes the 1400 Ma age to 1419 Ma and all but closes the age gap between the argon muscovite age and the Priest pluton

zircon age. Thus some of the new samples, as well as the pegmatite samples of Heizler et al. (1997) seem to closely record pegmatite emplacement age. Heizler et al. (1997) and Marcoline et al. (1999) both found substantial age gradients in deformed muscovites located in the Manzano Mountains and it is possible that some of the disturbed age spectra shown here are also the result of minor deformation that likely reduces the effective diffusion radius compared to large undeformed pegmatite crystals. In total the Manzano Mountains data are very similar to the Sandia Mountains data indicating that these two locations share similar plutonic histories and pegmatite emplacement histories.

4.2.d Manzanita Mountains

Three muscovite samples from Paleoproterozoic rocks in the Manzanita Mountains record the oldest apparent $^{40}Ar/^{39}Ar$ ages of muscovite in the state of New Mexico (Figures 8D, E, F). Sample KBP-99-3 is from a muscovite-bearing phase of the 1659±5 Ma Ojito granite (Karlstrom et al., 2004) and yields an analytically identical preferred age of 1670±6 Ma. A coarse muscovite (KBP-99-8) collected within the metamorphic contact aureole of the Ojito granite has a flat age spectrum and a preferred age of 1660±10 Ma. The CB-48 muscovite is the third sample from this group of rocks and is located in the northern Manzanita Mountains taken from the 1645 ± 10 Ma Manzanita granite (Karlstrom et al., 2004). The muscovite spectrum is characterized by a strong age gradient with a terminal age near 1510 ± 3.5 Ma. Because of the preserved Paleoproterozoic ages, the Manzanita Mountains area could not have been significantly heated above about 375°C during 1.4 Ga magmatism and metamorphism. As Shaw et al. (2005) showed, this block of rocks can best describe the Paleoproterozoic history of New Mexico and based on cross-cutting relationships between the muscovite bearing samples

and deformation fabrics (Thompson et al., 1996) outside the Ojito and Manzanita granites, the dates constrain the deformation fabrics to be of Mazatzal age.

4.3 Synthesis of New Mexico 40Ar/39Ar data from Precambrian rocks.

The geology of New Mexico Precambrian rocks plays a significant role in defining the 1.7 to 1.4 Ga history of Laurentia. Geochronology and thermochronology data provide important constraints on the overall tectonic history and specifically provide the temporal and spatial record of magmatism, an estimate for the timing of peak metamorphism and deformation and the subsequent exhumation history. The $^{40}Ar/^{39}Ar$ thermochronology and U/Pb zircon geochronology presented and summarized by Karlstrom et al. (1997; 2004) and Shaw et al. (2005) provide foundational data that recognizes two main pulses of magmatism at 1.7-1.6 Ga (Mazatzal orogeny) and 1.45-1.35 Ga and major 1.4 Ga heating of the presently exposed mid-crustal rocks. This heating is variable and regional in scale and only partially spatially controlled by 1.4 Ga granitoid intrusions. More focused and recent studies (i.e. Amato et al., 2011) are refining and shaping our understanding of magmatism and metamorphism at 1.4 Ga, and these studies continue to emphasize that the "1.4 Ga event" is a major tectonothermal orogeny. The so-called Picuris orogeny recently defined by Daniel et al. (2013) is a provocative and new model for the tectonic evolution of New Mexico and surrounding basement rocks challenges longstanding views for the tectonic evolution of southern Laurentia. The Picuris orogeny removes the ~1.65 Ga accretion of the Mazatzal juvenile arc in favor of accreting a Mazatzal microcontinent beginning at 1.46 Ga. New data presented here and a reassessment of the statewide thermochronology helps define the magmatic,

metamorphic, deformation and exhumation history and bears on current tectonic models for the evolution of New Mexico.

Selected published geo and thermochronology data from New Mexico along with new muscovite data collected here are summarized in Figure 12. Four panels of the $^{40}Ar/^{39}Ar$ data are presented as histograms and probability diagrams for the Burro, Manzano, Sandia and Tusas Mountains along with other relevant geochronology for these areas. As Karlstrom et al. (1997) noted, this summary shows older (1.44-1.40 Ga) ages in central New Mexico in comparison to younger (<1.40 Ga) ages in the northerly Tusas Mountains. The southerly Burro Mountains data of Amato et al. (2011) appear to continue this trend, as $^{40}Ar/^{39}Ar$ mica dates are as old as 1.47 Ga, nearly 100 Ma older than those from the Tusas Mountains. Karlstrom et al. (1997) recognized that age variation corresponded to variation in regional metamorphic grade differences across the state and suggested that the high-grade rocks in the Tusas Mountains cooled more slowly than those of the lower grade rocks in central New Mexico. Slower cooling in the Tusas block is not necessarily required because if micas from a deeper level of exposure could be sampled in the Manzano/Sandia block, micas could be equally as young as those in the Tusas. That is, if the timing of metamorphism is equal across northern and central New Mexico and uniform cooling is driven by exhumation, the structurally deeper samples will close to argon loss after the structurally shallower samples without a change in cooling rate. The structural offset that exposes the metamorphic grade rocks appears to have been established in the Precambrian, because similar aged Paleozoic strata unconformably overlie the Precambrian surface across the central and northern areas. Sanders et al. (2006) demonstrated substantial differential exhumation related to

Grenville aged tectonism in New Mexico and it is likely that different basement structural levels are the result of Grenville faulting.

Clearly there can be differences in $^{40}Ar/^{39}Ar$ mineral ages if the rocks themselves vary in age across the state. In order to evaluate this, the zircon ages for selected plutonic rocks are shown on the argon data summary plots along with metamorphic mineral ages from the Tusas Mountains (Figure 12). Unfortunately some of the U/Pb zircon ages have high uncertainties and therefore do not allow a high precision comparison of the magmatic history. In the Burro Mountains, Amato et al. (2011) show 1.46 Ga concordant U/Pb zircon and $^{40}Ar/^{39}Ar$ mica data that are equal to ~1.46 Ga U/Pb staurolite (Lanzarotti and Hanson, 1997) and Lu/Hf garnet dates (Aronoff et al., *in review*) in the Tusas Mountains. Also in the Burro Mountains, Amato et al. (2011) obtain a metamorphic zircon age of 1458±9 Ma that they claim equals the timing of amphibolite grade (4-6.5 kbar; 575-650°C) metamorphism. Combined, these data indicate similar metamorphic age and structural level for rocks in the Burro and Tusas Mountains, even though the Burro Mountain $^{40}Ar/^{39}Ar$ mica ages are nearly 100 Ma older (Figure 12). This implies a very different post 1.46 Ga thermal history in the two regions. The tectonic significance of this will be further discussed below.

There is no direct age for metamorphism in the Sandia and Manzano Mountains and the U/Pb zircon ages for the Sandia granite and the Priest pluton are too imprecise (Figure 12) to draw rigorous regional conclusions, however some bracketing models can be discussed. If the Sandia and Priest plutons are approximately 1.46 Ga, then the 1.44-1.42 Ga mica $^{40}Ar/^{39}Ar$ ages are discordant and younger by about 40-20 Ma. This would fit with an overall trend of equal metamorphic and plutonic histories and diachronous

cooling from north to south. It is equally likely that the older (~1.44 Ga) preferred ages of the muscovites from the Sandia and Manzano Mountain pegmatites closely equal emplacement ages. This would yield post-magmatic cooling rates similar to those in the Burro Mountains, however the timing would be younger because the granites are younger.

4.4 Tectonic models: Picuris Orogeny, Mazatzal Orogeny or Both

Lengthy discussion of large-scale tectonic models for New Mexico is well beyond the scope of this masters thesis, however some brief remarks are warranted. As mentioned, the Daniel et al. (2013) research in the Picuris Mountains has led to a new model for the timing of accretion of the Mazatzal aged crust. Their model, the Picuris orogeny, envisions 1.46 Ga collision of a Mazatzal microcontinent onto southeastern Laurentia, thereby eliminating the need to accrete the Mazatzal juvenile arc at ~1.65 Ga. Fundamentally, the model arises from discovering 1.49 to 1.45 Ga detrital zircons in metasedimentary rocks that have been presumed to be Paleoproterozoic (i.e. Mazatzal age). These ~1.47 Ga rocks have experienced Al_2SiO_5 triple-point metamorphism with likely burial to ~15 km. Also, in the Picuris and Tusas Mountains, Aronoff et al. (*in press)* interpret Lu/Hf isochron garnet ages of 1.46 to 1.40 Ga to reflect the rapid burial and metamorphism of sedimentary rocks during the onset of the Picuris orogeny. As discussed throughout this thesis there is little doubt that New Mexico experienced 1.46 Ga tectonism, metamorphism and plutonism and thus the Picuris orogeny is attractive from a geological perspective as well as a practical perspective as it rids the use of the term "1.4 Ga event".

If correct, the Picuris orogen is complex in tectonic style, but not unlike most major orogens. Daniel et al. (2013) and Aronoff et al. (*in press*) require a major compressional orogen that facilitates rapid burial and metamorphism under regional-scale thrusts knapps. In southern New Mexico, Amato et al. (2011) calls on an extensional orogen at 1.46 Ga to explain syntectonic metamorphism, plutonism and rapid exhumation. These contrasting tectonic styles along a single orogenic front are not in conflict, but rather attest to what is now becoming abundantly clear: that the Picuris orogeny is not a local phenomenon.

Mazatzal age rocks occur throughout New Mexico (Karlstrom et al., 2004; Amato et al., 2011) and $^{40}Ar/^{39}Ar$ muscovite ages (Figure 8) in the Manzanita Mountains bear on the timing of Paleoproterozoic deformation. Within the context of the Picuris orogeny, deformation of the 1.65 Ga Ojito pluton could be related to 1.46 Ga tectonism rather than syntectonic pluton emplacement during Mazatzal tectonism. However muscovite terminal ages of 1.66 and 1.67 Ga in the Ojito pluton and contact metamorphic assemblage argue that cleavage development occurred during Mazatzal time. This is mainly so because metamorphic garnet overgrows the fabric and thus not all deformation can be linked to the Picuris orogeny.

The discovery that once thought Paleoproterozoic metasedimentary successions are indeed Mesoproterozoic (Daniel et al., 2013; Jones et al., 2011, Doe et al., 2013) opens up a whole new tectonic model to consider for the evolution of the southern Laurentian margin. Current models are largely based on the geochronology and thermochronology and continued dating efforts should clarify debates on large-scale tectonothermal models for orogen development. Of particular importance, and perhaps

underappreciated, in this debate, is the large magmatic and tectonic gap between about 1.6 and 1.48 Ga. This gap is clearly defined in the zircon geochronology compilation of Karlstrom et al. (2004) and has long been recognized (e.g. Karlstrom and Bowring, 1988). The model of Daniel et al. (2013) does not seem to account for this gap in that they envision rafting in a Mazatzal microcontinent via long-lived convergent subduction zone geometry with north-westward subduction polarity under Laurentia. It appears hugely problematic for the model in that one would expect subduction related magmatism to be nearly continuous between about 1.65 and 1.45 Ga prior to collision, however there is absolutely zero record of magmatism of this age in southwest Laurentia. Thus, the magmatic gap may support a tectonic model where the 1.4 Ga granite-rhyolite province of central North America accreted via oblique (nonsubduction related) convergence onto a Laurentian continent that had indeed undergone Mazatzal age continental growth and orogenesis. At any rate, now is an exciting time of discovery in our understanding the Precambrian evolutionary history of New Mexico and geochronology and thermochronology are sure to play a pivotal role in this discovery.

5.0 Conclusions

$^{40}Ar/^{39}Ar$ muscovite dates from 27 pegmatites and 7 country rock samples yield 63 age spectra from the Tusas, Sandia and Manzano Mountains with ages between about 1450 and 1330 Ma. Three samples from the Manzanita Mountains yield Paleoproterozoic ages between 1670 and 1511 Ma. New and published Mesoproterozoic ages demonstrate statewide 1.46 Ga orogenesis and possibly a discrete younger magmatic event at about 1.44 Ga.

Both the Burro and Tusas Mountains experienced high-grade metamorphism at 1.46 Ga. However, the Burro Mountains cooled quickly through 300°C via exhumation driven by extension, whereas the Tusas Mountains were initially deeply buried by thrusting with later exhumed through 375°C by about 1375 Ma. The Sandia and Manzano Mountains experienced magmatism between about 1.46 and/or 1.44 Ga, and overall cooled quickly to 375°C by 1.43 Ga. Here, pegmatite muscovite $^{40}Ar/^{39}Ar$ ages closely approximate emplacement ages.

Attempts to directly date emplacement of Petaca district pegmatites using $^{40}Ar/^{39}Ar$ muscovite thermochronology were not successful because ambient conditions were in excess of 400°C during their emplacement. Preliminary electron microprobe monazite U+Th/Pb ages from the Globe and Meadow pegmatite yield ages at ~1430 Ma, confirming that muscovite ages are 10's of Ma younger than emplacement ages.

In situ dating and age correlation to muscovite grain size for Tusas Mountain pegmatites and metamorphic country rocks demonstrate that physical grain size

influences bulk argon closure temperature. Also, to first order, the MDD approach for recovering thermal histories from muscovite step-heating data appears successful.

An abundance of $^{40}Ar/^{39}Ar$, metamorphic mineral and magmatic zircon ages of ~1.46 Ga demonstrate a major Mesoproterozoic tectonothermal event throughout New Mexico that could fit into the definition of the newly coined Picuris orogeny (cf. Daniel et al., 2013). Paleoproterozoic muscovite ages in the Manzanita Mountains recordMazatzal age deformation, but not necessarily accretion of junvenile arcs to Laurentia between 1.7 to 1.65 Ga. between. The magmatic and tectonic lull between 1.6 and 1.48 Ga needs to be considered when defining the tectonic model for the Picuris orogeny that calls for a Mazatzal microcontinent to collide with southeast Laurentia at ~1.46 Ga. A long-lived subduciton zone with polarity under either southeast Laurentia or the Mazatzal microcontinent would likely generate calc-alkaline magmatism, although none was recorded during the magmatic lull.

6.0 References

Andronicos, C. L., Aronoff, R.F., Hunter, R. A. and Vervoort, J., 2013. A revised tectonic history for Proterozoic rocks of the southern rocky mountains in northern New Mexico (abstract). In: Rocky Mountain Section Geological Society of America Conference. May 15-17 2013. Geological Society of America Abstracts with Programs. Vol. 45, No. 5, p.37

Amato, J.M., Heizler, M.T., Boulion, A.O., Sanders, A.E., Toro, J., McLemore, V.T. and Andronicos, C.L., 2012. Syntectonic 1.46 Ga magmatism and rapid cooling of a gneiss dome in the southern Mazatzal Province: Burro Mountains, New Mexico. Geological Society of America Bulletin, v. 123, no. 9-10, p1720-1744.

Anderson, J.L., 1989, Proterozoic anorogenic granites of the southwestern United States, in Jenny, J.P., and Reynolds, S.J., eds., Geologic Evolution of Arizona: Arizona Geological Society Digest, v. 17, p. 211–238

Aronoff, R.F., Andronicos, C.L., Vervoort, J.D., and Hunter, R.A., *in press*. Redefining the Metamorphic History of the Oldest Rocks in the Southern Rocky Mountains.

Bauer, P.W., Karlstrom, K.E., Bowring, S.A., Smith, A.G. and Goodwin, L.B., 1993. Proterozoic plutonism and regional deformation: new constraints from the southern Manzano Mountains, central New Mexico: New Mexico Geology, v. 15, p. 49-53.

Brown, C.L., Karlstrom, K.E., Heizler, M.T, and Unruh, D., 1999. Paleoproterozoic deformation, metamorphism and Ar/Ar thermal history of the 1.65 Ga Manzanita pluton, Manzanita Mountains, New Mexico: New Mexico Geological Society, 50th Field Conference, Guidebook, p. 255-268

Danie13, C. G., Pfeifer, L.S., Jones III, J.V., and McFarlane, C.M., 2013. Detrital zircon evidence for non-Laurentian provenance, Mesoproterozoic (ca. 1490–1450 Ma) deposition and orogenesis in a reconstructed orogenic belt, northern New Mexico, USA: Defining the Picuris orogeny. Geological Society of America Bulletin, v. 125, no. 9-10, p. 1423-1441

Doe, M.F. et al., In Review. Using detrital zircon ages and Hf isotopes to identify 1.48 1 - 1.45 Ga sedimentary basins and fingerprint sources of exotic 1.6-1.5 Ga grains in southwestern Laurentia Precambrian Research.

Condie, K.C., 1982. Plate-tectonics model for the Proterozoic continental accretion in the southwestern United States: Geology, v. 10, p. 37-42.

Cosca M., Stunitz, H., Bourgeix, A.L., and Lee, J.P., 2011. 40Ar* loss in experimentally deformed muscovite and biotite with implications for 40Ar/39Ar geochronology of naturally deformed rocks. Geochim. Cosmochim. Acta, v. 75, p. 7759–7778.

Forster, M.A. and Lister, G. S., 2013.40Ar/39Ar geo-chronology and the diffusion of 39Ar in phengite – muscovite intergrowths during step-heating experiments invacuo. Geological Society, London, Special Publications, p. 378.

Hames, W.E., Bowring, S.A., 1994. An empirical evaluation of the argon diffusion geometry in muscovite, Earth and Planetary Science Letters, 124, p. 161-167.

Heizler, M. T., Perry, F. V., Crowe, B.M., Peters, L., and Appelt, R., 1999. The age of Lathrop Wells Volcanic Center: An 40Ar/39Ar dating investigation. Journal of Geophysical Research, v. 104, 767-804.

Heizler, M.T., Ralser S., and Karlstrom, K.E., 1997, Late Proterozoic (Grenville ?) deformation in central New Mexico determined from single crystal muscovite 40Ar/39Ar age spectra, Precambrian Research, v. 84, p. 1-15.

Harrison, T.M., Celerier, J., Aikman, A., Hermann, J., and Heizler, M.T., 2009. Diffusion of 40Ar in muscovite, Geochim. Cosmochim. Acta, v. 73, p. 1039-1051.

Harrison, T. M., and Lovera, O. M., 2012. The multi-diffusion domain model: past, present and future. Geological Society, London, Special Publications, 378.

Hodges, K. V. and Bowring, S. A., 1995. 40Ar/39Ar thermochronology of isotopically zoned micas: Insights from the south-western USA Proterozoic orogeny. Geochim. Cosmochim. Acta, v. 59, p. 3205–3220.

Hodges, K.V., Willis, H.E., Bowring, S.A. 1994. 40Ar/39Ar age gradients in micas from a high-temperature-low -pressure metamorphic terrain: Evidence for very slow cooling and implications for the interpretation of age spectra. Journal of Geology, v 22, p. 55-58

Jahns, R. H., 1974. Structural and Petrogenetic Relationships of Pegmatites in the Petaca District, New Mexico. New Mexico Geological Society Guidebook, 25th Field Conference, p. 371-375.

Jahns, R. H., 1946. Mica deposits of the Petaca District, Rio Arriba County, New Mexico, with brief descriptions of the Ojo Caliente District, Rio Arriba County, and the Elk Mountain District, San Miguel County, New Mexico Bureau Of Geology & Mineral Resources Bulletin, v. 25, p. 15-75.

Jahns, R.H. and Burnham, C.W., 1969. Experimental studies of pegmatite genesis; I, a model for the derivation and crystallization of granitic pegmatites. Economic Geology and the Bulletin of the Society of Economic Geologists, v. 64, p. 843-864.

Jahns, R. H. and Tuttle, O.F., 1963. Layered pegmatite-aplite intrusives. Special Papers Mineral Society of America, v. 1, p. 78-92.

Jones, J.V., III, Daniel, C.G., Frei, D., Thrane, K., 2011. Revised regional correlations and tectonic implications of Paleoproterozoic and Mesoproterozoic metasedimentary rocks in northern New Mexico, USA: New findings from detrital zircon studies of the Hondo Group, Vadito Group and Marquenas Formation. Geosphere, 7(4):

17.Karlstrom, K.E., Dallmeyer, R.D., and J.A. Grambling, 1997. 40Ar/39Ar evidence for 1.4 Ga regional metamorphism in New Mexico: Implications for thermal evolution of lithosphere in the Southwestern USA, Journal of Geology, v. 105, p. 205–223.

Karlstrom, K.E., Amato, J.M., Williams, M.L., Heizler, M., Shaw, C.A., Read, A.S., and Bauer, P., 2004, Proterozoic tectonic evolution of the New Mexico region, in Mack, G.H. and Giles, K.A., eds., The Geology of New Mexico: A Geologic History: New Mexico Geological Society Special Publication 11, p. 1-34.

Kelley, V. C. and Northrop, S. A., 1975, Geology of the Sandia Mountains and vicinity, New Mexico: New Mexico Bureau of Mines and Mineral Resources Memoir 29, p. 136

Kirby, E, Karlstrom, K.E. and Andronicos, C.1995. Tectonic setting of the Sandia pluton: An orogenic 1.4 Ga granite in New Mexico. Tectonics, v. 14, p. 185-201.

Kuiper, K. F., Deino, A., Hilgen, F. J., Krijgsman, W., Renne, P. R. and Wijbrans, J. R., 2008. Synchronizing rock clocks of earth history. Science, v. 320, p. 500–504.

Kula, J., Spell, T.L., 2012. Recovery of muscovite age gradients by 40Ar/39Ar vacuum furnace. Chemical Geology, v. 304-305, p. 166-174.

Lanzirotti, A. and Hanson, G.N., 1997. An assessment of the utility of staurolite in U-Pb dating of metamorphism. Contributions to Mineralogy and Petrology, v. 129, 4, p. 352-365.

London, D., 2008. Pegmatites. The Canadian Mineralogist Special Publication 10, Mineralogical Association of Canada

London, D., 2005. Granitic pegmatites: an assessment of current concepts and directions for the future. Lithos, v. 80, p. 281-303.

Lovera, O. M., Grove, M., and Harrison, T. M., 2002. Systematic analysis of K-feldspar 40Ar/39Ar step heating results II: Relevance of laboratory argon diffusion properties to nature. Geochim. Cosmochim. Acta. v. 66, no. 7, 1237-1255.

Lovera, O. M., Richter, F. M., and Harrison, T. M., 1989. The 40Ar/39Ar thermochronometry for slowly cooled samples having a distribution of diffusion domain sizes. Journal of Geophysical Research, 94(B12), 17917-17.

Macroline, J., Heizler, M.T., Goodwin, L., Rasler, S. and Clark, J. 1999. Thermal, structural, and petrological evidence for 1400-Ma metamorphism and deformation in central New Mexico. Rocky Mountain Geology, v. 34, no. 1, p. 93-119.

McDougall, I., Harrison, T. M. 1999. Geochronology and Thermochronology by the 40Ar/39Ar Method. Oxford University Press. Second Edition, p. 26, 123-130.

McIntosh, W. C., Heizler, M., Peters, L., & Esser, R., 2003. 40Ar/39Ar geochronology at the New Mexico Bureau of Geology and Mineral Resources. Socorro, New Mexico Bureau of Geology and Mineral Resources, Open File Report OF-AR-1, 7.

McLemore, V.T., 2012. Intermittent Globe Pegmatite Mine, Petaca District, Rio Arriba County, New Mexico. New Mexico Geological Society Guidebook, 63rd Field Conference, p. 109-110.

McLemore, V.T., Ramo, O.T., Heizler, M.T., and Heinonen, A.P., 2012. Intermittent Proterozoic plutonic magmatism and Neoproterozoic cooling history in the Caballo Mountains, Sierra County, New Mexico; Preliminary Results. New Mexico Geological Society Guidebook, 63rd Field Conference, p. 235-247.

Min, K., Mundil , R., Renne, P.R., Ludwig, K.R., 2000. A test for systematic errors in 40Ar/39Ar geochronology through comparison with U/Pb analysis of a 1.1-Ga rhyolite. Geochimica et Cosmochimica Acta, v. 64, 1, p. 73-98.

Nyman, M.W., Karlstrom, K.E., Kirby, E. and Graubard, C. M., 1994. Mesoproterozoic contractional orogeny in western North America: Evidence from ca. 1.4 Ga plutons. Geology, v. 22 (10), p. 901-904.

Parsons I., Rex, D.C., Guise, P., and Halliday, A.N., 1988. Argon-loss by alkali feldspars, Geochim. Cosmochim. Acta, v. 52, 1097-1112.

Providence, RI. Tarbuck, E.J. and Lutgens, F.K., 1999. Earth: An Introduction to Physical Geology. Sixth edition. Upper Saddle River, NJ: Prentice Hall. p. 64-65.

Robbins G.A. (1972) Radiogenic Ar diffusion in muscovite under hydrothermal conditions. M.S Thesis, Brown University,

Thompson et, A.G., Grambling, J., and Karlstrom, K., Dallmeyer, R. 1996 Mesoproterozoic 40Ar/39Ar Thermal History of the 1.4 Ga Priest Pluton, Manzano Mountains, New Mexico. Journal of Geology, v. 104, p. 583-598.

Tuttle, O.F. and Bowen, N.L. 1958. Origin of granite in the light of experimental studies in the system NaAlSi3O8-KAlSi3O8-SiO2-H2O. Geologic Society of America, Memoir 74.

Sanders, R.E., Heizler, M.T. and Goodwin, L.B., 2006. 40Ar/39Ar thermochronology constraints on the timing of Proterozoic basement exhumation and fault ancestry, southern Sangro De Cristo Range, New Mexico. Geological Society of America Bulletin, v. 118, p. 1489-1506.

Shaw, C., Heizler, M., Karlstrom, K.., 2005, Mid-Crustal temperatures during ca. 1.4 Ga metamorphism in the southwestern United States: A regional synthesis of 40Ar/39Ar data, in Karlstrom, K. E., and Keller, G. R., eds., Lithospheric structure and evolution of the Rocky Mountains, American Geophysical Union Monograph Series 154, p. 163-184.

Sletten, V.W., Onstott, T.C., 1998. The effect of the instability of muscovite during in vacuo heating on 40Ar/39Ar step-heating spectra. Geochim. Cosmochim. Acta, v. 62, p. 123-141.

Steiger, R.H. and Jäger, E., 1977. Subcommission on geochronology: Convention on the use of decay constants in geo and cosmochronology. Earth Planet. Sci. Lett., v. 36, p. 359–362.

Strickland, D., Heizler, M.T., Selverstone, J. and Karlstrom, K.E., 2003. Proterozoic evolution of the Zuni Mountains, western New Mexico: Relationship to the Jemez lineament and implication for a complex cooling history. New Mexico Geologic Society Guidebook, 54th Field Conference, p. 109-117.

Taylor, J.R., 1982. An Introduction to Error Analysis: The Study of Uncertainties in Physical Measurements. Mill Valley, CA. University Science Books.

Williams, M. (2014) Personal communication.

Williams, M., Jercinovic, M. and Hetherington, C. 2007. Microprobe Monazite Geochronology: Understanding Geologic Processes by Integrating Composition and Chronology. Annual Review of Earth and Planetary Sciences, v. 35, p. 137-175.

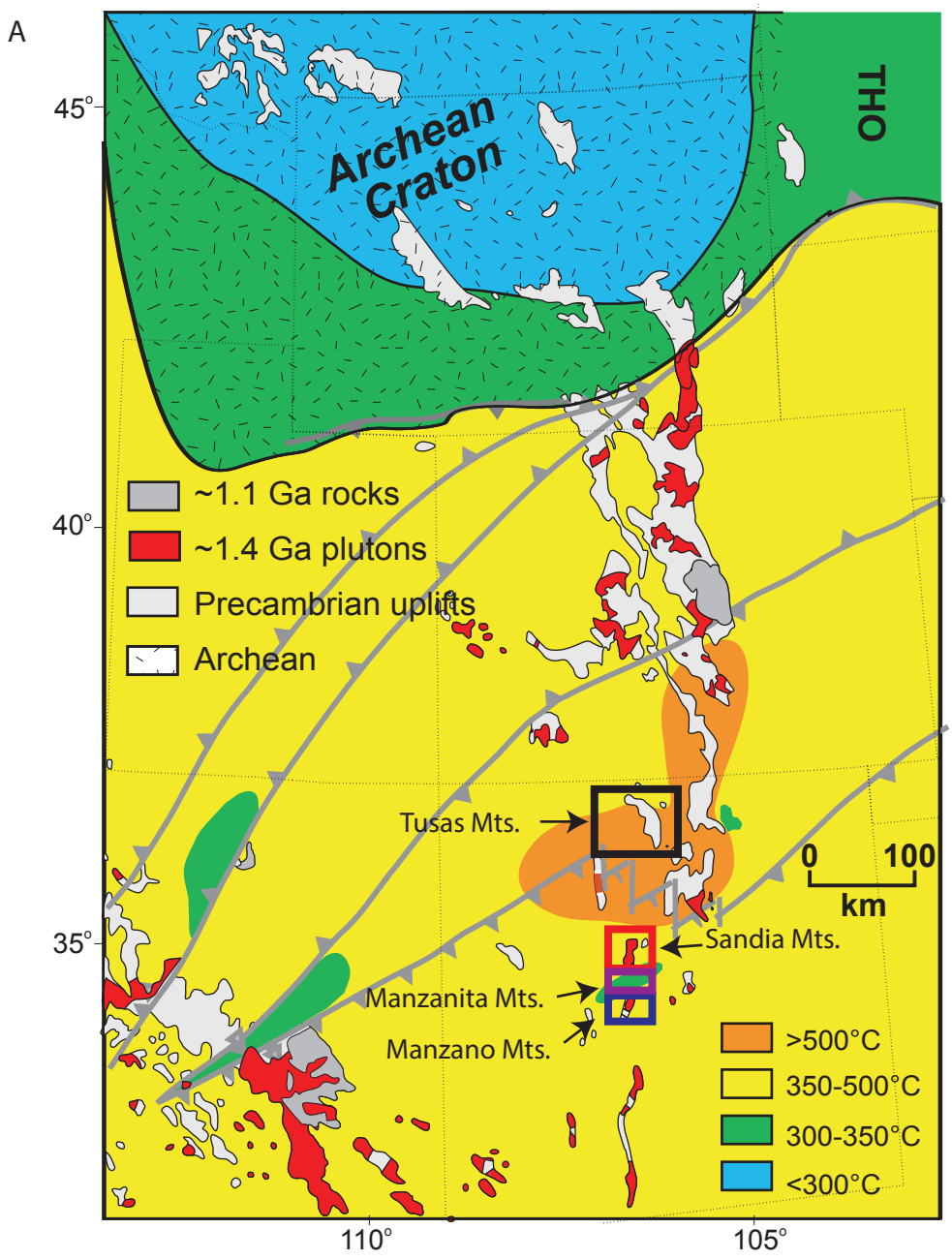

Figure 1: Inferred 1.4 Ga basement temperatures for presently exposed Precambrian rocks for parts of the SW USA (modified from Shaw et al., 2005). Tusas Mts. are located in the black box; Sandia Mts. are located in the red box; Manzanita Mts. are located in the purple box; Manzano Mts. are located in the blue box.

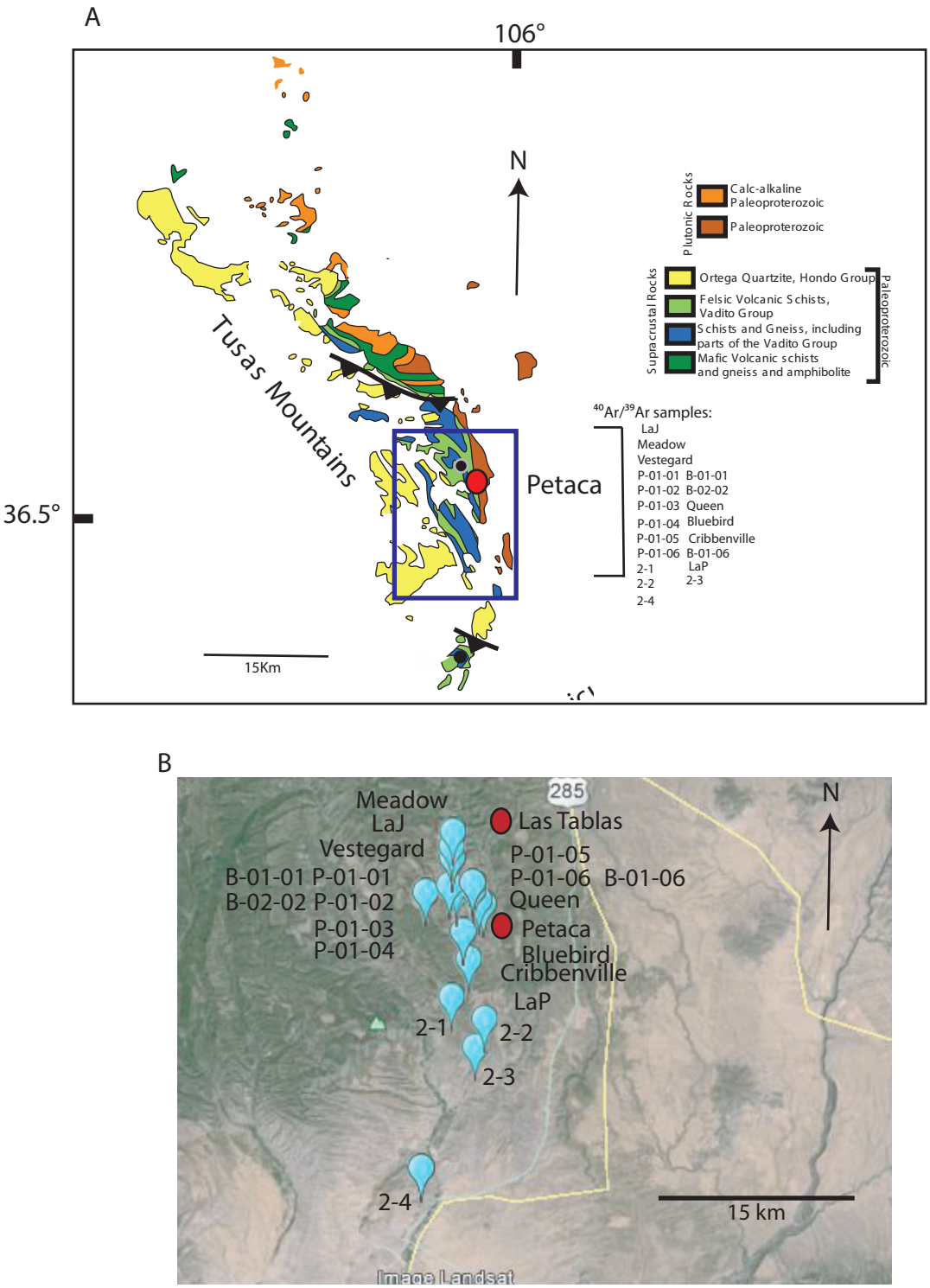

Figure 2: A: Geologic map of the Tusas Mountains (modified map from Aronoff et al., 2014). Samples collected from the Petaca district are indicated with the blue box. B: Google Earth image of sample locations from the Petaca District.

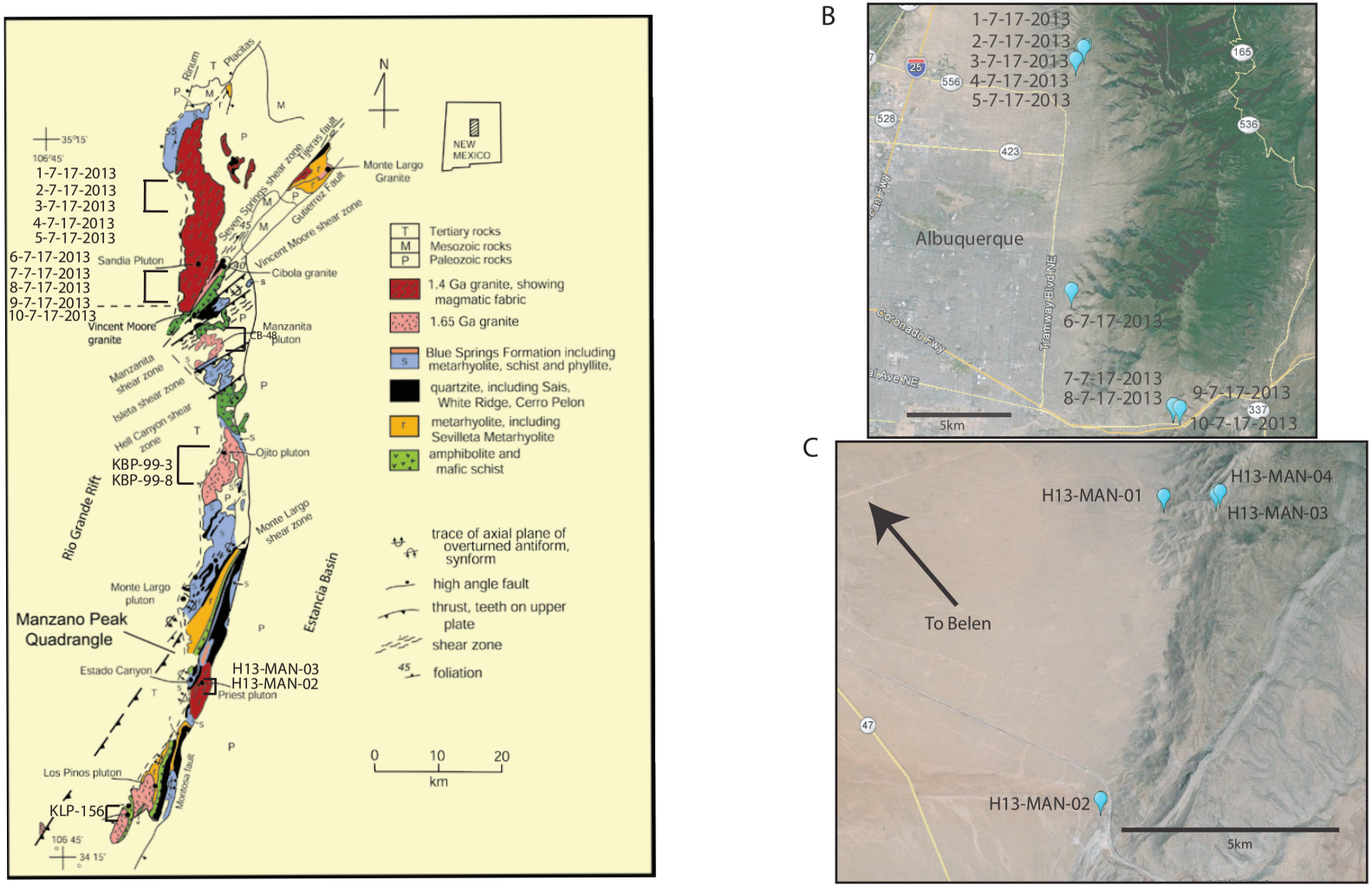

Figure 3: A: Geologic map of the Sandia, Manzanita and Manzano Mtns showing approximate location of dated samples (modified map from Karlstrom et al., 2004). B: Google Earth image of sample locations from the Sandia Mtns. C: Google Earth image of sample locations from the Manzano Mtns.

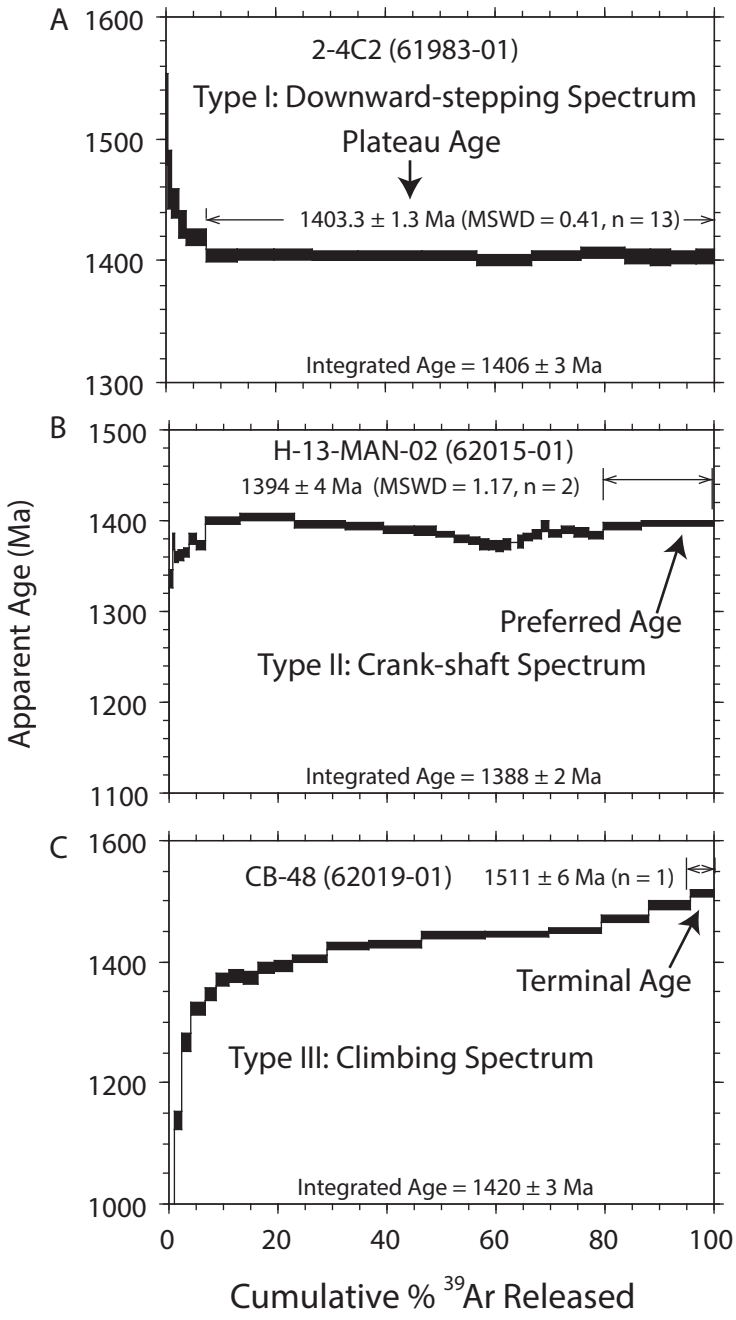

Figure 4: The three representative types of age spectra. A: Type I: Downward-stepping spectrum where the initial steps begin as old ages and get younger prior to a well-defined plateau segment. B: Type II: Crank-shaft spectrum with initially young ages followed by older ages and then repeats this pattern. C: Type III: Climbing spectrum where the initial steps are young and monotonically climb to either a terminal age or a plateau age.

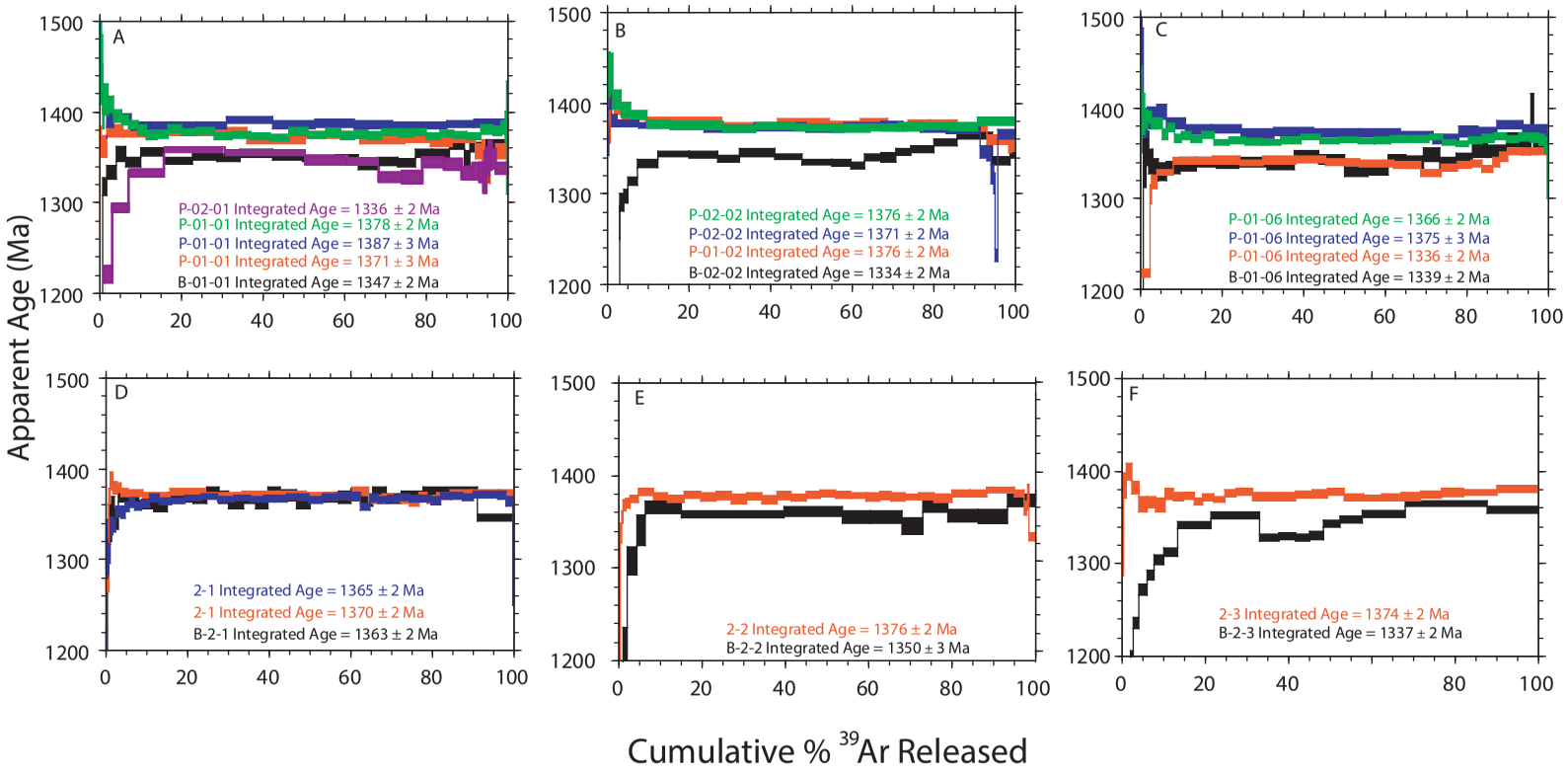

Figure 5: Comparison of pegmatite vs country rock muscovite age spectra for the Tusas Mt samples. All country rock muscovite data are shown in black, whereas all other spectra are from pegmatite muscovite samples. A-D have multiple aliquots of the same muscovite that show varying degrees of reproducibility. Data are arranged left-right in a north-south distribution.

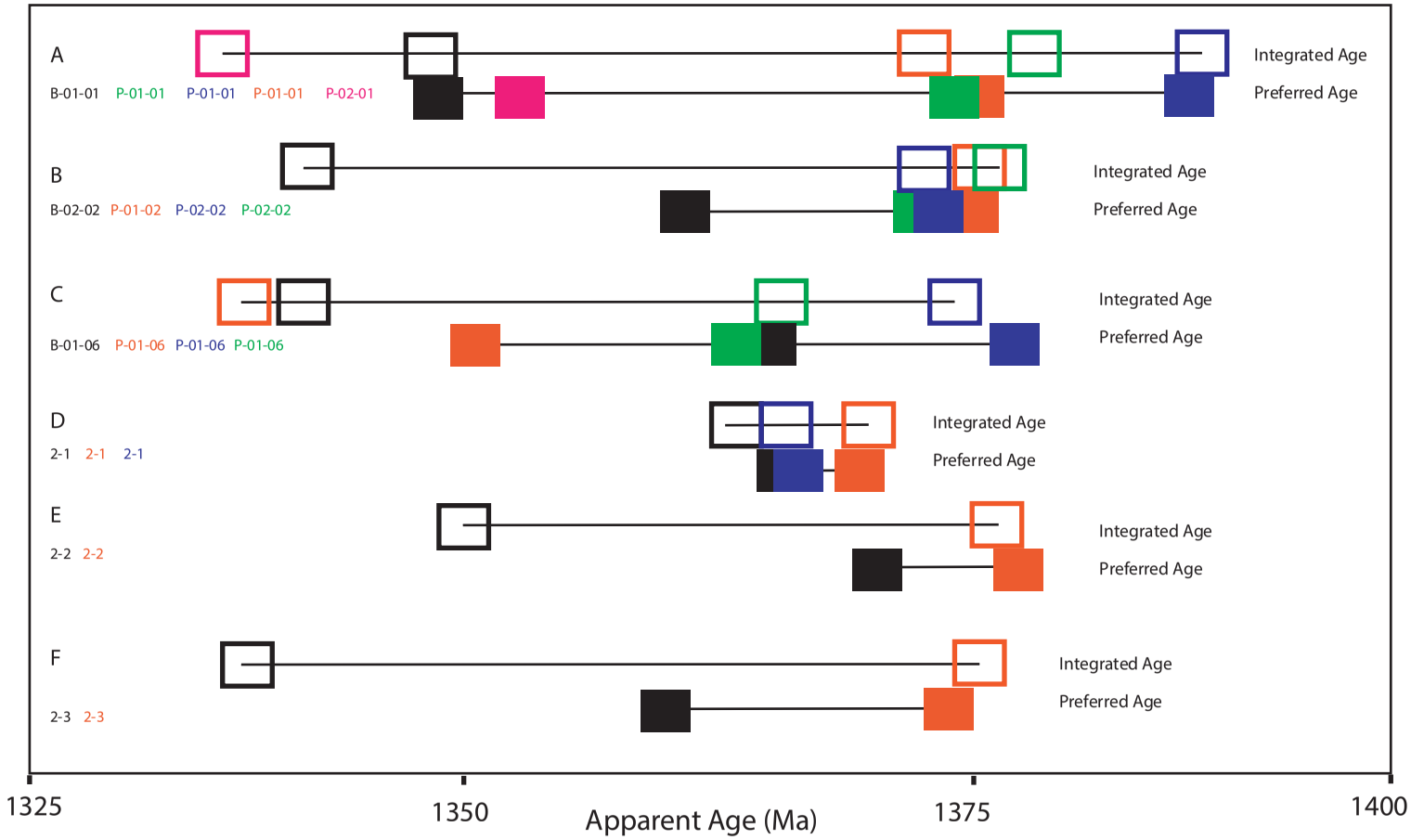

Figure 6: Comparison of country rock and pegmatite muscovite integrated and preferred ages. All colors and sample names correspond to Figure 5. Open boxes are integrated ages whereas solid boxes are preferred ages. Pegmatite muscovite ages are generally older than country rock pairs and this suggests finer grained muscovites have lower argon closure temperatures compared to coarse muscovite crystals.

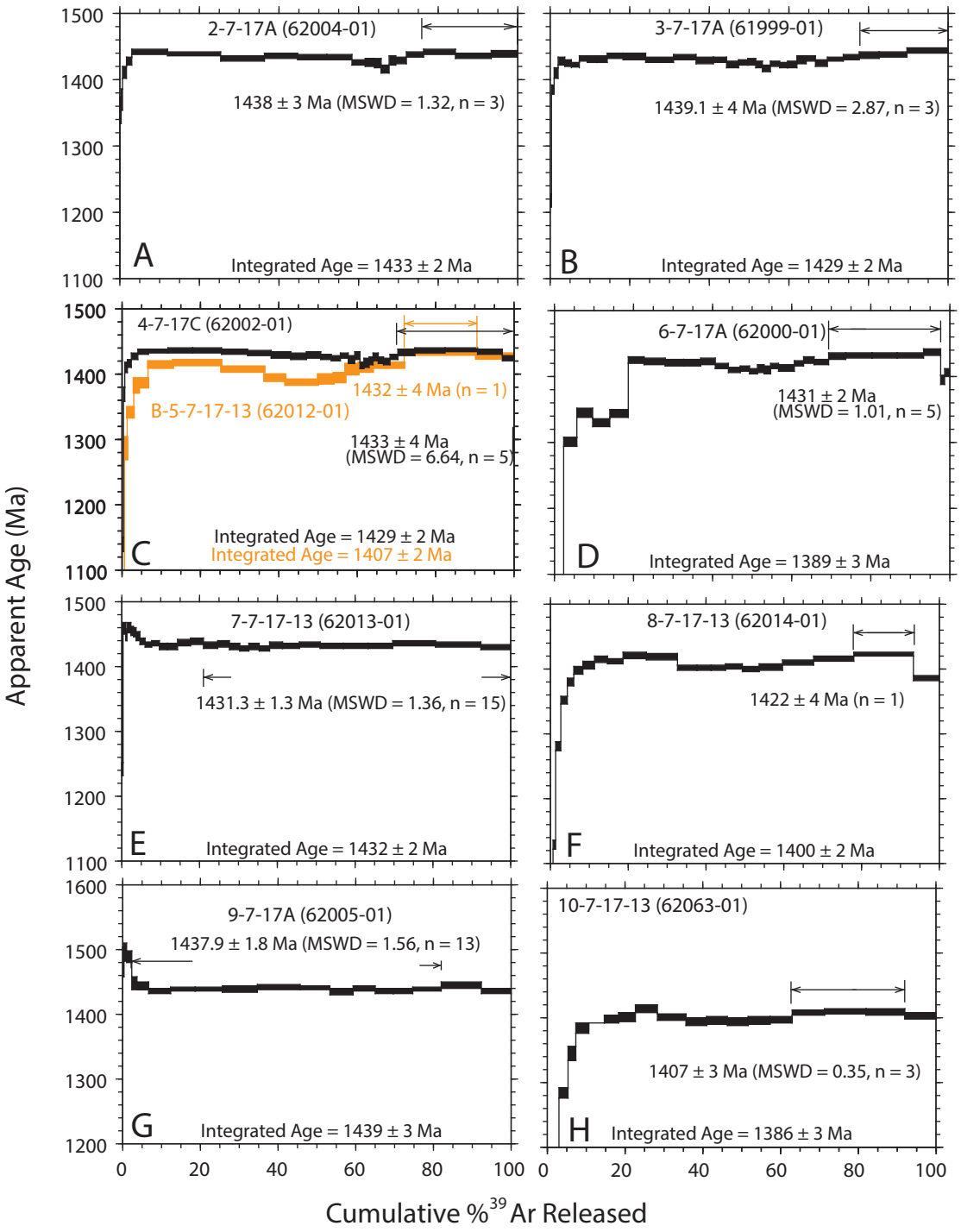

Figure 7: A-H: Pegmatite muscovite age spectra from the Sandia Mountains and a single country rock pair (C) shown in orange. Spectra are moderately variable in age and shape, however preferred ages group near 1440 Ma.

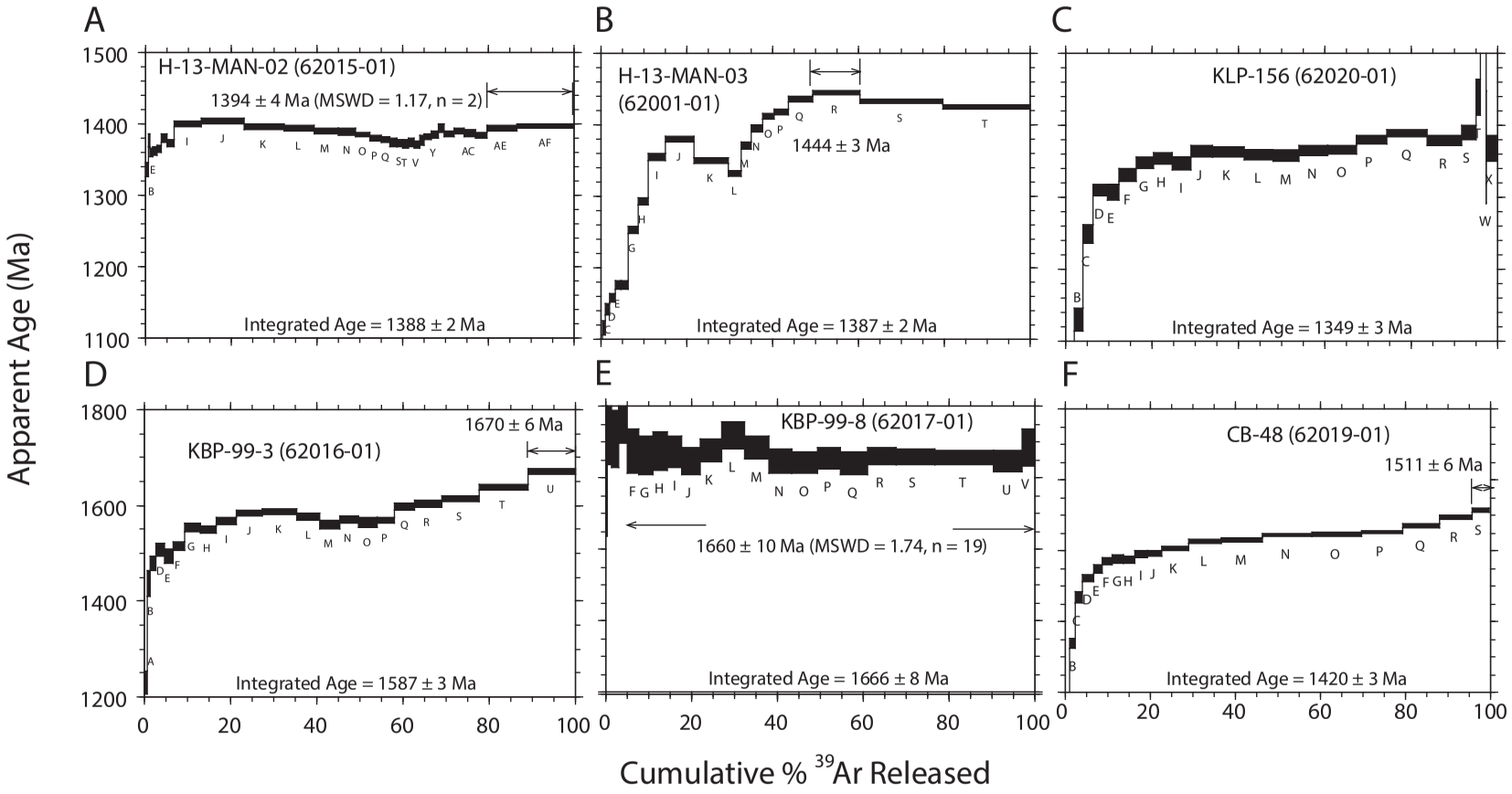

Figure 8: Muscovite age spectra for samples collected in the Manzano Mountains (A, B), Los Pinos pluton (C), Ojito pluton (D, E) and the Manzanita pluton (F). Samples north of the Monte Largo Shear Zone and south of the Sandia Mountains (see Figure 3A) are distinctly older than 1.4 Ga.

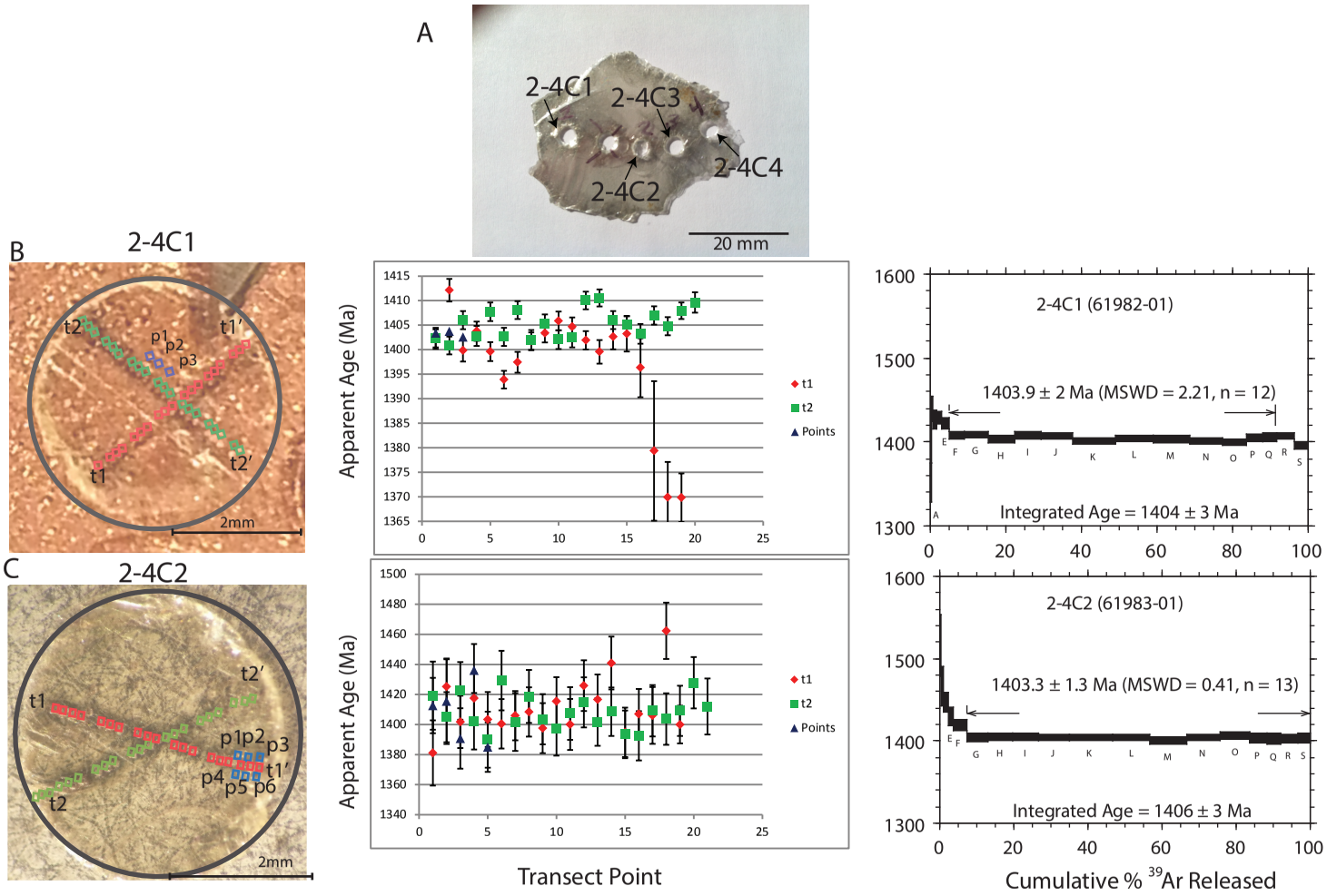

Figure 9: A: Image of whole 2-4C muscovite crystal. B (2-4C1) and C(2-4C2): Compilation of crystal image with UV transects, corresponding transect (t-t') vs age and corresponding age spectrum. The old ages in the age spectra for both samples were not sampled via the in situ analyses. The preferred ages from both of the age spectra are within error to the ages sampled in the corresponding in situ transects.

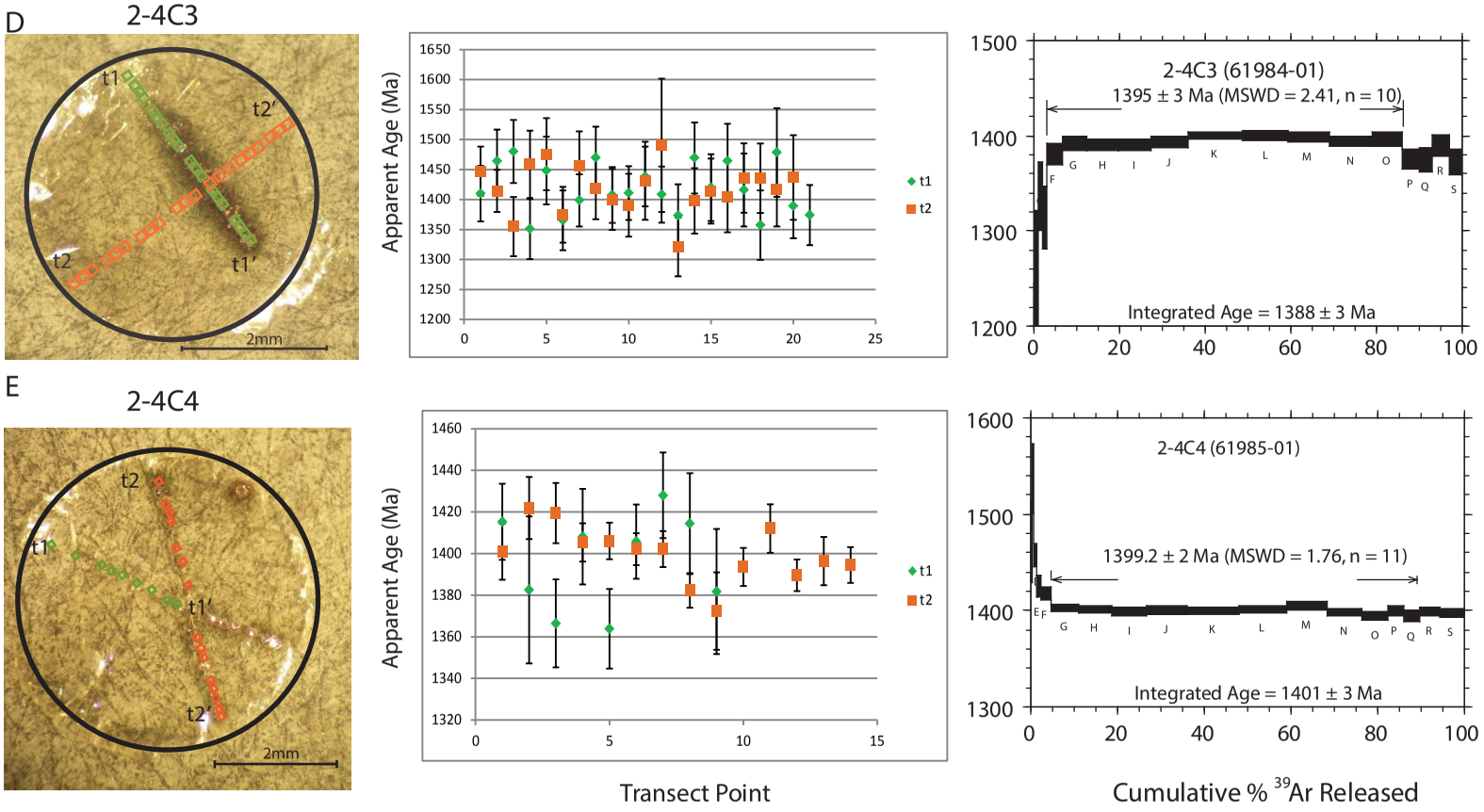

Figure 9 Continued: D (2-4C3) and E (2-4C4): Compilation of crystal image with UV transects, corresponding transect (t-t') vs age and corresponding age spectrum. The old ages in the age spectra for 2-4C4 were not sampled via the in situ analyses. The preferred ages from both of the age spectra are within error to the ages sampled in the corresponding in situ transects.

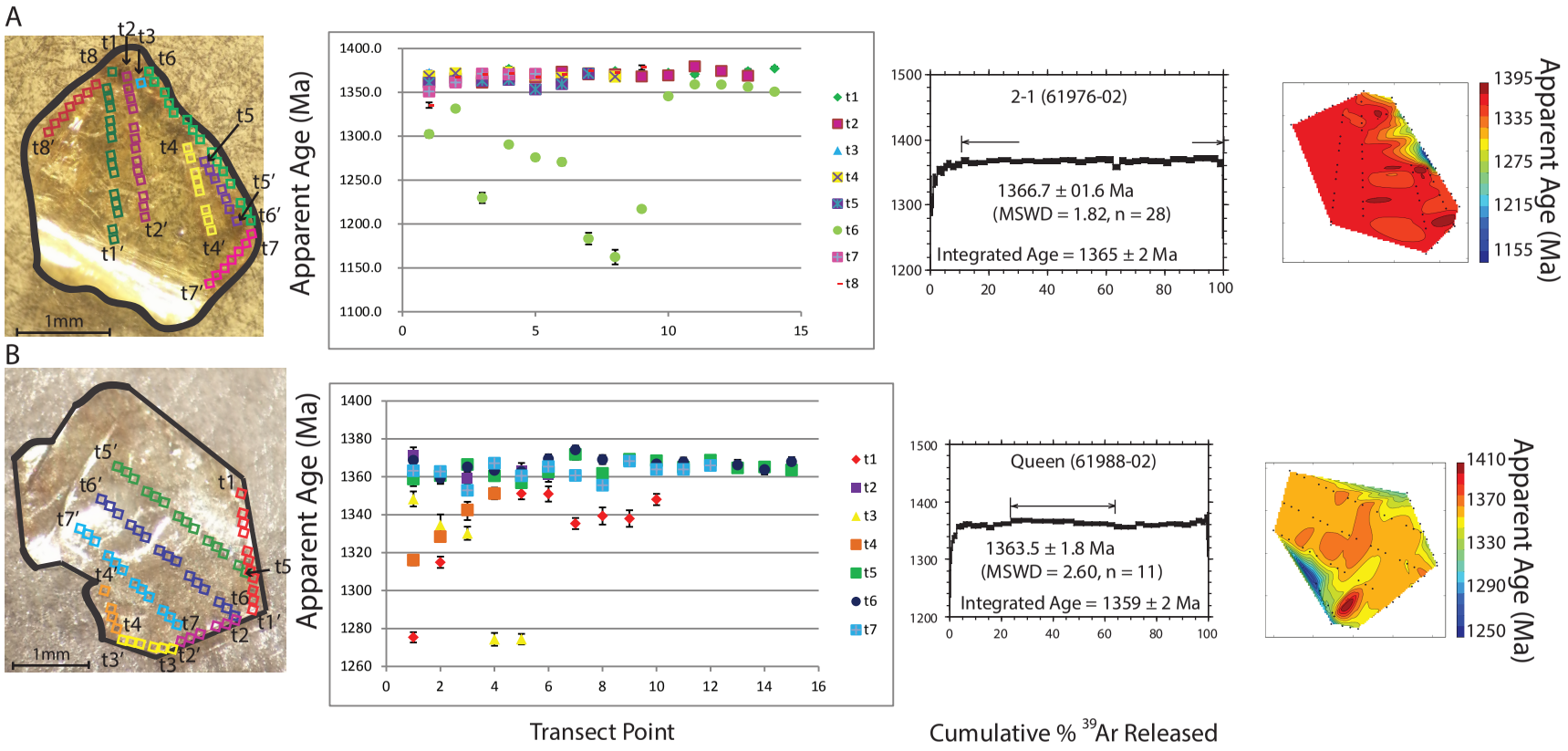

Figure 10: A (2-1) and B (Queen): Compilation of crystal image with UV transects, corresponding transect (t-t′) vs age, corresponding age spectrum and chrontour map. The ages are overall constant across the crystal and ages near the edge of the crystal are younger than the middle of the grain. The preferred ages from each of the age spectra correspond closely to the ages sampled from the center of the crystals via the in situ analysis.

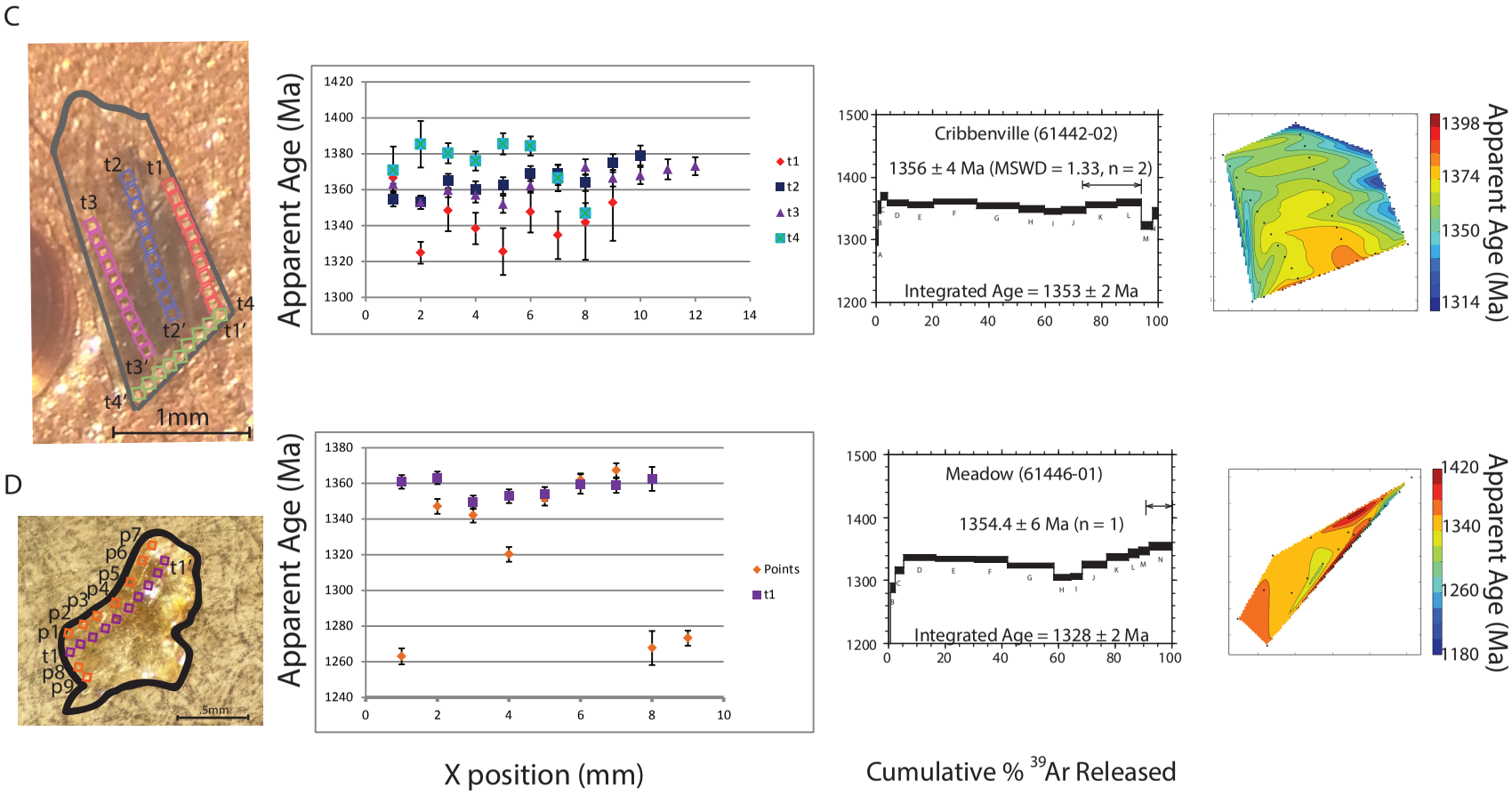

Figure 10 Continued: C (Cribbenville) and D (Meadow): Compilation of crystal image with UV transects, corresponding transect (t-t′) vs age, corresponding age spectrum and chrontour map. The ages are overall constant across the crystal and ages near the edge of the crystal are younger than the middle of the grain. The preferred ages from each of the age spectra closely correspond to the ages sampled from the center of the crystals via the in situ analysis.

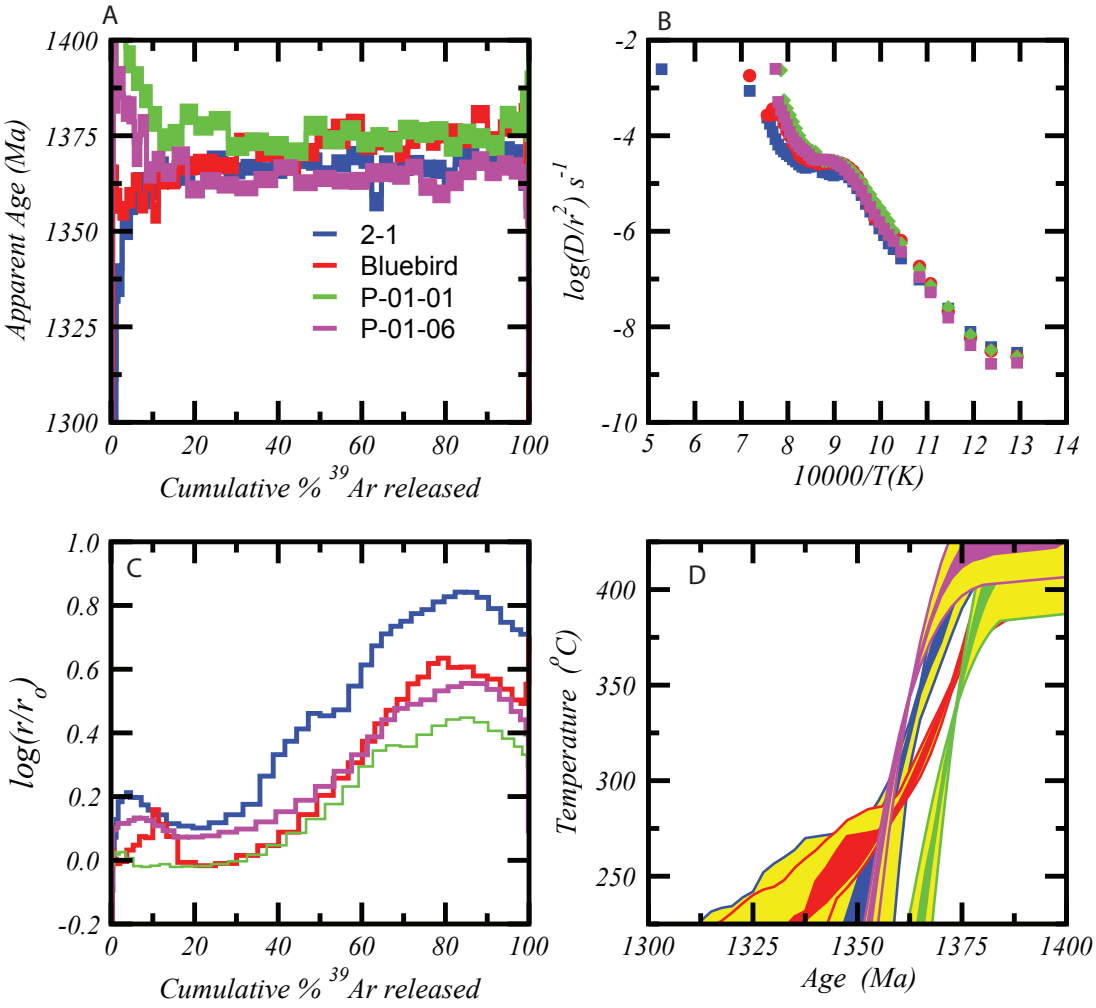

Figure 11. MDD analysis of muscovites from pegmatites from the Tusas Mountains. A: Measured age spectra using high resolution heating schedule similar to that recommended by Kula and Spell (2012). B: Arrhenius diagram determined from fractional release of ^{39}Ar showing similarity between all samples and a distinct kink beginning near 30% gas released. C: Log(r/r_0) plots constructed using the same reference Arrhenius law of 64.0 kcal/mol and D_0/r_0^2. Data appear to vary from 64.0 kcal/mol and the climbing pattern is consistent with multiple diffusion length scales. D: Thermal histories derived from kinetic data and age spectrum that indicate temperatures > 400°C prior to 1.4 Ga with cooling through 375°C by about 1375 Ma. See Appendix 3 for model fits

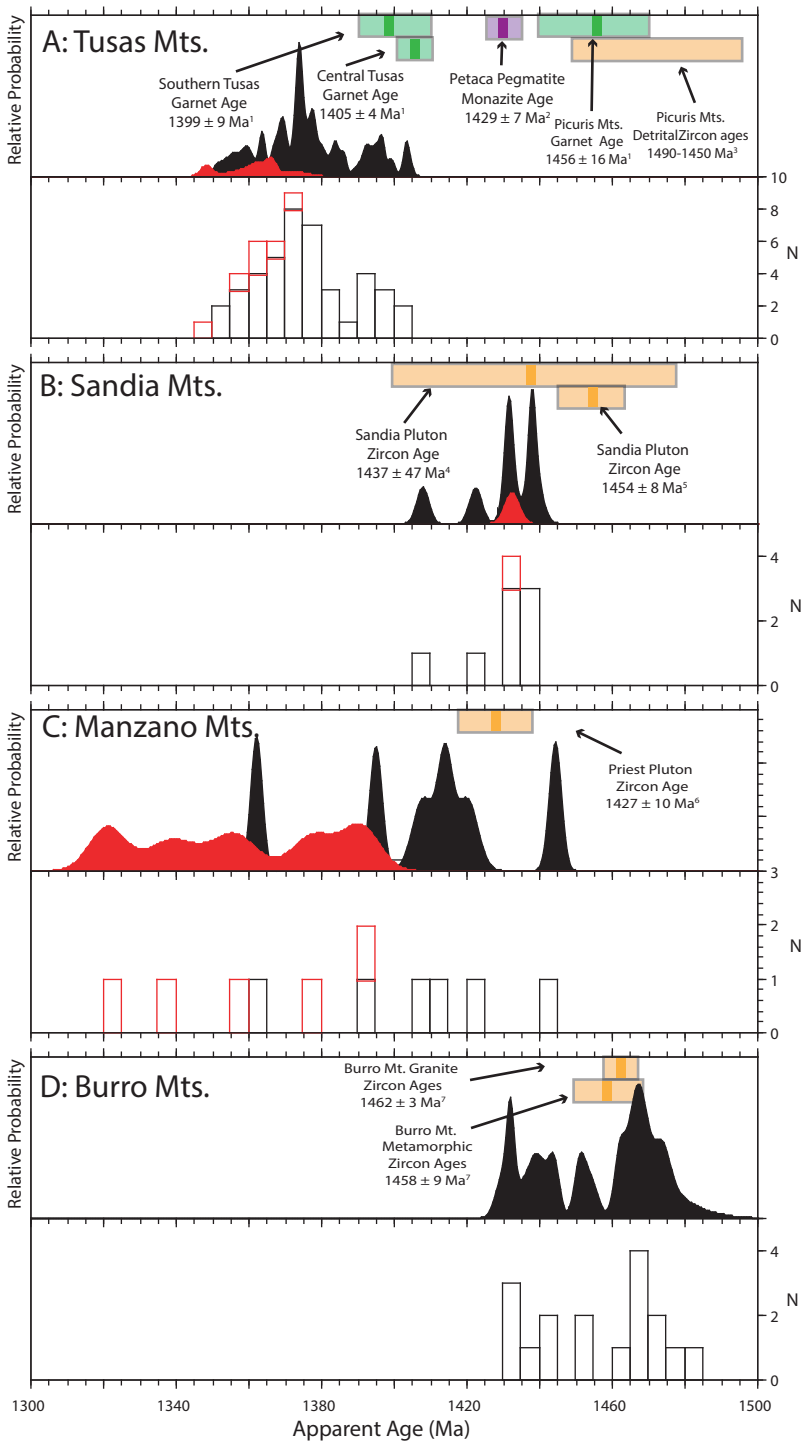

Figure 12: Age probability and histogram diagrams of micas and/or hornblendes from New Mexico Mt. regions. Country rock micas are shown in red whereas all other micas are shown in black. Other geochronology data shown by colored horizontal bars. A: Tusas muscovite ages range from 1407-1351 Ma. All ages are younger than the garnet and monazite ages indicating protracted cooling. B: Sandia Mts. pegmatite muscovites are as old as 1439 Ma which approaches the zircon age of 1454± 8 Ma. C: Manzano Mts. pegmatite muscovites get as old as 1444 Ma and closely approximate emplacement ages. Data shown for the Manzano Mts. include results presented here as well as micas from Heizler et al. (1997) and Macroline et al. (1999). D: Burro Mt. mica and hornblende ages are as old as zircon ages indicating rapid cooling and the onset of 1.46 Ga extension and metamorphism (Amato et al., 2012). 1. Aronoff et al. (in review) 2. Williams (pers. com.) 3. Daniel et al. (2013). 4. Karlstrom et al. (2004) 5. Karlstrom (pers. com.) 6. Bauer et al. (1993) 7. Amato et al. (2012).

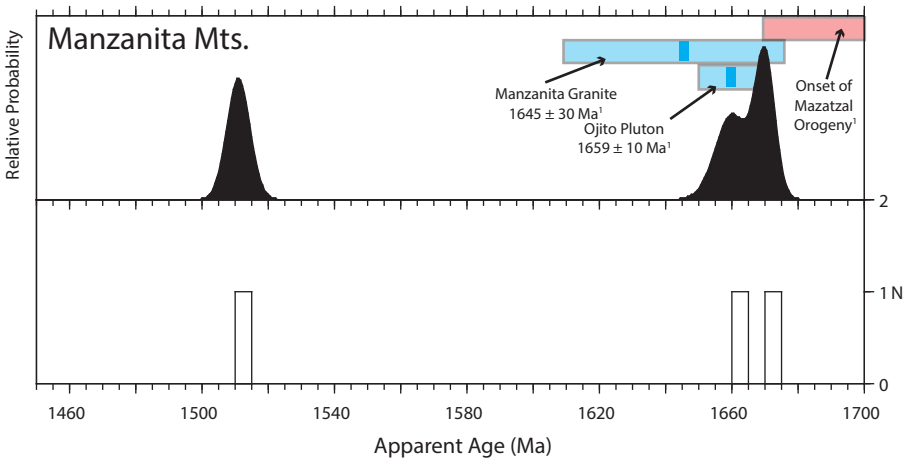

Figure 13: Age probability and histograms of micas from the Manzanita and Ojito Pluton located within the Manzanita Mts. Both plutons have zircon ages shown in blue. Muscovite and zircon ages are concordant and combined with other data (Thompson et al., 1996) demonstrate Mazatzal aged deformation. 1. Karlstrom et al. (2004).

Table 1

Samples with locations and other details

Run ID #	Sample	Location	Rock Type	Xl size (mm)			Comment	Type	Easting	Northing	Int Age	Plat Age	Term Age
Tusas Mtns													
61976-01	2-1	Globe Mine	P	3	x	2.5		I	0406803	4033239	1370	**1370**	
61976-02	2-1	Globe Mine	P	3	x	2.5		III	0406803	4033239	1365	**1367**	
62006-01	B-2-1	Globe Mine	CR	0.25	x	0.5		III	0406818	4033293	1363	**1366**	
61977-01	2-2	Unnamed	P	3	x	2.5		III	0409425	4031855	1376	**1378**	
62007-01	B-2-2	Vadito	CR	0.25	x	0.5		III	0409425	4031871	1350	1359	**1373**
61978-01	2-3	Salt Spring Mine	P	4	x	3		I	0408936	4029700	1374	**1373**	
62009-02	B-2-3	Vadito	CR	0.25	x	0.25		II	0408936	4029700	1337		**1361**
61996-01	5-1	Sandoval	P	4	x	4	Hole punch	I	0405954	4040930	1377	**1376**	
61997-01	5-2	Sandoval	P	4	x	4	Hole punch	I	0405954	4040930	1386	**1384**	
61998-01	5-3	Sandoval	P	4	x	4	Hole punch	I	0405954	4040930	1379	**1378**	
61979-01	2-4A	Joseph Mine	P	1	x	1		III	0405851	4020339	1373	**1374**	
61980-01	2-4B	Joseph Mine	P	5	x	1		III	0405851	4020339	1368	**1368**	
61982-01	2-4C1	Joseph Mine	P	4	x	4	Hole punch	I	0405851	4020339	1404	**1404**	
61983-01	2-4C2	Joseph Mine	P	4	x	4	Hole punch	I	0405851	4020339	1406	**1403**	
61984-01	2-4C3	Joseph Mine	P	4	x	4	Hole punch	III	0405851	4020339	1388	**1395**	
61985-01	2-4C4	Joseph Mine	P	4	x	4	Hole punch	I	0405851	4020339	1401	**1399**	
61482-01	B-01-01	Vadito	CR					III	0404078	4040780	1347	**1348**	
61469-01	B-01-06	Vadito	CR					III	0407606	4041371	1340	1337	**1366**
61468-01	B-02-02	Vadito	CR					II	0406376	4041048	1334		**1363**
61989-01	Bluebird	Bluebird	P	4	x	4		III	0405811	4043551	1368		**1381**
61989-02	Bluebird	Bluebird	P	4	x	4		I	0405811	4043551	1370	**1373**	
61444-01	Bluebird	Bluebird	P					II	0405811	4043551	1367	**1369**	
61442-02	Cribbenville	Cribbenville Excel Tunnel	P					II	0407180	4038165	1353		**1356**
61986-01	LaJ	La Jarita	P	4	x	4		I	0405674	4044377	1384	**1384**	
61981-01	LaP	La Paloma	P	4	x	4		I	0407802	4036168	1396	**1395**	
61981-02	LaP	La Paloma	P	4	x	4		I	0407802	4036168	1390	**1392**	
61446-01	Meadow	Meadow Contact	P					II	0405658	4045475	1328	1334	**1354**
61417-01	P-01-01	Prince	P					I	0404078	4040780	1371	1370	**1377**
61990-02	P-01-01	Prince	P	4	x	4		I	0404078	4040780	1387	**1386**	
61990-01	P-01-01	Prince	P	4	x	4		I	0404078	4040780	1378	**1374**	
61419-01	P-02-01	Prince	P					III	0404078	4040780	1336	1351	**1356**
61421-01	P-01-02	Keystone	P					I	0406371	4041045	1376	**1376**	

Run ID #	Sample	Location	Rock Type	Xl size (mm)			Comment	Type	Easting	Northing	Int Age	Plat Age	Term Age
61423-01	P-02-02	Keystone	P					I	0406376	4041048	1371	**1374**	
61991-01	P-02-02	Keystone	P	4	x	4		I	0406376	4041048	1376	**1374**	
61430-01	P-01-03	Conquestador	P					I	0406371	4041045	1392	1392	**1394**
61992-01	P-01-03	Conquestador	P	5	x	5		II	0406371	4041045	1397	**1397**	
61432-01	P-01-04	Wyoming	P		x			II	0406331	4041456	1357		**1364**
61993-01	P-01-04	Wyoming	P	4	x	4		I	0406331	4041456	1369	**1370**	
61434-01	P-01-05	Unnamed	P		x			II	0407508	4041838	1351		**1360**
61994-01	P-01-05	Unnamed	P	4	x	4		II	0407508	4041838	1373	**1373**	
61436-01	P-01-06	Pinos Altos	P		x			III	0407606	4041371	1336	1340	**1352**
61995-01	P-01-06	Pinos Altos	P	4	x	4		I	0407606	4041371	1375	1372	**1378**
61995-02	P-01-06	Pinos Altos	P	4	x	4		I	0407606	4041371	1366	**1364**	
61988-01	Queen	Queen	P	2	x	2		III	0408128	4040610	1363	1366	**1373**
61988-02	Queen	Queen	P	2	x	2		III	0408128	4040610	1359	**1364**	
61438-01	Queen	Queen	P					III	0408128	4040610	1355	**1360**	
61987-01	Vestegard	Vestegard	P	4	x	4		II	0405811	4038165	1375	**1390**	
61440-01	Vestegard	Vestegard	P					II	0405811	4038165	1360		**1380**
Sandia Mts.													
62004-01	2-7-17A	Sandias	P	4	x	4		III	0364427	3897858	1433	1435	**1438**
61999-01	3-7-17A	Sandias	P	5	x	4		III	0364485	3897928	1429	1431	**1439**
62002-01	4-7-17C	Sandias	P	4	x	3		III	0364087	3897245	1429	1432	**1433**
62012-01	B-5-7-17-13	Sandias	CR	0.5	x	1		III	0364087	3897245	1407		**1432**
62000-01	6-7-17A	Sandias White Wash	P	3	x	5		III	0364620	3886401	1389		**1432**
62013-01	7-7-17-13	Sandias	P	2	x	1		I	0369644	3881410	1432	**1431**	
62014-01	8-7-17-13	Sandias	P	2	x	1		III	0369700	3881409	1400		**1422**
62005-01	9-7-17A	Sandias	P	3	x	3		I	0369994	3881327	1439	**1438**	
62063-01	10-7-17-13	Sandias	P	1	x	1		III	0369994	3881327	1386		**1408**
Manzanita Mts.													
62019-01	CB-48	Manzanita Pluton	PL	0.2	x	0.25		III	370643.4	3874404.7	1420		**1511**
62016-01	KBP-99-3	Ojito Pluton	P	0.5	x	0.5		II	0366853	3846710	1587		**1670**
62017-01	KBP-99-8	Ojito Aureole	CR	0.5	x	0.5		I	0367175	3846688.9	1666	**1660**	
Manzano Mts.													
62015-01	H-13-MAN-02	Manzano	PL	2	x	1		II	0362542	3820230	1388		**1395**
62001-01	H-13-MAN-03	Manzano Estadio Canyon	P	2	x	3		II	0363635	3820334	1387		**1444**
Los Pinos Pluton													

Run ID #	Sample	Location	Rock Type	Xl size (mm)			Comment	Type	Easting	Northing	Int Age	Plat Age	Term Age
62020-01	KLP-156	Los Pinos	PL	1	x	1		III	353122.9?	3802230.5?	1349	**1362**	

Note: All samples were located at NAD 83 13 S.
Int= Integrated Age
Plat= Plateau Age
Term= Terminal Age
Xl= crystal
Rock Type: P = Pegmatite Muscovite, PL= Plutonic Muscovite Cr= Country Rock Muscovite
The preferred age for all samples is in bold.
?= Location is estimated

Table 2
Monazite Dating

Sample	Age (Ma)	Error (2 sigma)	ıtion in mineral
Petaca 9-46 Meadow Pegmatite	1431	6	Core
	1431	6	Core
	1421	7	Rim
	1432	7	Rim
*Petaca 4-19 Globe Pegmatite	1430		Core

* Petaca 4-19 is compatible in age to Petaca 9-46, but the specific ages and errors were not given. Information is from Mike Williams, personal communication (2014).

Appendix 1 $^{40}Ar/^{39}Ar$ analytical data.

	ID	Temperature (°C)	$^{40}Ar/^{39}Ar$	$^{37}Ar/^{39}Ar$	$^{36}Ar/^{39}Ar$ (x 10^{-3})	$^{39}Ar_K$ (x 10^{-15} mol)	K/Ca	$^{40}Ar^*$ (%)	^{39}Ar (%)	Age (Ma)	±1σ (Ma)
	P-01-01, Muscovite, .34 mg, J=0.0095565±0.10%, D=1.0012±0.0011, NM-254F, Lab#=61417-01										
X	A	630	141.7	0.0236	142.9	0.200	21.6	70.2	0.2	1222.8	18.0
X	B	680	123.7	0.0035	25.29	0.383	144.9	94.0	0.7	1367.3	8.6
X	C	730	119.3	0.0029	13.12	0.921	174.2	96.7	1.7	1360.8	5.9
X	D	780	118.4	0.0030	2.719	3.77	168.6	99.3	5.9	1378.8	3.2
X	E	830	117.4	0.0020	0.7516	9.56	248.9	99.8	16.7	1375.5	2.2
X	F	880	117.6	0.0005	0.2855	17.21	1081.4	99.9	36.1	1377.8	1.9
	G	900	116.4	0.0014	0.4228	12.78	353.3	99.9	50.5	1368.0	2.3
	H	930	117.3	0.0009	0.9054	11.92	552.1	99.8	63.9	1374.1	1.8
	I	960	116.4	0.0014	0.5351	9.66	377.5	99.9	74.8	1367.8	2.0
	J	990	116.8	0.0036	0.3845	5.67	141.9	99.9	81.2	1370.9	2.6
	K	1020	116.6	0.0029	0.9568	4.74	175.0	99.8	86.5	1368.1	3.2
	L	1050	116.8	0.0036	0.8057	5.12	141.8	99.8	92.3	1370.2	2.5
X	M	1070	115.0	0.0083	0.5034	1.422	61.3	99.9	93.9	1355.6	4.0
X	N	1090	117.1	0.0096	8.457	0.681	53.0	97.9	94.6	1353.9	7.5
X	O	1110	114.1	0.0050	4.282	0.513	102.5	98.9	95.2	1338.9	8.1
X	P	1140	113.7	0.0044	2.311	0.470	115.6	99.4	95.8	1340.3	9.4
X	Q	1350	115.5	0.0020	5.706	1.256	251.9	98.5	97.2	1347.7	5.0
X	R	1650	121.2	0.0094	21.44	2.51	54.4	94.8	100.0	1356.1	3.9
	Integrated age ± 1σ			n=18		88.8	235.7	K2O=10.50%		1370.7	1.6
	Plateau ± 1σ		steps G-L	n=6	MSWD=1.57	49.9			56.2	1370.3	1.5
	Terminal Age ± 1σ		steps E-F	n=2	MSWD=0.62	26.8			30.2	1376.8	1.7
	P-02-01, Muscovite, .44 mg, J=0.0095465±0.09%, D=1.0012±0.0011, NM-254F, Lab#=61419-01										
X	A	630	90.49	0.0323	65.86	1.503	15.8	78.5	1.3	947.5	5.0
X	B	680	112.7	0.0203	45.50	1.931	25.2	88.1	3.0	1220.0	4.3
X	C	730	109.2	0.0039	5.497	4.74	131.7	98.5	7.2	1293.4	2.3
X	D	780	112.6	0.0030	1.596	9.47	171.1	99.6	15.5	1332.0	2.2
	E	830	115.3	0.0012	0.5932	17.07	435.7	99.8	30.5	1357.5	2.1
	F	880	115.0	0.0024	0.4000	22.3	213.3	99.9	50.1	1355.1	1.9
x	G	900	114.0	0.0031	0.7763	11.84	163.2	99.8	60.5	1346.0	2.0
x	H	930	113.9	0.0024	0.6258	8.97	209.9	99.8	68.4	1345.0	2.0
X	I	960	111.9	0.0043	0.8356	6.56	117.7	99.8	74.1	1327.7	2.7
X	J	990	111.9	0.0023	0.8416	5.67	223.0	99.8	79.1	1327.7	3.2
X	K	1020	113.7	0.0025	0.5760	5.98	207.5	99.8	84.3	1344.2	2.8
X	L	1050	113.4	0.0024	0.3581	5.30	209.8	99.9	89.0	1341.7	2.9
X	M	1070	112.3	0.0060	0.4414	2.89	85.6	99.9	91.5	1332.6	3.4
X	N	1090	112.8	0.0102	1.399	1.783	50.0	99.6	93.1	1334.4	4.5
X	O	1110	112.9	0.0060	2.416	1.114	85.0	99.4	94.1	1332.7	5.3
X	P	1140	111.8	0.0125	1.401	0.850	40.7	99.6	94.8	1325.9	7.7
X	Q	1170	113.7	0.0110	-0.1376	0.706	46.3	100.0	95.5	1345.3	7.5
X	R	1200	114.6	0.0269	0.5991	0.654	19.0	99.8	96.0	1351.6	7.8
X	S	1350	114.7	0.0084	2.449	1.305	60.6	99.4	97.2	1347.5	5.4
X	T	1650	117.2	0.0102	15.09	3.22	49.9	96.2	100.0	1337.4	3.2
	Integrated age ± 1σ			n=20		113.9	127.0	K2O=10.41%		1336.1	1.5
	Terminal Age ± 1σ		steps E-F	n=2	MSWD=0.72	39.370			34.6	1356.18	1.6

Appendix 1 $^{40}Ar/^{39}Ar$ analytical data.

	ID	Temperature (°C)	$^{40}Ar/^{39}Ar$	$^{37}Ar/^{39}Ar$	$^{36}Ar/^{39}Ar$ (x 10^{-3})	$^{39}Ar_K$ (x 10^{-15} mol)	K/Ca	$^{40}Ar^*$ (%)	^{39}Ar (%)	Age (Ma)	±1σ (Ma)
	P-01-02, Muscovite, .88 mg, J=0.0095319±0.08%, D=1.0012±0.0011, NM-254F, Lab#=61421-01										
X	A	630	128.7	0.0020	41.81	2.01	254.5	90.4	0.8	1365.5	5.1
X	B	680	125.5	-0.0027	16.04	2.53	-	96.2	1.9	1402.4	4.4
X	C	730	121.4	-0.0013	5.907	5.06	-	98.6	4.0	1392.7	2.8
X	D	780	119.3	0.0003	2.067	13.11	1560.7	99.5	9.4	1385.0	2.1
	E	830	118.3	0.0001	0.5253	44.8	3454.3	99.9	28.1	1380.4	1.8
	F	850	117.4	0.0003	0.4718	33.3	1594.9	99.9	41.9	1373.5	1.9
	G	880	118.0	0.0009	0.2883	30.0	567.2	99.9	54.4	1378.4	1.9
	H	900	117.6	0.0000	0.5253	18.87	36705.3	99.9	62.2	1374.5	2.3
	I	930	117.9	0.0002	0.4813	16.28	2346.8	99.9	69.0	1377.2	2.3
	J	960	117.3	0.0010	0.8894	11.94	494.5	99.8	74.0	1372.0	1.8
	K	990	117.8	0.0006	0.7699	12.21	883.9	99.8	79.0	1376.1	2.3
	L	1020	117.8	0.0001	0.6116	16.47	8546.1	99.8	85.9	1376.1	2.2
	M	1050	117.4	0.0007	0.4770	17.37	746.6	99.9	93.1	1373.7	2.2
X	N	1090	115.9	0.0007	1.081	8.04	729.7	99.7	96.5	1359.4	2.4
X	O	1140	115.7	-0.0004	0.5003	4.89	-	99.9	98.5	1359.5	2.7
X	P	1350	116.1	0.0007	2.921	1.491	702.7	99.2	99.1	1356.4	5.5
X	Q	1650	121.8	0.0154	22.43	2.15	33.2	94.6	100.0	1355.9	4.5
	Integrated age ± 1σ			n=17		240.4		K2O=11.01%		1376.2	1.4
	Plateau ± 1σ		steps E-M	n=9	MSWD=2.03	201.1			83.7	1375.8	1.2
	P-02-02, Muscovite, 1.27 mg, J=0.0095294±0.08%, D=1.0012±0.0011, NM-254F, Lab#=61423-01										
X	A	630	129.2	-0.0100	49.27	1.381	-	88.7	0.4	1351.4	5.1
X	B	680	135.7	0.0000	50.28	2.24	17413.1	89.0	1.1	1402.5	4.6
	C	730	119.8	0.0001	5.994	4.41	6848.4	98.5	2.4	1379.6	3.4
	D	780	118.3	-0.0002	1.982	18.30	-	99.5	7.9	1377.1	2.0
	E	830	117.6	0.0001	0.5614	53.2	6023.7	99.9	23.8	1374.6	1.8
	F	850	117.1	-0.0001	0.2769	40.9	-	99.9	36.1	1370.9	1.9
	G	880	117.4	0.0004	0.3719	42.4	1314.6	99.9	48.7	1373.5	2.2
	H	900	117.2	0.0006	0.3412	31.0	924.3	99.9	58.0	1372.2	2.3
	I	930	117.5	0.0002	0.3553	30.3	2133.0	99.9	67.1	1374.1	2.0
	J	960	117.6	0.0005	0.6020	17.49	1130.0	99.8	72.3	1374.1	2.4
	K	990	117.5	0.0002	0.6602	14.91	3399.1	99.8	76.8	1373.5	2.3
	L	1020	117.2	0.0002	0.3158	21.6	3308.7	99.9	83.3	1371.6	2.4
	M	1050	117.0	-0.0001	0.2248	27.5	-	99.9	91.5	1370.7	2.2
X	N	1070	114.1	-0.0004	0.5182	6.01	-	99.9	93.3	1346.0	3.3
X	O	1090	114.0	-0.0052	1.072	2.92	-	99.7	94.2	1343.5	4.1
X	P	1110	111.0	-0.0039	0.0182	1.650	-	100.0	94.7	1320.6	5.3
X	Q	1140	110.0	0.0002	0.7379	1.460	2260.5	99.8	95.1	1310.5	5.6
X	R	1350	101.2	-0.0007	1.911	2.66	-	99.4	95.9	1231.2	3.6
X	S	1650	117.3	0.0008	3.440	13.67	663.0	99.1	100.0	1365.0	2.3
	Integrated age ± 1σ			n=19		333.9	7590.3	K2O=10.60%		1370.6	1.4
	Plateau ± 1σ		steps C-M	n=11	MSWD=1.14	301.9			90.4	1373.5	1.0

Appendix 1 $^{40}Ar/^{39}Ar$ analytical data.

	ID	Temperature	$^{40}Ar/^{39}Ar$	$^{37}Ar/^{39}Ar$	$^{36}Ar/^{39}Ar$	$^{39}Ar_K$	K/Ca	$^{40}Ar^*$	^{39}Ar	Age	±1σ
		(°C)			(x 10^{-3})	(x 10^{-15} mol)		(%)	(%)	(Ma)	(Ma)
	P-01-03, Muscovite, 1.11 mg, J=0.0095603±0.09%, D=1.0012±0.0011, NM-254F, Lab#=61430-01										
X	A	630	133.9	0.0016	69.33	2.25	322.6	84.7	0.7	1344.6	5.0
X	B	680	127.2	0.0010	22.02	3.15	530.2	94.9	1.8	1404.0	3.4
X	C	730	122.4	0.0000	6.627	7.61	10563.2	98.4	4.3	1402.3	3.8
	D	780	119.6	0.0007	1.798	16.47	689.9	99.5	9.8	1390.8	2.1
	E	830	119.6	0.0006	0.7511	40.8	802.1	99.8	23.3	1393.3	1.6
	F	850	119.1	0.0007	0.2601	37.2	768.3	99.9	35.7	1390.8	1.7
	G	880	119.5	0.0008	0.4136	39.0	668.0	99.9	48.6	1393.7	1.8
	H	900	119.7	0.0005	0.3874	30.6	951.0	99.9	58.8	1395.6	2.1
	I	930	119.0	0.0012	0.4484	30.9	433.6	99.9	69.0	1389.4	1.7
	J	960	119.0	0.0008	0.6650	20.4	659.9	99.8	75.8	1388.7	1.9
X	K	990	118.6	-0.0001	0.6037	17.00	-	99.8	81.5	1385.7	2.5
X	L	1020	119.7	0.0001	0.3695	20.5	5503.8	99.9	88.3	1395.8	2.4
X	M	1050	119.4	-0.0005	0.3015	20.2	-	99.9	95.0	1392.9	2.4
X	N	1070	118.5	0.0014	0.6429	4.47	363.2	99.8	96.5	1384.8	3.4
X	O	1090	118.0	0.0080	1.866	1.816	64.0	99.5	97.1	1377.6	5.4
X	P	1110	120.8	0.0038	3.392	1.161	134.9	99.2	97.4	1397.5	5.4
X	Q	1140	120.0	-0.0061	-0.4097	0.806	-	100.1	97.7	1399.9	8.6
X	R	1350	120.2	0.0016	3.898	1.538	316.3	99.0	98.2	1391.3	4.8
X	S	1650	121.0	0.0000	8.309	5.35	-	98.0	100.0	1386.6	3.0
	Integrated age ± 1σ			n=19		301.1	848.7	K2O=10.90%		1391.8	1.5
	Plateau ± 1σ		steps D-J	n=7	MSWD=1.77	215.4			71.5	1391.7	1.2
	Terminal Age ± 1σ		steps L-M	n=2	MSWD=0.74	40.6			13.5	1394.4	1.9
	P-01-04, Muscovite, 1.47 mg, J=0.0095628±0.09%, D=1.0012±0.0011, NM-254F, Lab#=61432-01										
X	A	630	118.0	0.0021	44.27	1.647	243.3	88.9	0.4	1272.0	5.7
X	B	680	123.7	0.0035	19.88	2.16	144.2	95.2	0.9	1381.0	4.2
X	C	730	120.6	0.0009	6.476	4.21	566.1	98.4	1.9	1388.4	3.5
X	D	780	116.6	0.0007	2.057	9.09	739.4	99.5	4.0	1366.0	3.2
X	E	830	116.3	0.0007	1.139	27.3	754.5	99.7	10.3	1365.8	1.9
X	F	850	116.5	0.0006	0.3948	59.7	880.6	99.9	24.1	1369.4	1.6
X	G	880	115.5	0.0005	0.3408	57.6	1023.7	99.9	37.5	1360.8	2.0
X	H	900	114.8	0.0011	0.4046	32.8	485.7	99.9	45.1	1355.0	2.0
X	I	930	111.8	0.0007	0.3623	29.8	727.3	99.9	52.0	1329.8	2.4
X	J	960	114.8	0.0005	0.4329	23.905	1074.1	99.9	57.5	1355.0	2.1
X	K	990	113.6	0.0013	0.5625	23.072	389.6	99.8	62.9	1344.9	2.0
X	L	1020	113.7	0.0007	0.6118	28.275	691.1	99.8	69.4	1345.1	3.0
	M	1050	116.3	0.0009	0.2492	44.7	585.2	99.9	79.7	1368.3	2.3
	N	1070	115.6	0.0006	0.2847	63.1	903.5	99.9	94.4	1362.2	1.6
X	O	1090	112.3	0.0015	0.5493	12.97	346.3	99.8	97.4	1333.9	2.7
X	P	1110	110.9	0.0021	2.028	4.03	243.8	99.5	98.3	1318.1	3.5
X	Q	1140	112.9	0.0015	0.5945	2.14	344.8	99.8	98.8	1338.8	4.9
X	R	1350	113.5	-0.0006	4.030	2.02	-	98.9	99.3	1334.9	4.1
X	S	1650	117.3	0.0045	12.45	3.21	113.8	96.9	100.0	1346.3	2.9
	Integrated age ± 1σ			n=19		431.7		K2O=11.80%		1357.2	1.5
	Terminal Age ± 1σ		steps M-N	n=2	MSWD=4.79	107.724			25.0	1364.18	3.0

Appendix 1 $^{40}Ar/^{39}Ar$ analytical data.

	ID	Temperature	$^{40}Ar/^{39}Ar$	$^{37}Ar/^{39}Ar$	$^{36}Ar/^{39}Ar$	$^{39}Ar_K$	K/Ca	$^{40}Ar^*$	^{39}Ar	Age	±1σ
		(°C)			(x 10^{-3})	(x 10^{-15} mol)		(%)	(%)	(Ma)	(Ma)
	P-01-05, Muscovite, .58 mg, J=0.009539±0.08%, D=1.0045±0.0011, NM-254G, Lab#=61434-01										
X	A	630	108.2	-0.0274	15.05	2.185	-	95.9	1.2	1258.9	4.1
X	B	680	116.5	-0.0052	7.938	2.553	-	98.0	2.6	1348.2	3.6
X	C	730	116.3	0.0066	6.705	4.09	77.4	98.3	4.8	1349.6	3.7
X	D	780	114.1	-0.0008	4.457	9.19	-	98.8	9.9	1337.1	2.4
x	E	830	114.4	0.0017	2.199	19.90	291.8	99.4	20.7	1345.0	1.6
x	F	850	114.6	0.0032	0.7619	19.88	160.3	99.8	31.6	1350.1	1.7
x	G	880	114.6	0.0017	0.7852	21.87	305.5	99.8	43.6	1349.9	2.1
x	H	900	114.7	0.0023	0.5668	15.36	217.8	99.8	52.0	1351.4	2.0
	I	930	115.7	0.0030	0.8684	13.52	171.9	99.8	59.4	1358.8	1.9
	J	960	115.6	0.0053	1.117	11.55	97.0	99.7	65.7	1357.6	2.0
	K	990	116.5	0.0043	1.452	10.39	117.4	99.6	71.4	1363.9	2.0
	L	1020	115.9	0.0023	1.259	13.21	219.4	99.7	78.6	1360.0	1.9
x	M	1050	115.7	0.0024	1.174	18.81	211.2	99.7	88.9	1358.0	1.7
X	N	1070	115.6	0.0020	0.9686	12.98	257.6	99.7	96.0	1358.2	1.9
X	O	1090	114.6	0.0032	1.786	5.00	159.3	99.5	98.7	1347.8	2.9
X	P	1110	116.8	-0.0040	13.72	1.292	-	96.5	99.4	1336.3	6.3
X	Q	1140	106.9	0.0345	13.19	0.397	14.8	96.4	99.6	1253.1	15.2
X	R	1350	118.9	0.1026	81.51	0.173	5.0	79.7	99.7	1179.3	26.0
X	S	1650	138.6	-0.0006	123.7	0.477	-	73.6	100.0	1243.9	12.0
	Integrated age ± 1σ			n=19		182.9		K2O=12.70%		1351.1	1.4
	Terminal Age ± 1σ		steps I-L	n=4	MSWD=1.83	48.670			26.6	1360.04	1.5
	P-01-06, Muscovite, 1.19 mg, J=0.0095275±0.07%, D=1.0045±0.0011, NM-254G, Lab#=61436-01										
X	A	630	105.0	0.0141	19.79	8.93	36.1	94.4	2.4	1217.4	2.5
X	B	680	109.5	0.0163	1.565	1.341	31.2	99.6	2.8	1304.4	5.5
X	C	730	111.2	0.0058	1.761	4.84	88.6	99.5	4.1	1317.6	3.6
X	D	780	112.2	0.0075	1.012	14.68	67.9	99.7	8.1	1328.3	1.8
	E	830	113.5	0.0039	0.5865	35.85	130.7	99.8	17.9	1340.4	1.9
	F	840	113.7	0.0036	0.4736	24.14	142.5	99.9	24.5	1342.4	2.2
	G	850	113.3	0.0036	0.5598	20.77	141.1	99.8	30.1	1339.0	1.5
	H	880	113.6	0.0025	0.4311	29.45	206.5	99.9	38.2	1341.8	1.9
	I	900	113.8	0.0036	0.4502	27.45	141.1	99.9	45.6	1342.9	1.8
	J	930	113.4	0.0025	0.3512	30.16	202.0	99.9	53.9	1339.9	2.0
	K	960	113.2	0.0036	0.5169	29.90	141.7	99.9	62.0	1337.9	2.1
	L	990	113.0	0.0028	0.5818	25.63	184.6	99.8	69.0	1336.1	1.8
X	M	1005	112.0	0.0046	0.6560	17.89	110.4	99.8	73.9	1327.8	1.7
X	N	1020	112.8	0.0057	0.7384	14.39	89.4	99.8	77.8	1333.7	2.0
X	O	1035	113.1	0.0058	0.6345	12.13	87.7	99.8	81.1	1336.7	2.2
X	P	1050	113.2	0.0020	0.5966	10.14	251.0	99.8	83.8	1338.1	2.1
X	Q	1070	112.6	0.0073	0.7199	9.35	69.8	99.8	86.4	1332.1	1.8
X	R	1090	113.4	0.0049	0.7095	6.14	103.9	99.8	88.1	1339.1	2.6
X	S	1350	114.5	0.0094	2.038	7.65	54.4	99.5	90.2	1345.4	2.5
X	T	1650	115.2	0.0021	1.594	36.12	241.9	99.6	100.0	1351.9	1.8
	Integrated age ± 1σ			n=20		366.9	123.4	K2O=12.43%		1336.3	1.3
	Plateau ± 1σ		steps E-L	n=8	MSWD=1.54	223.3			60.9	1339.9	1.1
	Terminal Age ± 1σ		steps T-T	n=1	MSWD=0.00	36.1			9.8	1351.9	1.8

Appendix 1 $^{40}Ar/^{39}Ar$ analytical data.

	ID	Temperature (°C)	$^{40}Ar/^{39}Ar$	$^{37}Ar/^{39}Ar$	$^{36}Ar/^{39}Ar$ (x 10^{-3})	$^{39}Ar_K$ (x 10^{-15} mol)	K/Ca	$^{40}Ar^*$ (%)	^{39}Ar (%)	Age (Ma)	±1σ (Ma)
	Meadow, Muscovite, .88 mg, J=0.0095456±0.11%, D=1.0045±0.0011, NM-254G, Lab#=61446-01										
X	A	680	106.9	0.0087	50.99	2.943	58.9	85.9	1.0	1152.0	5.6
X	B	730	108.8	0.0028	6.236	4.13	181.7	98.3	2.4	1287.9	3.5
X	C	780	110.7	-0.0017	1.718	9.21	-	99.5	5.5	1315.6	2.6
	D	830	112.8	0.0011	0.7910	33.68	474.2	99.8	16.9	1335.5	2.2
	E	850	112.4	0.0020	0.3268	39.7	258.5	99.9	30.3	1333.9	1.8
	F	880	112.3	0.0027	0.4505	35.16	189.2	99.9	42.2	1332.6	2.0
x	G	930	111.2	0.0028	0.2984	48.5	184.9	99.9	58.7	1323.2	2.2
x	H	960	109.0	0.0050	0.6259	17.33	101.8	99.8	64.5	1304.2	2.0
X	I	990	109.3	0.0063	0.7527	11.96	80.8	99.8	68.6	1305.7	2.3
X	J	1050	111.3	0.0062	0.3124	25.09	82.6	99.9	77.0	1324.2	2.4
X	K	1070	112.9	0.0033	0.5238	22.85	154.4	99.9	84.8	1337.2	2.6
X	L	1090	113.5	0.0014	0.5708	10.52	369.5	99.8	88.3	1342.4	3.3
X	M	1350	114.5	0.0389	2.157	11.77	13.1	99.4	92.3	1346.3	2.8
X	N	1650	115.6	0.0071	2.579	22.71	71.7	99.3	100.0	1354.4	3.0
	Integrated age ± 1σ			n=14		295.6	108.4	K2O=13.52%		1328.2	1.6
	Plateau ± 1σ		steps D-F	n=3	MSWD=0.49	108.569			36.7	1333.90	1.5
	Terminal Age ± 1σ		steps N-N	n=1	MSWD=0.00	22.7			7.7	1354.4	3.0
	Cribbenville, Muscovite, .88 mg, J=0.0095182±0.10%, D=1.0045±0.0011, NM-254G, Lab#=61442-02										
X	A	680	118.3	0.1139	31.72	2.245	4.5	92.1	0.8	1302.4	6.0
X	B	730	127.2	0.0009	41.93	3.102	569.9	90.3	2.0	1351.5	5.2
X	C	780	118.8	0.0020	6.415	6.03	249.0	98.4	4.2	1368.8	3.0
x	D	830	116.3	0.0032	2.531	19.47	158.5	99.4	11.4	1358.3	2.0
x	E	850	115.4	0.0043	0.5128	24.79	119.7	99.9	20.6	1355.1	2.4
x	F	880	116.0	0.0018	0.5301	41.1	290.1	99.9	35.9	1360.3	1.9
x	G	930	115.2	0.0028	0.5443	40.1	182.2	99.9	50.8	1354.0	2.0
x	H	960	114.6	0.0023	0.5444	24.65	225.0	99.9	59.9	1348.9	2.7
x	I	990	114.2	0.0020	0.7463	15.60	250.0	99.8	65.7	1344.9	2.4
x	J	1050	114.5	0.0028	0.7982	23.41	183.3	99.8	74.4	1347.5	2.5
	K	1070	115.3	0.0024	0.4935	29.86	215.0	99.9	85.5	1354.8	2.2
	L	1090	115.7	0.0010	0.2160	23.07	499.3	99.9	94.0	1359.0	2.9
X	M	1350	111.9	0.0006	1.862	11.33	831.1	99.5	98.2	1322.9	3.0
X	N	1650	115.7	-0.0035	7.335	4.75	-	98.1	100.0	1341.5	4.4
	Integrated age ± 1σ			n=14		269.4		K2O=12.36%		1352.7	1.6
	Terminal Age ± 1σ		steps K-L	n=2	MSWD=1.33	52.936			19.6	1356.33	2.2

Appendix 1 $^{40}Ar/^{39}Ar$ analytical data.

	ID	Temperature (°C)	$^{40}Ar/^{39}Ar$	$^{37}Ar/^{39}Ar$	$^{36}Ar/^{39}Ar$ (x 10^{-3})	$^{39}Ar_K$ (x 10^{-15} mol)	K/Ca	$^{40}Ar^*$ (%)	^{39}Ar (%)	Age (Ma)	±1σ (Ma)
	Queen , Muscovite, .43 mg, J=0.0095116±0.07%, D=1.0045±0.0011, NM-254G, Lab#=61438-01										
X	B	630	121.9	0.0155	114.4	0.946	32.9	72.3	0.7	1114.4	7.6
X	C	680	118.0	-0.0155	43.16	1.733	-	89.2	2.1	1270.0	4.4
X	D	730	114.0	-0.0039	7.587	4.18	-	98.0	5.4	1325.2	2.8
	E	750	115.9	-0.0066	2.667	3.380	-	99.3	8.1	1353.5	3.2
	F	780	115.8	-0.0011	1.741	5.56	-	99.5	12.4	1354.9	2.6
	G	810	116.0	-0.0030	1.277	8.74	-	99.7	19.3	1357.7	2.0
	H	830	115.7	0.0022	0.1489	9.98	232.6	100.0	27.1	1358.5	2.0
	I	840	115.5	-0.0011	0.3318	8.29	-	99.9	33.6	1355.6	2.4
	J	850	116.4	0.0014	0.1973	7.01	357.5	99.9	39.2	1363.5	2.6
	K	865	115.4	0.0058	-0.0996	6.97	87.2	100.0	44.6	1356.1	2.7
	L	880	116.2	0.0022	0.0852	6.67	233.0	100.0	49.9	1362.7	2.4
	M	900	116.0	0.0034	0.2789	7.06	151.9	99.9	55.4	1360.3	2.4
	N	915	116.4	0.0018	0.3274	5.60	287.9	99.9	59.8	1363.1	2.6
	O	930	115.7	0.0001	0.2976	4.88	10123.1	99.9	63.7	1357.9	3.5
	P	960	117.2	0.0093	0.9457	6.77	54.9	99.8	69.0	1369.0	3.3
	Q	990	115.8	0.0025	1.300	7.54	207.9	99.7	74.9	1356.0	2.2
	R	1020	115.8	0.0007	0.5214	10.12	738.7	99.9	82.9	1357.8	2.5
	S	1050	116.3	-0.0001	0.3120	8.92	-	99.9	89.9	1362.4	2.6
	T	1070	117.2	0.0006	0.1606	4.19	895.1	100.0	93.2	1370.4	3.1
X	U	1090	115.6	-0.0081	-0.6593	1.614	-	100.2	94.5	1359.0	5.0
X	V	1350	116.0	0.0030	3.825	3.007	172.0	99.0	96.8	1351.5	3.5
X	W	1650	117.6	0.0029	10.41	4.04	176.2	97.4	100.0	1348.3	3.3
	Integrated age ± 1σ			n=22		127.2		K2O=11.95%		1355.2	1.4
	Plateau ± 1σ		steps E-T	n=16	MSWD=2.90	111.7			87.8	1359.5	1.3
	Vestegard, Muscovite, 1.31 mg, J=0.0095097±0.07%, D=1.0045±0.0011, NM-254G, Lab#=61440-01										
X	A	600	127.0	0.0114	86.02	2.451	44.9	80.0	0.6	1237.5	5.3
X	B	630	110.6	-0.0050	2.713	0.701	-	99.3	0.8	1308.6	10.0
X	C	680	113.8	-0.0095	12.21	2.283	-	96.8	1.4	1311.7	4.7
X	D	710	114.6	-0.0057	10.57	3.310	-	97.3	2.2	1323.3	4.0
X	E	730	113.2	-0.0083	5.621	4.08	-	98.5	3.2	1323.2	3.3
X	F	750	113.7	0.0033	6.108	5.01	154.8	98.4	4.5	1326.4	3.2
X	G	780	113.8	0.0000	6.097	7.74	47241.1	98.4	6.5	1327.0	2.4
X	H	800	113.6	0.0023	3.798	10.62	224.5	99.0	9.1	1331.1	1.8
X	I	830	115.2	0.0019	1.507	24.50	263.0	99.6	15.3	1350.7	2.4
X	J	840	114.3	0.0000	0.6952	23.73	16044.2	99.8	21.3	1345.2	2.1
X	K	850	112.3	0.0011	0.6791	16.51	452.3	99.8	25.5	1328.1	1.8
X	L	865	112.4	0.0020	0.8581	17.53	255.4	99.8	29.9	1328.6	2.0
X	M	880	113.2	0.0025	0.6154	18.78	208.0	99.8	34.7	1335.6	2.0
X	N	900	115.1	0.0013	0.7213	22.07	402.9	99.8	40.3	1351.3	2.1
X	O	915	116.8	0.0024	1.206	19.72	208.5	99.7	45.2	1364.1	1.9
X	P	930	117.6	0.0017	1.032	16.59	298.2	99.7	49.4	1371.1	1.7
X	Q	945	117.8	0.0025	1.008	15.74	207.9	99.7	53.4	1373.5	1.7
	R	960	118.6	0.0037	1.266	17.42	136.7	99.7	57.8	1379.4	1.7
	S	990	119.0	0.0024	1.289	29.51	211.3	99.7	65.3	1382.4	1.9
	T	1005	118.6	0.0016	1.101	29.53	311.4	99.7	72.7	1379.5	2.3
	U	1020	118.2	0.0028	0.6303	30.16	179.4	99.8	80.3	1377.3	1.8
	V	1050	118.5	0.0035	0.3913	45.0	145.3	99.9	91.7	1380.7	1.6
X	W	1070	117.1	0.0036	0.7194	19.67	140.3	99.8	96.7	1368.5	2.0
X	X	1090	117.0	0.0084	-0.1544	4.85	60.7	100.0	97.9	1369.2	3.3
X	Y	1350	117.9	0.0069	3.011	4.57	73.8	99.2	99.1	1368.8	3.1
X	Z	1650	118.5	0.0024	9.621	3.696	209.5	97.6	100.0	1358.0	3.5
	Integrated age ± 1σ			n=26		395.8		K2O=12.20%		1360.1	1.3
	Terminal Age ± 1σ		steps R-V	n=5	MSWD=1.04	151.615			38.3	1379.85	1.1

Appendix 1 $^{40}Ar/^{39}Ar$ analytical data.

	ID	Temperature	$^{40}Ar/^{39}Ar$	$^{37}Ar/^{39}Ar$	$^{36}Ar/^{39}Ar$	$^{39}Ar_K$	K/Ca	$^{40}Ar^*$	^{39}Ar	Age	±1σ
		(°C)			(x 10^{-3})	(x 10^{-15} mol)		(%)	(%)	(Ma)	(Ma)
	Bluebird, Muscovite, 1.48 mg, J=0.0095297±0.11%, D=1.0045±0.0011, NM-254G, Lab#=61444-01										
X	A	630	129.8	-0.0074	69.13	2.183	-	84.3	0.5	1306.7	5.2
X	B	680	135.2	-0.0058	64.26	2.738	-	85.9	1.1	1364.6	4.6
X	C	700	116.6	-0.0174	4.929	2.827	-	98.7	1.8	1355.6	3.9
X	D	730	118.5	-0.0013	5.477	4.57	-	98.6	2.8	1369.9	3.3
X	E	750	117.0	-0.0054	4.456	5.23	-	98.9	4.0	1360.3	2.9
X	F	780	116.7	-0.0016	2.649	8.63	-	99.3	6.0	1362.0	2.3
	G	800	116.7	0.0002	0.8362	19.46	2235.8	99.8	10.5	1366.9	1.7
	H	815	117.1	0.0002	0.4685	29.86	2858.3	99.9	17.3	1370.4	2.0
	I	830	117.2	0.0019	0.2890	36.71	268.9	99.9	25.8	1371.9	2.0
	J	850	117.1	0.0021	0.2960	44.4	242.2	99.9	36.0	1370.9	1.6
	K	865	116.7	0.0014	0.2652	41.0	367.0	99.9	45.4	1367.7	2.0
	L	880	116.7	0.0016	0.2969	37.35	327.2	99.9	54.0	1367.9	1.7
	M	900	116.7	0.0032	0.2534	35.07	159.2	99.9	62.0	1368.4	2.0
	N	930	117.2	0.0023	0.5281	35.67	217.4	99.9	70.2	1371.1	1.7
	O	945	116.8	0.0020	0.4005	23.55	258.7	99.9	75.6	1368.2	1.9
X	P	960	115.6	0.0021	0.7232	16.87	240.6	99.8	79.5	1357.9	1.8
X	Q	975	115.8	0.0050	1.117	12.96	101.3	99.7	82.4	1358.8	2.1
X	R	990	116.4	0.0015	0.8169	11.33	347.3	99.8	85.0	1364.0	2.1
X	S	1020	116.6	0.0010	0.7333	17.11	521.6	99.8	89.0	1365.9	1.8
X	T	1035	116.4	0.0004	0.0949	15.88	1337.7	100.0	92.6	1365.7	2.0
X	U	1050	116.4	0.0031	0.4331	13.12	166.3	99.9	95.6	1364.8	2.0
X	V	1070	115.9	0.0024	0.1104	10.64	210.7	100.0	98.1	1361.6	2.1
X	W	1090	114.7	0.0020	-0.4426	4.26	256.6	100.1	99.1	1353.1	3.5
X	X	1650	117.3	-0.0043	11.60	4.11	-	97.1	100.0	1344.8	3.4
	Integrated age ± 1σ			n=24		435.5		K2O=11.86%		1366.8	1.6
	Plateau ± 1σ		steps G-O	n=9	MSWD=0.96	303.1			69.6	1369.3	1.2
	B-01-01, Muscovite, .53 mg, J=0.0095478±0.10%, D=1.0045±0.0011, NM-254G, Lab#=61482-01										
X	A	630	108.0	-0.0113	97.76	1.359	-	73.2	0.9	1029.6	6.7
X	B	680	113.8	-0.0311	11.78	1.357	-	96.9	1.8	1316.5	4.9
X	C	730	113.9	-0.0144	5.887	3.520	-	98.5	4.1	1332.7	3.4
X	D	750	115.2	-0.0107	1.867	3.591	-	99.5	6.4	1353.2	4.2
X	E	780	114.1	-0.0070	1.959	5.58	-	99.5	10.0	1343.5	2.7
X	F	810	115.1	0.0006	0.9014	9.10	850.3	99.8	16.0	1355.2	2.1
X	G	830	113.9	0.0015	0.7784	10.76	351.7	99.8	23.0	1345.0	1.9
	H	840	114.5	0.0004	0.3318	9.13	1147.3	99.9	28.9	1351.2	2.4
	I	850	114.2	-0.0013	0.3641	8.37	-	99.9	34.4	1349.0	2.3
	J	880	114.9	0.0031	0.5874	12.29	163.1	99.8	42.4	1354.0	2.2
	K	900	114.4	0.0011	0.4732	11.50	447.9	99.9	49.8	1350.2	2.0
	L	930	114.2	-0.0003	0.4436	12.46	-	99.9	58.0	1348.3	1.7
	M	945	114.2	-0.0051	0.4917	8.52	-	99.9	63.5	1348.1	2.2
	N	960	113.4	0.0003	0.5882	6.91	1524.4	99.8	68.0	1341.7	2.6
	O	990	113.7	0.0027	0.4446	8.07	191.4	99.9	73.3	1344.6	2.3
	P	1005	113.6	-0.0026	0.5616	6.74	-	99.8	77.7	1343.3	2.6
X	Q	1020	114.8	-0.0012	0.2230	5.75	-	99.9	81.4	1354.1	2.4
X	R	1050	114.7	-0.0031	0.5003	7.02	-	99.9	86.0	1352.7	2.5
X	S	1070	116.1	-0.0015	1.208	5.17	-	99.7	89.3	1362.1	2.1
X	T	1110	114.4	-0.0081	2.568	2.446	-	99.3	90.9	1345.1	5.6
X	U	1350	116.2	0.0003	2.369	5.78	1501.9	99.4	94.7	1360.8	2.8
X	V	1650	117.4	-0.0016	5.631	8.14	-	98.6	100.0	1362.6	2.7
	Integrated age ± 1σ			n=22		153.5		K2O=11.66%		1347.3	1.5
	Plateau ± 1σ		steps H-P	n=9	MSWD=2.77	83.983			54.7	1348.22	1.6

Appendix 1 $^{40}Ar/^{39}Ar$ analytical data.

	ID	Temperature	$^{40}Ar/^{39}Ar$	$^{37}Ar/^{39}Ar$	$^{36}Ar/^{39}Ar$	$^{39}Ar_K$	K/Ca	$^{40}Ar^*$	^{39}Ar	Age	±1σ
		(°C)			(x 10^{-3})	(x 10^{-15} mol)		(%)	(%)	(Ma)	(Ma)
	B-02-02, Muscovite, .88 mg, J=0.0094925±0.08%, D=1.0045±0.0011, NM-254K, Lab#=61468-01										
X	A	630	92.08	0.0092	17.73	7.70	55.7	94.3	3.0	1100.5	2.5
X	B	680	106.0	-0.0305	2.269	0.746	-	99.4	3.3	1268.3	9.0
X	C	730	108.1	0.0057	1.128	2.156	88.9	99.7	4.2	1289.8	4.7
X	D	750	108.9	-0.0004	1.033	2.828	-	99.7	5.3	1296.9	3.7
X	E	780	110.7	0.0028	0.4591	5.77	183.6	99.9	7.5	1313.3	2.4
X	F	810	113.0	-0.0012	0.6281	12.48	-	99.8	12.4	1332.9	2.0
x	G	830	114.2	0.0021	0.4868	20.04	245.1	99.9	20.3	1343.1	1.7
x	H	840	114.2	0.0048	0.5221	17.10	105.3	99.9	27.0	1343.0	1.8
x	I	850	113.6	0.0021	0.1761	14.12	247.2	99.9	32.6	1338.5	1.9
x	J	880	114.5	0.0032	0.5193	21.52	161.9	99.9	41.0	1345.2	2.3
x	K	900	113.9	0.0033	0.6068	17.48	155.6	99.8	47.9	1340.1	1.7
x	L	930	113.2	0.0047	0.3506	18.28	107.7	99.9	55.1	1334.5	1.7
x	M	945	113.0	0.0011	0.5025	12.00	452.5	99.9	59.8	1332.9	1.9
x	N	960	112.7	0.0036	0.3566	8.65	142.0	99.9	63.2	1330.5	2.1
x	O	990	113.8	0.0033	0.4709	10.51	156.5	99.9	67.3	1339.4	2.0
x	P	1005	113.8	0.0065	0.5194	9.40	78.6	99.9	71.0	1339.3	2.4
x	Q	1020	114.5	0.0073	0.4694	9.36	69.7	99.9	74.7	1345.5	2.1
x	R	1050	114.8	-0.0004	0.3864	13.99	-	99.9	80.2	1348.1	2.0
x	S	1070	115.7	0.0033	0.3458	14.38	155.4	99.9	85.8	1355.9	2.2
	T	1110	116.7	0.0032	0.6033	21.79	157.5	99.8	94.4	1363.3	2.1
X	U	1350	113.5	0.0221	1.213	11.04	23.1	99.7	98.7	1335.0	2.3
X	V	1650	118.8	0.0140	14.17	3.318	36.4	96.5	100.0	1347.8	4.6
	Integrated age ± 1σ			n=22		254.7		K2O=11.71%		1334.3	1.4
	Terminal Age ± 1σ		steps T-T	n=1	MSWD=0.0	21.790			8.6	1363.30	2.1

Appendix 1 $^{40}Ar/^{39}Ar$ analytical data.

	ID	Temperature (°C)	$^{40}Ar/^{39}Ar$	$^{37}Ar/^{39}Ar$	$^{36}Ar/^{39}Ar$ (x 10^{-3})	$^{39}Ar_K$ (x 10^{-15} mol)	K/Ca	$^{40}Ar^*$ (%)	^{39}Ar (%)	Age (Ma)	±1σ (Ma)
	B-01-06, Muscovite, .44 mg, J=0.0094845±0.09%, D=1.0045±0.0011, NM-254K, Lab#=61469-01										
X	A	630	83.81	0.0018	24.51	0.698	281.4	91.3	0.9	999.2	8.2
X	B	650	115.3	-0.0058	5.236	0.379	-	98.7	1.4	1339.1	13.5
X	C	680	116.6	-0.0155	3.783	0.553	-	99.0	2.1	1354.1	9.2
X	D	710	113.6	-0.0065	-0.7132	0.931	-	100.2	3.2	1340.3	6.8
X	E	730	113.0	-0.0270	0.6772	1.056	-	99.8	4.6	1331.3	5.9
	F	750	112.8	-0.0010	0.9809	1.426	-	99.7	6.4	1329.3	4.8
	G	780	113.1	0.0218	0.1221	2.705	23.4	100.0	9.8	1333.8	3.3
	H	800	113.4	0.0106	-0.1195	3.255	48.0	100.0	13.9	1337.3	3.8
	I	815	113.5	0.0128	-0.6370	3.77	39.7	100.2	18.7	1339.4	2.7
	J	830	113.6	0.0045	-0.1283	4.36	112.6	100.0	24.2	1338.7	3.1
	K	850	113.8	0.0056	0.2638	5.43	91.9	99.9	31.1	1339.5	2.8
	L	865	113.6	-0.0012	0.6793	5.26	-	99.8	37.7	1336.6	2.7
x	M	880	114.7	0.0065	0.2545	4.84	78.5	99.9	43.8	1347.0	2.9
x	N	900	114.2	0.0053	0.3103	5.03	96.0	99.9	50.2	1342.1	2.6
x	O	915	112.5	-0.0057	0.0862	4.43	-	100.0	55.8	1328.7	2.6
x	P	930	112.7	0.0074	-0.2636	3.87	69.4	100.1	60.7	1331.4	3.2
x	Q	945	114.1	0.0051	0.2381	3.603	99.4	99.9	65.2	1341.7	3.1
x	R	960	113.7	0.0022	-0.0410	3.481	233.1	100.0	69.6	1339.2	3.3
x	S	975	114.7	0.0033	0.0123	3.183	153.0	100.0	73.7	1347.5	3.6
x	T	990	113.4	0.0066	-0.4179	3.166	76.7	100.1	77.7	1337.6	3.6
x	U	1005	114.2	-0.0085	0.3239	3.076	-	99.9	81.5	1342.5	3.5
x	V	1020	115.4	-0.0122	-0.5639	2.957	-	100.1	85.3	1354.4	4.5
x	W	1050	115.3	0.0179	0.5160	3.610	28.6	99.9	89.8	1351.2	3.5
x	X	1070	116.6	0.0016	-0.2197	2.803	328.0	100.0	93.4	1363.8	3.7
x	Y	1090	116.2	0.0120	0.6467	1.814	42.4	99.8	95.7	1358.1	4.9
x	Z	1110	121.2	0.0525	2.027	0.673	9.7	99.5	96.5	1396.3	9.8
x	AA	1650	123.7	0.0171	24.57	2.741	29.8	94.1	100.0	1361.8	4.4
	Integrated age ± 1σ			n=27		79.1	109.1	K2O=7.28%		1339.8	1.5
	Plateau ± 1σ		steps F-L	n=7	MSWD=0.91	26.2			33.1	1337.2	1.5
	Terminal Age ± 1σ		steps V-X	n=3	MSWD=3.20	9.4			11.8	1356.5	4.1

Notes:

Isotopic ratios corrected for blank, radioactive decay, and mass discrimination, not corrected for interfering reactions.

Errors quoted for individual analyses include analytical error only, without interfering reaction or J uncertainties.

Integrated age calculated by summing isotopic measurements of all steps.

Integrated age error calculated by quadratically combining errors of isotopic measurements of all steps.

Plateau age is inverse-variance-weighted mean of selected steps.

Plateau age error is inverse-variance-weighted mean error (Taylor, 1982) times root MSWD where MSWD>1.

Plateau error is weighted error of Taylor (1982).

Isotopic abundances after Steiger and Jäger (1977).

Weight percent K_2O calculated from ^{39}Ar signal, sample weight, and instrument sensitivity.

X preceding sample ID denotes analysis excluded from plateau age calculations.

Ages calculated relative to FC-2 Fish Canyon Tuff sanidine interlaboratory standard at 28.201 Ma

Decay Constant (LambdaK (total)) = 5.463e-10/a

Correction factors:

$(^{39}Ar/^{37}Ar)_{Ca}$ = 0.000698 ± 8e-06

$(^{36}Ar/^{37}Ar)_{Ca}$ = 0.000273 ± 2e-07

$(^{38}Ar/^{39}Ar)_{K}$ = 0.013

$(^{40}Ar/^{39}Ar)_{K}$ = 0.008068 ± 6.8e-05

Appendix 1 $^{40}Ar/^{39}Ar$ analytical data.

	ID	Temperature (°C)	$^{40}Ar/^{39}Ar$	$^{37}Ar/^{39}Ar$	$^{36}Ar/^{39}Ar$ (x 10^{-3})	$^{39}Ar_K$ (x 10^{-15} mol)	K/Ca	$^{40}Ar^*$ (%)	^{39}Ar (%)	Age (Ma)	±1σ (Ma)
	2-1, Muscovite, .61 mg, J=0.014653±0.07%, D=1.0045±0.0011, NM-261A, Lab#=61976-01										
x	A	600	76.08	0.0076	26.09	1.91	67.4	89.9	0.8	1270.3	3.6
x	B	620	80.54	0.0031	15.55	1.073	162.3	94.3	1.2	1369.2	4.3
x	C	650	94.31	-0.0002	57.68	1.514	-	81.9	1.8	1385.9	5.1
x	D	680	80.42	0.0027	12.65	2.30	189.7	95.3	2.7	1378.5	3.2
x	E	700	80.01	0.0013	11.30	2.98	383.6	95.8	3.9	1378.4	2.8
x	F	720	78.22	0.0017	6.548	4.37	295.1	97.5	5.6	1373.5	2.5
	G	750	77.64	0.0010	4.802	9.31	529.6	98.2	9.3	1372.7	1.9
	H	770	76.42	0.0008	1.519	16.8	672.7	99.4	15.9	1369.5	1.9
	I	785	76.57	0.0008	0.9185	21.9	658.3	99.6	24.5	1373.7	1.8
	J	800	76.21	0.0010	0.6216	22.4	501.2	99.7	33.4	1370.2	1.6
	K	820	76.35	0.0010	0.5427	22.1	490.2	99.8	42.1	1372.3	1.6
	L	835	76.21	0.0012	0.6234	17.7	443.1	99.7	49.1	1370.2	2.0
	M	850	76.14	0.0010	0.6630	15.09	507.7	99.7	55.0	1369.2	2.0
	N	870	76.23	0.0008	0.7474	13.66	637.5	99.7	60.4	1369.9	1.9
	O	885	76.61	0.0011	0.8448	10.52	463.3	99.7	64.6	1374.4	2.2
	P	900	76.00	0.0015	1.088	8.20	337.5	99.6	67.8	1365.8	2.2
	Q	915	76.22	0.0014	1.328	6.50	367.1	99.5	70.4	1367.7	2.1
	R	930	76.03	0.0021	1.070	5.66	240.2	99.6	72.6	1366.2	2.0
	S	945	76.05	0.0014	1.534	5.13	352.5	99.4	74.6	1364.8	2.1
	T	960	75.79	0.0005	1.150	5.34	995.3	99.5	76.8	1362.9	2.3
x	U	975	76.36	0.0001	1.389	5.36	7105.9	99.5	78.9	1369.2	2.2
x	V	990	76.04	0.0019	1.223	5.79	269.4	99.5	81.2	1365.8	2.0
x	W	1020	76.32	0.0012	1.256	8.78	414.2	99.5	84.6	1369.3	2.1
x	X	1040	76.51	0.0010	0.8157	13.57	495.9	99.7	90.0	1373.3	1.8
x	Y	1060	76.38	0.0005	0.6326	16.8	965.4	99.7	96.6	1372.3	2.1
x	Z	1080	76.48	0.0014	1.109	8.60	357.4	99.6	100.0	1371.8	1.9
	Integrated age ± 1σ			n=26		253.3		K2O=10.88%		1370.1	1.3
	Plateau ± 1σ		steps G-T	n=14	MSWD=2.85	180.3			71.2	1369.6	1.1

Appendix 1 $^{40}Ar/^{39}Ar$ analytical data.

	ID	Temperature (°C)	$^{40}Ar/^{39}Ar$	$^{37}Ar/^{39}Ar$	$^{36}Ar/^{39}Ar$ (x 10^{-3})	$^{39}Ar_K$ (x 10^{-15} mol)	K/Ca	$^{40}Ar^*$ (%)	^{39}Ar (%)	Age (Ma)	±1σ (Ma)
	2-2, Muscovite, .64 mg, J=0.014653±0.07%, D=1.0045±0.0011, NM-261A, Lab#=61977-01										
x	A	600	75.09	0.0064	44.01	1.415	79.2	82.7	0.4	1184.2	4.3
x	B	620	78.58	0.0036	17.28	1.085	142.3	93.5	0.7	1337.5	5.1
x	C	650	76.91	0.0040	7.204	1.69	126.1	97.2	1.2	1354.3	3.6
x	D	680	78.20	0.0027	8.039	2.72	190.2	97.0	1.9	1367.7	2.9
x	E	700	77.59	0.0025	5.356	3.46	207.6	98.0	2.9	1369.9	2.5
x	F	720	77.25	0.0007	3.064	6.47	722.7	98.8	4.7	1374.2	1.8
	G	740	77.15	0.0005	0.8217	13.22	971.8	99.7	8.4	1381.3	2.0
	H	750	76.72	0.0010	0.4963	12.53	490.3	99.8	11.9	1377.1	2.0
	I	760	76.54	0.0006	0.5793	13.71	830.0	99.8	15.8	1374.5	2.0
	J	770	76.81	0.0013	0.4019	14.33	406.5	99.8	19.8	1378.6	1.9
	K	775	76.63	0.0011	0.6184	13.03	476.4	99.8	23.4	1375.6	2.2
	L	785	76.80	0.0008	0.5411	13.86	612.3	99.8	27.3	1377.9	2.1
	M	785	76.48	0.0006	0.5019	12.20	839.3	99.8	30.7	1374.1	2.3
	N	795	76.76	0.0012	0.6349	13.49	418.2	99.7	34.5	1377.1	2.2
	O	800	76.48	0.0010	0.5547	12.77	521.6	99.8	38.1	1373.9	2.2
	P	805	76.80	0.0005	0.5613	12.02	1094.2	99.8	41.5	1377.8	2.1
	Q	820	76.54	0.0009	0.3465	13.13	584.2	99.9	45.1	1375.4	2.1
	R	825	76.87	0.0007	0.5390	12.59	685.1	99.8	48.7	1378.8	1.8
	S	835	76.93	0.0012	0.5490	12.19	420.3	99.8	52.1	1379.6	1.9
	T	850	76.82	0.0011	0.5514	12.85	457.0	99.8	55.7	1378.1	2.1
	U	870	76.74	0.0009	0.4610	13.60	599.5	99.8	59.5	1377.6	1.7
	V	885	76.76	0.0010	0.7808	11.65	528.7	99.7	62.7	1376.6	2.1
	W	900	76.81	0.0009	0.7271	10.41	591.7	99.7	65.7	1377.4	2.3
	X	915	76.73	0.0007	0.7878	10.99	770.1	99.7	68.7	1376.2	2.2
	Y	930	76.76	0.0008	0.8851	11.95	605.0	99.6	72.1	1376.2	1.7
	Z	945	76.87	0.0007	1.110	13.94	709.3	99.6	76.0	1376.7	2.0
	AA	960	76.63	0.0007	0.7608	15.29	771.8	99.7	80.3	1375.0	2.0
	AB	975	76.97	0.0008	0.5926	14.84	639.1	99.8	84.4	1380.0	2.0
	AC	990	76.94	0.0008	0.6133	14.14	637.8	99.8	88.4	1379.5	1.9
	AD	1020	77.24	0.0006	0.4939	23.6	906.4	99.8	95.0	1383.6	1.7
	AE	1040	77.06	0.0014	0.8832	9.11	360.7	99.7	97.6	1380.0	2.2
x	AF	1060	76.29	0.0042	2.485	2.14	120.6	99.0	98.2	1364.3	3.6
x	AG	1080	78.51	0.0039	6.969	1.174	131.8	97.4	98.5	1375.6	4.5
x	AH	1620	76.23	0.0011	12.18	5.42	478.8	95.3	100.0	1326.6	2.4
	Integrated age ± 1σ			n=34		357.0		K2O=14.62%		1375.7	1.3
	Plateau ± 1σ		steps G-AE	n=25	MSWD=1.42	331.5			92.8	1377.73	0.8

Appendix 1 $^{40}Ar/^{39}Ar$ analytical data.

	ID	Temperature (°C)	$^{40}Ar/^{39}Ar$	$^{37}Ar/^{39}Ar$	$^{36}Ar/^{39}Ar$ (x 10^{-3})	$^{39}Ar_K$ (x 10^{-15} mol)	K/Ca	$^{40}Ar^*$ (%)	^{39}Ar (%)	Age (Ma)	±1σ (Ma)
	2-3, Muscovite, .64 mg, J=0.014653±0.07%, D=1.0045±0.0011, NM-261A, Lab#=61978-01										
x	A	610	112.5	0.0110	138.9	1.391	46.6	63.5	0.5	1311.5	12.7
x	B	650	82.14	0.0038	17.13	2.23	135.2	93.8	1.2	1383.5	6.9
x	C	690	81.02	0.0031	9.166	3.87	164.6	96.6	2.5	1398.9	4.7
x	D	720	78.21	0.0012	4.255	5.26	438.8	98.4	4.2	1381.9	3.4
x	E	740	76.69	0.0023	4.027	6.10	226.6	98.4	6.3	1363.6	4.3
x	F	750	76.14	0.0028	1.390	6.01	183.0	99.5	8.3	1366.4	3.0
x	G	760	75.78	0.0015	1.163	6.31	348.0	99.5	10.4	1362.7	3.6
x	H	770	76.84	0.0015	1.497	6.80	343.0	99.4	12.6	1374.9	2.9
x	I	775	76.55	0.0024	1.357	6.76	214.7	99.5	14.9	1371.8	2.1
x	J	785	76.49	0.0012	0.9731	7.70	434.1	99.6	17.5	1372.4	1.8
x	K	785	76.03	0.0026	1.024	6.48	199.9	99.6	19.6	1366.4	1.9
	L	795	76.32	0.0022	0.8608	7.85	231.0	99.7	22.2	1370.7	1.7
	M	800	76.23	0.0017	1.092	8.01	299.4	99.6	24.9	1368.7	1.6
	N	805	76.64	0.0016	0.7696	8.00	323.2	99.7	27.6	1375.2	1.9
	O	820	76.73	0.0014	0.5735	11.47	360.7	99.8	31.4	1376.9	2.0
	P	825	76.58	0.0016	1.389	10.72	322.0	99.5	35.0	1372.0	2.5
	Q	835	76.34	0.0018	0.6158	10.11	290.1	99.8	38.3	1371.8	2.2
	R	850	76.37	0.0016	0.8472	10.36	315.5	99.7	41.8	1371.3	2.3
	S	870	76.57	0.0018	0.8627	11.96	280.3	99.7	45.8	1373.8	2.0
	T	885	76.58	0.0016	0.7293	11.63	315.7	99.7	49.6	1374.5	2.1
	U	900	76.78	0.0014	0.8199	11.82	355.6	99.7	53.6	1376.7	2.0
	V	915	76.25	0.0018	0.6808	13.75	286.3	99.7	58.2	1370.5	2.0
	W	930	76.26	0.0016	0.7694	13.47	322.0	99.7	62.6	1370.3	1.9
	X	945	76.27	0.0013	0.7576	13.70	401.2	99.7	67.2	1370.5	2.0
	Y	960	76.41	0.0016	0.7664	13.98	321.3	99.7	71.9	1372.2	2.4
	Z	975	76.51	0.0013	0.7560	14.88	392.6	99.7	76.8	1373.4	1.9
	AA	990	76.80	0.0013	0.9016	15.74	390.4	99.6	82.1	1376.7	2.1
	AB	1020	76.70	0.0010	0.6769	24.2	499.2	99.7	90.1	1376.2	1.8
	AC	1070	76.99	0.0006	0.6282	29.6	899.5	99.7	100.0	1380.1	1.7
	Integrated age ± 1σ			n=29		300.2		K2O=12.30%		1373.5	1.3
	Plateau ± 1σ		steps L-AC	n=18	MSWD=2.78	241.3			80.4	1373.42	1.0

Appendix 1 $^{40}Ar/^{39}Ar$ analytical data.

	ID	Temperature (°C)	$^{40}Ar/^{39}Ar$	$^{37}Ar/^{39}Ar$	$^{36}Ar/^{39}Ar$ (x 10^{-3})	$^{39}Ar_K$ (x 10^{-15} mol)	K/Ca	$^{40}Ar^*$ (%)	^{39}Ar (%)	Age (Ma)	±1σ (Ma)
	2-4A, Muscovite, .75 mg, J=0.014594±0.06%, D=1.0045±0.0011, NM-261A, Lab#=61979-01										
x	A	610	82.48	0.0096	64.42	1.175	53.4	76.9	0.4	1199.6	5.1
x	B	650	75.76	0.0030	12.01	1.144	171.7	95.3	0.7	1317.4	4.1
x	C	690	75.80	0.0007	6.572	2.16	744.3	97.4	1.4	1338.6	3.4
x	D	720	76.36	0.0022	2.744	3.51	229.6	98.9	2.4	1360.3	2.8
x	E	740	76.74	0.0018	2.400	4.75	279.9	99.1	3.9	1366.3	2.1
x	F	750	76.12	0.0012	1.321	5.54	442.7	99.5	5.6	1362.5	2.0
x	G	760	76.46	0.0014	0.6720	8.01	356.0	99.7	8.0	1369.3	2.1
	H	770	76.54	0.0004	0.5495	10.72	1456.5	99.8	11.2	1370.8	2.1
	I	775	76.86	0.0005	0.6369	10.68	934.6	99.7	14.5	1374.5	2.3
	J	785	76.90	0.0012	0.5704	12.28	435.6	99.8	18.2	1375.2	2.2
	K	785	77.06	0.0014	0.5836	10.98	371.2	99.8	21.6	1377.1	2.0
	L	795	76.75	0.0011	0.5578	11.60	483.2	99.8	25.1	1373.4	2.2
	M	800	77.28	0.0006	0.6588	11.65	839.0	99.7	28.6	1379.7	1.9
	N	805	76.69	0.0016	0.4713	10.60	325.8	99.8	31.8	1373.0	2.2
	O	820	76.66	0.0011	0.5218	13.38	476.5	99.8	35.9	1372.3	1.9
	P	825	76.77	0.0010	0.6565	10.27	507.4	99.7	39.0	1373.3	2.3
	Q	835	76.78	0.0014	0.5339	9.49	362.3	99.8	41.9	1373.8	2.4
	R	850	76.91	0.0010	0.7163	10.30	514.2	99.7	45.0	1374.8	2.1
	S	870	76.69	0.0013	0.4103	12.41	386.3	99.8	48.8	1373.1	1.9
	T	885	76.86	0.0003	0.5821	11.67	1653.8	99.8	52.3	1374.7	1.8
	U	900	76.68	0.0005	0.7346	10.92	1037.0	99.7	55.7	1371.8	2.0
	V	915	77.08	0.0011	0.8706	10.65	453.8	99.7	58.9	1376.3	1.9
	W	930	76.94	0.0011	0.7689	9.78	482.1	99.7	61.9	1375.0	2.3
	X	945	76.38	0.0007	0.5411	9.40	699.2	99.8	64.7	1368.8	2.2
	Y	960	76.74	0.0012	0.5508	9.27	429.4	99.8	67.5	1373.3	2.2
	Z	975	76.72	0.0004	0.5677	9.96	1273.9	99.8	70.6	1372.9	2.1
	AA	990	76.76	0.0010	0.5575	11.04	510.2	99.8	73.9	1373.5	2.2
	AB	1020	76.80	0.0011	0.4420	18.9	454.2	99.8	79.7	1374.5	1.7
	AC	1070	77.21	0.0006	0.3016	49.2	848.4	99.9	94.6	1380.1	1.6
x	AD	1620	76.97	0.0011	3.718	17.8	455.5	98.6	100.0	1364.3	2.2
	Integrated age ± 1σ			n=30		329.2		K2O=11.55%		1372.8	1.3
	Plateau ± 1σ		steps H-AC	n=22	MSWD=1.81	285.2			86.6	1374.44	0.8

Appendix 1 $^{40}Ar/^{39}Ar$ analytical data.

	ID	Temperature (°C)	$^{40}Ar/^{39}Ar$	$^{37}Ar/^{39}Ar$	$^{36}Ar/^{39}Ar$ (x 10^{-3})	$^{39}Ar_K$ (x 10^{-15} mol)	K/Ca	$^{40}Ar^*$ (%)	^{39}Ar (%)	Age (Ma)	±1σ (Ma)
	2-4B, Muscovite, .41 mg, J=0.014594±0.06%, D=1.0045±0.0011, NM-261A, Lab#=61980-01										
x	A	610	68.46	0.0291	31.33	0.977	17.5	86.5	0.6	1139.8	5.8
x	B	650	73.88	0.0074	6.064	0.918	69.2	97.6	1.1	1315.8	5.3
x	C	690	76.76	0.0049	10.69	1.344	103.9	95.9	2.0	1335.3	4.3
	D	720	77.93	0.0057	6.489	1.80	88.9	97.5	3.1	1366.2	4.0
	E	740	79.61	0.0034	13.31	2.25	147.9	95.0	4.4	1361.8	3.4
	F	750	76.69	0.0044	2.929	2.12	115.7	98.9	5.7	1363.7	3.3
	G	760	77.17	0.0028	2.956	2.32	183.3	98.9	7.1	1369.7	3.2
	H	770	77.66	0.0040	3.203	2.76	128.3	98.8	8.8	1374.9	2.6
	I	775	76.86	0.0032	2.079	3.35	160.6	99.2	10.8	1369.1	2.3
	J	785	76.59	0.0017	1.289	4.91	299.0	99.5	13.8	1368.6	2.1
	K	785	76.44	0.0024	1.787	4.37	212.2	99.3	16.4	1364.9	2.4
	L	795	76.58	0.0024	0.6622	5.67	211.1	99.7	19.9	1370.8	2.2
	M	800	76.39	0.0016	1.042	5.82	311.0	99.6	23.4	1367.1	2.2
	N	805	76.31	0.0028	1.080	5.61	184.1	99.6	26.8	1365.8	2.2
	O	820	76.38	0.0017	0.6416	7.93	303.7	99.7	31.6	1368.5	2.0
	P	825	76.30	0.0028	0.8015	5.73	180.2	99.7	35.1	1366.8	2.2
	Q	835	76.28	0.0028	1.070	4.98	181.4	99.6	38.1	1365.5	2.1
	R	850	76.21	0.0022	0.8047	4.95	228.9	99.7	41.1	1365.7	2.2
	S	870	76.42	0.0012	0.9457	5.60	421.0	99.6	44.5	1367.7	2.2
	T	885	76.51	0.0009	0.7727	4.96	581.6	99.7	47.5	1369.5	2.1
	U	900	76.37	0.0006	1.147	4.55	817.1	99.5	50.2	1366.3	2.2
	V	915	76.35	0.0010	1.016	4.15	499.5	99.6	52.7	1366.6	2.6
	W	930	76.42	0.0044	0.9318	3.89	116.0	99.6	55.1	1367.8	2.3
	X	945	76.06	0.0031	1.271	3.73	165.4	99.5	57.4	1362.0	2.3
	Y	960	76.64	0.0035	1.146	3.91	143.9	99.5	59.7	1369.7	2.5
	Z	975	76.55	0.0031	1.153	4.06	167.0	99.5	62.2	1368.7	1.9
	AA	990	76.31	0.0008	1.277	4.35	631.9	99.5	64.8	1365.1	2.4
	AB	1020	76.27	0.0013	0.9277	6.35	392.8	99.6	68.7	1365.9	2.1
	AC	1070	76.82	0.0017	0.8290	15.35	305.5	99.7	78.0	1373.3	1.9
	AD	1620	77.45	0.0009	1.988	36.4	549.1	99.2	100.0	1376.9	1.7
	Integrated age ± 1σ			n=30		165.1		K2O=10.60%		1368.1	1.3
	Plateau ± 1σ		steps D-AD	n=27	MSWD=2.54	161.9			98.0	1368.24	0.9
	2-4C1, Muscovite, .32 mg, J=0.014539±0.06%, D=1.0045±0.0011, NM-261A, Lab#=61982-01										
x	A	550	132.5	-0.0232	194.2	0.496	-	56.7	0.4	1351.3	11.0
x	B	600	87.67	-0.0133	18.62	0.560	-	93.7	0.8	1438.6	7.7
x	C	650	86.10	-0.0036	16.87	1.061	-	94.2	1.7	1425.9	5.8
x	D	700	89.85	-0.0013	28.92	1.99	-	90.5	3.3	1428.3	4.1
x	E	720	85.92	0.0022	17.54	2.29	236.1	94.0	5.1	1421.3	3.6
	F	750	81.69	-0.0007	7.034	5.05	-	97.4	9.2	1407.5	2.2
	G	770	80.51	0.0001	2.858	8.01	9159.9	98.9	15.6	1408.1	2.1
	H	785	79.83	0.0003	2.112	8.61	1525.3	99.2	22.5	1402.4	2.2
	I	800	80.27	0.0002	2.271	8.85	2874.4	99.2	29.6	1407.2	2.6
	J	820	80.17	0.0006	2.078	10.33	864.5	99.2	37.9	1406.8	1.9
	K	850	79.60	0.0000	1.706	14.20	11755.9	99.4	49.3	1401.0	2.0
	L	870	79.92	0.0001	2.144	12.26	4948.6	99.2	59.1	1403.4	2.0
	M	890	79.87	0.0013	2.109	11.90	384.3	99.2	68.7	1402.9	2.2
	N	910	79.75	0.0011	2.360	10.82	455.6	99.1	77.4	1400.6	2.2
	O	930	79.86	0.0015	3.288	8.14	329.5	98.8	83.9	1398.5	1.9
	P	950	80.90	-0.0013	5.028	5.11	-	98.2	88.0	1405.0	2.3
	Q	980	81.35	0.0007	6.543	4.59	783.1	97.6	91.7	1405.0	2.4
	R	1010	81.17	0.0001	5.496	5.83	4098.0	98.0	96.4	1406.6	2.2
x	S	1040	82.03	0.0009	11.40	4.53	599.1	95.9	100.0	1395.6	2.4
	Integrated age ± 1σ			n=19		124.6		K2O=10.29%		1404.3	1.4
	Plateau ± 1σ		steps F-Q	n=12	MSWD=2.21	107.9			86.6	1403.9	1.1

Appendix 1 $^{40}Ar/^{39}Ar$ analytical data.

	ID	Temperature (°C)	$^{40}Ar/^{39}Ar$	$^{37}Ar/^{39}Ar$	$^{36}Ar/^{39}Ar$ (x 10^{-3})	$^{39}Ar_K$ (x 10^{-15} mol)	K/Ca	$^{40}Ar^*$ (%)	^{39}Ar (%)	Age (Ma)	±1σ (Ma)
	2-4C2, Muscovite, .41 mg, J=0.014539±0.06%, D=1.0045±0.0011, NM-261A, Lab#=61983-01										
x	A	550	147.6	-0.0152	212.2	0.156	-	57.5	0.2	1470.8	24.0
x	B	600	99.02	0.0287	35.21	0.199	17.8	89.5	0.5	1515.3	18.0
x	C	650	132.4	0.0136	162.5	0.428	37.6	63.7	1.1	1465.6	11.0
x	D	700	104.9	-0.0001	74.85	0.862	-	78.9	2.4	1446.5	6.2
x	E	720	90.71	-0.0015	31.63	1.013	-	89.7	3.9	1428.9	5.6
x	F	750	82.89	0.0004	8.062	2.50	1394.8	97.1	7.5	1418.5	3.3
	G	770	81.07	0.0018	5.847	3.92	282.3	97.9	13.2	1404.1	2.6
	H	785	80.84	0.0011	5.034	4.57	461.1	98.2	19.9	1404.2	2.4
	I	800	80.58	0.0018	4.240	4.81	277.6	98.4	26.9	1403.9	2.2
	J	820	80.53	0.0017	4.248	5.72	302.7	98.4	35.3	1403.2	2.0
	K	850	80.21	0.0020	3.069	7.86	259.0	98.9	46.7	1403.7	1.9
	L	870	80.33	0.0014	3.404	6.96	366.5	98.7	56.9	1403.9	2.0
	M	890	79.98	0.0012	3.286	6.91	411.6	98.8	67.0	1400.0	2.0
	N	910	80.44	0.0019	3.852	6.14	267.6	98.6	75.9	1403.6	2.1
	O	930	80.63	0.0003	3.960	5.44	2027.8	98.5	83.9	1405.6	2.2
	P	950	81.35	0.0030	7.101	3.27	170.1	97.4	88.6	1403.0	3.1
	Q	980	81.87	0.0026	9.162	2.49	197.7	96.7	92.3	1401.9	3.3
	R	1010	82.06	0.0036	9.880	3.06	141.1	96.4	96.7	1401.6	2.5
	S	1040	88.01	0.0066	29.69	2.25	77.0	90.0	100.0	1402.8	3.2
	Integrated age ± 1σ			n=19		68.6		K2O=4.42%		1405.6	1.4
	Plateau ± 1σ		steps G-S	n=13	MSWD=0.41	63.4			92.5	1403.26	0.8
	2-4C3, Muscovite, J=0.014539±0.06%, D=1.0045±0.0011, NM-261A, Lab#=61984-01										
x	A	550	123.1	0.2365	257.9	0.158	2.2	38.1	0.3	952.2	88.0
x	B	600	101.4	0.2111	151.3	0.177	2.4	55.9	0.5	1101.2	71.0
x	C	650	90.96	0.1245	80.02	0.339	4.1	74.0	1.1	1249.3	35.0
x	D	700	90.53	0.0627	56.18	0.654	8.1	81.7	2.1	1336.0	18.0
x	E	720	84.90	0.0463	43.11	0.712	11.0	85.0	3.3	1313.2	16.0
	F	750	81.92	0.0158	15.19	2.22	32.4	94.5	6.9	1380.4	5.7
	G	770	81.11	0.0109	9.525	3.55	47.0	96.5	12.7	1391.1	3.9
	H	785	80.56	0.0084	8.049	4.47	60.9	97.0	19.9	1389.8	3.3
	I	800	80.52	0.0099	7.867	4.68	51.8	97.1	27.5	1389.9	3.2
	J	820	80.51	0.0073	7.144	5.45	70.1	97.4	36.3	1392.4	3.0
	K	850	80.48	0.0049	5.108	7.70	104.3	98.1	48.8	1399.5	2.2
	L	870	80.64	0.0070	5.842	6.62	72.9	97.9	59.5	1398.8	2.6
	M	890	80.78	0.0064	6.406	6.00	79.7	97.6	69.2	1398.4	2.6
	N	910	80.38	0.0081	6.314	6.24	63.3	97.7	79.3	1393.8	2.8
	O	930	81.29	0.0111	9.004	4.32	45.8	96.7	86.3	1395.3	3.7
x	P	950	81.52	0.0161	15.48	2.44	31.6	94.4	90.3	1374.3	5.3
x	Q	980	82.79	0.0236	19.85	1.88	21.6	92.9	93.3	1374.0	6.6
x	R	1010	83.88	0.0217	19.55	2.27	23.5	93.1	97.0	1388.8	5.9
x	S	1040	86.41	0.0202	32.73	1.85	25.2	88.8	100.0	1371.6	7.0
	Integrated age ± 1σ			n=19		61.7		K2O=3.69%		1388.0	1.7
	Plateau ± 1σ		steps F-O	n=10	MSWD=2.41	51.3			83.0	1394.9	1.6

Appendix 1 $^{40}Ar/^{39}Ar$ analytical data.

	ID	Temperature (°C)	$^{40}Ar/^{39}Ar$	$^{37}Ar/^{39}Ar$	$^{36}Ar/^{39}Ar$ (x 10^{-3})	$^{39}Ar_K$ (x 10^{-15} mol)	K/Ca	$^{40}Ar^*$ (%)	^{39}Ar (%)	Age (Ma)	±1σ (Ma)
	2-4C4, Muscovite, .31 mg, J=0.014539±0.06%, D=1.0045±0.0011, NM-261A, Lab#=61985-01										
x	A	550	978.7	0.0078	2999.4	0.172	65.2	9.4	0.2	1557.9	63
x	B	600	172.0	-0.0140	294.7	0.198	-	49.3	0.3	1471.2	21
x	C	650	250.6	0.0201	542.2	0.441	25.4	36.1	0.8	1536.1	17
x	D	700	98.87	-0.0026	51.53	0.931	-	84.6	1.6	1456.5	5.8
x	E	720	96.79	0.0047	53.48	0.992	108.5	83.7	2.6	1424.3	5.5
x	F	750	84.24	0.0002	13.09	2.32	2636.7	95.4	4.8	1416.7	3.5
	G	770	79.96	0.0025	2.762	6.94	202.7	99.0	11.3	1401.7	2.1
	H	785	79.71	0.0022	2.308	8.12	233.8	99.1	19.0	1400.2	2.0
	I	800	79.56	0.0009	2.440	8.16	551.2	99.1	26.7	1397.9	2.1
	J	820	79.62	0.0012	2.159	9.89	409.1	99.2	36.0	1399.6	2.0
	K	850	79.48	0.0014	1.930	13.01	365.0	99.3	48.3	1398.8	1.9
	L	870	79.65	0.0021	2.102	11.32	246.2	99.2	59.0	1400.3	2.0
	M	890	80.07	0.0019	2.344	10.03	265.5	99.1	68.5	1404.6	2.1
	N	910	79.76	0.0007	3.105	8.37	735.2	98.8	76.4	1397.9	2.0
	O	930	79.64	0.0016	3.816	6.40	327.0	98.6	82.4	1393.9	2.2
	P	950	80.62	0.0052	5.656	4.13	98.9	97.9	86.3	1399.3	2.7
	Q	980	80.42	0.0077	6.345	3.70	66.3	97.7	89.8	1394.3	3.0
	R	1010	81.28	0.0047	8.050	4.82	108.0	97.1	94.3	1398.7	2.3
	S	1040	81.46	0.0021	9.299	6.00	242.8	96.6	100.0	1396.3	2.2
	Integrated age ± 1σ			n=19		105.9		K2O=9.03%		1401.3	1.5
	Plateau ± 1σ		steps G-Q	n=11	MSWD=1.76	90.1			85.0	1399.2	1.0
	5-1, Muscovite, .44 mg, J=0.014652±0.06%, D=1.0045±0.0011, NM-261B, Lab#=61996-01										
x	A	550	100.7	-0.0094	96.75	0.710	-	71.6	0.4	1320.1	7.9
x	B	600	85.28	-0.0002	17.90	0.756	-	93.8	0.7	1419.8	5.5
x	C	650	82.66	-0.0001	10.50	1.375	-	96.2	1.4	1414.4	4.1
x	D	700	93.18	0.0028	47.19	2.51	181.1	85.0	2.7	1410.4	3.6
x	E	720	91.26	0.0066	44.22	2.37	77.3	85.7	3.9	1397.4	3.8
x	F	750	80.57	0.0020	9.685	4.54	255.3	96.4	6.2	1391.3	2.5
	G	770	77.83	0.0019	3.599	8.05	274.4	98.6	10.3	1379.5	1.8
	H	785	77.44	0.0021	1.505	9.30	244.7	99.4	15.0	1382.3	2.5
	I	800	76.97	0.0020	1.028	11.52	250.8	99.6	20.9	1378.2	2.4
	J	820	76.77	0.0014	1.081	15.55	367.2	99.6	28.8	1375.6	2.3
	K	850	76.94	0.0007	0.8318	20.4	687.2	99.7	39.2	1378.5	1.8
	L	870	76.57	0.0018	0.9621	17.8	283.4	99.6	48.2	1373.4	2.0
	M	890	76.63	0.0015	1.192	15.53	348.6	99.5	56.1	1373.3	1.9
	N	910	76.65	0.0010	1.118	14.99	527.0	99.6	63.7	1373.9	1.8
	O	930	76.51	0.0023	1.532	11.38	224.2	99.4	69.5	1370.6	1.8
	P	950	76.75	0.0017	1.659	10.06	299.0	99.4	74.6	1373.1	2.4
	Q	980	77.10	0.0020	1.587	11.89	251.6	99.4	80.6	1377.8	2.1
	R	1010	76.85	0.0015	1.266	16.3	334.4	99.5	88.9	1375.8	2.2
	S	1040	76.80	0.0008	0.7345	21.8	645.7	99.7	100.0	1377.2	1.8
	Integrated age ± 1σ			n=19		196.9		K2O=11.73%		1377.3	1.3
	Plateau ± 1σ		steps G-S	n=13	MSWD=2.45	184.6			93.8	1375.9	1.1

Appendix 1 $^{40}Ar/^{39}Ar$ analytical data.

	ID	Temperature (°C)	$^{40}Ar/^{39}Ar$	$^{37}Ar/^{39}Ar$	$^{36}Ar/^{39}Ar$ (x 10^{-3})	$^{39}Ar_K$ (x 10^{-15} mol)	K/Ca	$^{40}Ar^*$ (%)	^{39}Ar (%)	Age (Ma)	±1σ (Ma)
	5-2, Muscovite, .29 mg, J=0.014652±0.06%, D=1.0045±0.0011, NM-261B, Lab#=61997-01										
x	A	550	203.1	0.0112	435.8	0.400	45.6	36.6	0.3	1348.0	17
x	B	600	103.5	0.0056	74.76	0.399	91.0	78.6	0.6	1437.1	11
x	C	650	88.48	0.0092	27.12	0.857	55.2	90.9	1.3	1425.6	5.6
x	D	700	117.5	0.0021	127.0	1.85	241.2	68.1	2.7	1419.6	6.0
x	E	720	88.45	0.0012	32.57	2.14	410.3	89.1	4.4	1405.3	3.9
	F	750	80.68	0.0027	10.84	5.60	186.8	96.0	8.7	1388.5	2.2
	G	770	78.04	0.0005	2.379	7.77	1029.7	99.1	14.8	1386.7	1.9
	H	785	77.62	0.0012	1.724	7.94	428.9	99.3	20.9	1383.8	1.8
	I	800	77.58	0.0012	1.228	8.58	430.1	99.5	27.6	1385.2	2.1
	J	820	77.54	0.0015	0.8725	10.37	351.6	99.7	35.6	1386.0	2.2
	K	850	77.42	0.0009	0.8539	14.09	593.8	99.7	46.5	1384.6	2.0
	L	870	77.40	0.0020	0.8830	13.23	258.0	99.7	56.8	1384.2	2.0
	M	890	77.18	0.0010	1.058	12.57	512.3	99.6	66.6	1380.8	2.1
	N	910	77.61	0.0015	1.064	10.54	329.2	99.6	74.7	1386.1	2.3
	O	930	77.04	0.0025	1.509	6.68	204.1	99.4	79.9	1377.4	2.2
	P	950	77.53	0.0039	1.990	4.74	129.9	99.2	83.6	1381.7	2.3
	Q	980	77.49	0.0011	1.919	5.85	445.8	99.3	88.1	1381.5	2.1
	R	1010	78.09	0.0020	1.777	8.64	258.5	99.3	94.8	1389.6	2.2
	S	1040	77.95	0.0020	1.702	6.66	249.5	99.3	100.0	1388.1	2.0
	Integrated age ± 1σ			n=19		128.9		K2O=11.65%		1385.8	1.4
	Plateau ± 1σ		steps F-P	n=11	MSWD=2.06	102.1			79.2	1384.1	1.1
	5-3, Muscovite, .29 mg, J=0.014652±0.06%, D=1.0045±0.0011, NM-261B, Lab#=61998-01										
x	A	550	211.9	-0.0278	472.7	0.408	-	34.1	0.3	1321.7	18.4
x	B	600	89.52	-0.0164	38.41	0.445	-	87.3	0.7	1397.1	9.4
x	C	650	91.00	-0.0048	40.47	0.786	-	86.9	1.3	1407.9	6.1
x	D	700	87.73	-0.0044	29.88	1.532	-	89.9	2.5	1406.2	4.0
x	E	720	96.11	-0.0029	62.65	1.457	-	80.7	3.7	1389.9	4.6
	F	750	80.61	-0.0007	11.93	3.08	-	95.6	6.2	1383.5	2.9
	G	770	77.43	-0.0001	2.631	5.20	-	99.0	10.3	1378.1	2.1
	H	785	77.16	-0.0001	1.949	6.06	-	99.2	15.1	1377.1	1.9
	I	800	76.79	0.0009	1.207	7.02	577.4	99.5	20.8	1375.2	1.9
	J	820	76.54	0.0008	0.8505	8.88	620.5	99.7	27.8	1373.5	2.0
	K	850	77.01	0.0000	0.9078	12.51	16248.5	99.6	37.8	1379.2	1.9
	L	870	76.98	0.0005	0.9339	11.81	1117.2	99.6	47.3	1378.8	2.1
	M	890	77.07	0.0008	1.149	10.78	664.0	99.6	55.9	1379.0	2.0
	N	910	77.12	0.0003	1.169	9.86	1599.4	99.5	63.7	1379.6	2.2
	O	930	77.11	0.0014	1.712	7.69	365.2	99.3	69.9	1377.4	1.9
	P	950	77.17	0.0008	1.582	5.54	611.5	99.4	74.3	1378.6	2.4
	Q	980	76.97	0.0000	1.908	6.06	28503.0	99.3	79.1	1374.9	2.0
	R	1010	77.06	0.0012	1.906	8.21	419.6	99.3	85.7	1376.1	1.8
	S	1040	77.34	0.0007	1.304	9.90	749.1	99.5	93.6	1381.8	2.6
	T	1070	77.33	0.0017	2.410	8.01	298.8	99.1	100.0	1377.6	2.1
	Integrated age ± 1σ			n=20		125.3		K2O=11.32%		1378.6	1.4
	Plateau ± 1σ		steps F-S	n=14	MSWD=1.36	112.6			89.9	1377.61	0.9

Appendix 1 $^{40}Ar/^{39}Ar$ analytical data.

	ID	Temperature (°C)	$^{40}Ar/^{39}Ar$	$^{37}Ar/^{39}Ar$	$^{36}Ar/^{39}Ar$ (x 10^{-3})	$^{39}Ar_K$ (x 10^{-15} mol)	K/Ca	$^{40}Ar^*$ (%)	^{39}Ar (%)	Age (Ma)	±1σ (Ma)
	LaP, Muscovite, .29 mg, J=0.014653±0.07%, D=1.0045±0.0011, NM-261A, Lab#=61981-01										
x	A	550	122.9	0.0065	158.6	0.217	79.1	61.8	0.2	1369.9	16.9
x	B	600	115.9	0.0333	95.86	0.244	15.3	75.5	0.4	1510.8	14.8
x	C	650	118.1	0.0159	114.2	0.502	32.1	71.4	0.8	1473.1	8.9
x	D	700	141.6	-0.0031	191.6	1.071	-	60.0	1.7	1480.8	8.5
x	E	720	84.73	0.0046	19.96	2.06	111.7	93.0	3.5	1405.5	3.3
	F	750	79.22	0.0038	3.124	6.08	135.0	98.8	8.6	1398.7	2.0
	G	770	78.81	0.0024	2.537	7.42	211.9	99.0	14.9	1395.8	2.0
	H	785	78.49	0.0017	2.994	7.74	300.8	98.9	21.4	1390.1	1.7
	I	800	79.03	0.0028	2.990	7.85	181.0	98.9	28.1	1396.9	1.8
	J	820	78.56	0.0020	2.332	9.63	260.5	99.1	36.2	1393.5	2.0
	K	850	78.67	0.0014	1.836	13.82	355.1	99.3	47.9	1396.7	2.2
	L	870	78.64	0.0024	1.957	13.05	210.6	99.3	59.0	1395.8	2.0
	M	890	78.74	0.0019	2.214	12.07	267.6	99.2	69.2	1396.1	2.3
	N	910	79.21	0.0028	2.395	9.86	182.5	99.1	77.6	1401.3	2.5
x	O	930	78.68	0.0040	4.195	6.52	126.3	98.4	83.1	1388.0	2.1
x	P	950	79.36	0.0050	6.275	4.04	102.5	97.7	86.5	1388.9	2.4
x	Q	980	80.25	0.0078	10.85	2.94	65.4	96.0	89.0	1383.1	3.0
x	R	1010	81.02	0.0042	13.07	3.52	120.5	95.2	92.0	1384.6	2.5
x	S	1040	83.35	0.0005	19.28	5.59	1068.3	93.2	96.7	1390.7	2.3
x	T	1070	87.57	0.0065	35.42	3.91	78.0	88.0	100.0	1383.8	3.1
	Integrated age ± 1σ			n=20		118.1		K2O=10.68%		1395.6	1.5
	Plateau ± 1σ		steps F-L	n=7	MSWD=2.37	65.6			55.5	1395.1	1.3
	LaJ, Muscovite, .35 mg, J=0.014543±0.05%, D=1.0045±0.0011, NM-261A, Lab#=61986-01										
x	A	550	130.5	0.0136	231.0	0.537	37.5	47.7	0.5	1179.3	11
x	B	600	100.5	0.0088	64.94	0.652	58.2	80.9	1.0	1429.0	6.8
x	C	650	103.2	0.0129	73.82	1.348	39.7	78.8	2.2	1429.0	6.0
x	D	700	82.88	0.0008	13.26	3.11	614.5	95.3	4.9	1399.6	2.8
x	E	720	79.52	-0.0003	3.977	3.30	-	98.5	7.7	1392.0	2.9
x	F	750	79.56	0.0018	3.713	5.21	278.8	98.6	12.2	1393.5	1.9
x	G	770	78.55	0.0018	3.413	6.15	289.1	98.7	17.6	1381.9	2.0
x	H	785	77.89	0.0008	2.829	7.18	659.9	98.9	23.8	1375.9	2.1
x	I	800	77.76	0.0018	2.467	8.07	290.1	99.1	30.8	1375.6	1.8
	J	820	78.51	0.0018	2.452	9.39	290.5	99.1	38.9	1385.1	2.2
	K	850	78.51	0.0024	2.015	11.42	215.6	99.2	48.8	1386.7	2.0
	L	870	78.27	0.0011	2.165	10.36	473.7	99.2	57.7	1383.2	1.9
	M	890	78.59	0.0026	2.675	8.38	199.4	99.0	65.0	1385.2	1.8
	N	910	78.56	0.0028	3.262	7.15	182.5	98.8	71.2	1382.7	2.1
	O	930	78.62	0.0044	3.295	6.19	115.1	98.8	76.6	1383.4	2.3
	P	950	78.55	0.0026	4.305	5.55	193.8	98.4	81.4	1378.7	1.9
	Q	980	79.58	0.0025	6.765	7.12	203.2	97.5	87.5	1382.5	1.9
	R	1010	79.70	0.0019	5.922	9.43	265.8	97.8	95.7	1387.1	2.4
	S	1040	83.31	0.0048	19.93	4.98	106.8	92.9	100.0	1380.5	2.9
	Integrated age ± 1σ			n=19		115.5		K2O=8.72%		1383.8	1.4
	Plateau ± 1σ		steps J-R	n=9	MSWD=1.68	75.0			64.9	1383.7	1.0

Appendix 1 $^{40}Ar/^{39}Ar$ analytical data.

	ID	Temperature (°C)	$^{40}Ar/^{39}Ar$	$^{37}Ar/^{39}Ar$	$^{36}Ar/^{39}Ar$ (x 10^{-3})	$^{39}Ar_K$ (x 10^{-15} mol)	K/Ca	$^{40}Ar^*$ (%)	^{39}Ar (%)	Age (Ma)	±1σ (Ma)
	Vestegard, Muscovite, .42 mg, J=0.014543±0.05%, D=1.0045±0.0011, NM-261A, Lab#=61987-01										
X	A	550	93.56	0.0237	77.54	0.269	21.6	75.5	0.2	1293.7	17
X	B	600	76.86	0.0074	18.35	0.310	69.3	92.9	0.5	1303.9	13
X	C	650	82.13	0.0157	26.60	0.586	32.5	90.4	1.0	1340.7	8.1
X	D	700	80.67	-0.0041	26.70	1.105	-	90.2	2.0	1321.5	5.5
X	E	720	76.88	0.0181	12.99	1.126	28.2	95.0	3.0	1324.9	4.8
X	F	750	77.78	0.0122	12.35	1.67	42.0	95.3	4.5	1338.8	3.9
X	G	770	77.79	0.0055	9.646	2.49	92.2	96.3	6.7	1349.1	3.5
X	H	785	77.10	0.0003	6.745	3.07	1873.0	97.4	9.5	1351.3	2.7
X	I	800	77.20	0.0024	3.042	4.86	208.9	98.8	13.8	1366.4	2.4
X	J	820	77.61	0.0016	1.669	9.41	319.4	99.4	22.1	1376.6	2.3
X	K	850	75.09	0.0025	1.660	9.02	206.5	99.3	30.2	1344.8	2.3
X	L	870	76.45	0.0028	1.749	7.87	184.9	99.3	37.1	1361.7	1.9
X	M	890	77.05	0.0028	1.664	8.76	181.7	99.4	44.9	1369.7	1.9
X	N	910	78.45	0.0035	2.434	6.39	147.1	99.1	50.6	1384.4	2.4
	O	930	78.88	0.0022	2.238	7.25	232.4	99.2	57.1	1390.5	2.0
	P	950	78.70	0.0019	2.011	9.48	262.3	99.2	65.5	1389.0	2.0
	Q	980	79.15	0.0013	2.078	16.6	404.0	99.2	80.2	1394.4	2.0
	R	1010	78.63	0.0021	2.064	18.8	246.1	99.2	96.9	1388.0	1.8
X	S	1040	83.87	0.0102	26.86	2.61	50.2	90.5	99.2	1361.7	4.1
X	T	1070	115.2	0.0116	133.1	0.880	43.8	65.9	100.0	1361.4	8.4
	Integrated age ± 1σ			n=20		112.5		K2O=7.08%		1375.1	1.4
	Terminal Age ± 1σ		steps O-R	n=4	MSWD=2.04	52.081			46.3	1390.33	1.5
	Queen, Muscovite, .49 mg, J=0.014543±0.05%, D=1.0045±0.0011, NM-261A, Lab#=61988-01										
x	A	550	89.54	0.0060	131.5	0.621	85.6	56.6	0.4	1010.5	8.8
x	B	600	83.31	-0.0009	37.89	0.705	-	86.6	0.9	1312.8	6.6
x	C	650	80.84	0.0083	23.75	1.64	61.8	91.3	1.9	1334.8	3.7
x	D	700	77.98	0.0059	12.19	3.77	87.0	95.4	4.4	1342.0	2.7
x	E	720	77.03	0.0039	5.168	3.88	131.1	98.0	6.9	1356.3	2.5
x	F	750	76.99	0.0028	4.138	6.14	185.3	98.4	10.8	1359.7	2.2
	G	770	77.68	0.0035	4.209	7.32	145.2	98.4	15.6	1368.2	1.9
	H	785	76.93	0.0027	3.207	9.28	188.5	98.8	21.6	1362.3	2.4
	I	800	76.92	0.0022	2.557	11.01	227.0	99.0	28.7	1364.7	2.0
	J	820	76.83	0.0016	1.934	13.05	316.8	99.2	37.1	1365.8	2.2
	K	850	76.94	0.0013	1.649	16.6	394.6	99.4	47.9	1368.3	1.9
	L	870	77.01	0.0015	2.408	12.21	341.9	99.1	55.8	1366.4	2.1
	M	890	76.90	0.0027	2.561	10.07	190.2	99.0	62.3	1364.4	2.2
	N	910	76.54	0.0023	2.704	8.97	223.5	98.9	68.1	1359.3	2.1
	O	930	77.27	0.0030	3.865	7.12	167.9	98.5	72.7	1364.2	2.1
	P	950	77.33	0.0014	4.297	6.83	372.8	98.3	77.1	1363.4	2.2
	Q	980	77.50	0.0021	4.208	9.17	248.0	98.4	83.0	1365.9	2.4
	R	1010	78.11	0.0021	5.659	13.18	246.6	97.9	91.6	1368.2	1.9
	S	1040	79.65	0.0017	9.644	13.05	292.6	96.4	100.0	1372.8	2.1
	Integrated age ± 1σ			n=19		154.6	222.6	K2O=8.33%		1363.2	1.3
	Plateau ± 1σ		steps G-S	n=13	MSWD=2.52	137.9			89.2	1365.9	1.1
	Terminal Age ± 1σ		steps S-S	n=1					8.4	1372.80	2.1

Appendix 1 $^{40}Ar/^{39}Ar$ analytical data.

	ID	Temperature (°C)	$^{40}Ar/^{39}Ar$	$^{37}Ar/^{39}Ar$	$^{36}Ar/^{39}Ar$ (x 10^{-3})	$^{39}Ar_K$ (x 10^{-15} mol)	K/Ca	$^{40}Ar^*$ (%)	^{39}Ar (%)	Age (Ma)	±1σ (Ma)
	Bluebird, Muscovite, .45 mg, J=0.014602±0.05%, D=1.0045±0.0011, NM-261A, Lab#=61989-01										
X	A	550	79.80	0.0559	86.96	0.561	9.1	67.8	0.4	1065.8	10
X	B	600	90.68	-0.0001	68.65	0.643	-	77.6	0.9	1294.0	8.5
X	C	650	81.41	0.0127	30.09	1.77	40.1	89.1	2.2	1321.9	3.6
X	D	700	77.31	0.0014	7.579	4.06	364.9	97.1	5.1	1354.7	2.4
X	E	720	76.13	0.0040	5.212	3.93	128.0	98.0	7.9	1348.5	2.2
X	F	750	75.93	0.0018	3.979	6.35	277.1	98.4	12.5	1350.7	2.2
X	G	770	76.12	0.0016	2.889	7.65	318.6	98.9	18.1	1357.2	2.0
X	H	785	76.41	0.0021	2.390	8.94	248.5	99.1	24.5	1362.7	2.0
X	I	800	76.66	0.0009	2.159	10.32	551.3	99.2	32.0	1366.8	2.6
X	J	820	76.46	0.0019	1.655	12.41	266.0	99.4	41.0	1366.1	2.1
x	K	850	76.87	0.0022	1.526	14.27	231.8	99.4	51.3	1371.8	2.0
x	L	870	77.22	0.0029	1.832	10.15	176.4	99.3	58.7	1375.1	2.2
x	M	890	77.18	0.0028	1.975	9.07	181.8	99.2	65.2	1374.1	2.2
x	N	910	77.62	0.0018	2.736	7.06	285.3	98.9	70.3	1376.8	2.2
x	O	930	77.54	0.0029	2.748	6.52	173.7	98.9	75.0	1375.7	1.9
x	P	950	77.61	0.0026	3.169	7.16	194.0	98.8	80.2	1375.0	2.0
	Q	980	78.90	0.0012	5.660	10.55	411.9	97.9	87.9	1382.0	2.4
	R	1010	80.98	0.0017	12.74	11.58	305.6	95.3	96.2	1381.8	2.4
	S	1040	85.12	0.0029	27.33	5.20	173.0	90.5	100.0	1379.7	2.7
	Integrated age ± 1σ			n=19		138.2		K2O=8.08%		1368.2	1.3
	Terminal Age ± 1σ		steps Q-S	n=3	MSWD=0.23	27.339			19.8	1381.28	1.5
	P-01-01, Muscovite, .38 mg, J=0.014602±0.05%, D=1.0045±0.0011, NM-261A, Lab#=61990-01										
x	A	550	371.8	0.0471	975.9	0.187	10.8	22.4	0.2	1458.4	37
x	B	600	140.5	0.0235	183.6	0.221	21.7	61.4	0.4	1491.8	19
x	C	650	121.3	0.0003	135.4	0.539	1911.6	67.0	0.8	1431.8	9.5
x	D	700	103.2	-0.0030	80.42	1.247	-	77.0	1.9	1410.0	6.1
x	E	720	83.96	0.0082	20.09	1.82	61.9	92.9	3.5	1391.9	4.5
x	F	750	79.92	0.0004	6.404	4.99	1179.1	97.6	7.8	1392.0	2.2
	G	770	79.00	0.0027	5.508	5.46	191.7	97.9	12.5	1383.8	2.3
	H	785	78.80	0.0024	4.584	6.01	213.8	98.3	17.7	1384.7	2.1
	I	800	78.62	0.0017	4.153	6.90	300.4	98.4	23.7	1384.0	1.9
	J	820	78.35	0.0023	3.201	8.77	221.4	98.8	31.3	1384.2	2.0
	K	850	78.57	0.0006	2.310	12.98	910.1	99.1	42.5	1390.2	2.0
	L	870	78.14	0.0019	2.116	11.94	265.2	99.2	52.9	1385.7	2.3
	M	890	78.29	0.0031	2.307	10.96	165.2	99.1	62.4	1386.8	2.0
	N	910	78.21	0.0019	2.425	10.99	264.9	99.1	71.9	1385.3	2.3
	O	930	78.38	0.0024	3.229	8.30	216.5	98.8	79.1	1384.5	1.9
	P	950	78.84	0.0037	4.822	7.00	139.7	98.2	85.1	1384.4	2.1
	Q	980	79.13	0.0024	5.209	7.74	212.5	98.0	91.8	1386.6	1.9
	R	1010	79.70	0.0017	7.058	9.41	302.7	97.4	100.0	1386.9	2.4
	Integrated age ± 1σ			n=18		115.5		K2O=7.99%		1387.1	1.4
	Plateau ± 1σ		steps E-R	n=14	MSWD=1.41	113.3			98.1	1386.13	0.8

Appendix 1 $^{40}Ar/^{39}Ar$ analytical data.

	ID	Temperature (°C)	$^{40}Ar/^{39}Ar$	$^{37}Ar/^{39}Ar$	$^{36}Ar/^{39}Ar$ (x 10^{-3})	$^{39}Ar_K$ (x 10^{-15} mol)	K/Ca	$^{40}Ar^*$ (%)	^{39}Ar (%)	Age (Ma)	±1σ (Ma)
	P-02-02, Muscovite, .3 mg, J=0.014602±0.05%, D=1.0045±0.0011, NM-261A, Lab#=61991-01										
x	A	550	138.1	-0.0027	201.2	0.276	-	56.9	0.3	1399.6	18
x	B	600	100.8	0.0080	66.24	0.362	63.4	80.6	0.7	1431.0	13
x	C	650	138.6	0.0008	193.6	0.824	611.8	58.7	1.6	1433.5	10
x	D	700	95.17	0.0034	55.02	1.86	147.9	82.9	3.6	1403.1	5.0
x	E	720	84.44	-0.0019	21.71	1.97	-	92.4	5.8	1391.9	4.2
x	F	750	80.53	-0.0001	9.899	3.72	-	96.4	9.9	1386.7	2.6
	G	770	78.36	0.0015	5.481	5.05	340.6	97.9	15.4	1375.8	2.3
	H	785	77.91	0.0013	4.376	5.76	386.2	98.3	21.7	1374.3	2.4
	I	800	77.71	0.0011	3.611	6.27	459.6	98.6	28.6	1374.7	1.9
	J	820	77.30	0.0007	3.196	7.19	685.9	98.8	36.5	1371.0	2.0
	K	850	77.36	0.0012	2.409	8.96	408.3	99.1	46.3	1374.7	1.9
	L	870	77.22	0.0030	2.648	8.33	168.8	99.0	55.5	1372.1	1.9
	M	890	77.20	0.0011	2.674	8.39	444.6	99.0	64.7	1371.7	2.0
	N	910	77.61	0.0020	3.734	6.27	252.1	98.6	71.5	1372.9	1.9
	O	930	77.82	0.0021	4.371	5.52	242.5	98.3	77.6	1373.2	2.2
	P	950	77.95	0.0013	4.535	5.72	398.5	98.3	83.9	1374.2	2.1
	Q	980	79.37	0.0004	9.581	6.33	1245.3	96.4	90.8	1373.3	2.2
	R	1010	81.97	0.0020	16.95	8.37	251.3	93.9	100.0	1378.7	2.2
	Integrated age ± 1σ			n=18		91.2		K2O=7.99%		1376.2	1.4
	Plateau ± 1σ		steps G-R	n=12	MSWD=0.97	82.2			90.1	1373.79	0.8
	P-01-03, Muscovite, .58 mg, J=0.014602±0.05%, D=1.0045±0.0011, NM-261A, Lab#=61992-01										
x	B	600	129.5	0.0059	193.5	0.810	86.5	55.8	0.6	1319.1	8.9
X	C	650	133.0	-0.0020	182.7	2.83	-	59.4	2.5	1404.8	5.6
	D	685	80.49	0.0002	8.505	3.85	3101.5	96.9	5.2	1391.3	2.7
	E	720	79.85	0.0012	4.620	6.70	440.9	98.3	9.9	1397.8	2.3
	F	740	79.31	0.0019	3.886	7.05	268.9	98.5	14.8	1393.7	1.9
	G	750	79.78	0.0017	4.195	6.34	305.6	98.4	19.2	1398.4	2.1
	H	760	79.84	0.0013	4.511	6.20	388.4	98.3	23.6	1398.0	2.0
	I	770	79.82	0.0002	3.964	6.33	2509.6	98.5	28.0	1399.7	2.0
	J	780	79.92	0.0004	4.093	6.67	1283.9	98.5	32.6	1400.5	1.9
	K	790	79.45	0.0009	3.910	7.27	559.6	98.5	37.7	1395.3	2.0
	L	800	79.41	0.0011	3.781	7.24	472.2	98.6	42.7	1395.4	2.0
	M	810	79.65	0.0032	4.046	6.44	157.6	98.5	47.2	1397.3	2.0
	N	820	79.78	0.0017	4.315	6.33	302.5	98.4	51.6	1398.0	2.2
	O	830	79.65	0.0030	4.168	6.12	169.4	98.4	55.9	1396.9	2.1
	P	840	79.64	0.0018	4.371	6.07	284.4	98.4	60.1	1396.0	2.0
	Q	850	79.89	0.0008	4.623	5.61	654.9	98.3	64.1	1398.2	2.1
	R	860	79.73	0.0034	5.139	5.13	150.0	98.1	67.6	1394.3	2.1
	S	870	79.94	0.0001	6.023	4.19	7405.0	97.8	70.6	1393.7	2.7
X	T	885	80.40	0.0011	5.271	4.88	449.4	98.1	74.0	1402.1	2.2
x	U	900	80.31	0.0034	4.611	5.05	149.0	98.3	77.5	1403.4	2.4
x	V	915	80.38	0.0014	5.639	4.64	370.0	97.9	80.7	1400.6	2.4
x	W	930	79.99	0.0045	5.664	4.53	112.6	97.9	83.9	1395.6	2.6
x	X	945	79.65	0.0022	5.886	4.73	229.9	97.8	87.2	1390.5	2.5
x	Y	960	80.64	0.0029	6.837	4.92	174.5	97.5	90.6	1399.4	2.5
x	Z	975	81.94	-0.0002	11.94	4.77	-	95.7	93.9	1396.7	2.8
x	AA	990	83.24	0.0011	17.52	4.21	464.6	93.8	96.9	1392.4	2.5
x	AB	1020	85.06	0.0052	22.74	4.49	97.5	92.1	100.0	1395.9	2.7
	Integrated age ± 1σ			n=27		143.4		K2O=6.50%		1396.7	1.4
	Plateau ± 1σ		steps D-S	n=16	MSWD=1.22	97.5			68.0	1396.72	0.7

Appendix 1 $^{40}Ar/^{39}Ar$ analytical data.

	ID	Temperature (°C)	$^{40}Ar/^{39}Ar$	$^{37}Ar/^{39}Ar$	$^{36}Ar/^{39}Ar$ (x 10^{-3})	$^{39}Ar_K$ (x 10^{-15} mol)	K/Ca	$^{40}Ar^*$ (%)	^{39}Ar (%)	Age (Ma)	±1σ (Ma)
	P-01-04, Muscovite, .4 mg, J=0.014658±0.06%, D=1.0045±0.0011, NM-261A, Lab#=61993-01										
x	A	550	124.6	0.0002	178.5	0.386	3376.6	57.7	0.4	1316.8	12
x	B	600	93.30	-0.0284	48.83	0.443	-	84.5	0.8	1406.2	8.8
x	C	650	97.10	-0.0140	61.89	0.884	-	81.2	1.7	1405.5	6.1
x	D	700	86.90	-0.0096	32.50	1.62	-	88.9	3.4	1386.5	4.3
x	E	720	83.00	-0.0008	20.78	1.73	-	92.6	5.1	1381.1	3.5
x	F	750	79.60	-0.0041	12.85	2.77	-	95.2	7.9	1367.7	2.6
x	G	770	77.44	0.0001	9.419	3.62	8560.5	96.4	11.5	1353.0	3.0
x	H	785	76.47	-0.0024	8.825	4.82	-	96.6	16.4	1342.8	3.1
	I	800	76.60	-0.0011	2.672	5.88	-	99.0	22.3	1367.8	2.1
	J	820	76.41	-0.0005	1.648	9.09	-	99.4	31.5	1369.2	2.2
	K	850	76.54	0.0009	2.066	10.96	549.1	99.2	42.5	1369.2	2.5
	L	870	76.79	0.0008	3.562	6.47	619.7	98.6	49.1	1366.9	2.1
	M	890	76.88	0.0010	3.303	6.07	508.5	98.7	55.2	1369.0	2.1
	N	910	77.21	0.0006	4.174	4.69	915.8	98.4	59.9	1369.9	2.4
	O	930	77.39	0.0003	5.683	4.30	2007.1	97.8	64.3	1366.5	2.4
	P	950	77.47	0.0005	5.220	4.42	1080.3	98.0	68.7	1369.3	2.5
	Q	980	78.81	0.0002	8.794	5.78	2434.2	96.7	74.5	1372.9	2.3
	R	1010	79.92	0.0004	13.01	8.72	1139.1	95.2	83.3	1371.2	2.2
	S	1040	80.50	0.0007	14.28	12.95	703.1	94.7	96.4	1373.7	2.1
	T	1070	104.2	0.0032	96.27	3.57	158.4	72.7	100.0	1367.6	4.2
	Integrated age ± 1σ			n=20		99.1		K2O=6.50%		1368.7	1.5
	Plateau ± 1σ		steps I-T	n=12	MSWD=1.00	82.9			83.6	1369.56	0.9
	P-01-05, Muscovite, .5 mg, J=0.014658±0.06%, D=1.0045±0.0011, NM-261A, Lab#=61994-01										
x	A	550	113.0	-0.0360	164.5	0.353	-	57.0	0.3	1217.0	14
x	B	600	89.91	0.0003	45.32	0.396	2040.0	85.1	0.7	1376.8	9.2
x	C	650	93.26	0.0011	57.15	0.924	466.5	81.9	1.6	1374.9	6.0
x	D	700	85.56	-0.0011	33.98	1.78	-	88.3	3.4	1364.1	4.2
	E	720	80.53	0.0055	14.00	1.95	93.6	94.9	5.3	1375.1	3.7
	F	750	79.33	0.0021	10.62	3.70	245.2	96.0	8.9	1372.6	2.6
	G	770	77.08	0.0011	4.220	6.60	482.2	98.4	15.4	1368.1	1.9
	H	785	76.94	0.0006	2.693	8.50	859.8	99.0	23.7	1372.0	1.9
	I	800	76.87	0.0021	2.235	9.32	239.5	99.1	32.8	1372.8	2.1
	J	820	77.34	0.0026	2.096	9.98	199.6	99.2	42.6	1379.3	2.2
	K	850	77.10	0.0018	1.673	11.22	285.5	99.3	53.6	1377.9	2.1
	L	870	77.15	0.0020	2.417	9.03	255.1	99.1	62.5	1375.7	2.2
	M	890	77.26	0.0018	3.852	5.39	290.3	98.5	67.8	1371.7	2.4
	N	910	77.37	0.0029	4.540	4.23	173.4	98.3	71.9	1370.5	2.6
	O	930	77.53	0.0025	6.109	3.67	201.9	97.7	75.5	1366.6	2.8
	P	950	78.76	0.0068	7.715	3.54	74.7	97.1	79.0	1376.3	2.6
	Q	980	79.13	0.0031	10.87	4.88	165.1	95.9	83.8	1369.1	2.4
	R	1010	81.39	0.0026	17.52	8.16	196.2	93.6	91.8	1373.0	2.2
	S	1040	82.15	0.0022	19.38	8.42	229.2	93.0	100.0	1375.5	2.5
	Integrated age ± 1σ			n=19		102.0		K2O=5.35%		1373.1	1.4
	Plateau ± 1σ		steps D-R	n=15	MSWD=2.68	92.0			90.1	1372.7	1.2

Appendix 1 $^{40}Ar/^{39}Ar$ analytical data.

	ID	Temperature (°C)	$^{40}Ar/^{39}Ar$	$^{37}Ar/^{39}Ar$	$^{36}Ar/^{39}Ar$ (x 10^{-3})	$^{39}Ar_K$ (x 10^{-15} mol)	K/Ca	$^{40}Ar^*$ (%)	^{39}Ar (%)	Age (Ma)	±1σ (Ma)
	P-01-06, Muscovite, .35 mg, J=0.014658±0.06%, D=1.0045±0.0011, NM-261A, Lab#=61995-01										
x	A	550	224.0	0.1277	474.8	0.221	4.0	37.4	0.3	1465.7	22
x	B	600	211.6	0.0707	439.0	0.287	7.2	38.7	0.8	1443.6	22
x	C	650	109.2	0.0298	108.9	0.728	17.1	70.5	1.9	1382.7	8.0
x	D	700	105.1	0.0149	93.53	1.391	34.3	73.7	4.0	1388.5	6.0
x	E	720	91.90	0.0079	47.08	1.66	64.6	84.9	6.6	1395.3	4.2
x	F	750	78.99	0.0065	6.955	3.01	78.9	97.4	11.2	1382.1	2.7
	G	770	77.71	0.0071	4.382	4.16	72.2	98.3	17.6	1375.4	2.6
	H	785	77.64	0.0035	3.783	4.77	144.4	98.6	24.9	1376.8	2.3
	I	800	76.97	0.0054	3.098	5.15	94.6	98.8	32.8	1370.9	2.6
	J	820	76.98	0.0035	2.541	6.45	146.4	99.0	42.7	1373.1	2.0
	K	850	76.81	0.0033	2.224	7.30	155.8	99.1	53.8	1372.1	2.1
	L	870	76.82	0.0043	2.395	6.58	118.9	99.1	63.9	1371.6	2.0
	M	890	76.72	0.0031	2.894	5.08	163.5	98.9	71.7	1368.5	2.1
	N	910	76.70	0.0065	3.946	4.28	78.6	98.5	78.3	1364.3	2.6
x	O	930	77.81	0.0065	5.159	3.00	78.7	98.0	82.9	1373.8	3.0
x	P	950	77.93	0.0087	5.977	3.02	58.7	97.7	87.5	1372.3	2.7
x	Q	980	79.59	0.0078	9.461	4.07	65.2	96.5	93.7	1380.3	2.3
x	R	1010	82.77	0.0058	21.52	4.10	88.2	92.3	100.0	1375.4	3.0
	Integrated age ± 1σ			n=18		65.3	79.8	K2O=4.89%		1374.8	1.5
	Plateau ± 1σ		steps G-N	n=8	MSWD=2.55	43.8			67.1	1371.7	1.4
	Terminal age 1σ		steps Q-R	n=2	MSWD=1.70	8.2			12.5	1378.4	2.4
	B-2-1, Schist Musc, .33 mg, J=0.014752±0.09%, D=1.0045±0.0011, NM-261C, Lab#=62006-01										
x	A	610	56.91	0.0349	46.54	0.421	14.6	75.8	0.5	901.8	12
x	B	650	72.00	-0.0026	6.162	0.314	-	97.5	0.9	1300.8	11
x	C	690	74.50	-0.0092	4.605	0.399	-	98.2	1.4	1339.6	9.9
x	D	720	74.59	0.0069	1.006	0.590	73.9	99.6	2.1	1354.6	7.2
x	E	740	73.86	0.0031	1.340	0.810	164.5	99.5	3.1	1343.8	5.4
x	F	750	75.64	0.0003	0.4783	1.473	1710.4	99.8	5.0	1370.0	3.8
	G	760	75.50	0.0004	0.4464	2.54	1438.8	99.8	8.1	1368.3	3.3
	H	770	74.98	0.0012	0.9802	3.06	422.1	99.6	11.9	1359.6	2.4
	I	775	74.77	0.0038	0.7001	2.59	132.8	99.7	15.1	1358.0	3.0
	J	785	75.44	-0.0004	0.4312	3.04	-	99.8	18.9	1367.6	3.0
	K	785	75.62	0.0028	0.6900	2.15	184.1	99.7	21.5	1368.9	3.4
	L	795	75.35	-0.0003	0.1742	2.62	-	99.9	24.8	1367.5	2.9
	M	800	75.90	0.0041	0.5283	2.38	124.2	99.8	27.7	1373.1	3.0
	N	805	75.28	0.0025	-0.2526	2.13	200.2	100.1	30.3	1368.1	3.1
	O	820	74.83	0.0018	0.3269	2.89	278.8	99.9	33.9	1360.1	2.4
	P	825	75.27	0.0037	0.0597	2.32	136.3	100.0	36.8	1366.8	2.9
	Q	835	75.15	0.0000	0.9699	2.41	-	99.6	39.8	1361.8	3.3
	R	850	75.91	0.0007	0.5741	2.60	701.3	99.8	43.0	1373.0	3.4
	S	870	75.75	0.0018	0.8922	3.08	286.1	99.6	46.8	1369.9	2.8
	T	885	74.95	0.0022	0.2733	2.81	228.5	99.9	50.3	1361.9	3.1
	U	900	75.32	0.0024	0.1221	2.79	210.0	99.9	53.7	1367.3	2.6
	V	915	75.40	0.0008	0.0450	2.87	611.0	100.0	57.3	1368.6	2.5
	W	930	75.68	0.0020	0.9953	2.32	256.7	99.6	60.1	1368.5	3.4
	X	945	75.63	0.0030	0.1910	2.12	168.9	99.9	62.8	1370.9	3.1
	Y	960	75.06	0.0020	0.2984	2.32	251.6	99.9	65.6	1363.2	2.8
	Z	975	75.91	0.0019	0.8218	2.54	271.3	99.7	68.8	1372.2	3.2
	AA	990	75.41	0.0004	0.6653	2.91	1392.9	99.7	72.4	1366.3	2.6
x	AB	1020	75.59	0.0006	0.4893	4.48	842.9	99.8	77.9	1369.3	2.4
x	AC	1070	76.03	0.0007	0.6686	10.76	759.8	99.7	91.3	1374.3	2.1
x	AD	1620	75.98	0.0012	8.168	7.06	421.4	96.8	100.0	1345.1	1.9
	Integrated age ± 1σ			n=30		80.8		K2O=6.37%		1363.1	1.5
	Plateau ± 1σ		steps G-AA	n=21	MSWD=2.30	54.5			67.4	1366.4	1.3

Appendix 1 $^{40}Ar/^{39}Ar$ analytical data.

	ID	Temperature (°C)	$^{40}Ar/^{39}Ar$	$^{37}Ar/^{39}Ar$	$^{36}Ar/^{39}Ar$ (x 10^{-3})	$^{39}Ar_K$ (x 10^{-15} mol)	K/Ca	$^{40}Ar^*$ (%)	^{39}Ar (%)	Age (Ma)	±1σ (Ma)
	B-2-2, Schist Musc, .18 mg, J=0.014736±0.08%, D=1.0045±0.0011, NM-261C, Lab#=62007-01										
x	A	610	61.68	0.1397	78.90	0.282	3.7	62.2	1.3	820.4	15.9
x	B	650	67.47	0.0447	14.11	0.224	11.4	93.8	2.3	1206.2	14.8
x	C	720	73.01	0.0825	7.725	0.496	6.2	96.9	4.5	1307.1	7.4
x	D	740	74.91	0.0951	5.615	0.415	5.4	97.8	6.3	1340.2	8.2
	E	770	75.45	0.0335	0.8620	2.00	15.2	99.7	15.3	1365.1	3.4
	F	820	74.95	0.0320	1.115	5.51	15.9	99.6	40.0	1357.8	1.9
	G	850	75.10	0.0590	0.8995	3.12	8.6	99.6	54.0	1360.6	2.5
	H	870	74.75	0.1092	1.413	1.455	4.7	99.4	60.5	1354.2	3.5
	I	930	75.01	0.1081	2.179	1.74	4.7	99.1	68.2	1354.7	3.3
x	J	945	74.25	0.0838	2.242	1.081	6.1	99.1	73.1	1344.5	4.7
x	K	960	75.82	0.0273	0.9731	1.324	18.7	99.6	79.0	1369.4	4.8
x	L	975	74.92	0.0214	1.405	1.66	23.9	99.4	86.5	1356.3	3.6
x	M	990	74.93	0.0205	1.886	1.570	24.9	99.2	93.5	1354.6	3.8
x	N	1020	76.16	0.0240	1.277	1.455	21.3	99.5	100.0	1372.5	3.7
	Integrated age ± 1σ			n=14		22.3	10.1	K2O=3.23%		1350.2	1.6
	Plateau ± 1σ		steps E-I	n=5	MSWD=1.87	13.8			61.9	1358.5	1.8
	Terminal Age ± 1σ		steps N-N	n=1	MSWD=0.0				6.5	1372.5	3.7
	B-2-3, Schist Musc, .25 mg, J=0.014681±0.07%, D=1.0045±0.0011, NM-261C, Lab#=62009-02										
X	A	550	41.18	0.1004	17.68	0.474	5.1	87.3	0.3	776.0	8.5
X	B	600	53.18	0.0473	13.13	0.377	10.8	92.7	0.6	996.7	8.2
X	C	650	57.98	0.0219	5.314	0.767	23.3	97.3	1.1	1104.3	5.3
X	D	700	61.99	0.0106	3.961	1.452	48.2	98.1	2.1	1168.0	3.5
X	E	720	63.85	0.0108	3.468	1.248	47.2	98.4	2.9	1196.3	4.5
X	F	750	66.17	0.0131	1.769	2.03	38.9	99.2	4.2	1235.3	2.9
X	G	770	68.72	0.0044	1.399	2.66	116.7	99.4	6.0	1271.3	2.7
X	H	785	69.86	0.0042	1.467	2.90	121.4	99.4	8.0	1286.3	2.6
X	I	800	71.02	0.0075	0.9848	3.48	68.3	99.6	10.3	1303.5	2.4
X	J	820	71.63	0.0046	0.9052	4.65	110.4	99.6	13.4	1311.8	2.3
x	K	850	73.75	0.0018	0.4928	12.05	290.8	99.8	21.5	1341.0	2.2
x	L	870	74.50	0.0021	0.3490	17.3	238.5	99.9	33.0	1351.3	1.9
x	M	890	72.78	0.0036	0.8177	7.41	141.3	99.7	38.0	1327.2	2.0
x	N	910	72.98	0.0035	1.012	5.78	147.3	99.6	41.9	1329.1	1.8
x	O	930	72.86	0.0044	1.132	5.10	116.5	99.5	45.3	1327.0	1.9
x	P	950	73.03	0.0050	0.9219	4.84	102.0	99.6	48.5	1330.1	2.1
x	Q	980	74.06	0.0039	1.044	5.80	129.6	99.6	52.4	1342.9	2.0
x	R	1010	74.30	0.0019	0.7789	8.16	275.5	99.7	57.9	1347.0	2.1
x	S	1040	74.65	0.0022	0.4560	15.53	236.2	99.8	68.3	1352.8	1.9
	T	1070	75.49	0.0011	0.3832	29.3	475.7	99.8	87.9	1363.8	1.6
	U	1110	75.17	0.0018	0.8191	18.1	289.7	99.7	100.0	1358.1	1.8
	Integrated age ± 1σ			n=21		149.4		K2O=15.64%		1336.8	1.3
	Terminal Age ± 1σ		steps T-U	n=2	MSWD=5.55	47.436			31.7	1361.28	2.9

Appendix 1 $^{40}Ar/^{39}Ar$ analytical data.

	ID	Temperature (°C)	$^{40}Ar/^{39}Ar$	$^{37}Ar/^{39}Ar$	$^{36}Ar/^{39}Ar$ (x 10^{-3})	$^{39}Ar_K$ (x 10^{-15} mol)	K/Ca	$^{40}Ar^*$ (%)	^{39}Ar (%)	Age (Ma)	±1σ (Ma)
	2-7-17A, , .49 mg, J=0.014565±0.05%, D=1.0045±0.0011, NM-261B, Lab#=62004-01										
X	A	550	100.5	0.0628	163.0	0.330	8.1	52.1	0.2	1037.1	14.4
X	B	600	82.13	0.0464	23.85	0.381	11.0	91.4	0.4	1352.5	9.9
X	C	650	82.13	0.0038	19.23	0.798	132.9	93.1	0.9	1369.7	7.9
X	D	700	86.51	0.0075	23.31	1.61	67.6	92.0	1.9	1409.3	4.4
X	E	720	86.01	0.0030	16.58	2.40	171.1	94.3	3.3	1427.6	3.2
	F	750	83.17	0.0004	3.365	14.64	1316.7	98.8	12.1	1440.6	2.0
	G	770	82.25	0.0010	1.089	22.4	512.6	99.6	25.5	1437.6	1.8
	H	785	81.77	0.0018	1.136	18.3	278.1	99.6	36.5	1431.6	1.9
	I	800	82.14	0.0007	1.465	14.07	754.7	99.5	44.9	1434.9	2.1
	J	820	82.04	0.0020	1.403	11.88	258.1	99.5	52.0	1433.9	2.0
	K	850	81.94	0.0019	1.449	10.71	275.4	99.5	58.4	1432.5	2.2
x	L	870	81.81	0.0033	3.043	5.91	155.0	98.9	62.0	1425.2	2.3
x	M	890	82.32	-0.0009	4.802	3.65	-	98.3	64.2	1425.1	2.8
x	N	910	82.44	0.0062	5.523	2.96	82.7	98.0	65.9	1423.9	3.7
x	O	930	81.79	0.0022	5.972	2.92	236.1	97.8	67.7	1414.3	3.1
x	P	950	82.70	0.0046	5.286	3.01	110.6	98.1	69.5	1428.0	3.2
x	Q	980	82.40	0.0008	4.255	4.24	638.6	98.5	72.0	1428.0	2.6
x	R	1010	82.66	0.0017	2.754	7.37	296.5	99.0	76.5	1436.6	1.9
x	S	1040	82.77	0.0006	2.089	13.20	788.0	99.2	84.4	1440.3	2.0
x	T	1070	82.63	0.0014	2.871	15.42	366.0	99.0	93.6	1435.8	2.0
x	U	1110	83.77	0.0019	5.959	10.68	272.1	97.9	100.0	1438.6	2.6
	Integrated age ± 1σ			n=21		166.9	287.9	K2O=8.98%		1433.0	1.3
	Plateau ± 1σ		steps F-K	n=6	MSWD=2.94	92.037			55.1	1435.33	1.5
	Terminal Age ± 1σ		steps S-U	n=3	MSWD=1.32	39.301			23.5	1438.10	1.5

Appendix 1 $^{40}Ar/^{39}Ar$ analytical data.

	ID	Temperature (°C)	$^{40}Ar/^{39}Ar$	$^{37}Ar/^{39}Ar$	$^{36}Ar/^{39}Ar$ (x 10^{-3})	$^{39}Ar_K$ (x 10^{-15} mol)	K/Ca	$^{40}Ar^*$ (%)	^{39}Ar (%)	Age (Ma)	±1σ (Ma)
	3-7-17A, Muscovite, .69 mg, J=0.014588±0.05%, D=1.0045±0.0011, NM-261B, Lab#=61999-01										
X	A	600	76.17	0.1178	38.80	1.156	4.3	85.0	0.5	1216.9	4.7
X	B	650	80.00	0.0150	8.774	1.59	34.1	96.8	1.3	1383.4	3.6
X	C	685	86.10	0.0121	22.48	2.00	42.1	92.3	2.2	1408.9	3.6
X	D	720	83.57	0.0057	9.020	3.27	90.1	96.8	3.8	1426.6	3.0
X	E	740	82.23	0.0056	5.161	4.01	91.7	98.1	5.6	1424.2	2.5
X	F	750	81.96	0.0056	5.109	3.79	91.4	98.1	7.4	1421.1	2.4
	G	760	82.34	0.0040	3.656	4.31	128.0	98.7	9.4	1431.0	2.5
	H	770	82.08	0.0009	3.024	4.99	575.1	98.9	11.8	1430.1	2.3
	I	780	81.74	0.0012	2.002	5.72	436.4	99.3	14.5	1429.6	2.2
	J	790	82.12	0.0020	1.982	8.28	256.1	99.3	18.3	1434.3	2.1
	K	800	81.83	0.0016	1.072	12.76	323.2	99.6	24.3	1434.1	2.1
	L	810	81.38	0.0015	0.9666	14.69	349.0	99.6	31.2	1429.0	1.9
	M	820	81.71	0.0017	1.005	12.03	294.4	99.6	36.8	1432.9	2.0
	N	830	81.40	0.0031	1.464	9.33	165.2	99.5	41.2	1427.4	2.3
	O	840	81.53	0.0032	1.582	7.28	158.9	99.4	44.6	1428.7	1.8
X	P	850	81.07	0.0037	1.890	5.84	137.1	99.3	47.4	1421.8	2.3
X	Q	860	81.37	0.0018	2.210	5.01	289.6	99.2	49.7	1424.3	2.1
X	R	870	81.54	0.0029	2.259	4.19	176.9	99.2	51.7	1426.3	2.4
X	S	885	81.31	0.0024	2.424	4.19	209.0	99.1	53.6	1422.8	2.5
X	T	900	80.70	0.0030	2.399	4.16	172.7	99.1	55.6	1415.5	2.4
X	U	915	81.30	0.0018	2.248	4.52	283.3	99.2	57.7	1423.3	2.2
X	V	930	81.13	0.0027	2.376	4.68	189.3	99.1	59.9	1420.8	2.4
X	W	945	81.12	0.0040	1.901	4.66	127.2	99.3	62.1	1422.4	2.3
X	X	960	81.67	0.0036	1.959	5.03	140.5	99.3	64.5	1429.0	2.9
X	Y	975	81.84	0.0034	2.019	5.34	149.9	99.3	67.0	1430.8	1.9
X	Z	990	81.24	0.0012	1.831	6.09	423.5	99.3	69.8	1424.1	2.1
X	AA	1020	81.58	0.0030	1.417	8.22	167.5	99.5	73.7	1429.8	1.9
X	AB	1035	81.95	0.0018	1.678	8.84	277.3	99.4	77.8	1433.4	2.3
X	AC	1050	82.08	0.0020	1.359	10.66	257.1	99.5	82.8	1436.1	2.4
X	AD	1070	82.21	0.0013	1.541	14.78	406.5	99.4	89.7	1437.1	2.1
X	AE	1120	82.66	0.0009	1.572	21.9	546.1	99.4	100.0	1442.4	1.8
	Integrated age ± 1σ			n=31		213.4		K2O=8.14%		1429.1	1.3
	Plateau ± 1σ		steps G-O	n=9	MSWD=1.43	79.402			37.2	1430.78	1.0
	Terminal Age ± 1σ		steps AC-AE	n=3	MSWD=2.87	47.334			22.2	1439.11	2.1

Appendix 1 $^{40}Ar/^{39}Ar$ analytical data.

	ID	Temperature (°C)	$^{40}Ar/^{39}Ar$	$^{37}Ar/^{39}Ar$	$^{36}Ar/^{39}Ar$ (x 10^{-3})	$^{39}Ar_K$ (x 10^{-15} mol)	K/Ca	$^{40}Ar^*$ (%)	^{39}Ar (%)	Age (Ma)	±1σ (Ma)
	4-7-17C, , .64 mg, J=0.014543±0.05%, D=1.0045±0.0011, NM-261B, Lab#=62002-01										
X	A	600	81.17	0.1250	74.25	1.094	4.1	73.0	0.4	1137.5	5.7
X	B	650	96.27	0.0189	67.22	1.393	27.0	79.4	1.0	1367.8	5.1
X	C	685	86.22	0.0086	21.89	1.67	59.0	92.5	1.6	1409.5	4.1
X	D	720	86.59	0.0033	21.63	2.61	156.4	92.6	2.6	1414.9	3.2
X	E	740	85.90	0.0042	16.05	3.74	120.5	94.5	4.1	1426.6	2.6
	F	750	83.77	0.0025	7.058	6.97	205.6	97.5	6.8	1433.1	2.0
	G	760	82.57	0.0015	2.758	12.41	336.1	99.0	11.7	1433.9	1.8
	H	770	82.44	0.0012	2.109	16.9	443.3	99.2	18.3	1434.7	2.0
	I	780	82.29	0.0010	1.452	18.3	491.0	99.5	25.5	1435.3	1.8
	J	790	82.04	0.0015	1.244	17.2	346.3	99.5	32.2	1433.0	1.9
	K	800	81.92	0.0013	1.331	15.12	391.9	99.5	38.1	1431.2	1.8
	L	810	81.66	0.0016	1.266	12.96	328.2	99.5	43.2	1428.2	2.4
	M	820	81.62	0.0014	1.694	10.63	371.9	99.4	47.3	1426.3	2.4
	N	830	81.82	0.0005	1.773	8.83	958.1	99.4	50.8	1428.4	2.4
	O	840	81.77	0.0020	2.358	7.35	256.9	99.1	53.7	1425.7	2.1
X	P	850	81.60	0.0024	2.621	5.96	210.5	99.0	56.0	1422.6	2.1
X	Q	860	82.04	0.0007	3.051	4.75	692.8	98.9	57.8	1426.4	2.1
X	R	870	81.72	0.0014	3.492	3.88	353.3	98.7	59.4	1420.9	2.9
X	S	885	82.36	0.0021	3.882	3.43	238.7	98.6	60.7	1427.4	2.9
X	T	900	81.33	-0.0002	4.697	3.14	-	98.3	61.9	1411.8	2.8
X	U	915	81.76	0.0036	4.998	2.83	141.6	98.2	63.0	1415.9	3.1
X	V	930	81.97	0.0031	4.834	2.97	163.2	98.2	64.2	1419.1	3.0
X	W	945	82.33	0.0027	4.248	3.26	187.3	98.5	65.5	1425.7	3.1
X	X	960	81.81	0.0006	3.895	3.65	872.9	98.6	66.9	1420.6	2.6
X	Y	975	81.70	0.0025	4.061	4.19	204.1	98.5	68.5	1418.6	2.6
X	Z	990	81.88	0.0016	2.953	5.42	322.3	98.9	70.7	1424.8	2.0
X	AA	1020	82.33	0.0011	2.726	10.81	444.4	99.0	74.9	1431.2	2.5
X	AB	1035	82.42	0.0014	1.913	19.2	372.5	99.3	82.4	1435.2	1.8
X	AC	1050	82.51	0.0011	1.841	21.7	476.3	99.3	90.9	1436.6	1.7
X	AD	1070	82.45	0.0014	2.456	16.0	360.5	99.1	97.2	1433.6	2.0
X	AE	1120	82.82	0.0034	6.532	7.24	149.1	97.7	100.0	1423.4	2.1
	Integrated age ± 1σ			n=31		255.7	231.0	K2O=10.55%		1428.6	1.3
	Plateau ± 1σ		steps F-O	n=10	MSWD=2.97	126.693			49.5	1431.55	1.2
	Terminal Age ± 1σ		steps AA-AE	n=5	MSWD=6.64	75.022			29.3	1432.75	2.3
	B-5-7-17-13, Muscovite, .14 mg, J=0.014576±0.11%, D=1.0045±0.0011, NM-261C, Lab#=62012-01										
x	A	610	62.78	0.0868	40.23	0.600	5.9	81.1	0.9	1015.8	7.2
x	B	650	73.32	0.0483	11.56	0.473	10.6	95.3	1.6	1286.1	8.4
x	C	720	76.52	0.0520	8.006	1.108	9.8	96.9	3.2	1341.4	4.2
x	D	740	78.48	0.0426	3.695	0.890	12.0	98.6	4.5	1382.3	5.3
x	E	770	78.64	0.0333	3.369	1.541	15.3	98.7	6.7	1385.5	3.7
x	F	795	80.35	0.0147	1.402	4.41	34.7	99.5	13.1	1414.0	2.3
x	G	820	80.42	0.0095	0.9505	8.39	53.7	99.6	25.3	1416.5	1.8
x	H	850	79.60	0.0113	0.7611	7.67	45.0	99.7	36.5	1407.0	1.9
x	I	870	78.64	0.0205	0.9278	3.68	24.9	99.6	41.9	1394.5	2.5
x	J	930	78.13	0.0220	1.224	5.70	23.1	99.5	50.2	1387.1	2.2
x	K	945	78.49	0.0229	1.150	2.65	22.3	99.6	54.0	1391.9	3.3
x	L	960	79.02	0.0193	2.367	2.20	26.4	99.1	57.2	1393.9	3.3
x	M	975	79.85	0.0157	1.625	2.19	32.5	99.4	60.4	1407.0	3.9
x	N	990	80.08	0.0148	1.605	2.48	34.5	99.4	64.0	1409.9	3.3
x	O	1020	80.24	0.0081	1.144	5.51	63.0	99.6	72.1	1413.5	2.1
	P	1070	81.69	0.0080	0.8400	12.70	64.2	99.7	90.5	1432.4	2.0
x	Q	1120	81.17	0.0207	0.7684	6.49	24.6	99.7	100.0	1426.4	2.0
	Integrated age ± 1σ			n=17		68.7		K2O=12.93%		1406.8	1.7
	Terminal Age ± 1σ		steps P-P	n=1	MSWD=0.00	12.701			18.5	1432.43	2.0

Appendix 1 $^{40}Ar/^{39}Ar$ analytical data.

	ID	Temperature (°C)	$^{40}Ar/^{39}Ar$	$^{37}Ar/^{39}Ar$	$^{36}Ar/^{39}Ar$ (x 10^{-3})	$^{39}Ar_K$ (x 10^{-15} mol)	K/Ca	$^{40}Ar^*$ (%)	^{39}Ar (%)	Age (Ma)	±1σ (Ma)
	6-7-17A, Muscovite, .6 mg, J=0.014588±0.05%, D=1.0045±0.0011, NM-261B, Lab#=62000-01										
X	A	600	185.1	0.0056	653.0	1.169	91.7	-4.2	0.5	-222.0	33
X	B	650	190.5	-0.0022	666.2	1.099	-	-3.3	0.9	-178.7	36
X	C	685	165.0	0.0009	502.3	1.305	556.2	10.1	1.4	397.4	20
X	D	720	127.7	0.0015	278.5	2.51	330.6	35.6	2.4	930.6	8.7
X	E	740	96.92	0.0013	88.17	8.12	394.9	73.1	5.7	1299.4	3.4
X	F	750	92.28	0.0004	60.77	9.91	1291.7	80.5	9.7	1344.2	3.3
X	G	760	93.37	0.0012	68.70	10.87	434.4	78.3	14.1	1328.1	3.0
X	H	770	90.45	0.0016	54.90	11.98	328.0	82.1	18.9	1343.0	2.8
x	I	780	80.81	0.0012	0.5539	9.85	440.2	99.8	22.9	1423.5	2.6
x	J	790	80.70	0.0018	0.7645	13.05	283.4	99.7	28.1	1421.4	2.4
x	K	800	80.70	0.0012	0.9872	11.74	408.4	99.6	32.8	1420.6	2.3
x	L	810	80.75	0.0018	1.375	10.79	276.9	99.5	37.2	1419.8	2.4
x	M	820	80.84	0.0031	1.131	9.50	166.3	99.6	41.0	1421.7	2.2
x	N	830	80.37	0.0030	1.642	8.16	169.0	99.4	44.3	1414.2	2.0
x	O	840	80.00	0.0017	1.586	7.06	297.2	99.4	47.1	1409.8	1.9
x	P	850	80.23	0.0044	2.195	5.87	115.0	99.2	49.5	1410.4	2.2
x	Q	860	80.00	0.0019	2.513	4.93	275.4	99.1	51.5	1406.4	2.1
x	R	870	80.50	0.0026	2.969	4.17	192.9	98.9	53.1	1410.9	2.9
x	S	885	80.36	0.0042	3.178	4.39	122.7	98.8	54.9	1408.4	2.8
x	T	900	80.72	0.0049	2.637	4.57	105.1	99.0	56.7	1414.8	2.4
x	U	915	80.44	0.0036	2.660	4.99	141.3	99.0	58.7	1411.3	2.4
x	V	930	80.37	0.0041	2.458	5.22	125.8	99.1	60.8	1411.1	2.6
x	W	945	80.92	0.0032	2.355	5.78	157.2	99.1	63.2	1418.3	1.9
x	X	960	81.20	0.0019	1.814	6.91	269.2	99.3	65.9	1423.7	2.2
x	Y	975	80.87	0.0020	1.629	8.93	260.1	99.4	69.5	1420.3	2.1
	Z	990	81.66	0.0021	1.723	10.57	247.1	99.4	73.8	1429.7	2.4
	AA	1020	81.64	0.0017	1.336	16.8	297.1	99.5	80.5	1430.9	1.9
	AB	1035	81.62	0.0013	1.161	15.25	378.7	99.6	86.7	1431.2	2.0
	AC	1050	81.70	0.0017	1.362	17.0	303.2	99.5	93.5	1431.5	1.9
	AD	1070	82.27	0.0022	2.110	10.88	236.2	99.2	97.9	1435.7	2.3
x	AE	1120	81.96	0.0070	12.59	2.24	72.9	95.5	98.8	1393.8	3.8
X	AF	1620	84.72	0.0042	18.82	3.02	121.9	93.4	100.0	1405.2	3.2
	Integrated age ± 1σ			n=32		248.6		K2O=10.91%		1388.6	1.6
	Terminal Age ± 1σ	steps Z-AD		n=5	MSWD=1.01	70.467			28.3	1431.71	1.0

Appendix 1 $^{40}Ar/^{39}Ar$ analytical data.

	ID	Temperature (°C)	$^{40}Ar/^{39}Ar$	$^{37}Ar/^{39}Ar$	$^{36}Ar/^{39}Ar$ (x 10^{-3})	$^{39}Ar_K$ (x 10^{-15} mol)	K/Ca	$^{40}Ar^*$ (%)	^{39}Ar (%)	Age (Ma)	±1σ (Ma)
	7-7-17-13, Muscovite, .8 mg, J=0.014571±0.12%, D=1.0045±0.0011, NM-261C, Lab#=62013-01										
x	A	600	82.08	0.0352	52.44	1.491	14.5	81.1	0.5	1241.3	5.0
x	B	650	84.86	0.0084	4.291	1.561	60.8	98.5	1.0	1458.1	4.7
x	C	685	84.89	0.0087	6.979	1.74	59.0	97.6	1.6	1448.9	4.5
x	D	720	84.73	0.0074	3.567	2.46	68.6	98.7	2.4	1459.1	3.8
x	E	740	83.68	0.0062	1.346	2.58	82.0	99.5	3.2	1454.4	3.6
x	F	750	83.82	0.0020	2.329	2.27	261.2	99.2	4.0	1452.6	3.5
x	G	760	83.05	0.0052	1.623	2.81	98.2	99.4	4.9	1445.8	3.2
x	H	770	82.24	0.0021	1.159	4.11	248.8	99.6	6.3	1437.6	2.5
x	I	780	81.80	0.0034	0.9846	4.87	151.0	99.6	7.9	1432.8	2.1
x	J	790	81.93	0.0030	0.9230	5.56	170.9	99.7	9.7	1434.7	2.2
x	K	800	81.49	0.0032	0.9397	6.75	158.1	99.7	11.9	1429.3	2.4
x	L	810	81.46	0.0022	0.6606	8.16	229.0	99.8	14.6	1429.9	2.2
x	M	820	81.94	0.0019	0.5026	9.60	264.9	99.8	17.8	1436.4	2.3
x	N	830	82.07	0.0020	0.5670	10.48	260.6	99.8	21.2	1437.7	2.7
	O	840	81.68	0.0017	0.6736	10.92	298.0	99.7	24.8	1432.5	2.4
	P	850	81.72	0.0015	0.4195	9.30	345.7	99.8	27.9	1433.9	2.5
	Q	860	81.46	0.0020	0.7031	7.98	261.1	99.7	30.5	1429.7	2.4
	R	870	81.22	0.0017	0.6747	7.37	294.5	99.7	32.9	1427.0	1.9
	S	885	81.47	0.0011	0.6474	7.61	448.0	99.8	35.4	1430.0	2.0
	T	900	81.16	0.0009	0.4244	8.51	591.6	99.8	38.2	1427.1	2.3
	U	915	81.62	0.0012	0.5448	10.39	423.9	99.8	41.7	1432.3	2.5
	V	930	81.53	0.0019	0.6087	12.88	266.3	99.8	45.9	1431.0	2.2
	W	945	81.66	0.0009	0.5445	15.9	538.1	99.8	51.2	1432.7	2.3
	X	960	81.56	0.0008	0.5392	18.2	636.1	99.8	57.2	1431.5	2.1
	Y	975	81.51	0.0012	0.4502	19.0	425.0	99.8	63.4	1431.2	2.0
	Z	990	81.50	0.0016	0.3651	19.9	321.7	99.9	70.0	1431.4	1.9
	AA	1020	81.83	0.0008	0.3658	33.3	612.6	99.9	80.9	1435.5	1.8
	AB	1035	81.62	0.0010	0.3758	35.5	503.3	99.9	92.6	1432.9	1.7
	AC	1050	81.36	0.0009	0.5224	22.4	558.8	99.8	100.0	1429.2	2.1
	Integrated age ± 1σ			n=29		303.7		K2O=10.01%		1432.3	1.7
	Plateau ± 1σ		steps O-AC	n=15	MSWD=1.36	239.2			78.8	1431.3	1.3
	8-7-17-13, Muscovite, .27 mg, J=0.014581±0.12%, D=1.0045±0.0011, NM-261C, Lab#=62014-01										
X	A	550	52.04	0.0536	66.54	1.257	9.5	62.2	0.8	707.8	5.8
X	B	600	59.38	0.0176	3.151	1.419	29.0	98.4	1.6	1128.2	3.7
X	C	650	70.30	0.0083	2.899	1.76	61.4	98.8	2.7	1280.2	3.5
X	D	700	75.37	0.0061	1.501	2.82	83.9	99.4	4.5	1351.5	3.0
X	E	720	77.39	0.0040	0.9062	2.59	128.0	99.6	6.1	1379.2	3.3
X	F	750	78.74	0.0018	0.7794	3.84	290.4	99.7	8.4	1396.6	3.0
x	G	770	79.35	0.0022	0.4862	4.97	228.4	99.8	11.5	1405.3	2.8
x	H	785	80.10	0.0007	0.6277	5.50	696.1	99.8	14.8	1414.0	2.4
x	I	800	79.81	0.0021	0.4333	6.72	246.0	99.8	19.0	1411.2	2.1
x	J	820	80.43	0.0011	0.2910	9.51	479.6	99.9	24.8	1419.3	2.5
x	K	850	80.40	0.0008	0.5602	12.88	618.3	99.8	32.7	1418.0	2.3
x	L	870	79.04	0.0013	0.4824	8.03	380.6	99.8	37.7	1401.4	2.2
x	M	890	79.01	0.0017	0.4160	6.26	308.2	99.8	41.5	1401.4	2.2
x	N	910	79.02	0.0011	0.5536	6.20	461.4	99.8	45.3	1400.9	2.2
x	O	930	79.18	0.0014	0.3697	6.64	372.2	99.9	49.4	1403.6	1.9
x	P	950	78.82	0.0015	0.2606	7.06	347.0	99.9	53.7	1399.5	2.0
x	Q	980	78.99	0.0015	0.2370	9.74	336.9	99.9	59.7	1401.7	2.4
x	R	1010	79.60	0.0015	0.4278	13.16	337.1	99.8	67.8	1408.6	2.2
x	S	1040	80.15	0.0011	0.3319	17.1	471.6	99.9	78.3	1415.7	1.9
	T	1070	80.73	0.0012	0.4361	24.9	429.6	99.8	93.6	1422.4	1.7
X	U	1110	77.75	0.0017	0.5792	10.43	295.3	99.8	100.0	1385.0	2.4
	Integrated age ± 1σ			n=21		162.7		K2O=15.88%		1399.7	1.7
	Terminal Age ± 1σ		steps T-T	n=1	MSWD=0.00	24.882			15.3	1422.41	1.721

Appendix 1 $^{40}Ar/^{39}Ar$ analytical data.

	ID	Temperature (°C)	$^{40}Ar/^{39}Ar$	$^{37}Ar/^{39}Ar$	$^{36}Ar/^{39}Ar$ (x 10^{-3})	$^{39}Ar_K$ (x 10^{-15} mol)	K/Ca	$^{40}Ar^*$ (%)	^{39}Ar (%)	Age (Ma)	±1σ (Ma)
	9-7-17A, Muscovite, .23 mg, J=0.014565±0.05%, D=1.0045±0.0011, NM-261B, Lab#=62005-01										
x	A	550	98.18	0.0200	128.3	0.311	25.5	61.4	0.3	1153.3	15
x	B	600	91.33	-0.0193	19.74	0.326	-	93.6	0.6	1480.4	11
x	C	650	92.56	0.0086	19.85	0.630	59.5	93.7	1.2	1494.6	6.9
x	D	700	90.31	0.0014	14.31	1.330	367.9	95.3	2.5	1487.4	4.3
x	E	720	86.05	0.0015	11.08	1.420	334.7	96.2	3.8	1447.9	5.0
	F	750	84.72	0.0013	8.018	3.02	385.6	97.2	6.7	1442.7	2.8
	G	770	82.67	-0.0001	3.263	5.90	-	98.8	12.4	1434.9	2.2
	H	785	82.91	0.0015	3.180	6.70	344.2	98.9	18.8	1438.1	1.9
	I	800	82.71	0.0006	2.631	7.53	915.5	99.1	26.0	1437.6	1.7
	J	820	82.54	0.0020	1.880	9.31	253.0	99.3	34.9	1438.3	2.4
	K	850	82.64	0.0010	1.640	11.46	497.5	99.4	45.8	1440.3	1.9
	L	870	82.93	0.0003	2.729	7.94	1855.3	99.0	53.4	1440.0	1.9
	M	890	82.58	0.0013	3.250	6.24	392.8	98.8	59.4	1433.8	2.3
	N	910	83.12	0.0019	3.592	6.05	271.1	98.7	65.2	1439.2	2.2
	O	930	82.75	0.0020	3.585	5.01	252.3	98.7	70.0	1434.8	2.3
	P	950	82.86	0.0036	3.931	5.21	141.2	98.6	75.0	1434.8	2.4
	Q	980	82.79	0.0017	2.788	7.52	298.9	99.0	82.1	1438.0	2.0
	R	1010	83.14	0.0016	2.241	10.68	310.5	99.2	92.4	1444.2	2.4
	S	1040	83.04	0.0014	4.442	7.99	368.9	98.4	100.0	1435.1	2.1
	Integrated age ± 1σ			n=19		104.6		K2O=11.99%		1438.8	1.3
	Plateau ± 1σ		steps E-Q	n=13	MSWD=1.56	83.3			79.7	1437.90	0.9
	10-7-17-13, Muscovite, .27 mg, J=0.014596±0.12%, D=1.0045±0.0011, NM-261C, Lab#=62063-01										
X	A	550	57.08	0.0286	57.70	0.482	17.8	70.1	0.8	842.2	10
X	B	600	51.83	0.0164	4.428	0.574	31.2	97.5	1.8	1011.0	7.5
X	C	650	62.43	0.0089	6.624	0.764	57.5	96.9	3.1	1158.1	6.3
X	D	700	70.40	0.0150	2.890	1.384	33.9	98.8	5.5	1282.5	4.2
X	E	720	74.57	0.0045	1.033	1.261	113.5	99.6	7.6	1344.0	5.1
X	F	750	77.56	0.0044	0.7565	1.96	116.7	99.7	11.0	1383.0	3.9
X	G	770	77.61	0.0053	0.4314	2.23	96.4	99.8	14.8	1384.8	3.2
x	H	785	78.62	0.0058	0.6140	2.26	87.3	99.8	18.6	1396.8	3.1
x	I	800	79.10	0.0043	1.176	2.52	118.3	99.6	22.9	1400.6	3.6
x	J	820	79.75	0.0031	0.0521	3.29	162.4	100.0	28.5	1412.9	2.6
x	K	850	78.97	0.0019	0.7715	4.27	262.0	99.7	35.8	1400.5	2.6
x	L	870	78.27	0.0042	0.4488	3.22	121.1	99.8	41.3	1392.9	2.8
x	M	890	78.52	0.0021	0.5133	3.02	246.1	99.8	46.4	1395.8	3.1
x	N	910	78.29	0.0032	0.3090	3.19	158.2	99.9	51.9	1393.8	3.0
x	O	930	78.48	0.0056	0.5381	3.24	90.8	99.8	57.4	1395.3	2.9
x	P	950	78.52	0.0025	0.3931	3.42	202.7	99.8	63.2	1396.3	2.7
	Q	980	79.36	0.0017	0.4556	4.85	295.8	99.8	71.5	1406.5	2.2
	R	1010	79.69	0.0032	0.9114	6.21	161.3	99.7	82.1	1409.0	2.1
	S	1040	79.52	0.0040	0.5963	5.99	127.4	99.8	92.3	1408.0	2.2
x	T	1070	79.48	0.0055	1.968	4.51	93.3	99.3	100.0	1402.4	2.3
	Integrated age ± 1σ			n=20		58.6		K2O=5.71%		1386.3	1.7
	Terminal Age ± 1σ		steps Q-S	n=3	MSWD=0.35	17.050			29.1	1407.86	1.7

Appendix 1 $^{40}Ar/^{39}Ar$ analytical data.

	ID	Temperature (°C)	$^{40}Ar/^{39}Ar$	$^{37}Ar/^{39}Ar$	$^{36}Ar/^{39}Ar$ (x 10^{-3})	$^{39}Ar_K$ (x 10^{-15} mol)	K/Ca	$^{40}Ar^*$ (%)	^{39}Ar (%)	Age (Ma)	±1σ (Ma)
	H-13-MAN-02, Muscovite, .48 mg, J=0.01462±0.11%, D=1.0045±0.0011, NM-261C, Lab#=62015-01										
X	A	600	70.66	-0.0019	81.83	0.721	-	65.8	0.3	949.0	7.4
X	B	650	75.87	0.0051	8.085	0.855	100.6	96.8	0.7	1335.5	5.0
X	C	685	77.51	-0.0091	2.939	1.066	-	98.9	1.1	1375.8	4.8
X	D	720	76.37	0.0022	3.671	1.90	232.1	98.6	2.0	1358.6	3.2
X	E	740	76.04	0.0018	1.901	2.23	289.8	99.3	2.9	1361.0	3.5
X	F	750	76.08	0.0013	1.350	2.39	383.4	99.5	4.0	1363.6	2.7
X	G	760	78.25	-0.0021	4.803	2.87	-	98.2	5.2	1378.2	3.0
X	H	770	76.82	0.0004	1.466	3.94	1294.3	99.4	6.9	1372.6	2.4
	I	780	78.56	0.0005	0.3684	14.47	1008.5	99.9	13.2	1398.5	2.0
	J	790	78.91	0.0004	0.4238	23.1	1227.0	99.8	23.2	1402.6	1.8
	K	800	78.33	0.0010	0.4710	21.2	510.5	99.8	32.4	1395.2	1.8
	L	810	78.13	0.0004	0.4540	16.7	1141.7	99.8	39.6	1392.8	1.8
	M	820	77.83	0.0009	0.6434	12.66	593.5	99.7	45.1	1388.4	2.2
x	N	830	77.78	0.0010	0.6718	9.66	499.8	99.7	49.2	1387.7	2.3
x	O	840	77.44	0.0019	0.4976	7.53	262.4	99.8	52.5	1384.0	1.9
X	P	850	77.16	0.0008	0.7501	5.95	613.6	99.7	55.1	1379.5	2.2
X	Q	860	77.03	0.0035	0.8784	4.63	146.3	99.7	57.1	1377.4	2.1
X	R	870	76.71	0.0013	0.9986	3.65	383.6	99.6	58.7	1373.0	2.6
X	S	885	76.56	0.0020	0.9438	3.45	256.1	99.6	60.2	1371.3	2.5
X	T	900	76.53	0.0009	0.8985	2.98	599.3	99.6	61.5	1371.1	3.0
X	U	915	76.85	0.0003	1.288	2.88	1501.0	99.5	62.7	1373.6	2.9
X	V	930	76.55	0.0031	1.308	3.00	165.8	99.5	64.0	1369.8	2.7
X	W	945	76.90	0.0014	0.9452	3.07	364.0	99.6	65.3	1375.5	3.3
X	X	960	77.41	0.0003	1.281	3.35	1661.9	99.5	66.8	1380.8	2.3
X	Y	975	77.53	0.0026	0.7012	3.61	194.6	99.7	68.3	1384.4	2.6
X	Z	990	78.34	-0.0003	1.170	3.71	-	99.5	69.9	1392.8	2.8
X	AA	1020	77.64	0.0014	0.9457	5.15	353.9	99.6	72.2	1384.9	2.2
X	AB	1035	77.83	0.0022	0.5066	5.35	236.6	99.8	74.5	1388.9	2.2
X	AC	1050	77.67	0.0006	0.7777	5.90	816.7	99.7	77.0	1385.8	2.2
X	AD	1070	77.59	0.0012	1.248	6.21	438.8	99.5	79.7	1383.1	2.0
X	AE	1120	78.19	0.0013	0.5023	16.1	396.5	99.8	86.7	1393.4	2.0
X	AF	1620	78.89	0.0007	2.139	30.7	694.8	99.2	100.0	1396.1	1.7
	Integrated age ± 1σ			n=32		230.9		K2O=12.64%		1387.8	1.6
	Terminal Age ± 1σ	steps AE-AF		n=2	MSWD=1.17	46.777			20.3	1394.96	1.7
	H-13-MAN-03, Muscovite, .37 mg, J=0.014588±0.05%, D=1.0045±0.0011, NM-261B, Lab#=62001-01										
X	A	550	51.41	0.0219	37.27	0.889	23.3	78.6	0.6	848.0	5.4
X	B	600	60.00	0.0074	8.480	0.839	68.6	95.8	1.1	1114.8	5.2
X	C	650	60.64	0.0062	4.593	1.436	82.6	97.8	2.0	1140.6	3.7
X	D	700	61.62	0.0012	3.946	2.42	419.0	98.1	3.6	1157.2	2.9
X	E	720	62.87	0.0010	3.923	2.00	489.6	98.1	4.9	1175.1	3.0
X	F	750	62.56	-0.0003	3.021	2.73	-	98.6	6.6	1174.4	2.8
X	G	770	68.24	0.0005	3.154	3.33	974.6	98.6	8.8	1252.1	2.4
X	H	785	71.11	0.0013	2.803	3.82	390.2	98.8	11.2	1291.7	2.4
X	I	800	75.65	0.0017	1.965	6.07	299.0	99.2	15.1	1353.8	2.3
X	J	820	77.35	0.0004	1.025	10.71	1297.2	99.6	22.0	1378.8	2.2
X	K	850	75.04	0.0014	1.321	12.20	358.7	99.5	29.8	1348.4	2.2
X	L	870	74.08	0.0017	2.586	4.70	301.6	99.0	32.9	1331.3	2.2
X	M	890	77.34	0.0046	3.530	3.74	110.0	98.6	35.3	1369.3	2.6
X	N	910	79.17	0.0025	3.053	3.97	200.4	98.9	37.8	1394.1	2.4
X	O	930	80.42	0.0027	2.718	4.43	190.4	99.0	40.7	1410.8	2.2
X	P	950	80.78	0.0028	2.086	5.09	185.2	99.2	43.9	1417.6	2.0
x	Q	980	82.19	0.0012	1.923	8.42	428.1	99.3	49.3	1435.5	1.8
	R	1010	82.71	0.0004	1.216	17.2	1146.3	99.6	60.4	1444.3	1.7
x	S	1040	81.53	0.0013	0.6603	30.2	402.0	99.8	79.8	1431.9	1.6
x	T	1070	81.07	0.0013	1.169	31.5	407.7	99.6	100.0	1424.5	1.7
	Integrated age ± 1σ			n=20		155.7		K2O=11.08%		1386.9	1.3
	Terminal Age ± 1σ	steps R-R		n=1	MSWD=0.00	17.226			11.1	1444.35	1.7

Appendix 1 $^{40}Ar/^{39}Ar$ analytical data.

	ID	Temperature (°C)	$^{40}Ar/^{39}Ar$	$^{37}Ar/^{39}Ar$	$^{36}Ar/^{39}Ar$ (x 10^{-3})	$^{39}Ar_K$ (x 10^{-15} mol)	K/Ca	$^{40}Ar^*$ (%)	^{39}Ar (%)	Age (Ma)	±1σ (Ma)
	KBP-99-3, Muscovite, .14 mg, J=0.014651±0.09%, D=1.0045±0.0011, NM-261C, Lab#=62016-01										
X	A	550	81.10	-0.0153	53.39	0.293	-	80.5	0.8	1228.9	12
X	B	600	89.76	0.0243	28.47	0.245	21.0	90.6	1.5	1436.4	14
X	C	650	90.30	0.0135	18.79	0.458	37.8	93.8	2.7	1477.5	7.9
X	D	700	89.32	0.0085	6.991	0.776	60.3	97.7	4.8	1507.2	6.7
X	E	720	87.48	0.0068	4.969	0.704	75.0	98.3	6.7	1492.6	7.0
X	F	750	88.94	0.0029	3.868	1.058	175.3	98.7	9.6	1513.6	5.1
x	G	770	91.84	0.0011	2.404	1.265	459.8	99.2	13.0	1552.3	4.4
x	H	785	91.12	0.0048	1.310	1.457	106.1	99.6	17.0	1547.7	3.8
x	I	800	93.03	0.0009	2.166	1.72	580.0	99.3	21.6	1566.8	3.9
x	J	820	94.28	0.0029	1.531	2.22	174.4	99.5	27.6	1583.1	3.4
x	K	850	94.35	0.0023	1.121	2.90	222.5	99.6	35.5	1585.2	3.2
x	L	870	93.62	0.0036	1.885	2.02	142.9	99.4	41.0	1574.4	3.6
x	M	890	92.30	0.0011	2.065	1.68	485.4	99.3	45.5	1558.8	4.6
x	N	910	93.09	0.0064	1.861	1.59	80.3	99.4	49.8	1568.4	3.9
x	O	930	92.75	0.0060	2.502	1.550	85.5	99.2	54.0	1562.4	5.0
X	P	950	93.06	0.0005	2.068	1.513	938.4	99.3	58.2	1567.4	3.6
X	Q	980	95.60	0.0037	1.989	1.71	136.1	99.4	62.8	1596.4	4.2
X	R	1010	96.01	0.0033	1.555	2.30	155.5	99.5	69.0	1602.4	3.5
X	S	1040	96.88	0.0056	1.451	3.21	91.2	99.6	77.7	1612.4	3.5
X	T	1070	99.04	0.0042	1.665	4.18	120.8	99.5	89.1	1635.6	2.7
	U	1110	102.4	0.0050	2.407	4.03	101.5	99.3	100.0	1670.2	3.1
	Integrated age ± 1σ			n=21		36.9		K2O=6.91%		1586.6	1.8
	Terminal Age ± 1σ		steps U-U	n=1	MSWD=0.00	4.034			10.9	1670.23	3.149
	KBP-99-8, Muscovite, .14 mg, J=0.014712±0.08%, D=1.0045±0.0011, NM-261C, Lab#=62017-01										
X	A	550	118.6	2.032	-358.6745	0.004	0.25	189.5	0.1	2674.7	604
X	B	600	89.34	0.0079	-70.2445	0.018	64.8	123.2	0.6	1762.9	164
X	C	650	98.82	0.1043	-43.5136	0.033	4.9	113.0	1.5	1779.2	73
	D	700	98.59	0.0747	-20.4041	0.067	6.8	106.1	3.3	1705.8	40
	E	720	101.3	0.0596	-32.4294	0.074	8.6	109.5	5.3	1770.5	38
	F	750	99.82	0.0307	-5.8666	0.096	16.6	101.7	7.9	1672.8	31
	G	770	96.03	0.0674	-14.8814	0.118	7.6	104.6	11.1	1660.8	27
	H	785	98.50	-0.0149	-10.0648	0.121	-	103.0	14.4	1671.9	26
	I	800	99.74	0.0513	-5.5483	0.127	9.9	101.6	17.8	1671.1	22
	J	820	96.22	0.0034	-8.8225	0.161	149.4	102.7	22.2	1643.2	19
	K	850	98.68	0.0357	-10.2707	0.185	14.3	103.1	27.2	1674.7	16
	L	870	104.0	-0.0086	-6.1162	0.191	-	101.7	32.3	1717.7	19
	M	890	101.4	0.0005	-3.5804	0.209	1112.5	101.0	38.0	1682.4	15
	N	910	97.93	0.0100	-3.4614	0.209	51.2	101.0	43.7	1644.5	16
	O	930	96.94	0.0111	-4.8902	0.214	46.2	101.5	49.4	1638.3	15
	P	950	98.74	0.0106	-3.2973	0.205	48.3	101.0	55.0	1652.9	15
	Q	980	97.62	-0.0132	-2.4664	0.228	-	100.7	61.1	1637.8	15
	R	1010	99.62	-0.0215	-1.4009	0.242	-	100.4	67.7	1656.3	12
	S	1040	99.56	0.0179	-1.2878	0.338	28.4	100.4	76.8	1655.4	11
	T	1070	99.82	-0.0009	-0.1635	0.501	-	100.0	90.4	1654.6	9.7
	U	1110	100.4	0.0169	5.050	0.248	30.3	98.5	97.1	1644.5	15
	V	1140	101.4	0.1040	-3.6994	0.108	4.9	101.1	100.0	1683.2	26
	Integrated age ± 1σ			n=22		3.70		K2O=0.69%		1666.1	4.3
	Plateau ± 1σ		steps D-V	n=19	MSWD=1.74	3.64			820.7	1660.0	5.0

Appendix 1 $^{40}Ar/^{39}Ar$ analytical data.

	ID	Temperature (°C)	$^{40}Ar/^{39}Ar$	$^{37}Ar/^{39}Ar$	$^{36}Ar/^{39}Ar$ (x 10^{-3})	$^{39}Ar_K$ (x 10^{-15} mol)	K/Ca	$^{40}Ar^*$ (%)	^{39}Ar (%)	Age (Ma)	±1σ (Ma)
	KLP-156, Muscovite, .21 mg, J=0.014762±0.09%, D=1.0045±0.0011, NM-261C, Lab#=62020-01										
X	A	550	57.78	0.2257	82.03	0.677	2.3	58.1	2.3	736.4	9.1
X	B	600	61.69	0.1071	13.26	0.512	4.8	93.7	4.0	1129.0	7.8
X	C	650	69.22	0.0769	9.965	0.729	6.6	95.7	6.5	1249.0	6.4
X	D	700	72.39	0.0611	5.623	0.988	8.4	97.7	9.9	1308.7	4.3
X	E	720	72.00	0.0745	5.086	0.804	6.8	97.9	12.6	1305.7	5.4
x	F	750	73.43	0.0595	3.754	1.125	8.6	98.5	16.5	1329.7	4.6
x	G	770	74.70	0.0404	3.635	1.199	12.6	98.6	20.5	1346.6	4.0
x	H	785	75.31	0.0355	3.860	1.219	14.4	98.5	24.7	1353.6	4.0
x	I	800	74.63	0.0336	3.494	1.286	15.2	98.6	29.1	1346.3	4.5
	J	820	75.97	0.0319	3.624	1.513	16.0	98.6	34.2	1363.0	3.8
	K	850	75.70	0.0295	3.009	2.18	17.3	98.8	41.7	1361.9	3.4
	L	870	75.35	0.0411	2.678	1.91	12.4	98.9	48.1	1358.6	3.4
	M	890	75.44	0.0395	3.273	1.76	12.9	98.7	54.1	1357.5	3.9
	N	910	75.84	0.0343	2.836	1.92	14.9	98.9	60.7	1364.3	3.4
	O	930	75.91	0.0308	2.801	2.04	16.5	98.9	67.7	1365.3	2.9
x	P	950	76.61	0.0289	1.659	2.05	17.7	99.4	74.6	1378.6	3.2
x	Q	980	77.48	0.0252	2.197	2.74	20.3	99.2	84.0	1387.6	2.3
x	R	1010	77.01	0.0232	2.963	2.34	22.0	98.9	91.9	1378.8	3.4
X	S	1040	78.54	0.0572	5.430	0.963	8.9	98.0	95.2	1388.9	4.7
X	T	1070	91.88	0.2347	37.35	0.304	2.2	88.0	96.3	1438.1	12
X	U	1110	120.0	0.6325	32.87	0.205	0.81	91.9	97.0	1769.7	16
X	V	1140	120.2	0.4284	41.05	0.129	1.2	89.9	97.4	1745.9	27
X	W	1170	98.31	0.1417	77.56	0.074	3.6	76.7	97.6	1369.5	39
X	X	1620	95.55	0.0043	68.82	0.691	118.1	78.7	100.0	1367.0	8.9
	Integrated age ± 1σ			n=24		29.4		K2O=3.64%		1348.8	1.7
	Plateau ± 1σ		steps J-O	n=6	MSWD=0.82	11.325			38.6	1362.11	1.6

Appendix 1 $^{40}Ar/^{39}Ar$ analytical data.

	ID	Temperature (°C)	$^{40}Ar/^{39}Ar$	$^{37}Ar/^{39}Ar$	$^{36}Ar/^{39}Ar$ (x 10^{-3})	$^{39}Ar_K$ (x 10^{-15} mol)	K/Ca	$^{40}Ar^*$ (%)	^{39}Ar (%)	Age (Ma)	±1σ (Ma)
	CB-48, Muscovite, .23 mg, J=0.014757±0.09%, D=1.0045±0.0011, NM-261C, Lab#=62019-01										
X	A	550	45.00	0.0147	59.32	0.456	34.7	61.0	1.2	622.9	10
X	B	600	60.80	-0.0093	8.423	0.469	-	95.9	2.4	1136.4	7.5
X	C	650	68.55	-0.0075	3.365	0.651	-	98.5	4.1	1265.8	7.1
X	D	700	72.11	-0.0052	1.411	1.027	-	99.4	6.8	1321.0	4.6
X	E	720	73.81	-0.0060	0.9753	0.773	-	99.6	8.8	1344.8	5.8
X	F	750	75.38	-0.0028	0.2541	0.987	-	99.9	11.3	1367.9	5.3
X	G	770	75.76	-0.0002	-0.1075	1.018	-	100.0	14.0	1374.1	5.1
X	H	785	76.29	-0.0060	2.032	1.011	-	99.2	16.6	1372.8	5.2
X	I	800	76.75	-0.0050	-0.8228	1.071	-	100.3	19.4	1389.2	4.8
X	J	820	77.42	-0.0022	0.8927	1.368	-	99.6	22.9	1391.4	4.0
X	K	850	78.36	0.0015	0.9196	2.42	339.3	99.6	29.2	1403.1	2.6
x	L	870	80.06	-0.0015	0.8322	2.95	-	99.7	36.9	1424.6	3.5
x	M	890	80.28	0.0006	0.7461	3.68	833.0	99.7	46.4	1427.7	2.5
x	N	910	81.47	0.0009	0.6152	4.57	594.0	99.8	58.3	1442.8	2.4
x	O	930	81.50	0.0009	0.1835	4.50	575.0	99.9	70.0	1444.8	2.4
x	P	950	82.24	0.0018	0.9492	3.62	280.3	99.7	79.4	1451.1	2.5
x	Q	980	83.54	0.0011	0.4800	3.37	447.5	99.8	88.1	1468.6	2.9
x	R	1010	85.61	0.0037	0.9028	2.93	136.4	99.7	95.7	1492.0	3.2
	S	1040	87.56	0.0010	1.988	1.66	515.1	99.3	100.0	1511.4	3.5
	Integrated age ± 1σ			n=19		38.5		K2O=4.36%		1419.6	1.6
	Terminal Age ± 1σ		steps S-S	n=1	MSWD=0.00	1.662			4.3	1511.35	3.5

Notes:

Isotopic ratios corrected for blank, radioactive decay, and mass discrimination, not corrected for interfering reactions.

Errors quoted for individual analyses include analytical error only, without interfering reaction or J uncertainties.

Integrated age calculated by summing isotopic measurements of all steps.

Integrated age error calculated by quadratically combining errors of isotopic measurements of all steps.

Plateau age is inverse-variance-weighted mean of selected steps.

Plateau age error is inverse-variance-weighted mean error (Taylor, 1982) times root MSWD where MSWD>1.

Plateau error is weighted error of Taylor (1982).

Isotopic abundances after Steiger and Jäger (1977).

Weight percent K_2O calculated from ^{39}Ar signal, sample weight, and instrument sensitivity.

X preceding sample ID denotes analysis excluded from plateau age calculations.

Ages calculated relative to FC-2 Fish Canyon Tuff sanidine interlaboratory standard at 28.201 Ma

Decay Constant (LambdaK (total)) = 5.463e-10/a

Correction factors:

$(^{39}Ar/^{37}Ar)_{Ca}$ = 0.00069 ± 2e-06

$(^{36}Ar/^{37}Ar)_{Ca}$ = 0.0002724 ± 2e07

$(^{38}Ar/^{39}Ar)_{K}$ = 0.01077

$(^{40}Ar/^{39}Ar)_{K}$ = 0.0072 ± 2e-05

Appendix 1 $^{40}Ar/^{39}Ar$ analytical data.

	ID	Power (Temperature)	$^{40}Ar/^{39}Ar$	$^{37}Ar/^{39}Ar$	$^{36}Ar/^{39}Ar$ (x 10^{-3})	$^{39}Ar_K$ (x 10^{-15} mol)	K/Ca	$^{40}Ar^*$ (%)	^{39}Ar (%)	Age (Ma)	±1σ (Ma)	Time (min)
	Bluebird, Muscovite, .69 mg, J=0.014602±0.05%, D=1.0035±0.001, NM-261A, Lab#=61989-02											
X	A	530	99.09	0.1118	142.3	0.489	4.6	57.6	0.2	1109.1	10	19
X	B	565	83.73	0.2450	41.57	0.271	2.1	85.3	0.3	1308.3	14	20
X	C	595	81.77	0.2585	31.04	0.339	2.0	88.8	0.4	1323.3	11	20
X	D	630	86.71	0.2018	37.75	0.766	2.5	87.1	0.7	1361.2	5.7	20
X	E	660	84.40	0.1007	29.36	1.63	5.1	89.7	1.3	1363.2	3.6	20
X	F	680	78.09	0.0932	9.389	2.19	5.5	96.4	2.1	1358.0	2.8	20
X	G	715	77.13	0.0651	6.830	4.42	7.8	97.4	3.8	1355.3	1.9	20
X	H	730	76.35	0.0842	3.279	4.09	6.1	98.7	5.3	1358.8	2.2	20
X	I	740	76.77	0.0784	3.627	4.00	6.5	98.6	6.8	1362.9	1.9	20
X	J	750	76.28	0.0606	3.432	3.95	8.4	98.7	8.3	1357.3	2.0	20
X	K	760	76.72	0.0539	3.383	4.58	9.5	98.7	10.0	1363.1	1.9	20
X	L	770	76.00	0.0777	3.151	3.59	6.6	98.8	11.3	1354.8	2.2	20
X	M	780	76.94	0.0501	4.050	5.24	10.2	98.4	13.3	1363.4	1.8	20
X	N	790	76.59	0.0385	2.885	7.14	13.3	98.9	16.0	1363.2	1.6	20
x	O	800	76.46	0.0224	1.412	11.32	22.8	99.4	20.2	1367.1	1.9	20
x	P	810	76.45	0.0198	1.252	12.77	25.7	99.5	25.0	1367.6	2.1	20
x	Q	820	76.32	0.0231	0.9227	13.51	22.1	99.6	30.0	1367.2	1.6	20
	R	830	76.77	0.0213	0.7741	13.50	23.9	99.7	35.1	1373.4	1.8	20
	S	840	76.58	0.0204	0.8483	13.38	25.0	99.7	40.1	1370.8	2.0	20
	T	850	76.27	0.0282	0.7301	12.79	18.1	99.7	44.9	1367.3	2.0	20
	U	860	76.60	0.0252	0.9188	11.70	20.3	99.6	49.3	1370.6	1.8	20
	V	870	76.89	0.0356	0.9665	10.48	14.3	99.6	53.2	1374.2	2.0	20
	W	880	77.06	0.0333	1.198	9.55	15.3	99.5	56.8	1375.5	3.4	20
	X	890	77.38	0.0483	1.541	9.07	10.6	99.4	60.2	1378.3	1.8	20
	Y	900	77.03	0.0529	1.971	7.88	9.6	99.2	63.1	1372.2	1.6	20
	Z	910	77.15	0.0496	2.042	7.23	10.3	99.2	65.8	1373.5	1.7	20
	AA	920	77.22	0.0640	2.162	6.99	8.0	99.2	68.4	1374.0	1.7	20
	AB	930	76.97	0.0517	2.311	6.97	9.9	99.1	71.0	1370.2	1.6	20
	AC	940	77.21	0.0461	2.178	6.44	11.1	99.2	73.4	1373.8	1.6	20
	AD	950	77.33	0.0381	2.054	6.69	13.4	99.2	75.9	1375.7	1.6	20
	AE	960	77.22	0.0374	2.310	6.22	13.6	99.1	78.3	1373.4	1.7	20
	AF	970	77.33	0.0231	2.136	6.44	22.0	99.2	80.7	1375.4	1.8	20
	AG	980	77.30	0.0222	1.841	7.94	23.0	99.3	83.7	1376.0	1.6	20
	AH	990	77.15	0.0237	1.957	8.11	21.5	99.2	86.7	1373.8	1.5	20
X	AI	1000	77.55	0.0159	1.449	8.92	32.1	99.4	90.0	1380.7	1.8	20
X	AJ	1010	77.13	0.0227	1.790	8.28	22.5	99.3	93.1	1374.1	1.5	20
X	AK	1020	77.40	0.0248	1.931	7.53	20.6	99.3	95.9	1377.0	1.6	20
X	AL	1030	77.57	0.0206	2.527	5.74	24.8	99.0	98.1	1376.9	1.7	20
X	AM	1040	78.19	0.0515	3.627	3.17	9.9	98.6	99.3	1380.7	2.3	20
X	AN	1050	78.16	0.0888	8.917	1.149	5.7	96.6	99.7	1360.6	4.4	20
X	AO	1060	81.66	0.0494	21.07	0.528	10.3	92.4	99.9	1359.4	7.7	20
X	AP	1070	88.04	0.9887	57.45	0.150	0.52	80.8	100.0	1304.5	27	20
X	AQ	1080	101.3	1.764	114.1	0.069	0.29	66.8	100.0	1259.4	56	20
X	AR	1150	141.2	3.926	248.5	0.057	0.13	48.2	100.0	1265.4	70	20
	Integrated age ± 1σ			n=44		267.3		K2O=10.19%		1370.1	1.1	
	Plateau ± 1σ	steps R-AH		n=17	MSWD=2.01	151.4			56.6	1373.4	0.8	

Appendix 1 $^{40}Ar/^{39}Ar$ analytical data.

	ID	Power (Temperature)	$^{40}Ar/^{39}Ar$	$^{37}Ar/^{39}Ar$	$^{36}Ar/^{39}Ar$ (x 10^{-3})	$^{39}Ar_K$ (x 10^{-15} mol)	K/Ca	$^{40}Ar^*$ (%)	^{39}Ar (%)	Age (Ma)	±1σ (Ma)	Time (min)
	2-1, Muscovite, .45 mg, J=0.014653±0.07%, D=1.0035±0.001, NM-261A, Lab#=61976-02											
X	A	530	79.99	-0.0421	75.96	0.341	-	71.9	0.2	1119.2	11	20
X	B	565	73.88	-0.4343	21.35	0.177	-	91.4	0.3	1259.0	18	20
X	C	595	81.40	-0.0950	32.44	0.248	-	88.2	0.5	1315.8	13	20
X	D	630	73.72	-0.0646	11.14	0.485	-	95.5	0.8	1297.6	7.4	20
X	E	660	75.02	-0.0074	13.44	0.729	-	94.7	1.2	1305.9	5.5	20
X	F	680	75.62	-0.0465	7.545	0.826	-	97.0	1.7	1336.3	4.7	20
X	G	715	79.11	-0.0265	19.23	1.530	-	92.8	2.7	1336.9	3.4	20
X	H	730	79.84	0.0003	17.74	1.66	1625.4	93.4	3.7	1352.0	3.2	20
X	I	740	76.73	0.0101	7.364	1.65	50.6	97.2	4.7	1351.5	3.1	20
X	J	750	78.16	-0.0116	10.54	1.95	-	96.0	5.9	1357.7	2.9	20
X	K	760	76.86	0.0148	4.937	2.18	34.5	98.1	7.2	1362.3	2.6	20
X	L	770	76.49	0.0076	4.648	2.71	66.8	98.2	8.9	1358.7	2.4	20
X	M	780	76.11	0.0000	2.740	3.25	-	98.9	10.9	1361.0	2.3	20
	N	790	76.58	-0.0075	2.738	3.86	-	98.9	13.2	1366.9	2.0	20
	O	800	76.25	-0.0017	2.481	4.84	-	99.0	16.2	1363.8	1.8	20
	P	810	76.10	0.0007	1.856	5.52	692.2	99.3	19.6	1364.2	1.7	20
	Q	820	76.18	0.0031	1.345	6.30	167.3	99.5	23.5	1367.1	1.7	20
	R	830	76.35	-0.0003	1.482	6.55	-	99.4	27.5	1368.8	1.7	20
	S	840	76.09	0.0040	1.401	6.64	127.0	99.4	31.6	1365.8	1.6	20
	T	850	76.13	0.0009	1.257	6.59	595.8	99.5	35.6	1366.7	1.6	20
	U	860	76.09	0.0053	1.424	5.17	96.3	99.4	38.8	1365.7	1.7	20
	V	870	76.26	0.0098	1.863	4.56	52.1	99.3	41.6	1366.1	1.8	20
	W	880	76.28	0.0022	1.674	4.55	233.5	99.3	44.4	1367.1	1.9	20
	X	890	76.39	0.0041	1.637	4.60	123.2	99.4	47.2	1368.7	1.8	20
	Y	900	76.40	-0.0013	1.786	4.56	-	99.3	50.0	1368.2	1.8	20
	Z	910	76.16	0.0103	1.833	5.35	49.6	99.3	53.3	1365.0	1.7	20
	AA	920	76.38	-0.0040	1.859	5.80	-	99.3	56.8	1367.8	1.7	20
	AB	930	76.70	0.0085	2.373	4.83	59.9	99.1	59.8	1369.8	1.9	20
	AC	940	76.55	0.0044	2.090	4.19	115.1	99.2	62.4	1369.0	2.0	20
	AD	950	75.89	0.0115	2.841	3.75	44.5	98.9	64.7	1357.7	1.9	20
	AE	960	76.54	0.0073	2.547	3.69	69.8	99.0	66.9	1367.1	2.1	20
	AF	970	76.49	0.0117	2.841	3.85	43.7	98.9	69.3	1365.4	2.0	20
	AG	980	76.53	0.0121	2.539	4.10	42.3	99.0	71.8	1367.0	1.9	20
	AH	990	76.44	-0.0057	2.115	4.16	-	99.2	74.4	1367.5	1.9	20
	AI	1000	76.43	-0.0025	2.365	4.37	-	99.1	77.1	1366.4	1.7	20
	AJ	1010	76.53	0.0096	2.764	4.28	53.1	98.9	79.7	1366.2	1.9	20
	AK	1020	76.37	0.0092	2.779	4.28	55.8	98.9	82.3	1364.1	1.9	20
	AL	1030	76.74	0.0109	2.641	4.21	46.8	99.0	84.9	1369.4	1.9	20
	AM	1040	76.90	0.0033	2.986	4.32	152.9	98.8	87.5	1370.1	1.9	20
	AN	1050	76.74	0.0050	2.938	4.52	101.9	98.9	90.3	1368.3	1.8	20
	AO	1060	76.87	-0.0005	2.778	4.76	-	98.9	93.2	1370.5	1.9	20
x	AP	1070	76.93	0.0128	2.812	4.52	39.8	98.9	96.0	1371.1	1.9	20
x	AQ	1080	77.14	0.0111	3.834	3.30	45.8	98.5	98.0	1370.0	2.2	20
X	AR	1150	77.24	-0.0074	5.832	2.96	-	97.8	99.8	1363.7	2.5	20
X	AS	1650	249.4	0.1924	605.9	0.245	2.7	28.2	100.0	1297.2	24	20
	Integrated age ± 1σ			n=45		163.0		K2O=9.49%		1364.6	1.3	
	Plateau ± 1σ	steps N-AO		n=28	MSWD=1.82	134.2			82.4	1366.76	0.83	

Appendix 1 $^{40}Ar/^{39}Ar$ analytical data.

	ID	Power (Temperature)	$^{40}Ar/^{39}Ar$	$^{37}Ar/^{39}Ar$	$^{36}Ar/^{39}Ar$ (x 10^{-3})	$^{39}Ar_K$ (x 10^{-15} mol)	K/Ca	$^{40}Ar^*$ (%)	^{39}Ar (%)	Age (Ma)	±1σ (Ma)	Time (min)
	Queen, Muscovite, .74 mg, J=0.014543±0.05%, D=1.0035±0.001, NM-261A, Lab#=61988-02											
X	A	530	72.16	-0.0457	113.9	0.498	-	53.3	0.2	813.7	11	19
X	B	565	69.34	0.0752	23.13	0.243	6.8	90.1	0.3	1183.6	14	20
X	C	595	70.86	0.0122	10.09	0.302	41.9	95.8	0.4	1256.9	12	20
X	D	630	78.47	0.1013	23.24	0.586	5.0	91.2	0.7	1306.3	6.7	20
X	E	660	78.13	0.1003	17.70	1.019	5.1	93.3	1.1	1323.1	4.3	20
X	F	680	77.60	-0.0474	12.89	1.373	-	95.1	1.7	1334.4	3.3	20
X	G	715	76.59	0.0136	7.852	2.90	37.5	97.0	2.9	1340.6	2.4	20
x	H	730	76.45	-0.0115	3.412	3.23	-	98.7	4.3	1355.5	2.0	20
x	I	740	76.44	0.0222	3.131	3.03	23.0	98.8	5.5	1356.5	2.1	20
x	J	750	76.75	0.0057	3.407	3.40	89.1	98.7	7.0	1359.4	2.2	20
x	K	760	76.74	0.0077	3.130	3.67	66.6	98.8	8.5	1360.3	2.0	20
x	L	770	76.02	-0.0054	1.613	4.11	-	99.4	10.2	1356.8	1.9	20
x	M	780	76.24	0.0153	2.197	4.67	33.3	99.1	12.2	1357.4	1.8	20
x	N	790	76.40	-0.0007	2.257	5.34	-	99.1	14.5	1359.2	1.7	20
x	O	800	75.80	0.0097	1.560	6.41	52.7	99.4	17.2	1354.3	1.6	20
x	P	810	76.25	0.0093	1.513	7.23	54.8	99.4	20.2	1360.1	1.5	20
x	Q	820	76.17	0.0042	1.084	8.50	120.6	99.6	23.8	1360.7	1.4	20
	R	830	76.52	0.0087	0.7902	9.34	58.5	99.7	27.7	1366.2	1.8	20
	S	840	76.56	0.0026	0.8024	10.03	197.6	99.7	31.9	1366.7	1.6	20
	T	850	76.44	0.0045	0.6773	10.10	112.5	99.7	36.2	1365.7	1.6	20
	U	860	76.42	0.0058	0.6491	9.88	87.6	99.7	40.3	1365.5	1.6	20
	V	870	76.36	0.0064	0.6146	9.41	80.2	99.8	44.3	1364.8	1.7	20
	W	880	76.50	0.0144	0.7639	8.97	35.4	99.7	48.0	1366.1	1.6	20
	X	890	76.26	0.0015	1.048	8.60	344.4	99.6	51.7	1362.0	1.5	20
	Y	900	76.13	0.0111	0.9823	8.03	46.1	99.6	55.0	1360.7	1.5	20
	Z	910	76.20	0.0081	0.9124	7.40	62.7	99.6	58.2	1361.7	1.5	20
	AA	920	76.32	0.0056	1.420	6.86	91.2	99.4	61.0	1361.4	1.6	20
	AB	930	76.19	-0.0021	1.302	6.50	-	99.5	63.8	1360.2	1.5	20
x	AC	940	75.88	0.0076	1.342	6.43	66.8	99.5	66.5	1356.0	1.6	20
x	AD	950	75.80	-0.0012	1.216	6.74	-	99.5	69.3	1355.5	1.6	20
x	AE	960	75.82	0.0059	1.314	6.92	86.7	99.5	72.2	1355.4	1.6	20
x	AF	970	76.34	0.0149	1.426	6.86	34.2	99.4	75.1	1361.6	1.6	20
x	AG	980	76.07	0.0057	1.297	7.02	89.1	99.5	78.1	1358.6	1.6	20
x	AH	990	76.01	0.0081	1.282	7.06	63.1	99.5	81.0	1357.9	1.5	20
x	AI	1000	76.17	0.0074	1.352	7.14	69.3	99.5	84.0	1359.7	1.4	20
x	AJ	1010	76.29	0.0106	1.374	7.31	48.3	99.5	87.1	1361.1	1.6	20
x	AK	1020	76.27	0.0039	1.480	7.30	132.3	99.4	90.2	1360.5	1.6	20
x	AL	1030	76.12	0.0088	1.393	6.94	58.1	99.5	93.1	1358.9	1.6	20
x	AM	1040	76.46	0.0140	1.683	6.07	36.3	99.3	95.7	1362.2	1.7	20
X	AN	1050	76.61	0.0142	1.146	4.71	35.9	99.5	97.6	1366.0	1.8	20
X	AO	1060	76.78	0.0274	2.237	3.03	18.6	99.1	98.9	1364.2	2.1	20
X	AP	1070	77.65	0.0203	3.475	1.513	25.1	98.7	99.5	1370.5	3.0	20
X	AQ	1080	77.49	-0.0956	8.816	0.561	-	96.6	99.8	1348.3	6.8	20
X	AR	1150	84.92	-0.1028	36.41	0.211	-	87.3	99.9	1339.0	16	20
X	AS	1650	168.3	-0.0974	316.1	0.307	-	44.5	100.0	1347.9	17	20
	Integrated age ± 1σ			n=45		237.8		K2O=8.49%		1359.1	1.1	
	Plateau ± 1σ	steps R-AB		n=11	MSWD=2.60	95.1			40.0	1363.55	0.93	

Appendix 1 $^{40}Ar/^{39}Ar$ analytical data.

	ID	Power (Temperature)	$^{40}Ar/^{39}Ar$	$^{37}Ar/^{39}Ar$	$^{36}Ar/^{39}Ar$ (x 10^{-3})	$^{39}Ar_K$ (x 10^{-15} mol)	K/Ca	$^{40}Ar^*$ (%)	^{39}Ar (%)	Age (Ma)	±1σ (Ma)	Time (min)
	LaP, Muscovite, .62 mg, J=0.014653±0.07%, D=1.0035±0.001, NM-261A, Lab#=61981-02											
X	A	530	131.7	-0.1141	196.4	0.405	-	55.9	0.2	1339.6	12	20
X	B	565	83.98	-0.0899	15.97	0.173	-	94.4	0.2	1410.6	21	20
X	C	595	84.19	-0.1028	7.314	0.252	-	97.4	0.3	1444.7	15	20
X	D	630	82.34	-0.0109	10.92	0.505	-	96.1	0.5	1408.9	8.0	20
X	E	660	96.20	0.0152	52.98	0.779	33.6	83.7	0.8	1426.7	6.1	20
X	F	680	83.53	-0.0856	16.11	0.913	-	94.3	1.2	1404.5	5.1	20
X	G	715	97.85	-0.0227	62.89	1.75	-	81.0	1.9	1410.9	3.8	20
X	H	730	87.44	0.0038	29.37	1.87	133.2	90.1	2.6	1404.6	3.3	20
X	I	740	81.83	0.0034	11.35	2.49	152.2	95.9	3.6	1401.0	2.7	20
X	J	750	80.28	0.0008	7.060	3.76	627.7	97.4	5.1	1397.5	2.1	20
X	K	760	78.67	0.0035	4.236	4.92	147.3	98.4	7.0	1387.7	1.7	20
X	L	770	78.06	0.0090	1.874	5.76	56.4	99.3	9.3	1388.9	1.7	20
X	M	780	77.64	0.0010	1.532	6.49	530.9	99.4	11.8	1384.9	1.7	20
X	N	790	77.56	0.0071	1.343	7.02	72.2	99.5	14.6	1384.6	1.6	20
X	O	800	77.71	0.0072	1.099	8.02	70.8	99.6	17.7	1387.4	1.5	20
X	P	810	77.57	0.0098	0.9405	8.71	52.1	99.6	21.2	1386.2	1.6	20
	Q	820	77.93	0.0085	0.6972	9.62	60.4	99.7	24.9	1391.6	1.8	20
	R	830	77.99	0.0060	0.8758	10.43	85.2	99.7	29.0	1391.7	1.7	20
	S	840	77.71	0.0060	0.5398	11.36	84.4	99.8	33.5	1389.4	1.6	20
	T	850	77.74	0.0049	0.4963	11.62	104.4	99.8	38.1	1389.9	1.6	20
	U	860	77.95	0.0092	0.3650	12.08	55.7	99.9	42.8	1393.2	1.7	20
	V	870	77.83	0.0000	0.5452	12.52	-	99.8	47.8	1391.0	1.7	20
	W	880	78.11	0.0088	0.7534	12.39	58.0	99.7	52.6	1393.7	1.8	20
	X	890	78.06	0.0070	0.6522	12.25	73.1	99.7	57.5	1393.4	1.7	20
	Y	900	78.07	0.0019	0.4919	11.53	262.0	99.8	62.0	1394.1	1.8	20
	Z	910	78.00	0.0063	0.6737	11.17	80.6	99.7	66.4	1392.6	1.7	20
	AA	920	78.23	0.0035	0.9239	10.60	144.8	99.6	70.6	1394.6	1.7	20
	AB	930	78.12	0.0062	0.7339	9.67	82.3	99.7	74.4	1393.8	1.8	20
X	AC	940	77.62	0.0117	0.9063	8.25	43.8	99.6	77.6	1387.0	1.6	20
X	AD	950	77.45	0.0086	1.037	6.50	59.3	99.6	80.2	1384.3	1.7	20
X	AE	960	77.63	0.0106	1.550	5.29	48.1	99.4	82.2	1384.7	1.7	20
X	AF	970	77.39	0.0098	1.299	4.76	51.8	99.5	84.1	1382.6	1.9	20
X	AG	980	77.73	-0.0013	1.398	4.50	-	99.5	85.9	1386.5	2.1	20
X	AH	990	77.57	0.0098	1.461	4.33	52.2	99.4	87.6	1384.3	1.9	20
X	AI	1000	77.91	0.0021	3.257	4.22	245.2	98.8	89.2	1381.9	1.9	20
X	AJ	1010	77.48	0.0052	1.454	4.09	97.8	99.4	90.9	1383.1	2.0	20
X	AK	1020	77.56	0.0106	1.426	4.22	48.2	99.4	92.5	1384.3	1.9	20
X	AL	1030	77.82	-0.0011	1.552	4.08	-	99.4	94.1	1387.1	2.2	20
X	AM	1040	77.72	0.0167	1.710	4.26	30.6	99.3	95.8	1385.3	2.0	20
X	AN	1050	77.41	0.0194	1.744	4.09	26.4	99.3	97.4	1381.2	2.0	20
X	AO	1060	77.95	0.0021	1.623	3.32	245.6	99.4	98.7	1388.5	2.1	20
X	AP	1070	78.11	-0.0133	1.781	2.14	-	99.3	99.5	1389.9	2.9	20
X	AQ	1080	78.39	-0.0298	4.246	0.849	-	98.4	99.9	1384.2	5.4	20
X	AR	1150	85.09	-0.1105	24.10	0.295	-	91.6	100.0	1394.5	13	20
	Integrated age ± 1σ			n=44		254.2	101.0	K2O=10.75%		1390.1	1.3	
	Plateau ± 1σ	steps Q-AB		n=12	MSWD=1.01	135.2	96.0 ±57.0		53.2	1392.3	0.9	

Appendix 1 $^{40}Ar/^{39}Ar$ analytical data.

	ID	Power (Temperature)	$^{40}Ar/^{39}Ar$	$^{37}Ar/^{39}Ar$	$^{36}Ar/^{39}Ar$ (x 10^{-3})	$^{39}Ar_K$ (x 10^{-15} mol)	K/Ca	$^{40}Ar^*$ (%)	^{39}Ar (%)	Age (Ma)	±1σ (Ma)	Time (min)
	P-01-01, Muscovite, .28 mg, J=0.014602±0.05%, D=1.0035±0.001, NM-261A, Lab#=61990-02											
X	A	530	395.7	-0.2113	1061.0	0.196	-	20.8	0.2	1442.7	35	19
X	B	565	192.1	-0.4124	361.0	0.111	-	44.4	0.3	1481.3	36	20
X	C	595	85.97	-0.0211	10.05	0.153	-	96.5	0.4	1453.1	23	20
X	D	630	201.5	-0.2874	400.8	0.348	-	41.2	0.8	1453.5	16	20
X	E	660	195.8	-0.1938	395.0	0.573	-	40.4	1.3	1404.9	12	20
X	F	680	139.0	-0.0943	200.5	0.790	-	57.4	2.0	1412.8	8.6	20
X	G	715	99.25	0.0002	67.52	1.63	2306.5	79.9	3.6	1407.8	4.2	20
X	H	730	81.64	-0.0309	11.41	1.88	-	95.9	5.3	1395.0	3.0	20
X	I	740	79.82	-0.0128	6.605	2.08	-	97.5	7.3	1389.9	2.6	20
X	J	750	78.58	-0.0196	3.672	2.22	-	98.6	9.4	1385.4	2.5	20
X	K	760	78.02	-0.0081	3.380	2.39	-	98.7	11.6	1379.4	2.7	20
X	L	770	77.17	-0.0242	1.946	2.62	-	99.2	14.1	1373.9	2.4	20
X	M	780	76.94	-0.0367	0.8543	3.08	-	99.7	17.0	1375.2	2.3	20
X	N	790	77.35	-0.0133	0.7719	3.46	-	99.7	20.3	1380.6	2.2	20
X	O	800	77.08	-0.0290	0.6707	3.91	-	99.7	23.9	1377.6	1.9	20
X	P	810	77.06	0.0040	0.2480	4.34	126.9	99.9	28.0	1378.9	1.9	20
	Q	820	76.59	-0.0151	0.4814	4.77	-	99.8	32.5	1372.2	1.9	20
	R	830	76.68	-0.0082	0.4449	5.00	-	99.8	37.2	1373.4	1.8	20
	S	840	76.64	-0.0014	0.5899	5.06	-	99.8	42.0	1372.4	1.9	20
	T	850	76.48	-0.0040	0.4542	4.96	-	99.8	46.6	1370.8	1.8	20
	U	860	76.97	-0.0068	0.2876	4.83	-	99.9	51.2	1377.6	2.0	20
	V	870	76.86	-0.0144	0.9152	4.45	-	99.6	55.4	1373.9	1.9	20
	W	880	77.02	-0.0218	0.8006	4.09	-	99.7	59.2	1376.4	2.1	20
	X	890	76.81	-0.0121	0.9090	3.60	-	99.6	62.6	1373.3	2.1	20
	Y	900	77.14	0.0013	1.666	3.36	384.3	99.4	65.8	1374.6	2.0	20
	Z	910	76.80	-0.0220	0.8760	3.62	-	99.7	69.2	1373.3	2.1	20
	AA	920	77.12	-0.0036	1.089	4.16	-	99.6	73.1	1376.6	1.9	20
	AB	930	77.06	-0.0121	1.089	3.85	-	99.6	76.7	1375.8	2.1	20
	AC	940	77.09	-0.0090	1.065	3.66	-	99.6	80.2	1376.3	1.9	20
	AD	950	76.85	-0.0085	1.367	3.54	-	99.5	83.5	1372.1	2.0	20
	AE	960	77.22	-0.0172	1.727	3.51	-	99.3	86.8	1375.5	2.0	20
	AF	970	76.94	0.0052	1.078	3.62	98.4	99.6	90.2	1374.3	2.0	20
	AG	980	76.87	-0.0224	1.357	3.57	-	99.5	93.6	1372.5	2.1	20
X	AH	990	77.55	-0.0192	1.660	3.01	-	99.4	96.4	1379.9	2.3	20
X	AI	1000	77.19	-0.0460	0.9055	2.11	-	99.6	98.4	1378.1	2.6	20
X	AJ	1010	77.40	-0.0705	0.3757	1.143	-	99.8	99.5	1382.7	3.9	20
X	AK	1020	77.12	-0.1795	-0.6317	0.450	-	100.2	99.9	1382.7	8.7	20
X	AL	1030	75.13	-0.7443	-4.5015	0.109	-	101.7	100.0	1371.0	31	20
	Integrated age ± 1σ			n=38		106.2		K2O=9.98%		1377.7	1.3	
	Plateau ± 1σ	steps Q-AG		n=17	MSWD=1.00	69.7			65.6	1374.13	0.66	

Appendix 1 $^{40}Ar/^{39}Ar$ analytical data.

	ID	Power (Temperature)	$^{40}Ar/^{39}Ar$	$^{37}Ar/^{39}Ar$	$^{36}Ar/^{39}Ar$ (x 10^{-3})	$^{39}Ar_K$ (x 10^{-15} mol)	K/Ca	$^{40}Ar^*$ (%)	^{39}Ar (%)	Age (Ma)	±1σ (Ma)	Time (min)
	P-01-06, Muscovite, .49 mg, J=0.014658±0.06%, D=1.0035±0.001, NM-261A, Lab#=61995-02											
X	A	15	332.9	-0.3038	890.7	0.245	-	20.9	0.2	1287.3	28	-1
X	B	565	222.8	-1.1646	484.4	0.097	-	35.7	0.2	1414.6	39	20
X	C	595	88.26	-0.2710	31.54	0.166	-	89.4	0.3	1406.7	19	20
X	D	630	132.3	-0.1054	189.2	0.380	-	57.7	0.6	1374.5	12	20
X	E	660	184.6	-0.0963	361.4	0.718	-	42.1	1.1	1392.7	11	20
X	F	680	88.00	-0.0712	36.13	0.910	-	87.9	1.7	1386.8	5.4	20
X	G	715	89.93	-0.0528	42.03	1.84	-	86.2	2.9	1389.2	3.4	20
X	H	730	80.47	-0.0666	11.93	1.99	-	95.6	4.2	1382.1	2.8	20
X	I	740	85.35	-0.0676	28.55	1.95	-	90.1	5.6	1381.6	3.0	20
X	J	750	78.71	-0.0248	9.143	2.05	-	96.6	6.9	1370.3	2.9	20
X	K	760	77.66	-0.0354	3.625	2.31	-	98.6	8.5	1377.6	2.4	20
X	L	770	76.78	-0.0353	3.898	2.70	-	98.5	10.3	1365.4	2.3	20
X	M	780	77.87	-0.0177	6.843	3.27	-	97.4	12.5	1368.3	2.1	20
X	N	790	76.33	-0.0169	2.381	3.93	-	99.1	15.1	1365.4	1.8	20
X	O	800	76.70	-0.0172	2.493	4.79	-	99.0	18.3	1369.8	1.8	20
	P	810	75.81	-0.0069	1.813	5.33	-	99.3	21.9	1360.9	1.7	20
	Q	820	75.81	-0.0072	1.209	5.89	-	99.5	25.8	1363.2	1.7	20
	R	830	75.72	-0.0025	1.192	6.32	-	99.5	30.0	1362.1	1.6	20
	S	840	75.61	-0.0005	1.067	6.88	-	99.6	34.7	1361.3	1.5	20
	T	850	75.84	-0.0091	1.236	7.11	-	99.5	39.4	1363.5	1.6	20
	U	860	76.00	-0.0141	0.9111	7.11	-	99.6	44.2	1366.7	1.5	20
	V	870	75.69	-0.0037	0.9301	7.03	-	99.6	48.9	1362.7	1.6	20
	W	880	75.85	-0.0082	1.165	6.71	-	99.5	53.4	1363.8	1.6	20
	X	890	75.77	-0.0070	1.080	6.19	-	99.6	57.5	1363.2	1.6	20
	Y	900	75.84	0.0104	1.323	5.69	49.2	99.5	61.3	1363.2	1.7	20
	Z	910	76.03	-0.0091	1.383	5.11	-	99.5	64.8	1365.3	1.9	20
	AA	920	76.13	-0.0242	1.704	4.63	-	99.3	67.9	1365.4	1.8	20
	AB	930	76.11	-0.0089	1.834	4.52	-	99.3	70.9	1364.7	1.9	20
	AC	940	76.20	-0.0007	1.589	4.82	-	99.4	74.1	1366.8	1.6	20
X	AD	950	75.84	-0.0189	1.743	5.00	-	99.3	77.5	1361.6	1.7	20
X	AE	960	75.73	-0.0267	1.831	4.75	-	99.3	80.6	1359.8	1.8	20
X	AF	970	76.08	0.0045	2.162	4.73	114.4	99.2	83.8	1363.1	2.0	20
X	AG	980	76.29	0.0038	2.096	4.61	135.6	99.2	86.9	1366.0	2.0	20
X	AH	990	76.29	-0.0146	1.435	4.53	-	99.4	89.9	1368.4	1.9	20
X	AI	1000	76.12	-0.0184	1.599	4.47	-	99.4	92.9	1365.7	1.9	20
X	AJ	1010	76.34	-0.0208	1.924	4.17	-	99.2	95.7	1367.2	2.0	20
X	AK	1020	76.26	-0.0273	1.878	3.33	-	99.3	97.9	1366.4	2.3	20
X	AL	1030	76.78	-0.0439	4.188	1.96	-	98.4	99.2	1364.3	2.7	20
X	AM	1040	76.93	-0.0938	6.214	0.878	-	97.6	99.8	1358.5	4.7	20
X	AN	1050	77.92	-0.2888	17.91	0.249	-	93.2	100.0	1326.4	14	20
	Integrated age ± 1σ			n=40		149.4		K2O=7.99%		1365.6	1.3	
	Plateau ± 1σ	steps P-AC		n=14	MSWD=1.31	83.3			55.8	1363.74	0.79	

Appendix 1 $^{40}Ar/^{39}Ar$ analytical data.

ID	Power (Temperature)	$^{40}Ar/^{39}Ar$	$^{37}Ar/^{39}Ar$	$^{36}Ar/^{39}Ar$ (x 10^{-3})	$^{39}Ar_K$ (x 10^{-15} mol)	K/Ca	$^{40}Ar^*$ (%)	^{39}Ar (%)	Age (Ma)	±1σ (Ma)	Time (min)

Notes:

Isotopic ratios corrected for blank, radioactive decay, and mass discrimination, not corrected for interfering reactions.
Errors quoted for individual analyses include analytical error only, without interfering reaction or J uncertainties.
Integrated age calculated by summing isotopic measurements of all steps.
Integrated age error calculated by quadratically combining errors of isotopic measurements of all steps.
Plateau age is inverse-variance-weighted mean of selected steps.
Plateau age error is inverse-variance-weighted mean error (Taylor, 1982) times root MSWD where MSWD>1.
Plateau error is weighted error of Taylor (1982).
Isotopic abundances after Steiger and Jäger (1977).
X preceding sample ID denotes analysis excluded from plateau age calculations.
Weight percent K_2O calculated from ^{39}Ar signal, sample weight, and instrument sensitivity.
Ages calculated relative to FC-2 Fish Canyon Tuff sanidine interlaboratory standard at 28.201 Ma
Decay Constant (LambdaK (total)) = 5.463e-10/a
Correction factors:
$(^{39}Ar/^{37}Ar)_{Ca}$ = 0.00069 ± 2e-06
$(^{36}Ar/^{37}Ar)_{Ca}$ = 0.0002724 ± 2e-07
$(^{38}Ar/^{39}Ar)_K$ = 0.01077
$(^{40}Ar/^{39}Ar)_K$ = 0.0072 ± 2e-05

Appendix 1 Continued: In situ $^{40}Ar/^{39}Ar$ analytical data.

	ID	Power (Pulses)	$^{40}Ar/^{39}Ar$	$^{37}Ar/^{39}Ar$	$^{36}Ar/^{39}Ar$ (x 10^{-3})	$^{39}Ar_K$ (x 10^{-15} mol)	K/Ca	$^{40}Ar^*$ (%)	Age (Ma)	±1σ (Ma)
	2-4C1, Muscovite, J=0.0144374±0.06%, D=1±0, NM-261A, Lab#=61982									
	03	500	79.78	0.0070	0.0973	0.094	72.9	100.0	1402.3	2.1
	04	500	80.62	0.0080	0.2119	0.115	63.8	99.9	1412.1	2.3
	05	500	79.63	0.0070	0.2821	0.106	72.9	99.9	1399.8	2.3
	07	500	79.99	0.0070	0.3911	0.112	72.9	99.8	1403.8	2.0
	08	500	79.64	0.0070	0.3805	0.117	72.9	99.9	1399.6	1.9
	09	500	79.16	0.0070	0.3164	0.117	72.9	99.9	1393.9	1.8
	11	500	79.41	0.0070	0.1927	0.113	72.9	99.9	1397.4	2.1
	12	500	79.79	0.0070	0.2989	0.112	72.9	99.9	1401.7	1.8
	13	500	79.93	0.0070	0.3179	0.118	72.9	99.9	1403.4	1.9
t1	15	500	80.13	0.0070	0.3190	0.113	72.9	99.9	1405.8	1.9
	16	500	80.02	0.0070	0.2541	0.118	72.9	99.9	1404.7	1.9
	17	500	79.94	0.0070	0.7304	0.119	72.9	99.7	1401.9	1.9
	19	500	83.33	0.0070	12.86	0.096	72.9	95.4	1399.6	2.4
	20	500	80.86	0.0070	3.654	0.072	72.9	98.7	1402.6	2.6
	21	500	85.35	0.0070	18.69	0.048	72.9	93.5	1403.2	3.6
	23	500	81.88	0.0070	8.837	0.021	72.9	96.8	1396.3	6.0
	24	500	88.77	0.0070	36.78	0.007	72.9	87.7	1379.4	14.2
	25	500	78.58	0.0070	4.901	0.017	72.9	98.1	1369.9	7.2
	27	500	77.67	0.0070	1.839	0.028	72.9	99.3	1369.8	5.0
	28	500	80.66	0.0070	3.084	0.125	72.9	98.9	1402.3	1.8
	29	500	80.88	0.0070	4.229	0.115	72.9	98.4	1400.9	1.8
	31	500	80.89	0.0070	2.840	0.121	72.9	99.0	1406.0	1.9
	32	500	80.06	0.0070	0.9034	0.110	72.9	99.7	1402.8	2.0
	33	500	80.27	0.0070	0.2514	0.114	72.9	99.9	1407.7	1.9
	35	500	79.91	0.0070	0.4438	0.121	72.9	99.8	1402.6	1.9
	36	500	80.28	0.0070	0.2052	0.114	72.9	99.9	1408.1	1.8
	37	500	79.97	0.0070	0.8424	0.118	72.9	99.7	1402.0	2.0
	39	500	80.30	0.0080	1.053	0.116	63.8	99.6	1405.2	2.0
t2	40	500	80.50	0.0070	2.596	0.114	72.9	99.0	1402.1	1.9
	41	500	79.85	0.0070	0.2952	0.103	72.9	99.9	1402.5	2.0
	43	500	80.48	0.0070	0.3366	0.109	72.9	99.9	1410.0	1.8
	44	500	80.61	0.0070	0.6452	0.115	72.9	99.8	1410.5	1.7
	45	500	80.20	0.0070	0.4938	0.117	72.9	99.8	1406.0	1.8
	47	500	80.31	0.0070	1.122	0.119	72.9	99.6	1405.1	1.7
	48	500	80.40	0.0070	1.942	0.107	72.9	99.3	1403.2	2.0
	49	500	81.63	0.0070	5.078	0.121	72.9	98.2	1407.0	1.9
	51	500	80.47	0.0070	1.754	0.108	72.9	99.3	1404.8	1.9
	52	500	80.73	0.0070	1.750	0.131	72.9	99.4	1407.9	1.7
	53	500	81.50	0.0070	3.893	0.112	72.9	98.6	1409.6	2.1
p1	54	500	79.99	0.0070	0.5351	0.126	72.9	99.8	1403.3	5.1
p2	55	500	79.96	0.0070	0.3342	0.119	72.9	99.9	1403.7	4.2
p3	56	500	79.84	0.0070	0.2292	0.131	72.9	99.9	1402.5	3.3

Appendix 1 Continued: In situ $^{40}Ar/^{39}Ar$ analytical data.

	ID	Power (Pulses)	$^{40}Ar/^{39}Ar$	$^{37}Ar/^{39}Ar$	$^{36}Ar/^{39}Ar$ ($\times 10^{-3}$)	$^{39}Ar_K$ ($\times 10^{-15}$ mol)	K/Ca	$^{40}Ar^*$ (%)	Age (Ma)	$\pm 1\sigma$ (Ma)
	2-4C2, Muscovite, J=0.0145099±0.06%, D=1±0, NM-261A, Lab#=61983									
	01	500	78.27	0.0080	2.108	0.072	63.8	99.2	1381.1	21.7
	02	500	81.90	0.0070	2.314	0.067	72.9	99.2	1425.2	18.1
	03	500	80.09	0.0070	2.659	0.071	72.9	99.0	1401.7	17.4
	04	500	80.77	0.0070	0.6346	0.071	72.9	99.8	1417.5	17.0
	06	500	79.61	0.0070	0.5809	0.068	72.9	99.8	1403.4	18.3
	07	500	79.39	0.0070	0.5989	0.075	72.9	99.8	1400.5	16.4
	08	500	80.04	0.0070	1.325	0.076	72.9	99.5	1405.9	16.4
	10	500	80.00	0.0070	0.5227	0.071	72.9	99.8	1408.4	16.3
	11	500	79.19	0.0070	0.7355	0.074	72.9	99.7	1397.6	16.6
t1	12	500	80.57	0.0070	0.5027	0.075	72.9	99.8	1415.5	16.1
	14	500	79.44	0.0070	0.9286	0.073	72.9	99.6	1400.0	16.9
	15	500	82.25	0.0070	3.310	0.074	72.9	98.8	1425.8	16.8
	16	500	80.75	0.0070	0.7758	0.074	72.9	99.7	1416.6	16.7
	18	500	82.73	0.0070	0.7345	0.072	72.9	99.7	1440.9	17.5
	19	500	79.05	0.0070	1.035	0.075	72.9	99.6	1394.8	16.4
	20	500	81.47	0.0070	5.861	0.072	72.9	97.9	1407.1	16.6
	22	500	83.42	0.0070	12.72	0.068	72.9	95.5	1406.1	18.9
	23	500	370.7	0.0070	969.4	0.070	72.9	22.7	1462.3	18.8
	24	500	83.46	0.0070	14.53	0.092	72.9	94.8	1400.0	12.5
	25	500	80.86	0.0070	0.4520	0.053	72.9	99.8	1419.2	22.7
	26	500	79.74	0.0070	0.5922	0.072	72.9	99.8	1404.9	16.6
	27	500	81.26	0.0070	0.9142	0.067	72.9	99.7	1422.4	19.2
	28	500	79.60	0.0070	0.8682	0.064	72.9	99.7	1402.2	18.8
	29	500	78.52	0.0070	0.5389	0.064	72.9	99.8	1390.0	18.6
	30	500	81.78	0.0070	0.7643	0.063	72.9	99.7	1429.3	19.8
	32	500	79.32	0.0070	0.0628	0.069	72.9	100.0	1401.7	19.2
	33	500	80.77	0.0070	0.2755	0.068	72.9	99.9	1418.7	17.6
	34	500	79.51	0.0070	0.1932	0.072	72.9	99.9	1403.6	16.7
	36	500	78.99	0.0070	0.1640	0.074	72.9	99.9	1397.3	17.9
t2	37	500	79.83	0.0070	0.2293	0.071	72.9	99.9	1407.3	17.5
	38	500	80.41	0.0070	0.1670	0.075	72.9	99.9	1414.7	16.6
	40	500	79.40	0.0070	0.3342	0.076	72.9	99.9	1401.7	15.8
	41	500	80.26	0.0070	1.370	0.074	72.9	99.5	1408.5	16.1
	42	500	78.81	0.0070	0.5746	0.078	72.9	99.8	1393.5	15.8
	44	500	78.65	0.0070	0.3035	0.075	72.9	99.9	1392.5	16.4
	45	500	80.40	0.0070	1.670	0.075	72.9	99.4	1409.1	17.1
	46	500	79.87	0.0070	1.387	0.072	72.9	99.5	1403.7	17.1
	48	500	114.6	0.0070	117.3	0.077	72.9	69.7	1409.1	16.7
	49	500	86.30	0.0070	16.49	0.073	72.9	94.3	1427.8	17.1
	50	500	98.38	0.0070	61.74	0.065	72.9	81.5	1412.0	18.6
p1	52	500	82.10	0.0080	6.478	0.068	63.8	97.7	1412.6	18.4
p2	53	500	80.58	0.0070	0.5168	0.042	72.9	99.8	1415.5	28.4
p3	54	500	79.87	0.0070	4.922	0.061	72.9	98.2	1390.7	20.1
p4	55	500	137.6	0.0070	187.8	0.072	72.9	59.7	1436.0	17.5
p5	56	500	78.99	0.0070	3.500	0.077	72.9	98.7	1384.9	16.5

Appendix 1 Continued: In situ $^{40}Ar/^{39}Ar$ analytical data.

	ID	Power (Pulses)	$^{40}Ar/^{39}Ar$	$^{37}Ar/^{39}Ar$	$^{36}Ar/^{39}Ar$ ($\times 10^{-3}$)	$^{39}Ar_K$ ($\times 10^{-15}$ mol)	K/Ca	$^{40}Ar^*$ (%)	Age (Ma)	$\pm 1\sigma$ (Ma)
	2-4C3, Muscovite, J=0.0145099±0.06%, D=1±0, NM-261A, Lab#=61984									
	01	500	80.24	0.0070	0.9115	0.025	72.9	99.7	1409.9	46.2
	02	500	84.56	0.0070	0.4302	0.024	72.9	99.8	1464.0	52.7
	03	500	86.22	0.0070	1.496	0.023	72.9	99.5	1480.0	52.6
	05	500	75.45	0.0070	0.7208	0.024	72.9	99.7	1350.8	50.2
	06	500	83.32	0.0090	0.6828	0.022	56.7	99.7	1448.3	56.5
	07	500	76.47	0.0070	0.2960	0.024	72.9	99.9	1365.2	49.8
	09	500	79.35	0.0070	1.034	0.028	72.9	99.6	1398.5	43.4
	10	500	85.16	0.0070	0.8860	0.024	72.9	99.7	1469.5	52.1
	11	500	79.89	0.0070	0.3553	0.026	72.9	99.9	1407.6	46.7
	13	500	80.18	0.0070	0.4736	0.026	72.9	99.8	1410.8	44.8
t1	14	500	82.43	0.0070	0.4189	0.024	72.9	99.8	1438.4	49.9
	15	500	79.97	0.0070	0.4623	0.026	72.9	99.8	1408.2	46.8
	17	500	77.18	0.0070	0.5006	0.023	72.9	99.8	1373.4	52.2
	18	500	84.98	0.0070	0.3560	0.021	72.9	99.9	1469.2	59.3
	19	500	80.92	0.0070	0.4952	0.022	72.9	99.8	1419.8	55.8
	21	500	84.52	0.0070	0.1844	0.021	72.9	99.9	1464.4	61.8
	22	500	80.90	0.0070	1.500	0.020	72.9	99.4	1415.9	61.0
	23	500	75.85	0.0070	0.3241	0.021	72.9	99.9	1357.4	57.9
	25	500	85.81	0.0070	0.5477	0.017	72.9	99.8	1478.5	73.8
	26	500	78.43	0.0070	0.5473	0.023	72.9	99.8	1388.9	53.6
	27	500	77.25	0.0070	0.5697	0.024	72.9	99.8	1374.0	50.2
	29	500	83.20	0.0070	0.5318	0.031	72.9	99.8	1447.3	40.9
	30	500	80.40	0.0070	0.2398	0.034	72.9	99.9	1414.3	35.2
	31	500	75.59	0.0070	0.1095	0.025	72.9	99.9	1354.8	49.3
	33	500	84.02	0.0070	0.1306	0.023	72.9	99.9	1458.6	56.3
	34	500	85.36	0.0070	-0.1478	0.022	72.9	100.0	1475.5	60.1
	35	500	77.08	0.0070	-0.1502	0.025	72.9	100.0	1374.5	46.5
	37	500	83.82	0.0070	0.2342	0.022	72.9	99.9	1455.8	57.7
	38	500	80.72	0.0070	0.2782	0.024	72.9	99.9	1418.1	50.9
	39	500	79.26	0.0070	0.2958	0.023	72.9	99.9	1400.1	51.0
t2	41	500	78.44	0.0070	0.0807	0.023	72.9	100.0	1390.7	52.4
	42	500	81.80	0.0070	0.2593	0.020	72.9	99.9	1431.3	65.0
	43	500	86.64	0.0070	-0.0494	0.012	72.9	100.0	1490.3	111.3
	45	500	72.92	0.0080	-0.0085	0.024	63.8	100.0	1321.1	49.2
	46	500	78.89	0.0070	-0.2852	0.023	72.9	100.1	1397.7	54.5
	47	500	80.33	0.0070	0.0452	0.022	72.9	100.0	1414.1	54.3
	49	500	79.58	0.0070	0.1722	0.021	72.9	99.9	1404.5	59.2
	50	500	82.17	0.0070	0.2296	0.020	72.9	99.9	1435.9	57.8
	51	500	82.22	0.0070	0.5164	0.021	72.9	99.8	1435.5	57.7
	53	500	82.46	0.0070	6.379	0.019	72.9	97.7	1417.4	62.4
	54	500	82.34	0.0070	0.5743	0.018	72.9	99.8	1436.8	70.5

Appendix 1 Continued: In situ $^{40}Ar/^{39}Ar$ analytical data.

	ID	Power (Pulses)	$^{40}Ar/^{39}Ar$	$^{37}Ar/^{39}Ar$	$^{36}Ar/^{39}Ar$ (x 10^{-3})	$^{39}Ar_K$ (x 10^{-15} mol)	K/Ca	$^{40}Ar^*$ (%)	Age (Ma)	±1σ (Ma)
	2-4C4, Muscovite, J=0.0145099±0.06%, D=1±0, NM-261A, Lab#=61985									
	01	500	80.55	0.0070	0.5003	0.054	72.9	99.8	1415.2	18.3
	04	500	77.93	0.0070	0.5722	0.029	72.9	99.8	1382.5	35.4
	06	500	76.62	0.0070	0.4806	0.048	72.9	99.8	1366.4	21.1
	07	500	79.98	0.0070	0.5175	0.045	72.9	99.8	1408.1	23.0
t1	08	500	76.61	0.0070	1.130	0.051	72.9	99.6	1363.9	19.1
	10	500	79.88	0.0090	0.8221	0.058	56.7	99.7	1405.7	17.9
	12	500	81.61	0.0070	0.5452	0.049	72.9	99.8	1428.0	20.6
	14	500	82.06	0.0070	5.839	0.041	72.9	97.9	1414.4	24.3
	15	500	78.46	0.0070	2.592	0.034	72.9	99.0	1381.7	30.1
	19	500	87.86	0.0070	23.97	0.018	72.9	91.9	1400.9	13.5
	20	500	83.53	0.0070	3.438	0.015	72.9	98.8	1421.9	14.9
	21	500	138.0	0.0070	188.5	0.021	72.9	59.6	1419.5	14.5
	22	500	86.65	0.0070	18.65	0.019	72.9	93.6	1405.4	9.2
	23	500	99.07	0.0080	60.47	0.021	63.8	82.0	1406.1	8.8
	25	500	81.33	0.0070	1.531	0.023	72.9	99.4	1402.1	7.7
	26	500	82.37	0.0070	5.045	0.018	72.9	98.2	1402.2	8.6
t2	27	500	79.97	0.0070	2.454	0.019	72.9	99.1	1382.3	8.3
	29	500	79.37	0.0070	3.165	0.007	72.9	98.8	1372.3	18.6
	30	500	80.81	0.0070	2.166	0.018	72.9	99.2	1393.5	9.2
	31	500	82.20	0.0070	1.722	0.013	72.9	99.4	1412.0	11.7
	33	500	80.25	0.0070	1.391	0.025	72.9	99.5	1389.6	7.6
	34	500	81.30	0.0070	3.046	0.014	72.9	98.9	1396.4	11.6
	35	500	80.55	0.0070	1.021	0.021	72.9	99.6	1394.5	8.6
	37	500	79.86	0.0070	1.273	0.021	72.9	99.5	1385.1	8.5

Appendix 1 Continued: In situ $^{40}Ar/^{39}Ar$ analytical data.

	ID	Power (Pulses)	$^{40}Ar/^{39}Ar$	$^{37}Ar/^{39}Ar$	$^{36}Ar/^{39}Ar$ (x 10^{-3})	$^{39}Ar_K$ (x 10^{-15} mol)	K/Ca	$^{40}Ar^*$ (%)	Age (Ma)	±1σ (Ma)
	Queen, Muscovite, J=0.0144413±0.06%, D=1±0, NM-261A, Lab#=61988									
	03	500	70.02	0.0070	0.9313	0.142	72.9	99.6	1275.3	2.7
	05	500	72.96	0.0070	0.5734	0.136	72.9	99.8	1314.9	3.0
	06	500	75.03	0.0070	0.4327	0.143	72.9	99.8	1342.0	4.8
	07	500	75.76	0.0080	0.4273	0.146	63.8	99.8	1351.3	2.8
t1	09	500	76.08	0.0070	1.555	0.138	72.9	99.4	1351.1	3.0
	10	500	76.08	0.0070	1.575	0.149	72.9	99.4	1351.0	4.0
	11	500	84.88	0.0070	35.53	0.150	72.9	87.6	1335.3	3.0
	13	500	75.09	0.0070	1.351	0.141	72.9	99.5	1339.3	4.5
	14	500	75.02	0.0070	1.485	0.147	72.9	99.4	1338.0	4.4
	15	500	75.76	0.0070	1.292	0.141	72.9	99.5	1348.0	2.9
	17	500	77.51	0.0070	0.9559	0.143	72.9	99.6	1371.3	4.2
	18	500	76.56	0.0070	0.7419	0.154	72.9	99.7	1360.2	3.9
t2	19	500	76.54	0.0070	0.9701	0.153	72.9	99.6	1359.1	3.0
	21	500	77.52	0.0070	3.339	0.142	72.9	98.7	1362.6	3.9
	22	500	77.07	0.0070	1.646	0.148	72.9	99.4	1363.2	4.0
	23	500	78.40	0.0070	6.727	0.150	72.9	97.5	1361.1	3.7
	25	500	75.59	0.0070	0.6371	0.139	72.9	99.7	1348.3	3.9
	26	500	74.44	0.0070	0.4193	0.139	72.9	99.8	1334.6	5.6
t3	27	500	74.49	0.0070	1.751	0.141	72.9	99.3	1330.2	3.5
	29	500	71.45	0.0070	6.040	0.132	72.9	97.5	1274.3	3.4
	30	500	70.10	0.0070	1.435	0.132	72.9	99.4	1274.4	2.7
	31	500	73.32	0.0070	1.495	0.145	72.9	99.4	1316.1	2.9
t4	33	500	74.19	0.0070	1.212	0.144	72.9	99.5	1328.4	2.8
	34	500	75.88	0.0070	3.165	0.150	72.9	98.8	1342.5	2.7
	35	500	75.94	0.0070	1.061	0.149	72.9	99.6	1351.2	3.2
	36	500	76.29	0.0070	0.1828	0.135	72.9	99.9	1358.8	3.7
	37	500	76.49	0.0070	0.3959	0.132	72.9	99.8	1360.5	2.8
	38	500	76.94	0.0070	0.3445	0.146	72.9	99.9	1366.4	2.6
	40	500	76.64	0.0070	0.9289	0.144	72.9	99.6	1360.5	2.3
	41	500	76.39	0.0070	1.094	0.147	72.9	99.6	1356.8	2.3
	42	500	76.80	0.0070	0.9680	0.138	72.9	99.6	1362.4	2.4
	44	500	79.21	0.0070	6.581	0.141	72.9	97.5	1371.8	2.8
t5	45	500	76.84	0.0070	1.276	0.152	72.9	99.5	1361.7	2.4
	46	500	77.30	0.0070	0.8121	0.150	72.9	99.7	1369.2	2.5
	48	500	77.14	0.0070	0.4570	0.142	72.9	99.8	1368.5	2.8
	49	500	76.79	0.0070	0.2296	0.151	72.9	99.9	1365.0	2.2
	50	500	77.17	0.0090	0.4926	0.153	56.7	99.8	1368.7	2.3
	52	500	77.92	0.0070	4.153	0.150	72.9	98.4	1364.6	2.3
	53	500	78.54	0.0070	6.108	0.155	72.9	97.7	1365.2	2.5
	54	500	76.65	0.0070	0.1229	0.143	72.9	99.9	1363.6	2.4
	56	500	77.08	0.0070	0.2276	0.137	72.9	99.9	1368.6	2.7
	57	500	76.42	0.0070	0.5033	0.150	72.9	99.8	1359.3	2.4
	58	500	77.04	0.0070	1.037	0.149	72.9	99.6	1365.1	2.2
	60	500	76.63	0.0070	0.1255	0.133	72.9	99.9	1363.4	2.6
	61	500	76.70	0.0070	0.5541	0.146	72.9	99.8	1362.6	2.4
	62	500	77.31	0.0070	0.8122	0.146	72.9	99.7	1369.4	2.5
	64	500	77.90	0.0070	1.491	0.147	72.9	99.4	1374.1	2.3
t6	65	500	77.33	0.0070	0.9555	0.157	72.9	99.6	1369.1	2.4
	66	500	77.50	0.0070	1.738	0.142	72.9	99.3	1368.3	2.5
	68	500	76.92	0.0070	0.1750	0.147	72.9	99.9	1366.8	2.4
	69	500	76.99	0.0070	0.1611	0.152	72.9	99.9	1367.7	2.4
	70	500	76.94	0.0070	0.4061	0.151	72.9	99.8	1366.2	2.4

Appendix 1 Continued: In situ $^{40}Ar/^{39}Ar$ analytical data.

	ID	Power (Pulses)	$^{40}Ar/^{39}Ar$	$^{37}Ar/^{39}Ar$	$^{36}Ar/^{39}Ar$ (x 10^{-3})	$^{39}Ar_K$ (x 10^{-15} mol)	K/Ca	$^{40}Ar^*$ (%)	Age (Ma)	±1σ (Ma)
	72	500	76.90	0.0070	0.2512	0.139	72.9	99.9	1366.3	2.7
	73	500	76.90	0.0070	0.9232	0.151	72.9	99.6	1363.8	2.6
	74	500	77.24	0.0070	0.9450	0.150	72.9	99.6	1367.9	2.5
	76	500	76.73	0.0070	0.5121	0.150	72.9	99.8	1363.2	2.5
	77	500	76.70	0.0070	0.4919	0.151	72.9	99.8	1362.8	2.4
	78	500	76.56	0.0070	2.697	0.139	72.9	99.0	1352.9	2.4
	80	500	77.48	0.0070	1.974	0.149	72.9	99.2	1367.2	2.5
	81	500	76.47	0.0070	0.3647	0.157	72.9	99.9	1360.5	2.5
t8	82	500	76.98	0.0070	0.7907	0.158	72.9	99.7	1365.3	2.4
	84	500	76.62	0.0070	0.8329	0.133	72.9	99.7	1360.6	2.6
	85	500	76.14	0.0070	0.5773	0.142	72.9	99.8	1355.5	2.3
	86	500	77.84	0.0070	2.919	0.155	72.9	98.9	1368.2	2.3
	88	500	76.80	0.0070	0.5767	0.153	72.9	99.8	1363.9	2.6
	89	500	77.07	0.0070	1.487	0.153	72.9	99.4	1363.8	2.3
	90	500	80.67	0.0070	13.09	0.153	72.9	95.2	1365.9	2.6

Appendix 1 Continued: In situ $^{40}Ar/^{39}Ar$ analytical data.

	ID	Power	$^{40}Ar/^{39}Ar$	$^{37}Ar/^{39}Ar$	$^{36}Ar/^{39}Ar$	$^{39}Ar_K$	K/Ca	$^{40}Ar^*$	Age	±1σ
		(Pulses)			(x 10^{-3})	(x 10^{-15} mol)		(%)	(Ma)	(Ma)
	2-1, Muscovite, J=0.0145506±0.07%, D=1±0, NM-261A, Lab#=61976									
	03	500	76.77	0.0070	1.568	0.109	72.9	99.4	1367.0	2.8
	04	500	76.93	0.0080	2.614	0.150	63.8	99.0	1365.1	2.5
	05	500	77.46	0.0070	2.765	0.165	72.9	98.9	1371.2	2.2
	07	500	78.13	0.0070	3.561	0.153	72.9	98.6	1376.7	2.5
	08	500	77.14	0.0070	1.518	0.143	72.9	99.4	1371.9	2.5
	09	500	77.64	0.0070	4.333	0.156	72.9	98.3	1367.7	2.3
t1	11	500	77.20	0.0070	1.506	0.152	72.9	99.4	1372.6	2.4
	12	500	77.07	0.0070	0.6063	0.158	72.9	99.8	1374.3	2.1
	13	500	76.60	0.0070	0.3384	0.147	72.9	99.9	1369.4	2.5
	15	500	76.87	0.0070	0.4841	0.160	72.9	99.8	1372.3	2.3
	16	500	76.69	0.0070	0.3269	0.167	72.9	99.9	1370.6	2.1
	17	500	76.99	0.0070	0.3828	0.167	72.9	99.8	1374.2	2.2
	19	500	81.65	0.0070	16.23	0.164	72.9	94.1	1374.0	2.6
	20	500	77.36	0.0070	0.8199	0.164	72.9	99.7	1377.2	2.0
	21	500	76.18	0.0070	0.9187	0.109	72.9	99.6	1361.9	2.7
	23	500	76.29	0.0070	0.1821	0.144	72.9	99.9	1366.1	2.1
	24	500	76.11	0.0070	0.9403	0.165	72.9	99.6	1361.0	2.0
	25	500	76.79	0.0070	1.419	0.161	72.9	99.4	1367.8	2.1
	27	500	77.86	0.0070	5.258	0.156	72.9	98.0	1367.0	2.2
	28	500	77.22	0.0070	1.375	0.144	72.9	99.5	1373.4	2.5
t2	29	500	76.66	0.0070	0.2716	0.157	72.9	99.9	1370.4	2.2
	31	500	76.69	0.0070	0.3456	0.152	72.9	99.9	1370.5	2.1
	32	500	76.44	0.0070	0.1529	0.156	72.9	99.9	1368.1	2.0
	33	500	76.52	0.0070	0.1207	0.144	72.9	99.9	1369.3	2.2
	35	500	77.36	0.0080	0.2147	0.156	63.8	99.9	1379.4	1.9
	36	500	76.92	0.0070	0.1190	0.165	72.9	99.9	1374.2	2.1
	37	500	76.46	0.0070	0.0609	0.166	72.9	100.0	1368.7	2.2
t3	39	500	76.94	0.0070	0.7539	0.143	72.9	99.7	1372.1	2.4
	40	500	76.62	0.0070	0.7313	0.156	72.9	99.7	1368.2	2.3
	41	500	76.97	0.0070	0.9881	0.156	72.9	99.6	1371.6	2.3
	43	500	77.85	0.0070	5.050	0.157	72.9	98.1	1367.6	2.2
t4	44	500	77.11	0.0070	1.236	0.144	72.9	99.5	1372.5	2.2
	45	500	76.66	0.0070	0.3780	0.154	72.9	99.8	1370.0	2.1
	47	500	76.54	0.0070	0.9562	0.153	72.9	99.6	1366.4	2.3
	48	500	76.68	0.0070	0.0298	0.158	72.9	100.0	1371.6	2.1
	49	500	76.42	0.0070	0.1619	0.158	72.9	99.9	1367.8	2.5
	51	500	76.19	0.0070	1.250	0.156	72.9	99.5	1360.8	2.1
	52	500	76.25	0.0070	0.9938	0.147	72.9	99.6	1362.6	2.3
	53	500	77.42	0.0070	4.789	0.151	72.9	98.2	1363.2	2.1
t5	55	500	77.37	0.0070	4.358	0.151	72.9	98.3	1364.2	2.1
	56	500	75.56	0.0070	1.094	0.154	72.9	99.6	1353.4	2.5
	57	500	75.91	0.0070	0.6829	0.153	72.9	99.7	1359.4	2.3
	59	500	76.80	0.0070	0.4713	0.146	72.9	99.8	1371.5	1.9
	60	500	71.55	0.0070	0.9124	0.076	72.9	99.6	1302.4	3.7
	61	500	73.79	0.0070	0.9235	0.098	72.9	99.6	1331.4	2.8
	63	500	66.21	0.0070	1.273	0.029	72.9	99.4	1229.8	5.9
	64	500	70.52	0.0070	0.5221	0.087	72.9	99.8	1290.5	3.2
	65	500	69.46	0.0070	0.7019	0.066	72.9	99.7	1275.8	3.2
	67	500	69.04	0.0070	0.5766	0.061	72.9	99.7	1270.7	3.8
t6	68	500	62.57	0.0070	0.3513	0.027	72.9	99.8	1183.4	6.7
	69	500	61.86	0.0070	3.018	0.017	72.9	98.5	1162.4	8.4
	71	500	65.08	0.0070	0.6156	0.091	72.9	99.7	1217.0	2.8

Appendix 1 Continued: In situ $^{40}Ar/^{39}Ar$ analytical data.

	ID	Power (Pulses)	$^{40}Ar/^{39}Ar$	$^{37}Ar/^{39}Ar$	$^{36}Ar/^{39}Ar$ (x 10^{-3})	$^{39}Ar_K$ (x 10^{-15} mol)	K/Ca	$^{40}Ar^*$ (%)	Age (Ma)	±1σ (Ma)
	72	500	74.71	0.0070	0.3022	0.113	72.9	99.9	1345.6	3.1
	73	500	75.98	0.0070	1.039	0.113	72.9	99.6	1359.0	2.7
	75	500	75.78	0.0070	0.4078	0.109	72.9	99.8	1358.8	2.6
	76	500	75.65	0.0070	0.6713	0.114	72.9	99.7	1356.1	2.5
	77	500	76.14	0.0070	3.802	0.114	72.9	98.5	1350.6	2.6
	79	500	75.37	0.0070	1.109	0.116	72.9	99.6	1351.0	2.5
	80	500	77.64	0.0070	6.103	0.117	72.9	97.7	1361.1	2.3
t7	82	500	76.70	0.0070	0.1803	0.119	72.9	99.9	1371.2	2.5
	83	500	76.67	0.0070	0.3262	0.124	72.9	99.9	1370.4	2.8
	84	500	76.74	0.0070	0.3816	0.124	72.9	99.8	1371.0	2.4
	86	500	74.00	0.0070	0.5902	0.080	72.9	99.8	1335.4	3.1
	87	500	76.40	0.0070	0.3882	0.085	72.9	99.8	1366.7	3.4
	88	500	77.04	0.0070	1.510	0.056	72.9	99.4	1370.6	3.9
	90	500	76.75	0.0070	0.1795	0.072	72.9	99.9	1371.9	3.0
t8	91	500	76.79	0.0070	1.528	0.110	72.9	99.4	1367.4	2.7
	92	500	79.11	0.0070	8.658	0.130	72.9	96.8	1370.1	2.3
	94	500	77.66	0.0070	2.570	0.125	72.9	99.0	1374.5	2.4
	95	500	77.23	0.0070	1.552	0.122	72.9	99.4	1372.8	2.5
	96	500	78.08	0.0070	3.000	0.099	72.9	98.9	1378.2	2.5

Appendix 1 Continued: In situ $^{40}Ar/^{39}Ar$ analytical data.

	ID	Power	$^{40}Ar/^{39}Ar$	$^{37}Ar/^{39}Ar$	$^{36}Ar/^{39}Ar$	$^{39}Ar_K$	K/Ca	$^{40}Ar^*$	Age	±1σ
		(Pulses)			(x 10^{-3})	(x 10^{-15} mol)		(%)	(Ma)	(Ma)
	Cribbenville, Muscovite, J=0.0094706±0.05%, D=1±0, NM-254G, Lab#=61442									
	04	500	117.5	0.0070	1.173	0.059	72.9	99.7	1366.5	3.2
	05	500	112.9	0.0070	2.584	0.023	72.9	99.3	1324.8	6.1
	06	500	116.1	0.0070	3.952	0.012	72.9	99.0	1348.3	11.5
	07	500	114.3	0.0070	2.036	0.017	72.9	99.5	1338.3	8.8
t1	08	500	113.3	0.0070	3.710	0.010	72.9	99.0	1325.5	13.0
	09	500	116.6	0.0070	5.752	0.010	72.9	98.5	1347.6	11.5
	10	500	115.3	0.0070	6.713	0.009	72.9	98.3	1334.6	13.3
	11	500	117.7	0.0070	12.14	0.006	72.9	97.0	1341.8	20.8
	12	500	117.4	0.0070	6.410	0.005	72.9	98.4	1352.8	21.3
	13	500	119.8	0.0070	4.393	0.003	72.9	98.9	1377.7	33.5
	14	500	111.9	0.0070	5.509	0.003	72.9	98.5	1309.2	28.9
	15	500	115.8	0.0070	0.3940	0.056	72.9	99.9	1354.5	3.9
	16	500	115.7	0.0070	0.7402	0.055	72.9	99.8	1352.9	3.8
	17	500	117.2	0.0070	0.7024	0.062	72.9	99.8	1364.9	3.9
	18	500	117.2	0.0070	2.603	0.052	72.9	99.3	1360.2	4.4
t2	19	500	118.7	0.0070	6.741	0.045	72.9	98.3	1362.3	4.6
	21	500	120.6	0.0080	10.57	0.053	63.8	97.4	1368.9	4.2
	22	500	123.9	0.0070	21.74	0.044	72.9	94.8	1368.8	5.2
	23	500	120.4	0.0070	12.09	0.044	72.9	97.0	1363.9	4.6
	24	500	126.8	0.0070	29.09	0.046	72.9	93.2	1374.8	5.0
	25	500	129.2	0.0070	35.62	0.042	72.9	91.8	1379.0	5.5
	26	500	125.9	0.0070	30.94	0.064	72.9	92.7	1363.1	3.9
	27	500	118.2	0.0070	9.091	0.065	72.9	97.7	1352.9	3.7
	28	500	118.1	0.0070	6.069	0.061	72.9	98.5	1359.7	3.9
	29	500	117.1	0.0070	3.685	0.066	72.9	99.1	1356.9	4.2
	30	500	176.3	0.0070	206.0	0.066	72.9	65.5	1351.9	4.8
t3	31	500	117.8	0.0070	3.946	0.060	72.9	99.0	1362.2	4.0
	32	500	117.5	0.0070	0.9553	0.056	72.9	99.8	1367.0	4.5
	33	500	125.9	0.0070	27.18	0.054	72.9	93.6	1372.6	4.4
	34	500	119.4	0.0070	7.702	0.053	72.9	98.1	1366.4	4.6
	35	500	117.7	0.0070	1.288	0.046	72.9	99.7	1367.8	4.8
	36	500	118.8	0.0070	3.563	0.043	72.9	99.1	1371.3	5.6
	37	500	118.5	0.0070	1.897	0.045	72.9	99.5	1373.1	5.0
	39	500	119.3	0.0070	5.438	0.010	72.9	98.7	1370.8	13.2
	40	500	124.3	0.0070	16.56	0.010	72.9	96.1	1385.3	13.0
	41	500	119.2	0.0070	1.185	0.037	72.9	99.7	1380.3	5.6
t4	42	500	118.4	0.0090	0.2401	0.039	56.7	99.9	1375.9	5.4
	43	500	120.0	0.0070	1.625	0.032	72.9	99.6	1385.5	6.0
	44	500	120.0	0.0070	2.182	0.034	72.9	99.5	1384.4	5.3
	45	500	119.5	0.0070	7.771	0.026	72.9	98.1	1366.4	7.4
	46	500	115.5	0.0070	2.398	0.032	72.9	99.4	1346.8	5.7

Appendix 1 Continued: In situ $^{40}Ar/^{39}Ar$ analytical data.

	ID	Power (Pulses)	$^{40}Ar/^{39}Ar$	$^{37}Ar/^{39}Ar$	$^{36}Ar/^{39}Ar$ (x 10^{-3})	$^{39}Ar_K$ (x 10^{-15} mol)	K/Ca	$^{40}Ar^*$ (%)	Age (Ma)	±1σ (Ma)
	Meadow, Muscovite, J=0.0094979±0.04%, D=1±0, NM-254G, Lab#=61446									
p1	03	500	105.7	0.0070	3.624	0.060	72.9	99.0	1263.0	4.5
p2	04	500	115.4	0.0070	3.191	0.079	72.9	99.2	1347.1	4.2
p3	05	500	115.0	0.0070	3.613	0.073	72.9	99.1	1342.1	4.0
p4	06	500	113.2	0.0070	6.301	0.064	72.9	98.3	1320.2	4.1
p5	07	500	115.7	0.0070	2.394	0.078	72.9	99.4	1351.4	3.9
p6	08	500	116.9	0.0080	2.203	0.077	63.8	99.4	1361.9	3.7
p7	09	500	117.2	0.0070	0.9073	0.074	72.9	99.8	1367.3	4.0
p8	10	500	107.0	0.0070	6.160	0.020	72.9	98.3	1267.7	9.5
p9	11	500	107.5	0.0070	5.921	0.056	72.9	98.4	1273.2	4.2
t1	12	500	117.2	0.0070	3.454	0.078	72.9	99.1	1360.8	3.8
	13	500	118.0	0.0070	5.487	0.079	72.9	98.6	1363.1	3.5
	14	500	115.4	0.0070	2.074	0.074	72.9	99.5	1349.4	3.8
	15	500	115.3	0.0070	0.4084	0.075	72.9	99.9	1352.8	3.9
	16	500	115.5	0.0070	0.3772	0.076	72.9	99.9	1354.1	3.9
	17	500	116.6	0.0070	1.904	0.048	72.9	99.5	1359.7	5.5
	18	500	117.9	0.0070	6.707	0.073	72.9	98.3	1358.7	4.1
	19	500	116.6	0.0080	1.017	0.032	63.8	99.7	1362.5	6.7

Notes:

Isotopic ratios corrected for blank, radioactive decay, and mass discrimination, not corrected for interfering reactions.

Errors quoted for individual analyses include analytical error only, without interfering reaction or J uncertainties.

Mean age is weighted mean age of Taylor (1982). Mean age error is weighted error of the mean (Taylor, 1982), multiplied by the root of the MSWD where MSWD>1, and also incorporates uncertainty in J factors and irradiation correction uncertainties.

Isotopic abundances after Steiger and Jäger (1977).

Ages calculated relative to FC-2 Fish Canyon Tuff sanidine interlaboratory standard at 28.201 Ma

Decay Constant (LambdaK (total)) = 5.463e-10/a

Correction factors:

$(^{39}Ar/^{37}Ar)_{Ca}$ = 0.000698 ± 8e-06

$(^{36}Ar/^{37}Ar)_{Ca}$ = 0.000273 ± 2e-07

$(^{38}Ar/^{39}Ar)_{K}$ = 0.013

$(^{40}Ar/^{39}Ar)_{K}$ = 0.008068 ± 6.8e-05

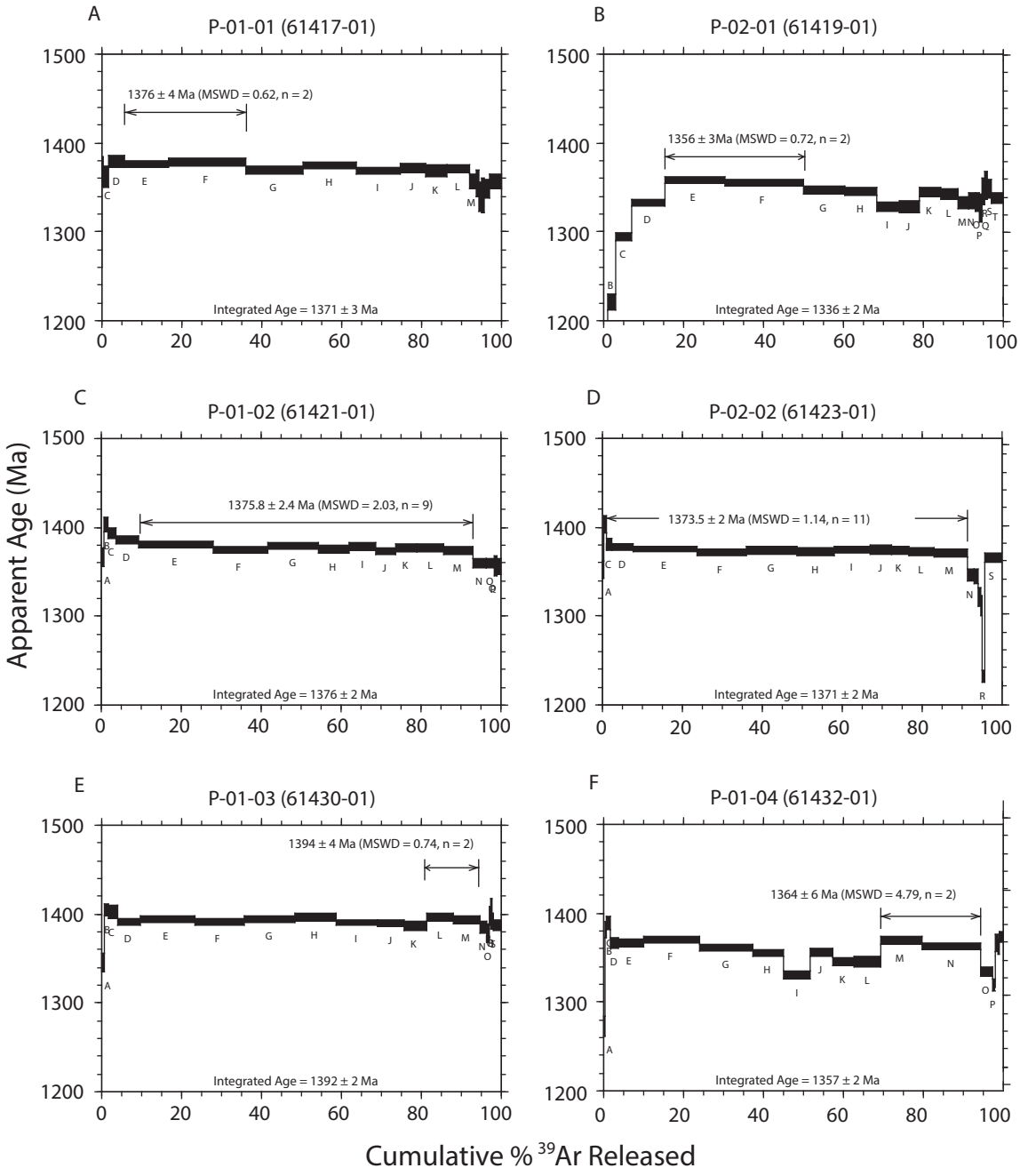

Appendix 2: A-F: Pegmatite muscovites from the Tusas Mountains with preferred ages shown.

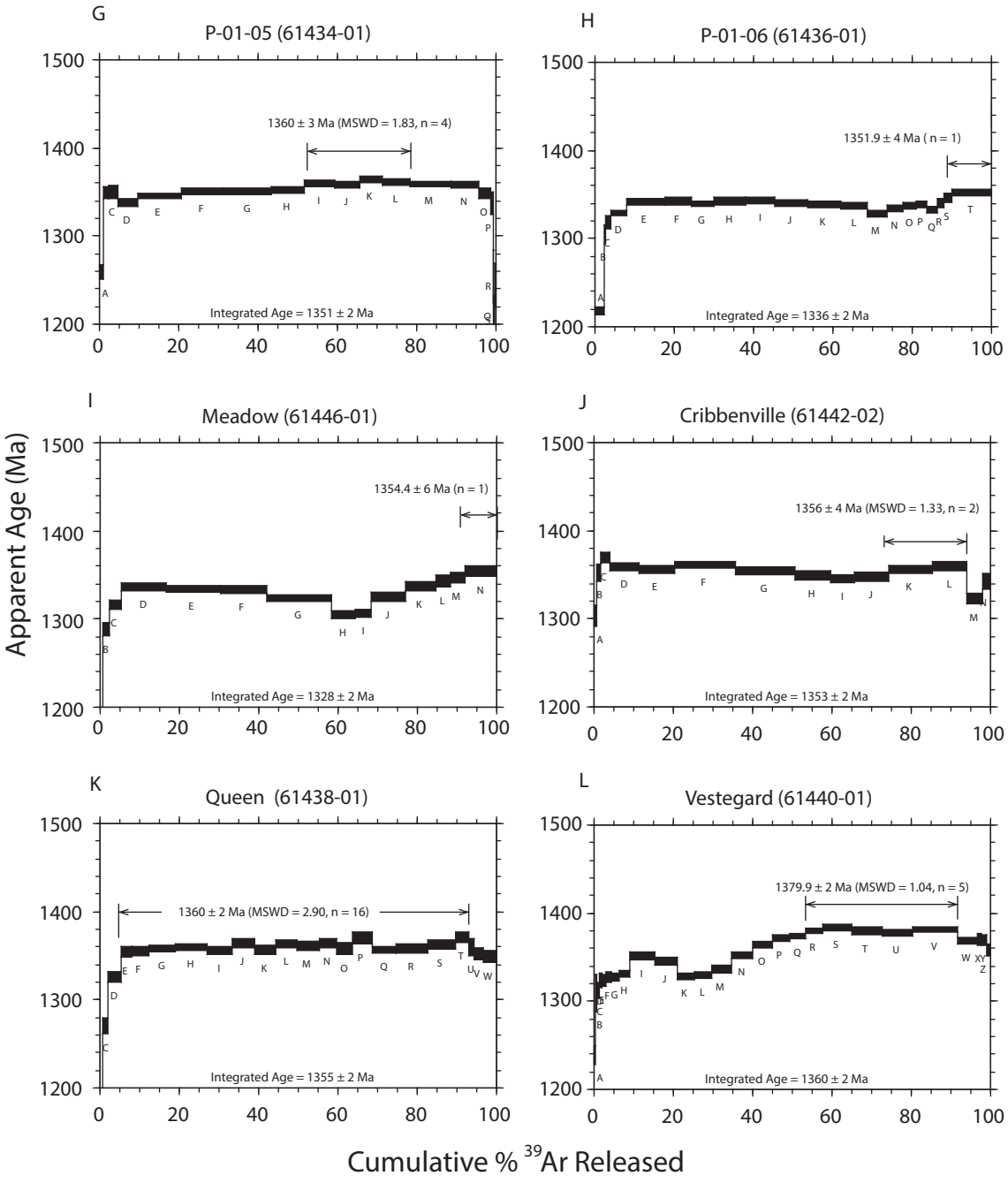

Appendix 2 Continued: G-L: Pegmatite muscovites from the Tusas Mountains with preferred ages shown.

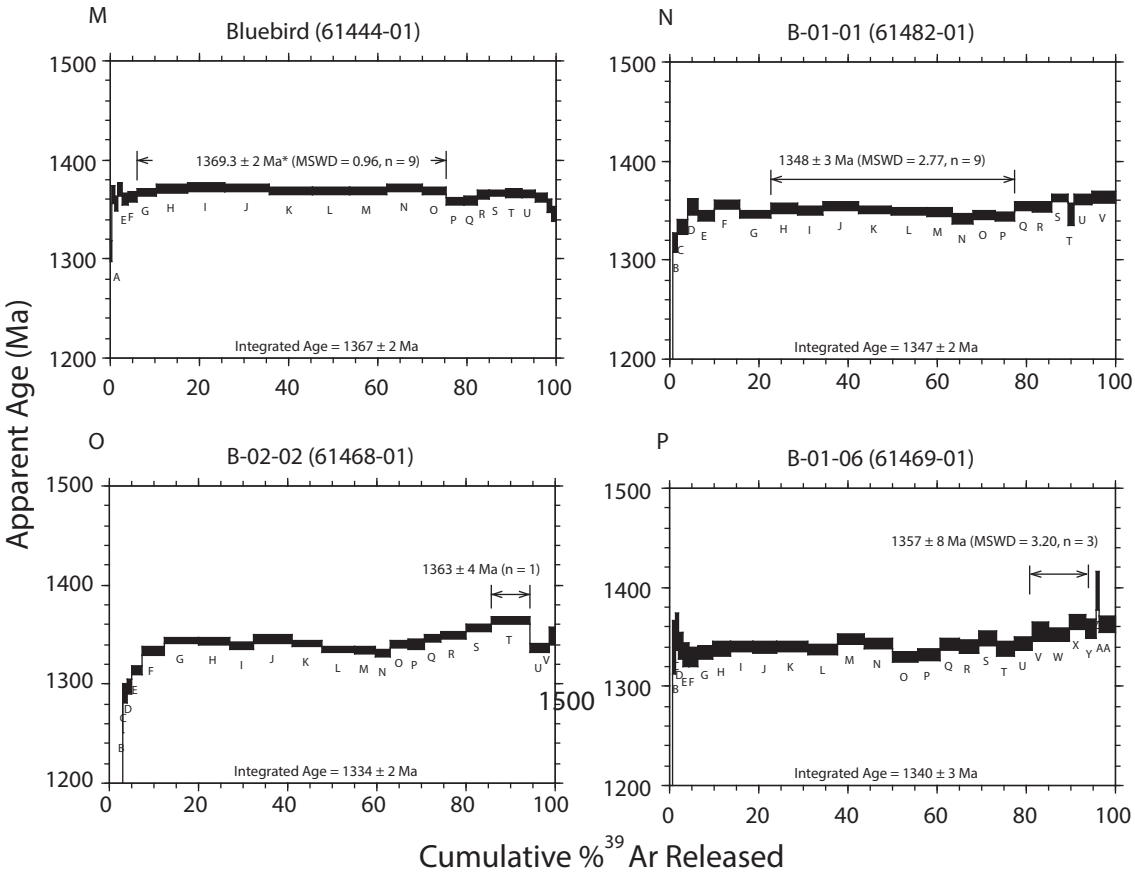

Appendix 2 Continued: M: Pegmatite muscovite from the Tusas Mountains;
N-P: Country Rcok muscovites from the Tusas Mountains with preferred ages shown.

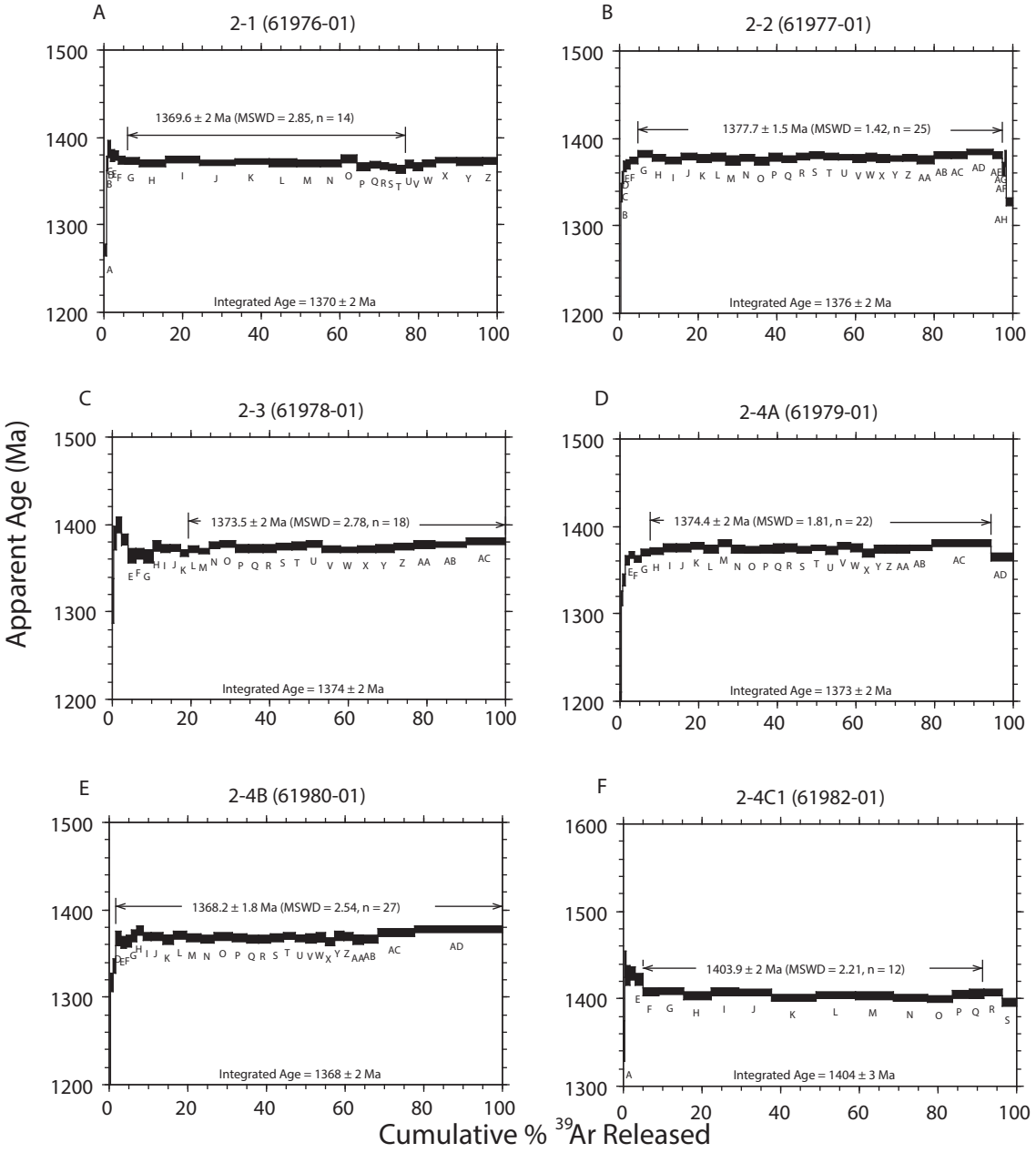

Appendix 2: A-F: Pegmatite muscovites from the Tusas Mountains with preferred ages shown.

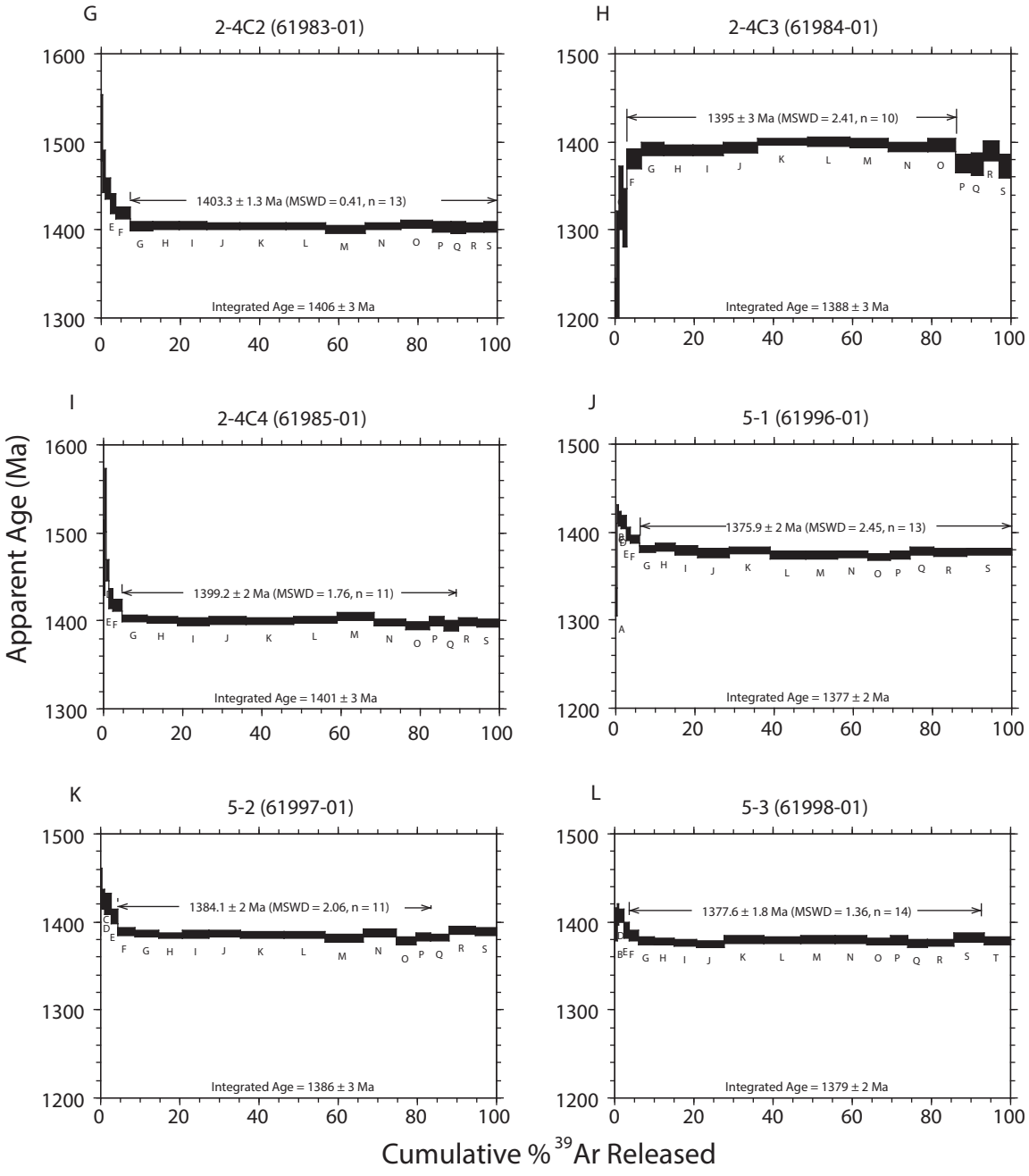

Appendix 2 : G-L: Pegmatite muscovites from the Tusas Mountains with preferred ages shown.

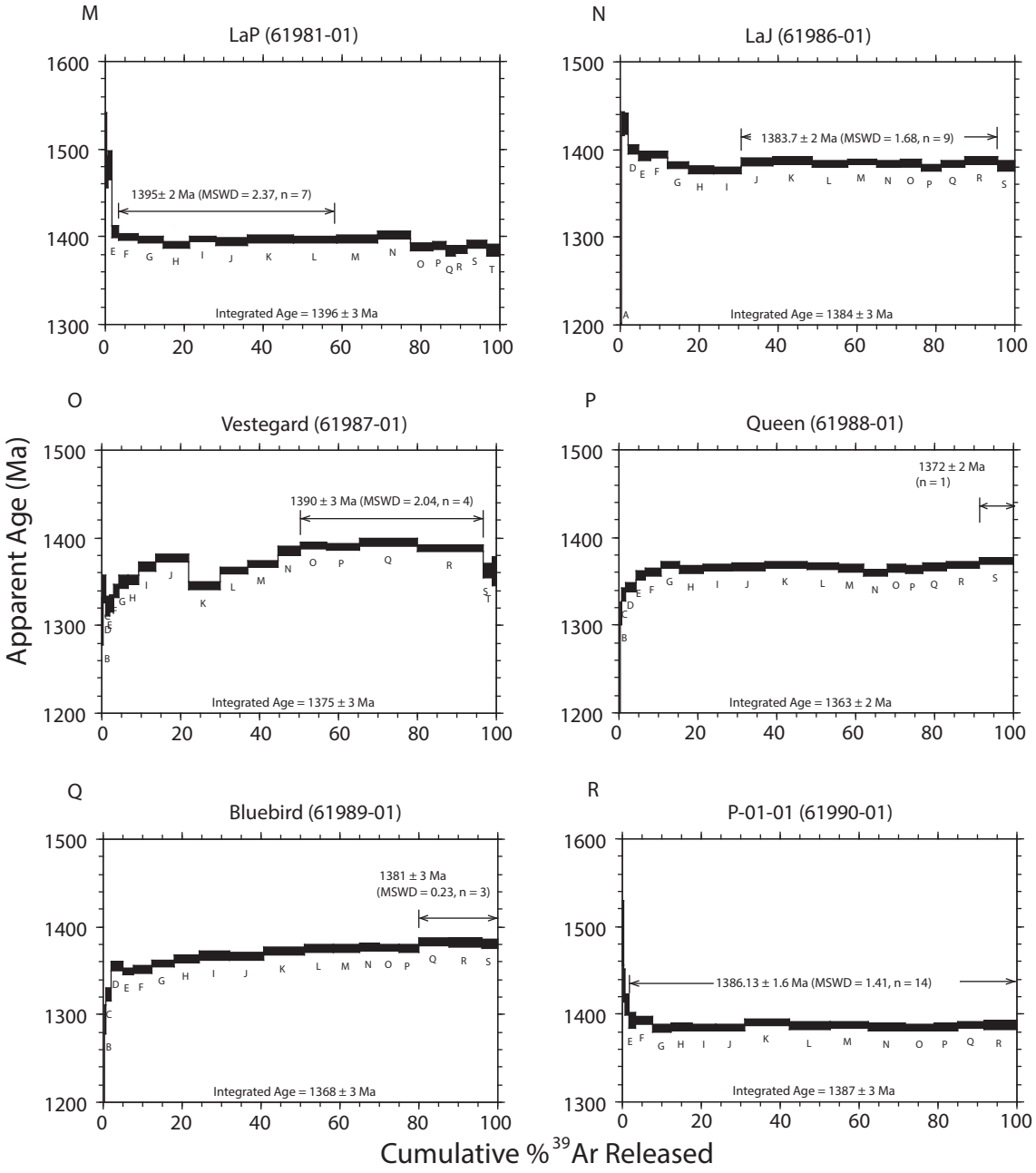

Appendix 2: M-R: Pegmatite muscovites from the Tusas Mountains with preferred ages shown.

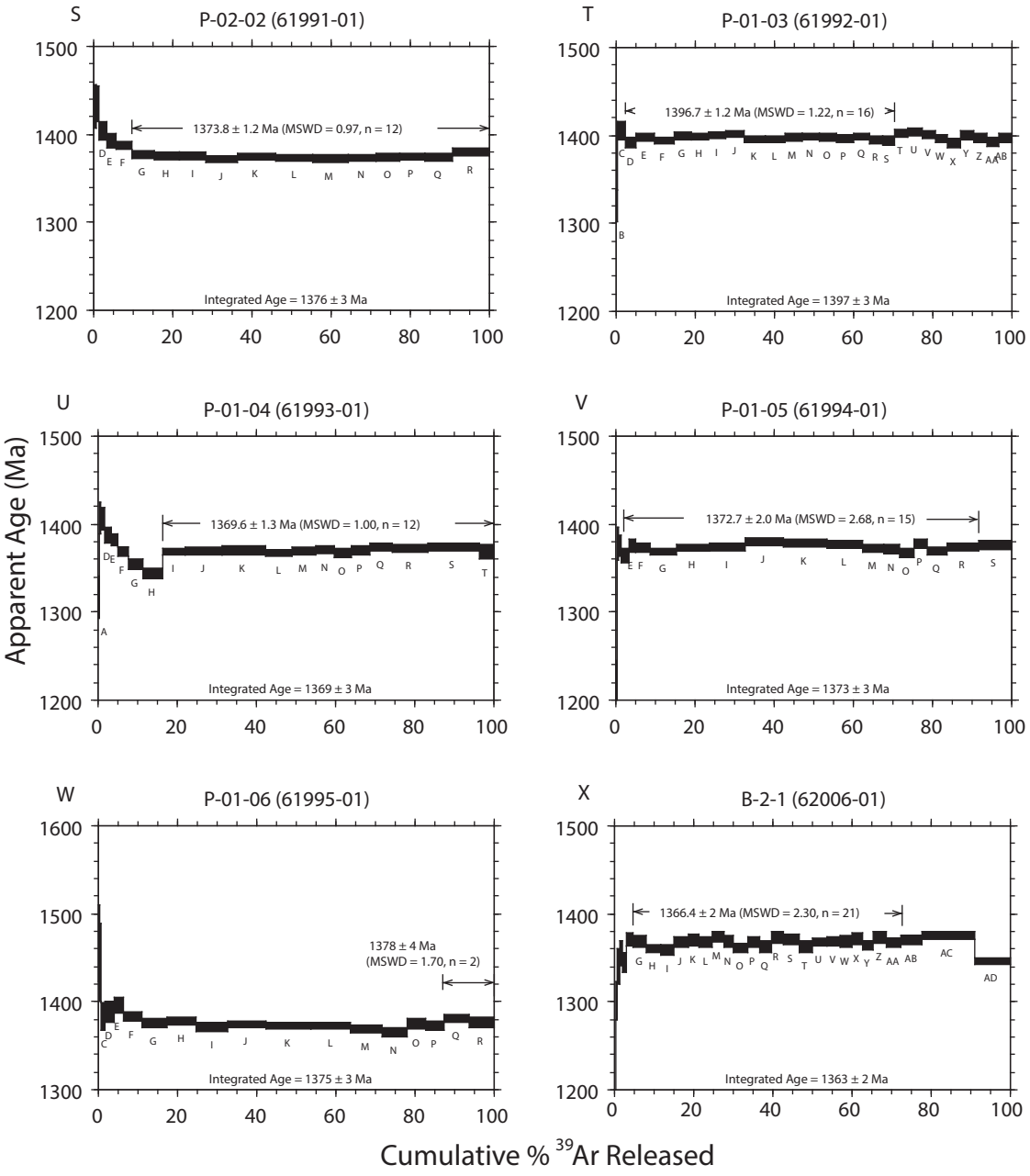

Appendix 2 : S-W: Pegmatite muscovites from the Tusas Mountains; X: Country Rock muscovites from the Tusas Mountains with preferred ages shown.

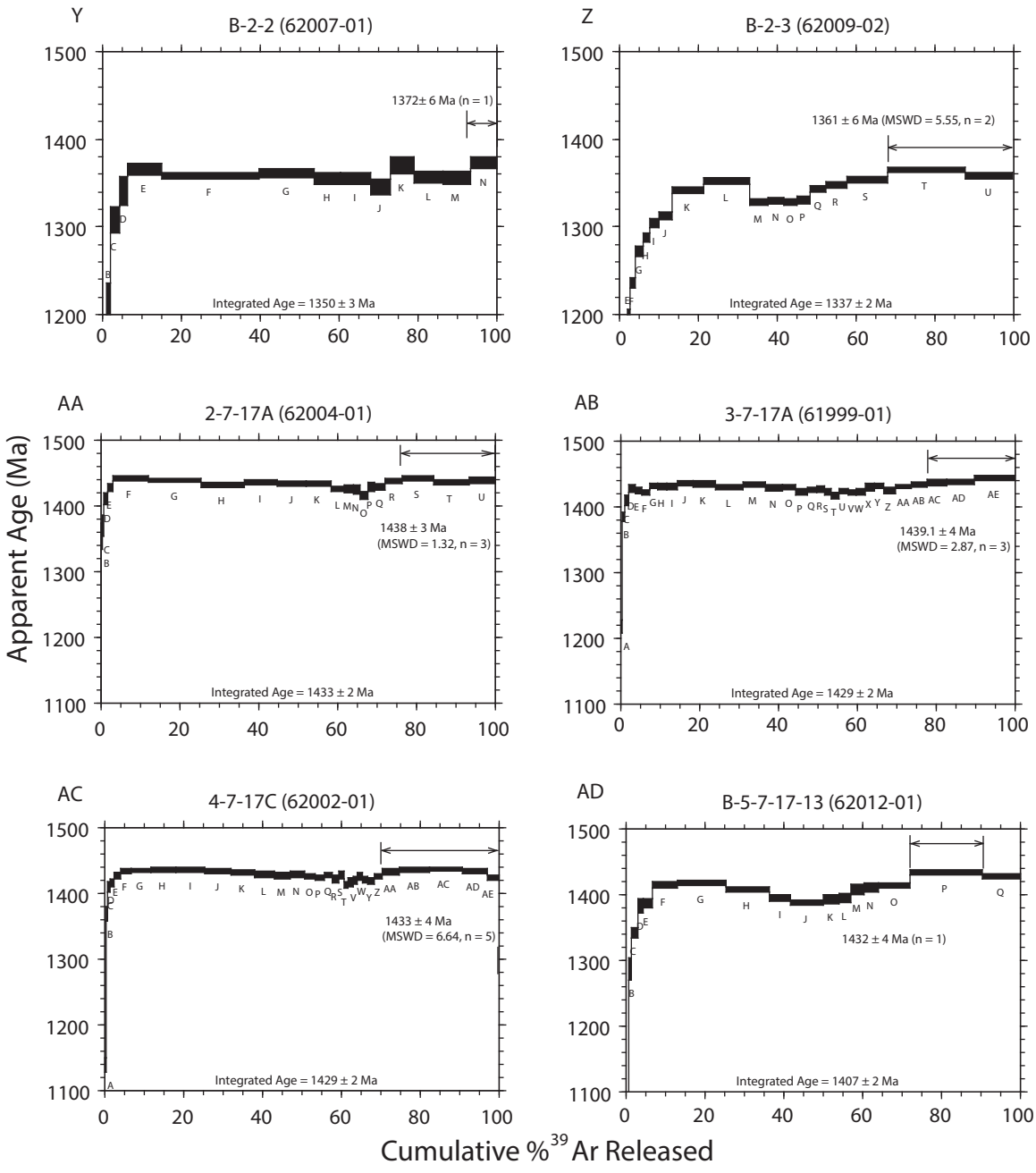

Appendix 2 : Y-Z: Country Rock muscovites from the Tusas Mountains; AA-AC: Pegmatite muscovite from the Sandia mountains; AD: Country Rock muscovite from the Sandia Mountains. All spectra with preferred ages shown.

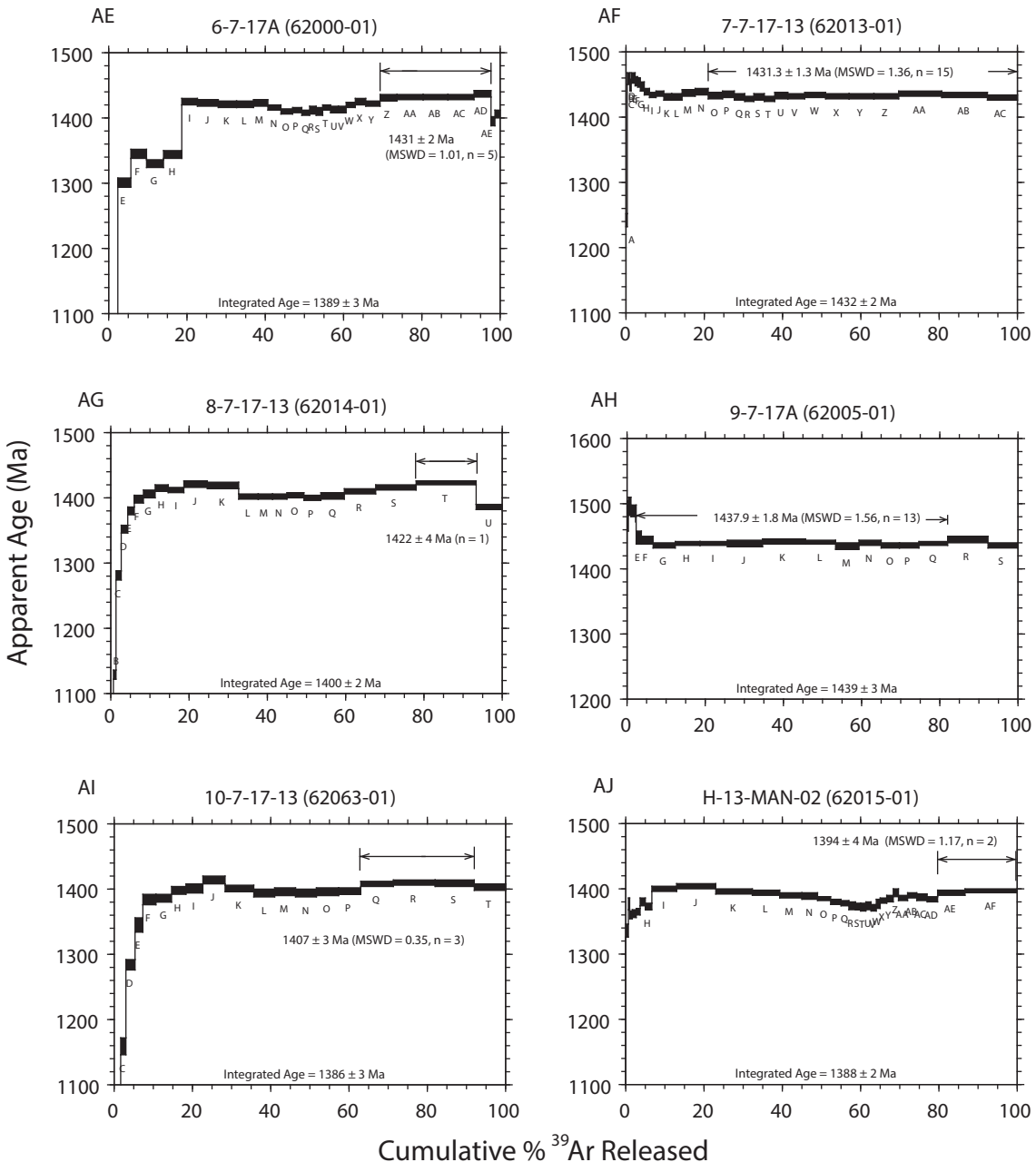

Appendix 2 : AE-AI: Pegmatite muscovites from the Sandia Mountains; AJ: Pegmatite Muscovite from the Manzano Mountains. All spectra with preferred ages shown.

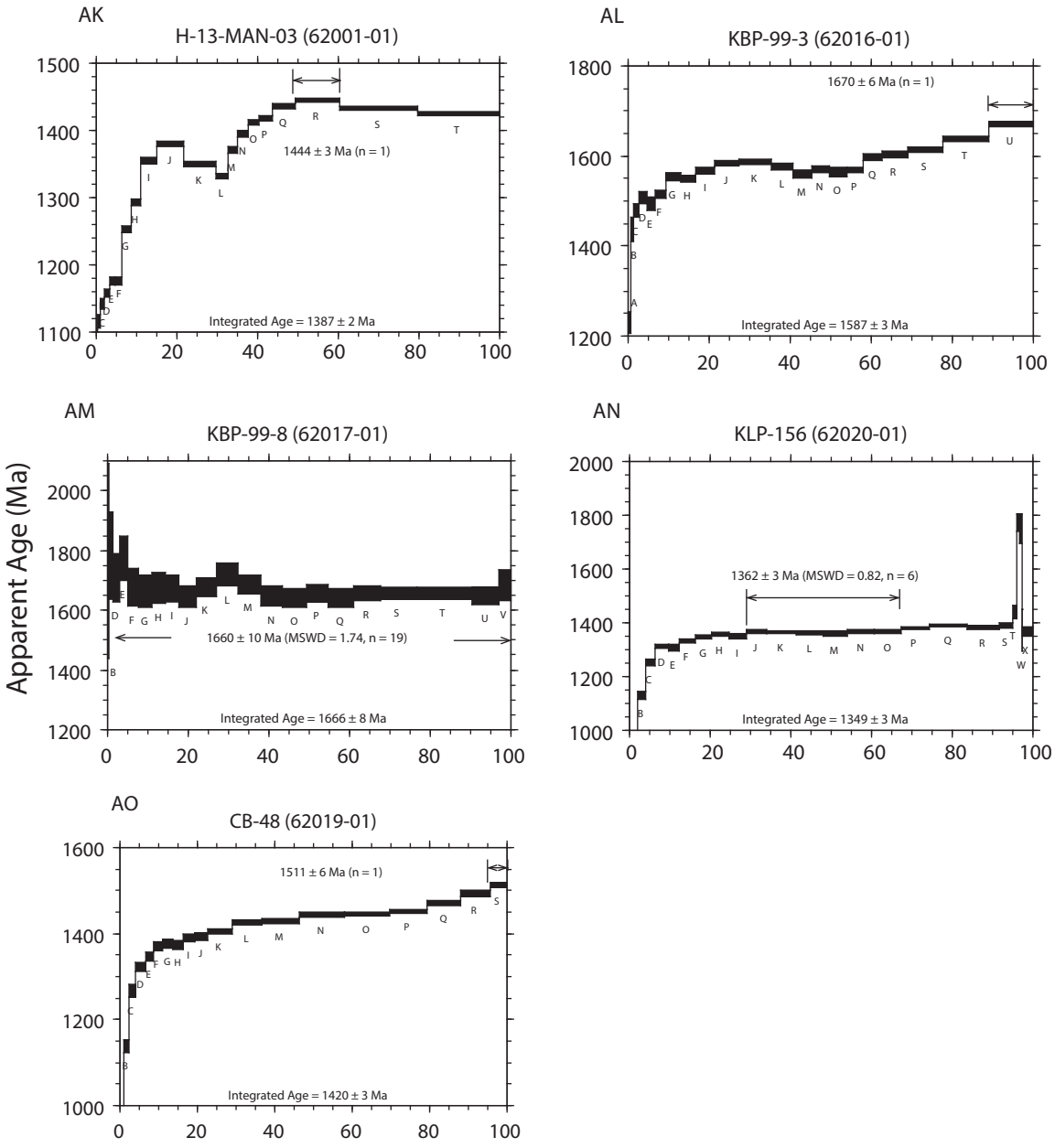

Appendix 2 : GAK: Pegmatite muscovites from the Manzano Mountains; AL-AM: Pegmatite muscovite from the Ojito Pluton; AN: Pegmatite muscovite from Los Pinos Pluton; AO:Pegmatite muscovite from the Manzanita Pluton. All spectra with with preferred ages shown.

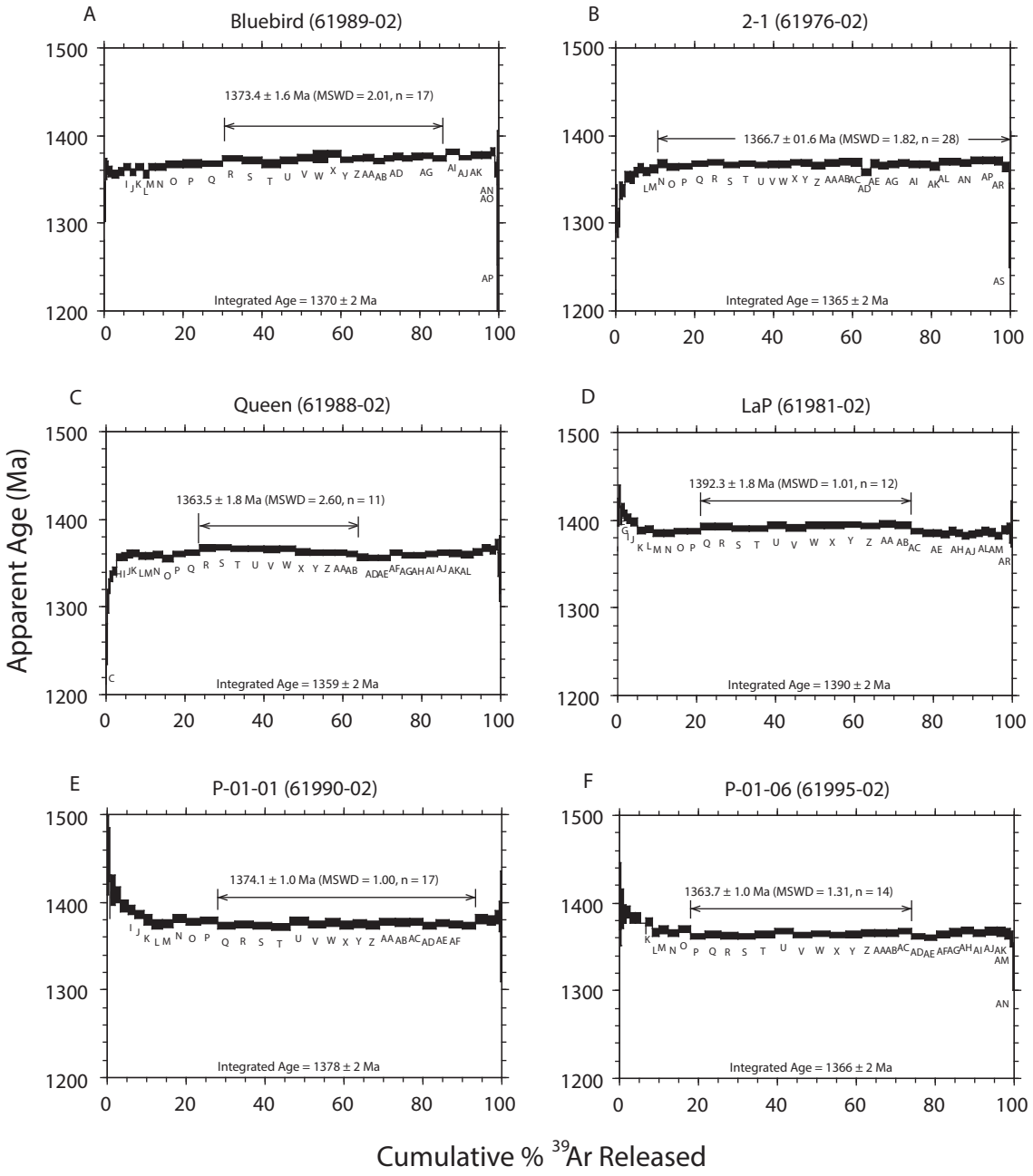

Appendix 2 Continued : A-F: Pegmatite muscovites from the Tusas Mountains with preferred ages shown. Samples where analysed according to Kula and Spell (2012) methods.

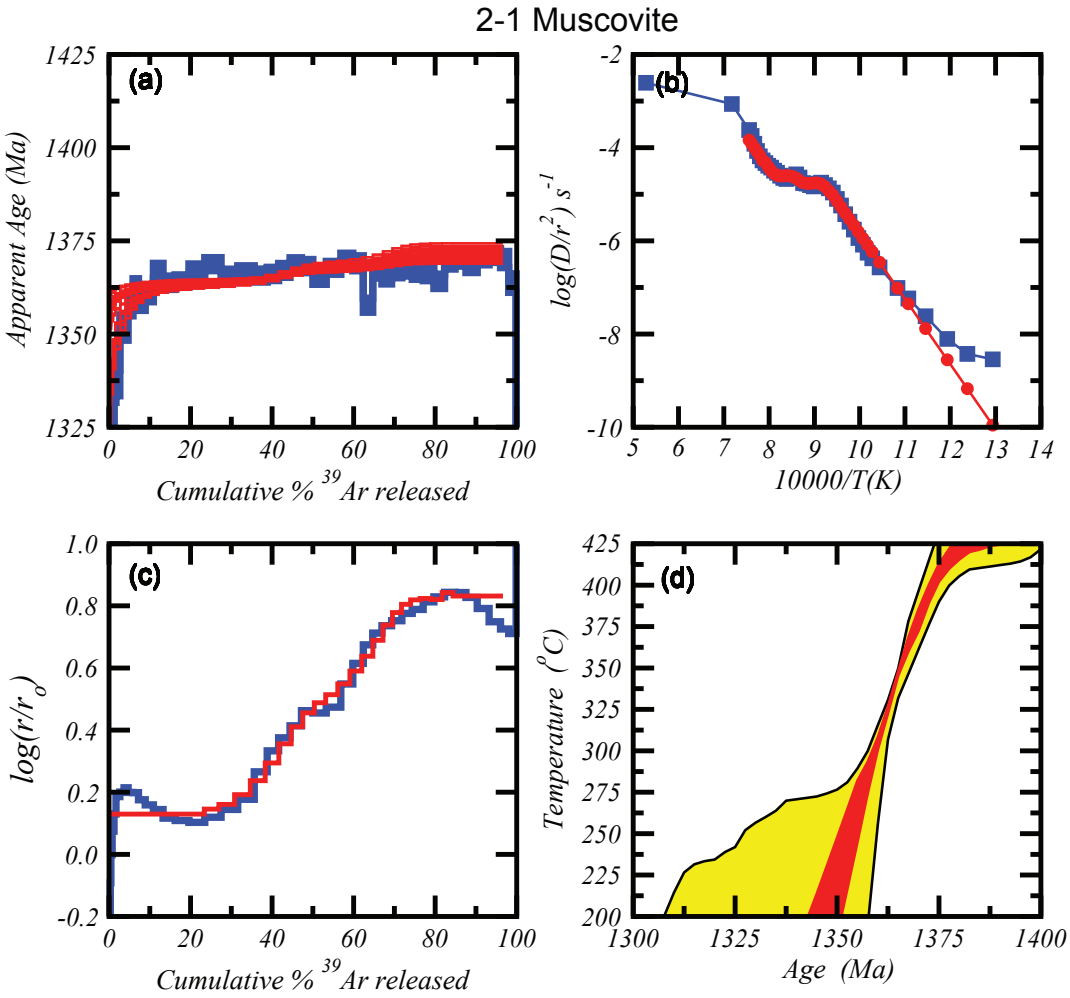

Appendix 3: MDD analysis of sample 2-1 from the Tusas Mountains. A: Measured age spectra using high resolution heating schedule similar to that recommended by Kula and Spell (2012). B: Arrhenius diagram determined from fractional release of ^{39}Ar. C: Log(r/r_0) plot constructed using the same reference Arrhenius law of 64.0 kcal/mol and D_0/r_0^2. Data appears to vary from 64.0 kcal/mol and the climbing pattern is consistent with multiple diffusion length scales. D: Thermal history derived from kinetic data and age spectrum that indicates temperatures > 400°C prior to 1.4 Ga with cooling through 375°C by about 1375 Ma.

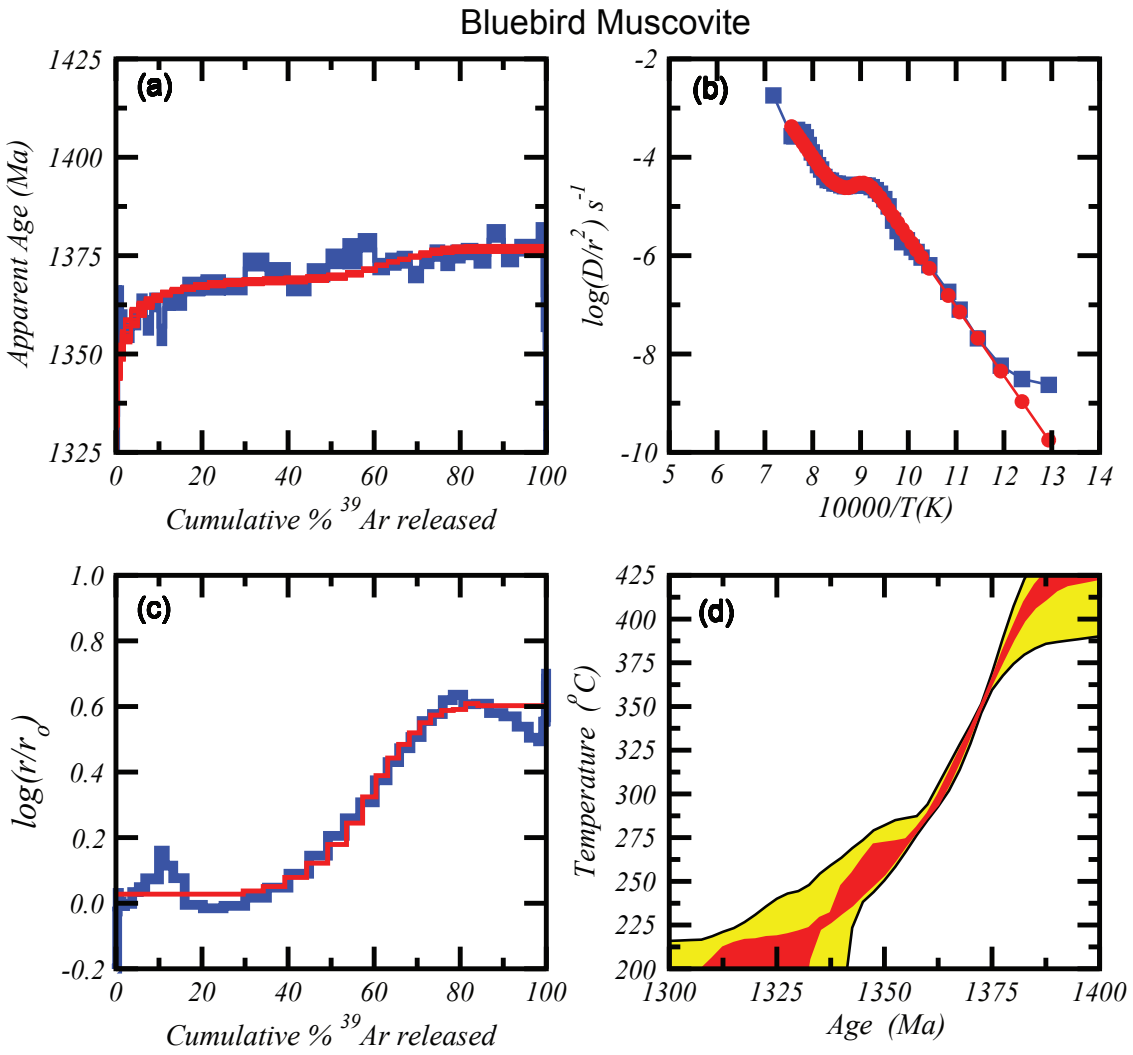

Appendix 3 continued: MDD analysis of sample Bluebird from the Tusas Mountains. A: Measured age spectra using high resolution heating schedule similar to that recommended by Kula and Spell (2012). B: Arrhenius diagram determined from fractional release of ^{39}Ar. C: Log(r/r_0) plot constructed using the same reference Arrhenius law of 64.0 kcal/mol and D_0/r_0^2. Data appears to vary from 64.0 kcal/mol and the climbing pattern is consistent with multiple diffusion length scales. D: Thermal history derived from kinetic data and age spectrum that indicates temperatures > 400°C prior to 1.4 Ga with cooling through 375°C by about 1375 Ma.

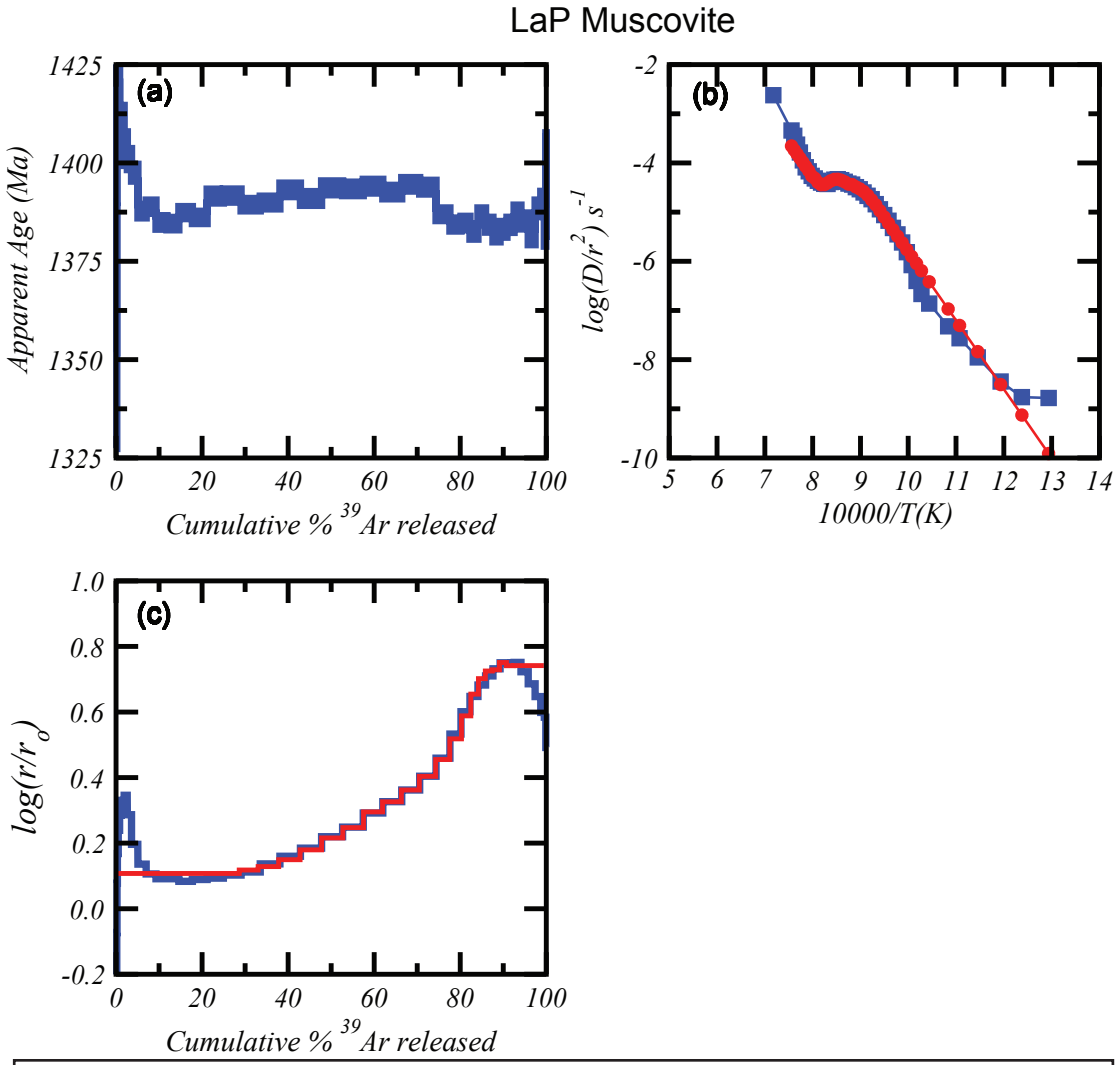

Appendix 3 continued: MDD analysis of sample LaP from the Tusas Mountains. A: Measured age spectra using high resolution heating schedule similar to that recommended by Kula and Spell (2012). B: Arrhenius diagram determined from fractional release of ^{39}Ar. C: Log(r/r_0) plot constructed using the same reference Arrhenius law of 64.0 kcal/mol and D_0/r_0^2. Data appears to vary from 64.0 kcal/mol and the climbing pattern is consistent with multiple diffusion length scales.

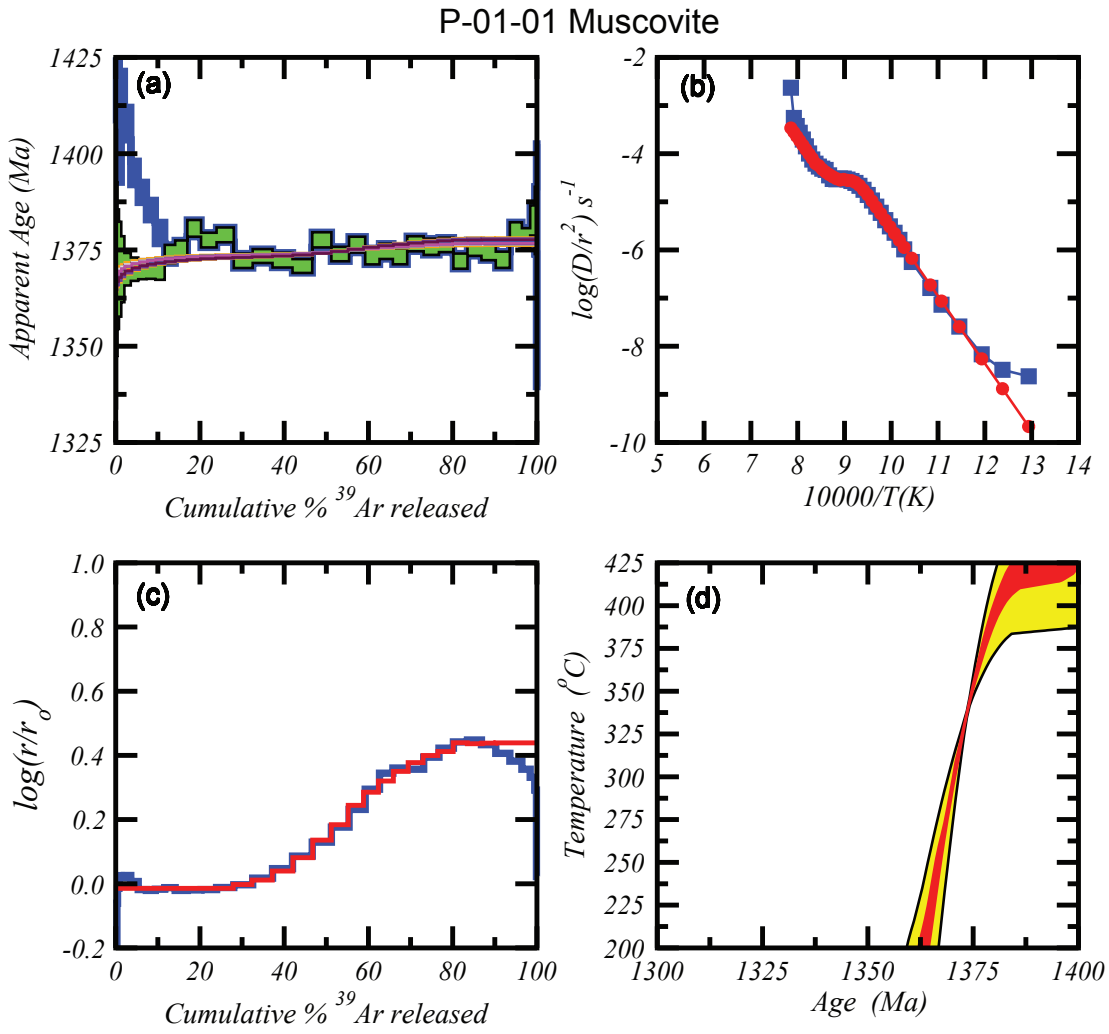

Appendix 3 continued: MDD analysis of sample P-01-01 from the Tusas Mountains. A: Measured age spectra using high resolution heating schedule similar to that recommended by Kula and Spell (2012). B: Arrhenius diagram determined from fractional release of ^{39}Ar. C: Log(r/r_0) plot constructed using the same reference Arrhenius law of 64.0 kcal/mol and D_0/r_0^2. Data appears to vary from 64.0 kcal/mol and the climbing pattern is consistent with multiple diffusion length scales. D: Thermal history derived from kinetic data and age spectrum indicates temperatures > 400°C prior to 1.4 Ga with cooling through 375°C by about 1375 Ma.

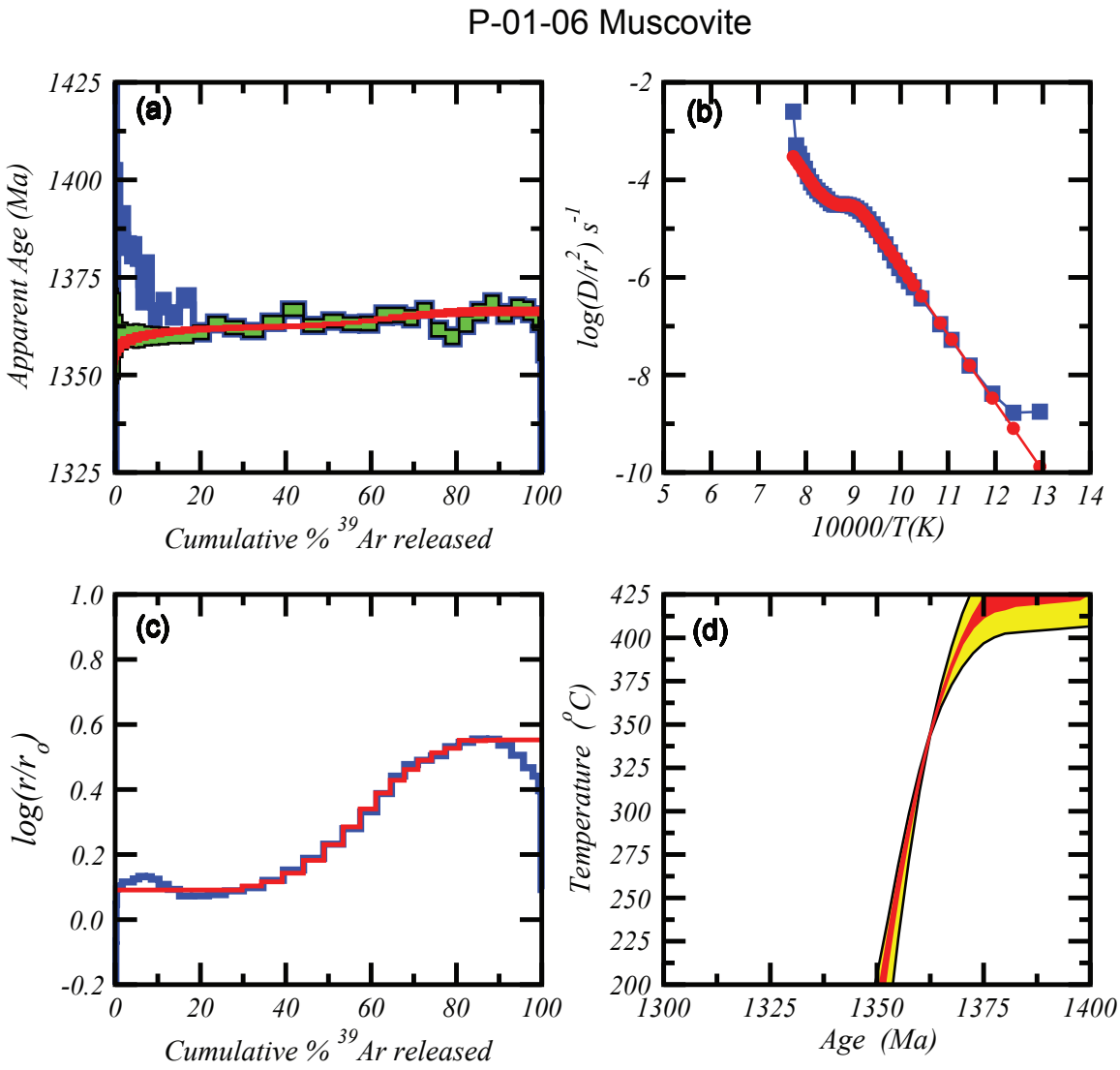

Appendix 3 continued: MDD analysis of sample P-01-06 from the Tusas Mountains. A: Measured age spectra using high resolution heating schedule similar to that recommended by Kula and Spell (2012). B: Arrhenius diagram determined from fractional release of ^{39}Ar. C: Log(r/r_0) plot constructed using the same reference Arrhenius law of 64.0 kcal/mol and D_0/r_0^2. Data appears to vary from 64.0 kcal/mol and the climbing pattern is consistent with multiple diffusion length scales. D: Thermal history derived from kinetic data and age spectrum that indicates temperatures > 400°C prior to 1.4 Ga with cooling through 375°C by about 1375 Ma.

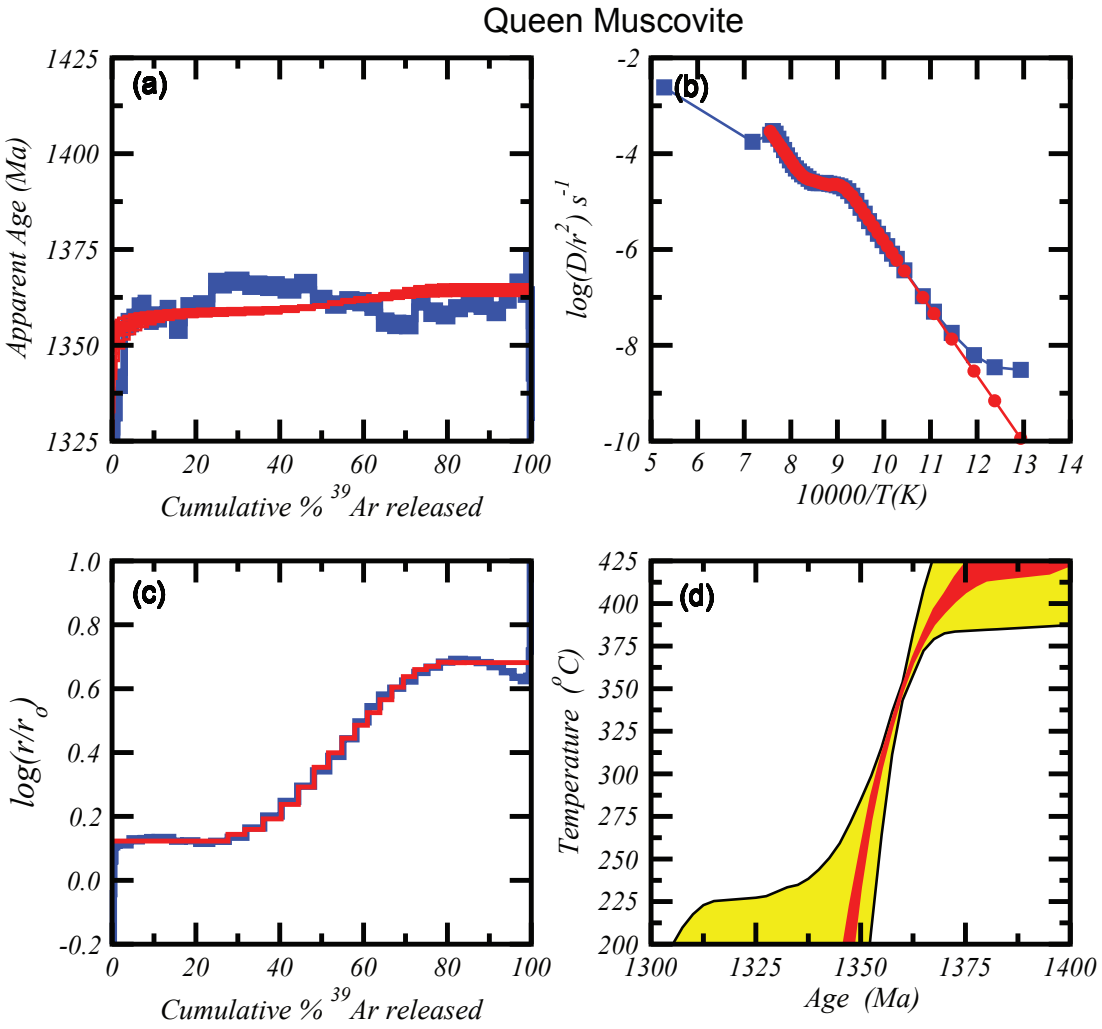

AAppendix 3 continued: MDD analysis of sample Queen from the Tusas Mountains. A: Measured age spectra using high resolution heating schedule similar to that recommended by Kula and Spell (2012). B: Arrhenius diagram determined from fractional release of ^{39}Ar. C: Log(r/r_0) plot constructed using the same reference Arrhenius law of 64.0 kcal/mol and D_0/r_0^2. Data appears to vary from 64.0 kcal/mol and the climbing pattern is consistent with multiple diffusion length scales. D: Thermal history derived from kinetic data and age spectrum that indicates temperatures > 400°C prior to 1.4 Ga with cooling through 375°C by about 1375 Ma.

Appendix 4

4.1 Geologic Setting and Existing Geochronology

Granite magmatism is an important component of multiple orogenic events that shape the Precambrian history of New Mexico. Igneous activity is temporal with continental assembly related to arc terrain accretion that grew the southern margin of Laurentia between ~1.8-1.6 Ga and the New Mexico Precambrian basement holds rich record of this magmatism (Condie, 1982). The Yavapai orogeny occurred from 1.8-1.7 Ga and the Mazatzal orogeny followed from 1.7-1.66 Ga. In many parts of New Mexico, metamorphism is polyphase and broadly described by 1.7 Ga compressional deformation related to the assembly of Laurentia. In northern New Mexico this compressional deformation is seen as a northwest striking foliation trend that is thought to be related to the accretion and subduction of the volcanic arc (Karlstrom et al., 2004) Between 1.6 Ga and 1.5 Ga (fig 2A) there was a lack of active tectonism and magmatism which was then followed by a pervasive orogenic event between 1.45 Ga and 1.35 Ga (Karlstrom et al., 2004). The lack of tectonic activity between 1.60-1.45 Ga is shown by the compilation of Karlstrom et al. (2004) of 181 U-Pb zircon ages with no values of this age. There are two main pulses, one from 1.8-1.6 Ga, which is during the Yavapai and Mazatzal orogenies and then another pulse from 1.48-1.35 Ga. This plot shows a lull in active tectonism between the igneous pulses and likely represents a period of minimal tectonism.

The 1.4 Ga orogenic event has been extensively studied throughout the southwest USA and remains enigmatic (Karlstrom et al., 2004; Karlstrom et al. 1997, Shaw et al., 2005; Anderson et al., 1989; Andronicos et al., 2013; Daniel et al., 2013). Once thought

to be "anorogenic" (Anderson et al., 1989) it is now recognized that extensive deformation, metamorphism and magmatism occurred over a time span of ~100 Ma (Karlstrom et al., 1997).

Recent multidisciplinary studies, including thermochronology, record spatially variable metamorphism and significant deformation at 1.4 Ga in New Mexico (Shaw et al., 2005 and Karlstrom et al., 1997). However, there has been discovery of deformation within the pluton aureoles (e.g. Kirby et al., 1995; Amato et al., 2012) and it has since been proposed that the 1.4 Ga event is thought to be an accretionary orogenic event that is responsible for much of the tectonism that was previously thought to have occurred during the Mazatzal orogeny (Karlstrom et al., 2004).

The 1.4 Ga event caused metamorphic temperatures and pressures to become greater than 500˚C and 3.5 kbar. Karlstrom et al. (2004) conclude that the 1.4 Ga event is related to basaltic underplating. The basaltic underplating, which the petrologic and geochemistry data support, is thought to be the source of the tholeiitic magmatism in addition to the metamorphism. The "high crustal temperatures caused regional greenschist to amphibolite grade metamorphism and reset argon systematics throughout the SW," (Karlstrom et al., 2004).

The Precambrian plutonic rocks of the southwest USA have been extensively studied and their geochronology is fairly well established (Karlstrom et al., 2004, Shaw et al., 2005, Amato et al., 2012, Jahns, 1946; 1974). In contrast, the widely prevalent pegmatite occurrences have not received as much attention and their geochronology is not well known. This is important because if emplaced at shallow depths (at temperatures lower than the closure temperature of coarse muscovite crystals), $^{40}Ar/^{39}Ar$ dating of the

muscovite may record pegmatite emplacement. The common definition of a pegmatite is an igneous rock with coarse grained crystals that are all larger than one centimeter in diameter (Tarbuck and Lutgens, 1999). However, it has been accepted that pegmatites do not need to be coarse grained and perhaps a better definition is given by London (2008) in his publication on pegmatites. He states pegmatites are "an essentially igneous rock, commonly of granitic composition, that is distinguished from other igneous rocks by its extremely coarse but variable grain-size, or by an abundance of crystals with skeletal, graphic, or other strongly directional growth-habits. Pegmatites occur as sharply bounded homogenous to zoned bodies within igneous or metamorphic host-rocks" (London, 2008).

The origin of pegmatites has long been investigated. Originally, pegmatites were thought to have undergone slow cooling in order to allow for growth of coarse minerals. However, it is now believed they cool quickly to ambient temperatures and the minerals grow to large sizes due to high vapor content produced by fractionation within the granitic body (London, 2005). Knowing that Tuttle and Bowen (1958) had shown that the "granite system at elevated H_2O pressures demonstrated the low-temperature, hydrous, near minimum origins of most granites," in 1963, Jahns and Tuttle were able to clearly relate the last stages of granite magmatism to pegmatites. They did this by verifying that pegmatites had granitic minimum compositions (London, 2008).

4.2 Tusas Mountains

The Tusas Mountains are located approximately 25 miles south of the Colorado border, west of the Rio Grande Rift. Samples were collected from the Petaca District in the Tusas Mountains which is well known for its rich mining history. There are 5 major

formation groups within the Petaca district: the Kiawa, Persimmons Peak-Las Tablas, La Jarita-Apache, Cribbenville and Alamos groups. The Petaca district has over 200 pegmatites. Pegmatites occur as dikes, sills, branches and pods spanning the entire district and have an average linear dimension of ~200 meters, but range from 2-1000 meters. The thickness of the pegmatites range from 10's of centimeters to 100 meters (Jahns, 1974). The pegmatites crosscut the Precambrian metasedimentary and metavolcanic rocks (Karlstrom et al., 2004). The Petaca pegmatites have been described Jahns (1946 and 1974) as alkalic granites based on bulk chemical analyses. The majority of the pegmatites are internally zoned and exhibit a "sugary" to very coarse grained albite. Muscovite concentrations are commonly found around quartz masses (Jahns, 1974). These coarse muscovites were historically mined as sheet mica for stove windows and electrical circuits (McLemore, 2012).

The Tusas Mountains are located within the Yavapai-Mazatzal transition zone (Karlstrom et al. 2004). Williams (2007) shows evidence for a 1.4 Ga thermal event in the Tusas. Using an electron microprobe to date monazite he reports ~1.7 Ga cores over grown by much younger ~1.4 Ga rims. Additionally, Andronicos et al. (2013) published Lu/Hf garnet ages of 1.4 Ga from the Tusas Mountains that indicate metamorphism at this time as well. As seen in Figure 1, the Tusas Mountains were at high temperatures (>500˚C) 1.4 Ga. (Shaw et al., 2005). No 1.4 Ga plutons have been found in the Tusas and therefore the high metamorphic temperatures at 1.4 Ga are somewhat enigmatic. However, the Petaca pegmatites that were emplaced may be part of the heat source that drove the 1.4Ga metamorphism.

4.3 Sandia Mountains

The Sandia Mountains are located east of Albuquerque, NM on the eastern flank of the Rio Grande Rift. They are part of an eastward-tilted, rift-flank fault block composed of Paleozoic, Cenozoic and Precambrian rocks (Kelley and Northrop, 1975). The Sandia Mountains are within the Mazatzal zone and at 1.4 Ga were at temperatures between 350˚C and 500˚C (Karlstrom et al., 2004, Shaw et al., 2005). Pegmatites occur throughout the Sandia pluton and according to Kirby et al. (1995) result from the crystallization of the Sandia pluton.

The Cibola Gneiss is part of the northwest belt of the Tijeras Canyon Metamorphics. It is located between the Sandia Granite and the Tijeras fault. Kelley and Northrop (1975) note it has a distinct foliation that dips 40 to 65 degrees northwestward toward the granite contact. The Rincon Ridge Metamorphics are made primarily of micaceous quartzite and quartz-mica schist. Other present lithologies include feldspar, sillimanite, greenstone and chlorite schists. The Sandia Granite is primarily made up of the Sandia Pluton. The granite is porphyritic and consists of quartz, feldspars and micas (Kelley and Northrop, 1975). The pluton intruded into the area at 1.42 Ga (zircon age, Kirby et al., 1995). Since the Sandia Mountains are part of a colder 1.4 Ga block, their pegmatite muscovite ages are more likely to produce emplacement ages, in contrast to the cooling ages expected from the hotter Tusas block.

4.4 Manzano Mountains

The Manzano Mountains are located to the southeast of Albuquerque on the eastern side of the Rio Grande Rift. They are a fault-bounded mountain range that is primarily composed of Proterozoic rocks (Thompson et al., 1996) and is located within

the Mazatzal terrain, (Karlstrom et al., 2004). The mountain range stretches approximately 60 km north-south and 15 km east-west (Macroline et al., 1999). The mountains are divided by a northeast striking shear zone, which juxtaposes the southern and the northern portions (Thompson et al., 1996).

The Paleoproterozoic rocks, found in the central and south portions of the Manzano Mountains, consist of metarhyolite, amphibolite, schist, phyllite, and quartzite (Thompson et al., 1996). Two of the main plutons within the Manzanos are the Monte Largo pluton and the Priest pluton. Pegmatites are rare in the Manzanos, but can be found within the metarhyolite of the Monte Largo Pluton (Bauer et al., 1993). There are three main phases of Proterozoic deformation that occurred in the mountains. The first two occurred between 1650 Ma and 1400 Ma. These deformations are marked by folding and foliation within the mountain range. The third deformation phase is marked by low temperature deformation in the Priest pluton after 1400 Ma (Macroline et al., 1999; Heizler et al., 1997).

Deformation in the area decreases south from the shear zone on the upper plate. North of the shear zone on the lower plate, rocks record plutonism and deformation, primarily from the approximately 1.65 Ga Monte Largo pluton. The Monte Largo pluton and surrounding area of the lower plate are overprinted with greenschist-facies metamorphism that probably occurred around the time of crystallization of the pluton (Thompson et al., 1996). The upper plate consists of amphibolite-facies supracrustal rocks intruded by the approximately 1.43 Ga Priest Pluton (Thompson et al., 1996).

The Manzano Mountains are within a colder geologic block (~350-500˚C) than

the Tusas Mountains (>500˚C) and therefore pegmatite muscovites are more likely to record emplacement ages, rather than the cooling ages expected from the Tusas block.

4.5 Previous $^{40}Ar/^{39}Ar$ Geochronology

Shaw et al. (2005) compiled a large thermochronological dataset of $^{40}Ar/^{39}Ar$ ages that span from northern New Mexico to southern Wyoming. Similarly Karlstrom et al. (1997) published a large argon dataset and compiled zircon ages from central and northern New Mexico.

Shaw et al.'s (2005) compilation of biotite, muscovite and hornblende ages suggest that the southwest underwent a regional thermal episode from 1.45-1.35 Ga. Using the $^{40}Ar/^{39}Ar$ method, he reports ages for biotite and muscovite of 1.4 Ga and hornblende of 1.7-1.4 Ga. These ages are consistent with 300-500˚C temperatures at 1.4 Ga. The Tusas Mountain data is composed of ages less than 1.45 Ga, suggesting a resetting of the argon ages due to heating above 500°C. Coarse-grained muscovites from this region exhibit flat age spectra with plateau ages around 1375 Ma. Hornblende ages from this area are less than 1.4 Ga and are believed to represent cooling from greater than 500˚C temperatures. In addition to Shaw's findings, Sanders' et al. (2006) research in the Sangre de Cristo Range in northern NM supports a 1.4 Ga metamorphic event. He dated hornblende and micas by the $^{40}Ar/^{39}Ar$ method and concluded that much of the region was above 500˚C 1.4 Ga.

Karlstrom et al. (1997) also reports hornblende ages of 1.43-1.35 Ga that are interpreted to indicate cooling through temperatures greater than 500˚C. This correlates to a regional amphibolite facies metamorphism at 1.4 Ga followed by rapid cooling to ambient conditions of less than 300˚C. The muscovite ages of 1.37-1.31 Ga from

northern New Mexico come from a higher grade tectonic block compared to older ages from lower grade rocks of southern New Mexico.

Zircons from the same area have been dated at 1.7 Ga which suggest that the muscovite may have crystallized at 1.7 Ga and remained above 350°C or were reset during 1.4 Ga reheating. Ages for minerals collected from deeper in the crust in northern New Mexico are younger compared to minerals from the less metamorphosed areas in southern New Mexico which suggest uneven exhumation of the Precambrian rocks.

Daniel et al. (2013) did extensive research in the Picuris Mountains of northern New Mexico and concluded that high grade metamorphism occurred post 1.4 Ga. Their data includes detrital zircons that indicate deposition between 1490-1450 Ma of metasedimentary rocks, as well as evidence of regional deformation, crustal thickening, plutonism and metamorphism following the zircon deposition. They concluded that the accretion of the Mazatzal province could have occurred at 1.46 Ga instead of 1.7 Ga (Daniel et al., 2013).

Research completed in the central to south-western part of New Mexico also supports a 1.4 Ga event. Strickland et al. (2003) dated hornblende, mica, diabase and potassium feldspar from the Zuni Mountains via the $^{40}Ar/^{39}Ar$ method. Their data suggests that the deformation present is not due to the presupposed Paleoproterozoic Yavapai/Mazatzal accretion, but rather a 1430 Ma event. There is also an undeformed granite in the area that could be 1.4 Ga. Similarly, there is evidence of 1.4 Ga plutonism in the Burro and Caballo Mountains (Amato et al., 2012; McLemore et al., 2012). Zircon ages from the Burro Mountains indicate metamorphism and pluton emplacement 1.4 Ga (Amato et al., 2012). Amato et al. (2012) also dated micas and hornblendes and compared

them to zircon ages from the same area. The concordance of these ages record rapid cooling related to extension ~1460 Ma.

4.6 Muscovite Thermochronology

Muscovite is a useful, but somewhat complex thermochronological tool. Incremental heating, when compared to in situ age mapping of micas, can produce complex results. Hodges et al. (1994) found when they compared Crazy Basin muscovite and biotite ages done by both methods their results were in apparent disagreement. The laser in situ dating of the muscovite showed ages that varied by 300-400 Ma, recording slow cooling over 100's of millions of years. In contrast, the incremental step-heating data did not show age variation, suggesting rapid cooling (Hodges et al., 1994). Biotite data from an area nearby the Crazy Basin also showed large age gradients, suggesting that the incremental heating method was not the best approach for interpreting the cooling history. In situ UV laser can be used to directly date small areas on a muscovite, and could would allow recovery of accurate cooling histories without the complication of annealing of diffusion domains that might occur during incremental heating (Cosca et al., 2011).

Although the findings of Hodges et al. (1994) are a compelling case against incremental heating of muscovites, Forester and Lister (2013), Harrison et al. (2009) and Kula and Spell (2012) all show that incremental heating of muscovites can produce accurate thermal history results. These studies show that if heated slowly, muscovite does not catastrophically break down under vacuum, and can produce age spectra that record argon diffusion profiles.

The diffusion of argon in some potassium bearing minerals has been thoroughly investigated. McDougall and Harrison (1999) explain diffusion of argon as moving from a high concentration, i.e. the center of the crystal, to an area of low concentration, i.e. the rim of the crystal. The Arrhenius equation, $D=D_oe^{-E/RT}$, where D is the diffusion coefficient, D_o is the frequency factor, E is the activation energy, R is a gas constant and T is temperature, is used to model the diffusion of argon within a sample (Harrison et al., 2009).

The idea that there could be multiple domains within Kspar was introduced by Lovera et al. (1989). The multi domain (MDD) model suggests that argon from the small domains will dominate the first ^{39}Ar released during step heating, and then once those domains are exhausted, the degassing of the larger domains will dominate in the ^{39}Ar released. Each domain has its own closure temperature and therefore its own apparent age (McDougall and Harrison, 1999). With this knowledge, the MDD model can be applied to more accurately interpret complex age spectra. Also, by calculating the diffusion coefficients based on fractional loss of ^{39}Ar, and plotting them against the inverse temperature of laboratory heating, an Arrhenius diagram can be constructed.

Once an Arrhenius plot is constructed a reference line is calculated. A reference line is the slope of the line that the initial diffusion coefficients make when plotted on the Arrhenius diagram and is proportional to activation energy. With the reference line the Arrhenius diagram can be recast to create $Log(r/r_o)$ plots. A $Log(r/r_o)$ plot is a visual tool to represent the domain distribution is independent of the heating schedule. Correlation of the $Log(r/r_o)$ plot with the age spectrum indicates equal diffusion kinetics for ^{39}Ar and $^{40}Ar^*$ (Lovera et al., 2002; Harrison and Lovera, 2013).

In order for the MDD model to work, several conditions need to be met. The most important condition is that argon diffuses in the lab the same as it diffuses in nature. This has become an important and controversial topic in thermochronology today but ample data support MDD accuracy for Kspar. The presence of water in mica lattice has been thought to cause break down during heating in a vacuum and the release of argon by non-diffusive mechanisms. However, recent experiments by Harrison et al. (2009) and Kula and Spell (2012) found that this may not be the case. Harrison et al. (2009) experimented on muscovites by hydrothermally heating them in a piston-cylinder apparatus to cause $^{40}Ar^*$ loss. These experiments produced an Arrhenius law that predicted higher argon closure temperatures than those of Robins (1972).

Kula and Spell (2012) compared a slow, detailed step heated age spectrum, for muscovites to a shorter, less detailed step heated spectrum. Their results from Crazy Basin muscovites can be compared to Hames and Bowring (1994) results on the same material. Hames and Bowring (1994) used in situ analysis to study the concentration of argon within micas. They found that the oldest ages were in the middle of the crystal and the younger ages were near the rim. Hodges et al. (1994) also observed older ages in the center of their micas. Kula and Spell (2012) were able to show that step heating the muscovite over a long period of time yielded age spectra with the same age range as found by the in situ analysis of Hames and Bowring (1994). Additionally, with their more detailed age spectra, they were able to determine a thermal history. Their $\log(r/r_o)$ plots correlate well with their age spectra. This correlation is a strong indication that argon diffusion under lab conditions is similar to argon diffusion in nature. This data gives hope for using muscovite to record thermal histories, and specifically to this study

of coarse grained muscovites may provide a better means to extract emplacement ages from muscovite age spectra.

New Mexico Institute of Mining and Technology
Center For Graduate Studies

Student's Full Name: Lisa Anne Gaston
Title: $^{40}Ar/^{39}Ar$ Muscovite Thermochronology and Geochronology of New Mexico Pegmatites
Degree: ☒ MS ☐ PhD Department: EES Graduation Date 5/14

NMT Copyright Agreement

I hereby certify that this is my original work and I have the authority to grant the non-exclusive right and license specified herein. I further certify that, if appropriate, I have obtained and attached hereto a written permission statement from the owner(s) of each third party copyrighted matter to be included in my thesis, dissertation, or record of study, allowing distribution as specified below.

I certify that the version I submitted is the same as the approved by my advisory committee.

I hereby grant in perpetuity, without restriction, royalty free to New Mexico Tech or its agents the non-exclusive right and license to archive and make accessible, under the conditions specified below, my thesis, dissertation, or record of study in while or in part in all forms of media, now or hereafter known. This agreement shall survive assignment of any and all exclusive rights provided to copyright holders in Section 106 or the United States copyright law.

FERPA. To the extent this thesis, dissertation, or record of study is an educational record as defined in the Family Educational Rights and Privacy Act (FERPA) (20 USC 1232g), I consent to disclosure of it to anyone who requests a copy.

I retain all other ownership rights to the copyright of the thesis, dissertation, or record of study. I also retain the right to use in future works (such as articles or books) all or part of this thesis, dissertation, or record of study.

Availability Option (check one)

☑ Release the work immediately for **worldwide access on the Internet.**
☐ (*Patent Hold*) Secure the work temporarily for patent and/or proprietary purposes, then release the work for **worldwide access on the Internet.**
☐ (*Journal Hold*) Hold the work for one year, then release the work for **worldwide access on the Internet.** (*One-year extension on request, if needed*)

Chair/Co-Chair Certification

I have discussed the availability choices with my student and I am aware of the choice my student has made.

Chair/Co-Chair's Signature: _____ 5/6/14
(*Only one Chair or Co-Chair signature is required*).

Student Copyright Agreement

I have read and fully agree to the NMT copyright agreement regarding my thesis/dissertation. I agree to the thesis/dissertation availability option I selected above. I understand that the availability option is my choice and that there may be publishing consequences to my selection.

Student's Signature: _____ 5/5/14

Approval _____ Effective Date _____